Ministry of Higher Education and Scientific Research

Hassiba Benbouali University of Chlef

Faculty of Technology

Department Process engineering

THESIS Cotutelle with the University of

Gheorghe Asachi Iaşi, Romania

Presented to obtain the diploma of

DOCTORATE

Sector: Process engineering

Specialty: Process engineering

By

Chahrazed MAHMOUDI

Theme:

NEW HYDROGELS IN PARTICLE AND FILM FORM FOR THE ENCAPSULATION AND CONTROLLED RELEASE OF BIOLOGICALLY ACTIVE COMPOUNDS

Presented on 11/02/2025, before a jury comprising:

M. Bensaber BENSEBIA	Pr.	University Hassiba Benbouali Chlef	President
M. Mohamed DELLALI	Dr. MCA	University Hassiba Benbouali Chlef	Examiner
Mme Cătălina Anisoara PEPTU	Dr. MCA	University Gheorghe Asachi de Iasi, Romania	Examiner
Mme Naïma TAHRAOUI DOUMA	Pr.	University Hassiba Benbouali Chlef	Director
M. Marcel POPA	Pr.	University Gheorghe Asachi de Iasi, Roumani	Co-director
Mme Camelia Elena IURCIUC	Dr. Reasercher	University Gheorghe Asachi de Iasi, Romania	Examiner
M. Hacène MAHMOUDI	Pr.	National Higher School of Nanotechnologies, Algiers.	Invited

Acknowledgements

First and foremost, I would like to thank God ALLAH The Almighty for the courage, willpower, patience and health he has given me during these long years of study, so that I could reach this stage.

This thesis was carried out in the biomaterials laboratory of the Gheorghe Asachi Technical University, Romania and the Water and Environment laboratory of the Hassiba Benbouali University of Chlef under the supervision of Dr. ***Tahraoui Douma Naïma*** *and Professor* ***Marcel Popa****.*

I would like to thank my thesis supervisor for the trust he placed in me and the autonomy I was able to acquire during these enriching years. Additionaly, I would like to express my heartfelt gratitude to Dr. ***Camelia Elena Iurciuc (Tincu)*** *for her invaluable support and patience in the laboratory. Her guidance and dedication have been instrumental in my experimental work, and I am deeply appreciative of the time she invested in teaching me every aspect in the lab work.*

I would like to express my deep gratitude to Professor ***Mahmoudi Hacene*** *for his invaluable support throughout my university journey. His patience, guidance, and insightful advice have helped me overcome numerous academic and personal challenges. His dedication to his students' success and his passion for teaching has been a great source of inspiration, motivating me to strive for my best. I sincerely thank him for all the assistance and mentorship he has provided. His kindness and availability have left an indelible mark on my university experience, and I am honored to have benefited from his guidance.*

I want to thank sincerely my parents ***MAHMOUDI Djelali*** *and* ***CHAFEI Khadidja****, and to my sisters, , and my brothers for their contributions, their support and their patience, without whom this modest work would never have seen the light of day.*

Thank you to my husband ***BOUKACEM Hamza*** *and my family in-laws for their support and help.*

I would also like to thank my companions and friends who have helped me in many ways, I would like to thank them for always being there for me: ***Sened Nassiba****,* ***Fettah Nadjiya****,* ***Ayadi Khadidja, Maimoun Bekhta, Maouche Wahiba, Sahraoui Noura, Fekaouni Ayda, Kaltoum*** *and all my friends at UHBC*

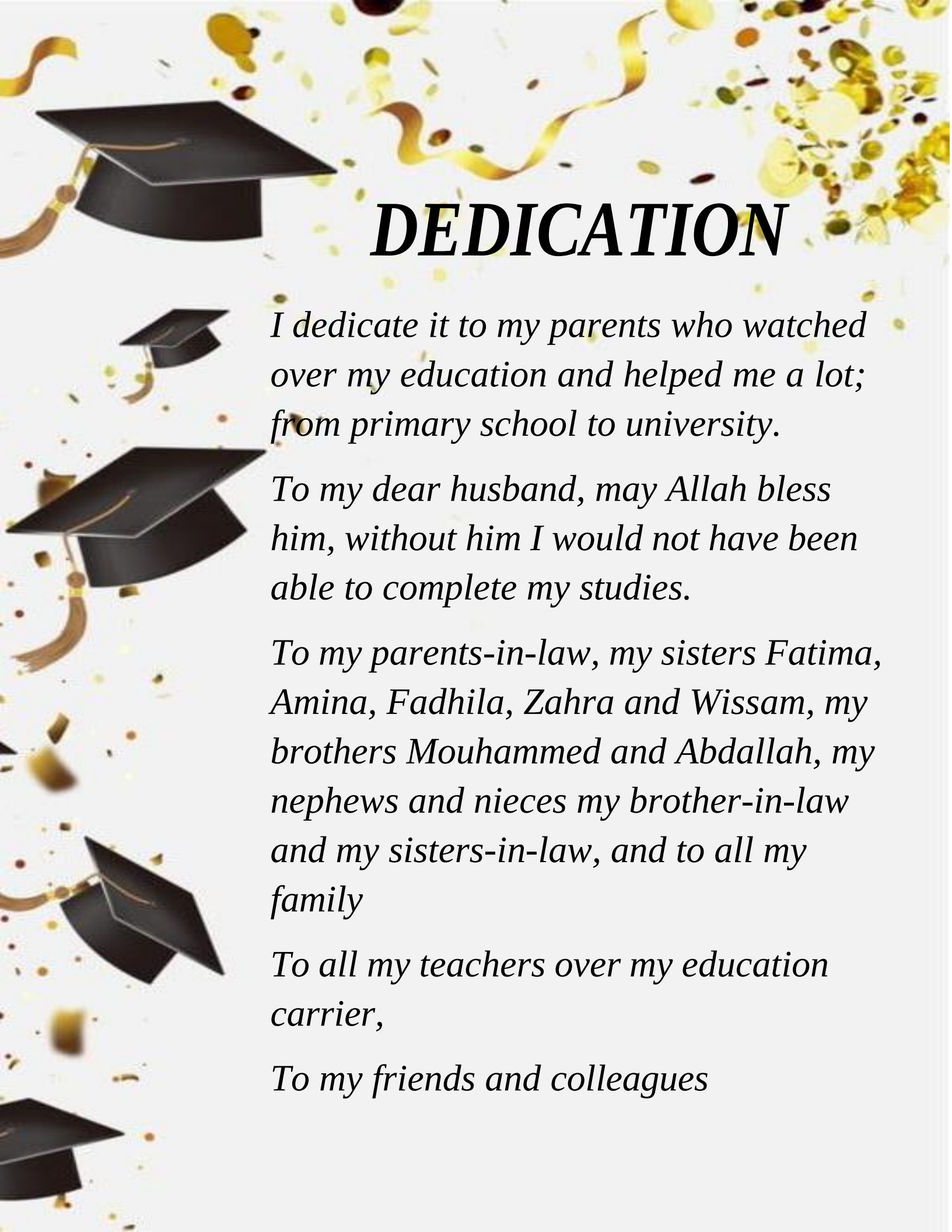

DEDICATION

I dedicate it to my parents who watched over my education and helped me a lot; from primary school to university.

To my dear husband, may Allah bless him, without him I would not have been able to complete my studies.

To my parents-in-law, my sisters Fatima, Amina, Fadhila, Zahra and Wissam, my brothers Mouhammed and Abdallah, my nephews and nieces my brother-in-law and my sisters-in-law, and to all my family

To all my teachers over my education carrier,

To my friends and colleagues

ABSTRACT

ملخص

RESUME

Abstract

The main objective of this research is to synthesize biocompatible gelatin-based hydrogels by cross-linking protein-free amino groups with aldehyde groups obtained by oxidation of sodium alginate, a dual cross-linking approach that incorporates both covalent and ionic bonds for propolis immobilization. The covalent bonds are formed by Schiff base bonds between the free amino groups (NH_2) of the lysine residues in the protein and the aldehyde groups (CHO) generated by the oxidation of sodium alginate using $NaIO_4$. Ionic bonds are created using Mg^{2+} ions. Hydrogel films were synthesized by varying the molar ratios of -CHO to -NH_2 under different pH conditions (3.7 and 5.5).

The presence of aldehyde groups in oxidized sodium alginate (OSA) was confirmed by FTIR and NMR spectroscopy. The degree of oxidation was monitored for 48 hours and the effect of temperature was also studied.

The results indicate that higher -CHO/-NH_2 molar ratios lead to an increase in the conversion index values for NH_2 groups, while a decrease in the swelling degree values was observed in media with pH values of 5.5 and 7.4.

In addition, the effectiveness of encapsulation and release of propolis decreases as the degree of cross-linking of the hydrogel increases. In particular, UV irradiation enhanced the antioxidant activity of both free and encapsulated propolis.

These results provide valuable insights into the design of biocompatible hydrogels for propolis immobilization, highlighting their potential for controlled release applications in the biomedical and pharmaceutical sectors.

Key words: polysaccharides, gelatin, aldehyde groups, sodium alginate, propolis, hydrogels.

ملخص

الهدف الرئيسي من هذا البحث هو تخليق هيدروجيلات متوافقة حيوياً قائمة على الجيلاتين، من خلال الربط التبادلي بين مجموعات الأمين الحرة الخالية من البروتين ومجموعات الألدهيد التي يتم الحصول عليها عن طريق أكسدة ألجينات الصوديوم، وهي مقاربة ثنائية الربط التبادلي تدمج الروابط التساهمية والأيونية لتثبيت مادة البروبوليس. يتم تكوين الروابط التساهمية عبر روابط شيف بين مجموعات الأمين الحرة(NH_2) لمخلفات الليسين في البروتين ومجموعات الألدهيد (CHO) التي تنتج عن أكسدة ألجينات الصوديوم باستخدام $NaIO_4$. وتُنشأ الروابط الأيونية باستخدام أيونات Mg^{2+}. تم تخليق أفلام الهيدروجيل عن طريق تغيير النسب المولية من CHO- إلى NH_2- تحت ظروف مختلفة من درجة الحموضة (3.7 و5.5.) تم تأكيد وجود مجموعات الألدهيد في ألجينات الصوديوم المؤكسدة (OSA) من خلال التحليل الطيفي FTIR و .NMRتم مراقبة درجة الأكسدة على مدار 48 ساعة، وتمت دراسة تأثير درجة الحرارة أيضًا.

تشير النتائج إلى أن النسب المولية الأعلى من NH_2-CHO/- تؤدي إلى زيادة في قيم مؤشر التحويل لمجموعاتNH_2 ، بينما لوحظ انخفاض في قيم درجة الانتفاخ في الأوساط ذات قيم pH تبلغ 5.5 و7.4.

بالإضافة إلى ذلك، تقل فعالية التغليف وإطلاق البروبوليس مع زيادة درجة الربط التبادلي للهيدروجيل. وعلى وجه الخصوص، عزز التشعيع بالأشعة فوق البنفسجية النشاط المضاد للأكسدة لكل من البروبوليس الحر والمغلف.

توفر هذه النتائج رؤى قيمة حول تصميم هيدروجيلات متوافقة حيوياً لتثبيت مادة البروبوليس، مما يبرز إمكاناتها في تطبيقات الإطلاق المُتحكم فيه في القطاعات الطبية والصيدلانية.

لكلمات المفتاحية: السكريات المتعددة، الجيلاتين، مجموعات الألدهيد، ألجينات الصوديوم، البروبوليس، الهيدروجيلات.

Résumé

L'objectif principal de cette recherche est de synthétiser des hydrogels biocompatibles à base de gélatine en réticulant des groupes amine libres de protéines avec des groupes aldéhyde obtenus par oxydation de l'alginate de sodium, une approche de double réticulation qui intègre à la fois des liaisons covalentes et ioniques pour l'immobilisation de la propolis. Les liaisons covalentes sont formées par des liaisons de Schiff entre les groupes amine libres (NH_2) des résidus de lysine de la protéine et les groupes aldéhyde (CHO) générés par l'oxydation de l'alginate de sodium à l'aide de $NaIO_4$. Les liaisons ioniques sont crées en utilisant des ions Mg^{2+}. Les films d'hydrogel ont été synthétisés en faisant varier les rapports molaires de -CHO à -NH_2 sous différentes conditions de pH (3,7 et 5,5). La présence de groupes aldéhyde dans l'alginate de sodium oxydé (OSA) a été confirmée par spectroscopie FTIR et RMN. Le degré d'oxydation a été suivi pendant 48 heures, et l'effet de la température a également été étudié.

Les résultats indiquent que des rapports molaires -CHO/-NH_2 plus élevés entraînent une augmentation des valeurs de l'indice de conversion des groupes NH_2, tandis qu'une diminution des valeurs de degré de gonflement a été observée dans des milieux avec des valeurs de pH de 5,5 et 7,4. De plus, l'efficacité de l'encapsulation et de la libération de la propolis diminue à mesure que le degré de réticulation de l'hydrogel augmente. En particulier, l'irradiation UV a renforcé l'activité antioxydante de la propolis, tant libre qu'encapsulée. Ces résultats fournissent des informations précieuses sur la conception d'hydrogels biocompatibles pour l'immobilisation de la propolis, mettant en évidence leur potentiel pour des applications de libération contrôlée dans les secteurs biomédical et pharmaceutique.

Mots-clés: polysaccharides, gélatine, groupes aldéhyde, alginate de sodium, propolis, hydrogels.

- **List of figures**
- **List of Tables**
- **List of Abbreviations**

List of figures

List of Tables

List of Abbreviations

SA: Sodium Alginate

Gel (G): Gelatin

Pro: Propolis

OSA: Oxidized Sodium Alginate

FTIR: Fourier Transform Infrared Spectroscopy

NMR: Nuclear Magnetic Resonance Spectroscopy

TGA: Thermogravimetric Analysis

SEM: Scanning Electron Microscopy

TEMPO: 2, 2, 6, 6-tetramethylpiperidine-1-oxyl radical.

LMS: laccase-mediator system

CI: Conversion Index

PCA: Para-Coumaric Acid

ABS: Acetate Buffer Solution

OD: Degree of Oxidation

UV: Ultra Violet Spectrophotometer

HPLC: High-Performance Liquid Chromatography

I (%): Inhibition percentage.

Tmax: temperature at which the maximum rate of weight loss occurs during the thermal decomposition

IC50: represents the concentration of the sample required to neutralize 50% of the free radicals present in the DPPH solution

Table of Content

Table of content

GENERAL INTRODUCTION

Intrroduction

A hydrogel is a three-dimensional, hydrophilic polymer network that absorbs and retains large amounts of water [1]. Despite their high water content, hydrogels usually behave as solids. Their inflated shape resembles certain elements of living systems, making them useful in a variety of sectors, including medical, pharmaceuticals, food, agriculture, and environmental science [1, 4].

Polysaccharides are complex carbohydrates made up of long chains of monosaccharide units linked by glycosidic bonds, characterized by their high molecular weights [5]. Naturally occurring in microorganisms, algae, plants, and animals, they play key roles in biological processes such as cell wall formation and energy storage [6, 7]. Their bioactive properties offer promising potential for therapeutic applications in pharmaceuticals [8]. Additionally, their unique physicochemical characteristics make them valuable in industries such as food [9,10], cosmetics [11], and materials science [12]. Ongoing research is enhancing our understanding of the structure-function relationships of polysaccharides, enabling innovative advancements. Scientists are also modifying their branching patterns, chain lengths, and functional groups to improve their versatility for specific applications [13].

A key approach to modifying polysaccharides is through the introduction of carbonyl groups into the biopolymer chain via oxidation [13, 14]. This targeted modification is designed to enhance the functionality and performance of polysaccharides for specific applications. Adding carbonyl groups imparts new chemical and physical properties to the polysaccharide structure, improving characteristics such as solubility, stability, and reactivity [15]. This process expands the potential uses of polysaccharides across various fields. Chemical oxidation methods are commonly employed to introduce these carbonyl functional groups into the polysaccharide backbone [15–17].

Introducing carbonyl groups into polysaccharides enhances their capacity to form hydrogels and imparts unique functionalities to the resulting materials. The addition of carbonyl groups increases the polysaccharide’s reactivity and cross-linking potential, allowing for precise control over the hydrogel's mechanical properties, swelling behavior, and responsiveness to external stimuli. Furthermore, these carbonyl groups facilitate the incorporation of other functional molecules, such as amino groups from protein chains. Cross-linking modified polysaccharides, particularly those with added carbonyl groups, with proteins is an important technique in biomaterials and biomedical research [18, 19].

Proteins are natural polymers made up of amino acids linked by peptide bonds and further stabilized by cross-links such as sulfhydryl bonds, hydrogen bonds, and van der Waals forces, resulting in complex, functional structures [20]. Common proteins like collagen, gelatin, albumin, and soy protein are frequently used to form hydrogels [21]. Their wide array of functional groups—such as amino, carboxyl, hydroxyl, and sulfhydryl groups—enables diverse interactions and crosslinking techniques, making proteins ideal for hydrogel creation [22].

As the fundamental building blocks of life, proteins offer a rich variety of chemical functionalities and structural patterns that are particularly well-suited for developing advanced hydrogels. These protein-based hydrogels can promote cell growth, support tissue regeneration, and feature customizable mechanical properties and degradation rates [22]. The integration of protein-derived materials into hydrogel technology represents a cutting-edge area in biomaterials research, offering innovative solutions to complex challenges in healthcare and environmental sustainability.

Carbonyl-modified polysaccharides cross-linked with protein-based hydrogels represent a promising class of materials for biomaterials and biomedical applications. These hydrogels combine the beneficial properties of both polysaccharides and proteins, offering key features such as biocompatibility, biodegradability, and adjustable mechanical properties. One of the main mechanisms for cross-linking in these systems is Schiff base formation, which occurs when carbonyl groups introduced into the polysaccharide backbone react with amino groups in proteins to form covalent Schiff base bonds [8, 23].

This cross-linking process, which involves the condensation of the carbonyl groups in polysaccharides with the amino groups in proteins, creates a stable, pH-dependent network that can be tuned for desired cross-linking levels [9]. The resulting hybrid hydrogel structure combines the structural and mechanical properties of polysaccharides with the bioactivity and functionality of proteins, making it ideal for a variety of applications. The tunability of the Schiff base reaction allows precise control over the physical and chemical characteristics of the hydrogel.

The Schiff base hydrogels are widely applicable in biomedical fields. They enable precise control over drug release kinetics, enhancing therapeutic outcomes [11, 24, 25]. To develop an effective controlled drug delivery system using biopolymers, the first crucial step is selecting the appropriate biopolymer(s). This requires a deep understanding of the biopolymers' surface and

intrinsic properties, which are essential for designing systems that deliver optimal therapeutic outcomes [26, 27]. The choice of biopolymer significantly influences the hydrogel's characteristics, including its mechanical strength, porosity, and responsiveness to external stimuli. Common biopolymers used in hydrogel synthesis include alginate, chitosan, hyaluronic acid, collagen, and gelatin, each contributing unique properties to the resulting material.

Gelatin (Gel) is a water-soluble compound derived from collagen through partial hydrolysis. It readily dissolves at 37°C, is non-immunogenic, and exhibits amphoteric properties [28, 29]. The molecular weight and characteristics of Gel are influenced by two main factors: the source of collagen and the manufacturing process. The type of collagen used, along with the method of production—such as heat and enzymatic denaturation or extraction under alkaline (gelatin type B) or acidic (gelatin type A) conditions—significantly affect Gel's molecular weight, viscosity, and gelling strength [30]. Structurally, Gel is characterized by a repeating amino acid sequence and a high concentration of hydroxyproline and hydroxylysine. Due to these unique properties, hydrogels made from Gel are extensively used in the development of drug delivery systems, contact lens composites, and tissue engineering matrices [30].

Additionally, the mechanical and chemical properties of Gel can be adjusted by using various cross-linking agents, such as glutaraldehyde [31], genipin [32], and dialdehydes derived from oxidized polysaccharides [33, 34]. Sodium alginate (SA) is a non-toxic, naturally occurring polysaccharide extracted from brown seaweed, like kelp, and is widely utilized in the food [35], pharmaceutical [36], and textile industries [37]. It is a water-soluble salt that forms a viscous, gel-like substance upon contact with water, making it an excellent thickener, stabilizer, and emulsifier.

SA can be modified through oxidation with sodium periodate in an aqueous solution, which reduces its molecular weight and enhances its reactivity and biodegradability [38, 39]. This modification broadens the potential applications of SA in various industries, including food, pharmaceuticals, and biomedicine. The oxidation process transforms the hydroxyl groups at the C-2 and C-3 vicinal bonds in the uronic units of the alginate chains into dialdehyde groups [40]. These dialdehyde groups can subsequently undergo additional chemical reactions, such as cross-linking, resulting in more complex structures with diverse properties.

Hydrogels based on oxidized sodium alginate (OSA) have demonstrated significant potential in numerous applications, including drug delivery [41], tissue engineering [42], and wound healing

[43]. The carbonyl groups present in the hydrogel can interact with various functional groups in drugs or proteins, enabling controlled release of these molecules over time. Furthermore, reactions involving amino groups can produce hydrogels with enhanced cell adhesion properties, making them suitable for a variety of applications [44]. The varying degrees of cross-linking in OSA-based hydrogels also contribute to the development of scaffolds for tissue engineering and drug delivery systems with improved stability and durability [45].

The Gel-OSA-based hydrogel is notable for its abundance and advantageous properties for creating functional materials, including biocompatibility, non-toxicity, flexibility, and biodegradability [40,46]. When the free amino groups of lysine and hydroxylysine residues in Gel react with the aldehyde groups of OSA, covalent bonds are formed through Schiff base linkages. This reaction results in the formation of highly stable, physiologically degradable networks that enhance cell adhesion and biocompatibility.

Pettignano et al. developed a Gel-based hydrogel cross-linked with OSA using borax, resulting in hybrid hydrogels with self-healing capabilities due to the reversible nature of Schiff base formation. This bio-hydrogel merges the properties of both materials, enabling it to self-repair after mechanical damage. Their findings indicate that optimizing self-healing properties in these hydrogels requires a careful balance of concentration, the stoichiometric ratio of the two biopolymers, and the specific source of Gel. Additionally, the healing process is significantly affected by pH, underscoring the importance of the dynamic Schiff base linkages between the amine groups of Gel type B and the aldehyde groups of OSA in reconstructing the damaged hydrogel interface [46].

A study by Rottensteiner et al. [47] demonstrated that alginate-gelatin hydrogels exhibited favorable biocompatibility both in vitro and in vivo, along with strong cell adhesion and proliferation of mesenchymal stem cells. These encouraging results indicate that alginate-gelatin hydrogels hold significant potential for applications in bone tissue engineering and merit further research in this field [47].

Propolis (Pro) is a natural, resinous substance collected and processed by bees from various plant sources [48]. It contains over 300 components [49], including resins, gummy substances, waxes, essential oils, aromatic oils, phenolic compounds, and bioactive substances such as phenolic acids, flavonoids, ketones, and aldehydes[49,50]. The composition of propolis varies based on its botanical origin [51]. This diverse array of chemical compounds contributes to its wide range of

biological activities, which differ among samples from various geographical locations. These activities include anesthetic, antimicrobial, antioxidant, anti-inflammatory, and, more recently, antiproliferative and antitumor effects [50, 52]. Additionally, Pro is non-toxic, safe, and can exhibit antimicrobial synergism when used in combination with certain antibiotics [53]. Recently, novel biopolymer hydrogels containing Pro have been developed for various biomedical applications [54].

The primary objective of this study was to optimize the reaction parameters for producing hydrogel films by cross-linking gelatin with oxidized sodium alginate (OSA) to achieve the most favorable physicochemical properties for the controlled and sustained release of propolis (Pro). Within the propolis used, three phenolic acids were quantified: caffeic acid, p-coumaric acid, and ferulic acid [55], with para-coumaric acid selected as the key component for investigating the encapsulation and release performance of the fabricated hydrogels.

The structure of the obtained OSA was analyzed using FTIR and ^{1}HNMR spectroscopy to determine the degree of oxidation and assess the effects of varying oxidation times and temperatures. We also evaluated the capacity of the aldehyde groups in OSA to cross-link the free amino groups in gelatin by analyzing the conversion index of NH_2 groups to Schiff bases, utilizing different NH_2/CHO molar ratios and two distinct pH environments. The hydrogels, both with and without encapsulated propolis, were characterized using FTIR spectroscopy, scanning electron microscopy, and measurements of swelling degree. Furthermore, we investigated the protective role of the polymer matrix by assessing the antioxidant activity of propolis-containing films exposed to UV light for 30 minutes. We also evaluated the hydrogels' ability to control and sustain the release of p-coumaric acid from propolis in vitro, in buffer solutions at pH 5.5 and pH 7.4.

This thesis is organized into three parts:

The first part is a bibliographic research being composed of three (chapters describing the oxidation of polysaccharides and their reaction with proteins to form hydrogels, their classification and various biomedical applications, and a description of Schiff base cross-linked hydrogels based on oxidised alginate and gelatin for biomedical applications.

The second part presents the methods and materials, being organized in one chapter.

Chapter 4 is dedicated to the presentation of the characterization synthesis methods and the equipment used for this purpose.

The third part represents the part of Results and discussion composed of one chapter which is chapter 5 presents the obtained results and their discussions.

Finally, a general conclusion and suggestions for future are presented

PART I:
BIBLIOGRAPH
IC RESEARCH

CHAPTER I:
Oxidation Of Polysaccharides And Their Reaction With Proteins To Form Hydrogels

Chapter I: Oxidation of Polysaccharides and Their Reaction with Proteins to Form Hydrogels

I.1 Introduction

This chapter presents a bibliographic summary of the generalities on the chemical and physical properties of polysaccharides as well as their periodic periodat oxidation or enzymatic oxidation which improves their crosslinking with proteins to form hydrogels.

I.2 Polysaccharides

Polysaccharides or essential carbohydrates are versatile molecules in the form of short sequences of oligosaccharides or polymeric repeating units. Both substances are found in abundance in plants and animals, and play a variety of roles such as structural support, energy storage and facilitating gel formation. Their specific functions depend on factors such as chemical composition, molecular weight and, in some cases, ionic properties. Because of their multiple capabilities, polysaccharides find applications in both food and non-food industries, serving as crucial components in a variety of products and processes [56]. Chemical modification of polysaccharides results in hydrophilic, acidic, basic or other functional groups in the polysaccharide structure, thus modifying their properties [19].

I.2.1. Introduction of carbonyl groups in polysaccharides chains by oxidation

Chemical oxidation of polysaccharides enables the creation of structures that can be applied in a variety of fields. This method improves product value by triggering the oxidative cleavage of glycol, converting primary alcohols to carboxylic acids and enzymatically converting them to aldehydes [19]. These oxidation techniques modify the hydroxyl groups in the polysaccharide backbone, producing carboxyl or carbonyl groups. This modification lengthens the chains and enhances the reactivity of polysaccharides, thus broadening their potential applications [25]. Recent studies highlight the effectiveness of selective oxidation in introducing carbonyl (aldehydes, CHO) and carboxyl (COOH) groups to the polysaccharide backbone [13, 39]. More specifically, hydroxyl groups in the primary C-6 position can be oxidized to form aldehydes or carboxylic acids [19]. Among oxidation methods, the nitroxyl radical TEMPO appears to be a promising route for the production of polyuronic acids produced from polysaccharides, targeting the selective oxidation of primary alcohol groups (C-6) [57, 59]. Researchers in this field have

explored chemoenzymatic modifications using biocatalysts such as laccase and mediators such as TEMPO or 4-Amino-TEMPO under mild aqueous conditions to introduce aldehydes and surface-active carboxylic groups onto cellulose nanofibers. In addition, variable proportions of dicarboxylic and dialdehyde chemical functions can be obtained by using other oxidizing agents such as sodium hypochlorite and hydrogen peroxide to oxidize secondary hydroxyl groups (C-2 and C-3) [14, 57, 60, 61].

The introduction of carbonyl groups into the backbone chain of polysaccharides is of great importance, as it profoundly influences their structural and reactive characteristics. The main methods for incorporating carbonyl groups into polysaccharide chains involve chemical and enzymatic oxidation [62]. These oxidation techniques are used to target the hydroxyl group at the C-6 position, resulting in the formation of aldehyde groups, as well as to cleave vicinal diols at C-2 and C-3, thus introducing dicarbonyl functional groups [19].

I.2.2 Enzymatic oxidation

A commonly employed method for modifying and enhancing the properties of polysaccharides involves enzymatic oxidation. Instead of relying on chemical catalysts, enzymes like galactose oxidase (D-galactose: oxygen 6-oxidoreductase, E.C.1.1.3.9) are utilized. This enzyme exhibits selectivity in catalyzing the oxidation of the C-6 primary hydroxyl group of D-galactose moieties, yielding corresponding aldehydes, as depicted in **Figure 1** [62]**.** The resulting galactoaldehyde products possess heightened reactivity, rendering them suitable for various applications, including the formation of hydrogel by cross-linking reactions [63] and the fabrication of new aerogels [64]. The enzymatic oxidation reaction catalyzed by galactose oxidase proceeds via oxidative and reductive half-reactions, utilizing oxygen as an oxidant and generating hydrogen peroxide as the by-product [65, 66].

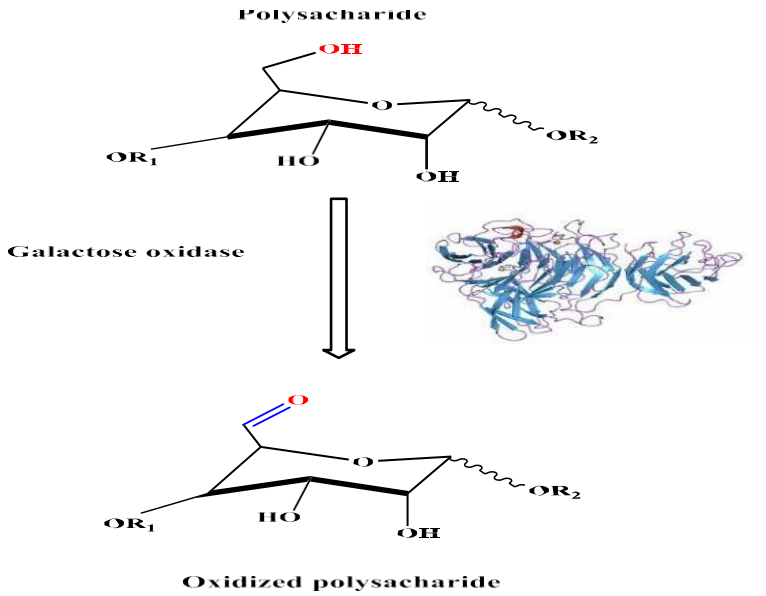

Figure 1. Enzymatic oxidation reaction by galactose oxidase.

Parikka et al [67] employed a selective oxidation technique on various galactose containing polysaccharides, including spruce galactoglucomannan (O-acetyl galactoglucomannan), guar galactomannan (guar gum), larch arabinogalactan (corn arabinoxylan), and tamarind seed xyloglucan. They utilized a consistent three-enzyme system comprising Galactose oxidase, catalase, and horseradish peroxidase. Their study aimed to assess how temperature, substrate concentration, enzyme-to-substrate ratio, and polysaccharide structure influence both the quantity and quality of the resulting products through oxidation. Their findings indicate that higher degrees of oxidation were achieved with oxidized O-acetyl galactoglucomannan, guar gum, and xyloglucan compared to oxidized larch arabinogalactan and corn fiber gum [67].

Previous studies have also demonstrated the oxidation of polysaccharides using galactose-6-oxidase. Mollerup *et al* [68] used chemoenzymatic approaches involving galactose-6-oxidase to oxidize galactoglucomann and xyloglucan units in polysaccharides. The oxidized polysaccharides can then be adsorbed onto cellulose surfaces, improving the reactivity and barrier properties of cellulose-based materials. This study was undertaken with the aim of advancing this system for renewable energy and materials applications [68].

A number of studies have also focused on the chemoenzymatic alteration of cellulose pulps using the laccase-mediator system (LMS), which comprises laccase (EC 1.10.3.2) and the 2,2,6,6-tetramethylpiperidine-1-oxyl radical (TEMPO). Operating under mild aqueous conditions (sodium citrate buffer, pH 6, 30 °C), this system introduces mainly aldehyde groups into

cellulose, with carboxyl groups forming a smaller fraction of the carbonyl groups. The reaction proceeds uniformly, even in the high-b-weight region, distinguishing it from other methods of chemical oxidation of cellulose. The effectiveness of LMS in modifying cellulose fibers, particularly those derived from softwood (bleached softwood kraft pulp), has been convincingly demonstrated [69]. Thanks to the combination of laccase and TEMPO, fibers can be endowed with carboxyl and aldehyde groups, with process parameters tailored for optimum enhancement of functional group content. The effectiveness of this approach derives from its catalytic oxidation pathways, highlighting enzymatic modifications suitable for papermaking applications. In addition, research indicates that increasing pulp consistency enhances the biorefinery potential of the laccase-TEMPO system. Higher pulp consistency yields heightened levels of aldehyde and carboxyl groups, accompanied by more pronounced reductions in pulp viscosity during enzymatic treatment. These not only impacts fiber strength and tear resistance but also results in improved water retention capabilities and mechanical properties like dry tensile index and burst index. The treatment fosters enhanced inter-fiber hydrogen bonding, leading to energy savings during refining and bolstering wet tensile strength. The observed increase in wet tensile strength is ascribed to inter-fiber covalent bonding facilitated by aldehyde groups [70, 71].

I.2.3. Periodate oxidation

Periodate oxidation in aqueous solutions emerges as a highly effective method for modifying polysaccharide chains by introducing carbonyl groups, thereby potentially transforming the physical and chemical properties of the resulting biopolymer derivatives [15, 72]. Typically, this oxidation process occurs with sodium metaperiodate as the oxidizing agent, leading to the ring-opening of 1,2-diols at positions C-2 and C-3 of polysaccharides, resulting in dialdehyde groups with remarkable selectivity and efficiency [19]. Malaprade first identified this cleavage reaction through the rapid oxidation of polyols by the periodate ion [73, 74]. Subsequently, Criegee noted that lead tetraacetate can cleave 1, 2-diols [75], while Fleury and Lange further validated Malaprade's cleavage reaction, emphasizing the role of vicinal hydroxyl groups in the compound [65]. Prior literature has extensively reviewed periodate oxidation [15, 40, 76], and only a brief overview will be provided here.

The process of oxidizing polysccharides with sodium periodate to introduce carbonyl groups into the polysccharide backbone starts with hydroxyl groups binding directly to iodine via

two successive ion-pair attacks on each hydroxyl group (**Figure 2**). This sequence forms a cyclic intermediate known as the periodate ester. Next, the cyclic iodate ester is decomposed to give dialdehyde groups. The crucial step in this mechanism is the formation of the periodate ester. Factors such as substrate structure, reaction pH and temperature can influence this process. In addition, the periodate oxidation reaction is exothermic and the periodate compound itself has relatively low light stability. Consequently, the reaction is generally carried out in the dark, at a temperature below 30 °C and at a pH between 3 and 7 [77].

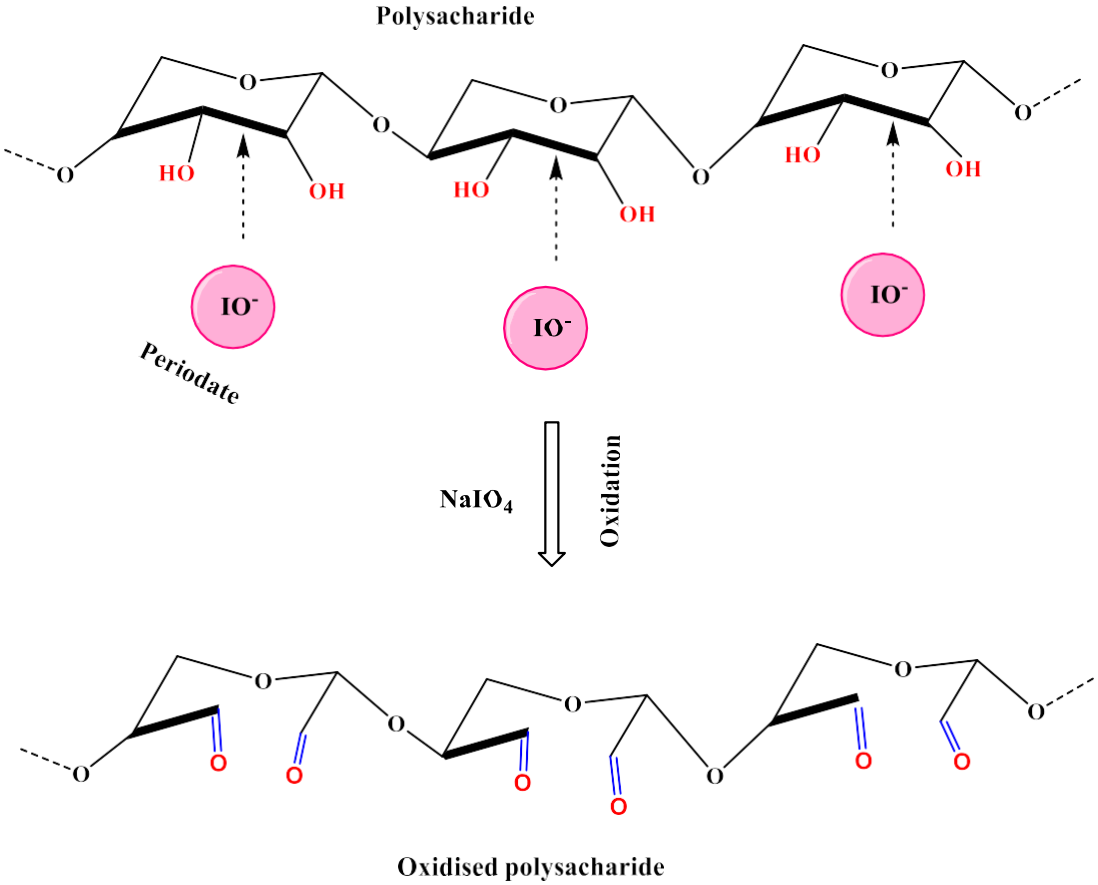

Figure 2. Mechanism of polysaccharide oxidation by sodium periodate.

In general, the properties of dialdehyde products are influenced by various processing parameters, such as periodate dosage, temperature and pH. Aldehyde content is influenced by increasing periodate dosage, but excessive molar ratios between periodate and the monomer unit of the polysaccharide can lead to a slight increase in aldehyde content due to the formation of hemiacetals. These hemiacetals are created when an aldehyde group reacts with a hydroxyl group, which is particularly noticeable when the aldehyde content is higher [38]. For example,

during the oxidation of sodium alginate, the degree of oxidation generally reaches a maximum of around 50% due to the formation of stable inter-residue hemiacetals, which protect the hydroxyl groups from further oxidation [15, 79]. In addition, temperature affects the density of dialdehyde products, with higher temperatures leading to deterioration of periodate ions and consequently reducing aldehyde content. To achieve maximum aldehyde density, it is crucial to keep the oxidation temperature below 30 °C, as demonstrated by Kholiya et al. [65]. Other studies have shown that the aldehyde density of dialdehyde-carboxymethylagarose fell from 81% to 64% when the temperature was raised from 30 °C to 60 °C [65]. The pH of the reaction medium also plays an important role in determining aldehyde density [66]. The optimum density of dialdehydes in oxidized polysaccharides lies within a pH range of 3 to 7. At pH values below 2.0, the dialdehyde product undergoes acidic degradation, while pH values above 7 result in a reduction in aldehyde content and molecular weight due to β-elimination reactions [66].

Furthermore, under alkaline conditions, some aldehyde groups may undergo further oxidation to form carboxyl groups through the Cannizzaro reaction [72]. Additionally, the type of saccharide blocks can influence the rate at which dialdehyde groups are generated. For instance, the periodate oxidation rate for guluronic residues of alginate was approximately 50 % faster than that for mannuronic residues [63]. Therefore, comprehending the impact of periodate oxidation factors and the structural characteristics of polysaccharides is crucial for achieving high dialdehyde content with the desired structure.

When dealing with derivatives of periodate-oxidation products, caution is paramount to prevent unintentional or undesirable modifications. One concern involves the precipitation of free iodine, which can lead to adverse effects. Studies have shown that iodine can react with specific periodate-oxidation products, resulting in unwanted alterations. Additionally, treating the typical dialdehydic oxidation product with a strong base poses risks, as it may trigger an internal Cannizzaro reaction. For instance, the oxidation of methyl P-L-rhamnopyranoside can quantitatively undergo this reaction within a short period when exposed to strong bases like sodium hydroxide at elevated temperatures [79]. Moreover, water can produce the hydrolysis of polysaccharides under certain conditions, particularly in acidic or alkaline environments. This hydrolytic reaction breaks glycosidic bonds within polysaccharides, producing smaller oligosaccharides or monosaccharides. While hydrolysis is typically undesired during oxidation

reactions, it may occur as a side reaction if the reaction conditions are not meticulously controlled [79,80].

To mitigate undesirable reactions like free iodine precipitation or internal Cannizzaro reactions during the isolation of derivatives from periodate-oxidation products, several precautions can be implemented. Firstly, it's essential to ensure complete removal of excess periodate from the reaction mixture before isolation. Thorough washing or purification steps, such as dialysis or chromatography, can effectively separate desired oxidation products from unreacted periodate, thus preventing free iodine formation. Additionally, optimizing reaction conditions during periodate oxidation is crucial to minimize the formation of unwanted by-products and side reactions. Controlling factors such as pH, temperature, and reaction time can facilitate the selective formation of desired oxidation products [79].

I.3. Proteins

Proteins are complex biological macromolecules made up of chains of amino acids. They are fundamental components of all living organisms and play crucial roles in various biological processes. Proteins are involved in structural support, enzymatic reactions, immune responses, cell signaling, transport of molecules, and many other functions within cells and organisms [81]. Proteins constitute more than half of the dry weight of cells, surpassing all other biomolecules in abundance. They stand out among macromolecules by orchestrating virtually every biochemical reaction within biological systems. However, it's crucial not to overlook the essential roles played by other components of living systems, as they also contribute indispensably to the intricate workings of life [82].

The structure of a protein is hierarchical, with primary, secondary, tertiary, and sometimes quaternary levels of organization. The primary structure refers to the linear sequence of amino acids in the protein chain. Secondary structure involves the folding of the polypeptide chain into alpha-helices, beta-sheets, or other structural motifs stabilized by hydrogen bonds. Tertiary structure is the overall three-dimensional folding of the protein chain, driven by interactions between amino acid side chains and the surrounding environment. Quaternary structure, present in proteins with multiple subunits, refers to the arrangement of these subunits in the protein complex [83].

Proteins are derived from natural sources such as plants, animals, fungi, and microorganisms. They can be obtained through dietary sources or extracted and purified for various applications in research, medicine, biotechnology, and food industry.

I.3.1. Protein's shape and structure

Chemically speaking, proteins represent the pinnacle of structural complexity and functional sophistication among known molecules. This complexity is not surprising considering that each protein's structure and chemistry have been honed over billions of years of evolutionary history. Even experts are often astounded by the remarkable versatility of proteins [84].

The shape of a protein is dictated by its sequence of amino acids and they are synthesized as linear chains of amino acids, forming a polyamide (polypeptide) structure. However, they adopt intricate three-dimensional shapes to fulfill their functions. While there are approximately 300 amino acids found across various animal, plant, and microbial systems, only 20 amino acids (essential amino acids) are encoded by DNA for incorporation into proteins. Additionally, many proteins contain modified amino acids and associated components known as prosthetic groups [81, 84].

Various chemical techniques are employed to isolate and characterize proteins based on criteria such as mass, charge, and three-dimensional structure. Proteomics, an emerging field, focuses on studying the complete spectrum of protein expression within a cell or organism, including alterations in protein expression in response to factors such as growth, hormones, stress, and aging [82]. Every amino acid features a central carbon, known as the α-carbon, to which four distinct groups are connected (**Figure 3**):

A basic amino group (—NH_2).

An acidic carboxyl group (—COOH).

A hydrogen atom (—H).

A unique side chain (—R).

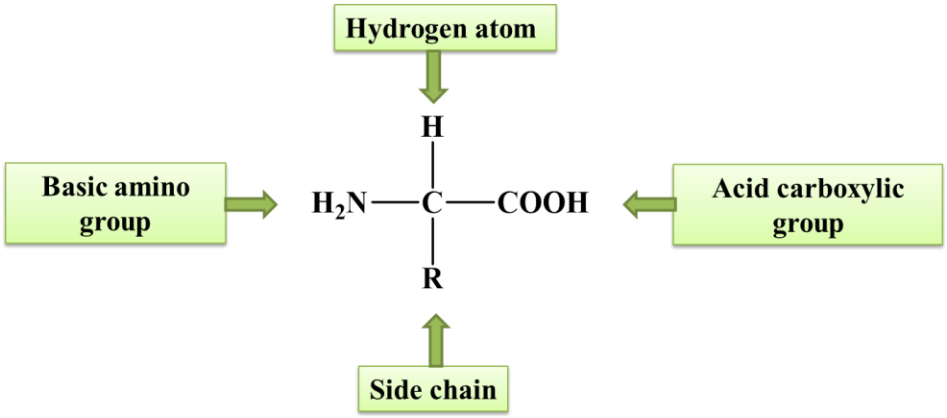

Figure 3. Structure of a protein.

I.4. Hydrogels

Hydrogels are characterized as a distinctive category of cross-linked polymer networks, whether natural or synthetic, with the capability to absorb and retain substantial amounts of aqueous solutions and biological fluids [85, 86]. This water-holding ability stems from the presence of a hydrophilic polymer network, which can be formed through in situ physical or chemical cross-linking methods [85, 86]. Typically, physical networks are established through non-covalent interactions, including hydrogen bonding, ionic interactions (such as electrostatic interactions in polyelectrolyte complexes), metal coordination (for instance, the formation of hydrogels using metal-coordinated ligands), hydrophobic interaction (like the aggregation of hydrophobic segments in proteins), and host-guest interaction (such as cyclodextrin inclusion complexes). Alternatively, ionic cross-linking involves the use of divalent cations, such as calcium ions, to cross-link polymers that contain carboxylic groups as a substituent on the base chain [alginate, gellan, poly (acrylic acid) or its copolymers]. Chemical cross-linking can be achieved through various methods, each offering unique advantages and applications. One common approach is cross-linking polymerization where acrylamide-based monomers undergo radical polymerization to form polyacrylamide hydrogels. Another method employs chemical cross-linking agents like glutaraldehyde or genipin, which react with functional groups on polymer chains to create cross-links. Additionally, hydrogel formation can be facilitated through Michael addition, where thiol-containing polymers react to form cross-linked networks [87]. Enzymatic cross-linking utilizes enzymes such as transglutaminase to cross-link gelatin, resulting in gelatin hydrogels [88]. Metal coordination cross-linking occurs through the formation of

coordination bonds between polymer chains and transition metal ions. Lastly, photochemical cross-linking relies on exposure to UV light to induce the photo-polymerization of acrylate-based monomers, forming cross-linked structures [88]. These diverse methods offer versatility in designing hydrogels with tailored properties to suit various biomedical and industrial applications. Hydrogels can be created by cross-linking either a single water-soluble polysaccharide or a mixture thereof, resulting in a wide array of chemical and physical characteristics. Conversely, hydrogels can also be engineered in various physical formats, including slabs (sheets), microparticles, nanoparticles, coatings, and films [85].

Recently, hydrogels have garnered considerable attention, especially in biomedical and pharmaceutical domains. They have been utilized for controlled drug release, particularly for proteins, and for encapsulating living cells. Moreover, hydrogels find applications in various biomedical contexts such as contact lenses, artificial corneas, wound dressings, and coatings for sutures.

I.4.1. Synthesis of hydrogels

Hydrogels are versatile three-dimensional polymer structures defined by their cross-linking, a fundamental trait influencing their performance. The density of these cross-links profoundly affects hydrogel properties. Achieving this density entails diverse techniques like physical cross-linking, chemical cross-linking, grafting polymerization, and radiation cross-linking. These modifications are pivotal in enhancing hydrogels' viscoelasticity and mechanical traits, rendering them suitable for various biomedical and pharmaceutical applications [85, 89].

I.4.1.1. Chemical cross-linking

Chemically cross-linked hydrogels emerge from the establishment of covalent bonds between the chains of one or multiple polymers. These cross-links are generated through diverse methods like polymerization with multifunctional monomers, exposure to high-energy radiation, chemical reactions involving complementary or pendant groups, or reactions facilitated by cross-linking agents. Enzymes can also serve as cross-linking agents [90, 91]. The **figure 4** illustrates various techniques for synthesizing chemically cross-linked hydrogels.

Polymerization with a multifunctional monomer can be accomplished through step or condensation polymerization, as well as free radical or chain polymerization methods [92]. These

polymerization reactions can occur in solution, bulk, emulsion or suspension. Typically, the polymerization process is initiated by adding a quantity of initiator after mixing the monofunctional and multifunctional monomers [92, 93].

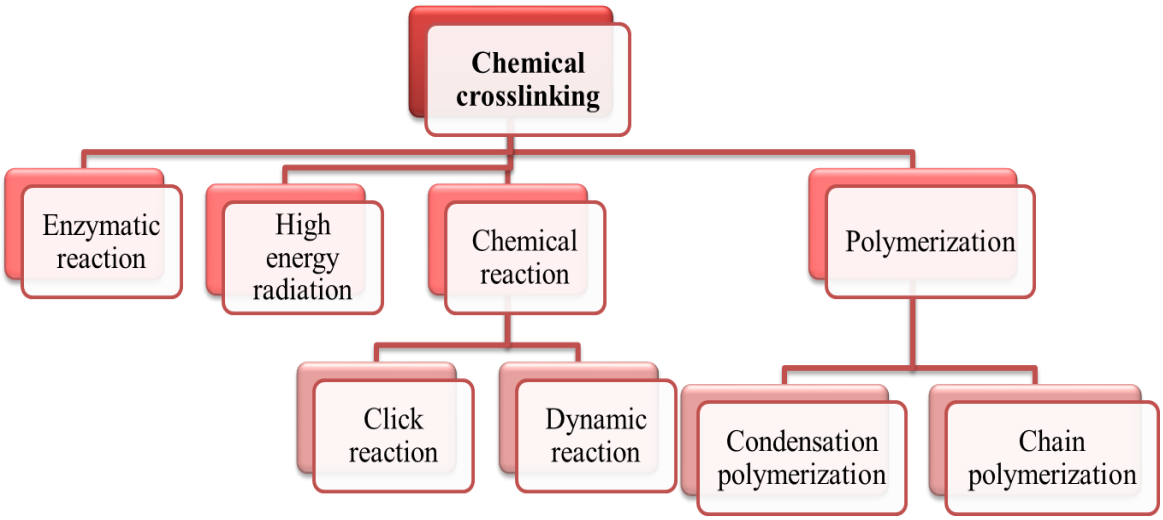

Figure 4. Diagram representing different chemical methods of hydrogels fabrication.

Cross-linking can manifest through various mechanisms, including free radical or oxidizing reactions facilitated by elevated temperatures and the presence of air. Alternatively, UV light or other radiation sources may also induce cross-linking. Another mechanism involves chemical reactions, such as the condensation of an alcohol or an amine with a carboxylic acid. When polymers undergo cross-linking, a three-dimensional network structure emerges as chemical bonds or bridges form between the polymer chains. This process enhances the mechanical properties and stability of the polymer. Cross-links can be established through chemical reactions triggered by factors like heat, pressure, pH changes, or irradiation [93].

Various initiators, including azo compounds, peroxides, and redox initiators, can be employed to initiate polymerization. Chemical initiation offers the advantage of yielding relatively pure, residue-free hydrogels [92].

High-energy electromagnetic irradiation, particularly gamma and electron beams, can be employed to chemically cross-link water-soluble monomers or polymers. This process generates free radicals on polymer chain ends without requiring the addition of a cross-linker [91,92]. Such high-energy irradiation can transform the water-soluble polymers into hydrogels, by vinyl groups

polymerization. Subsequently, the resulting radicals combine to form bonds between polymer backbones, resulting in a polymer network [87, 91, 92].

Moreover, chemically cross-linked hydrogels can be synthesized through click chemistry and dynamic reactions, particularly utilizing cross-linking reactions involving Schiff base formation for water-soluble polymers [86, 91].

Click reactions are regarded as faster, more versatile, regiospecific, and efficient compared to Schiff base reactions, as they typically generate no byproducts [91, 94]. Hydrogels can be produced using click reactions (**Figure 5**), which encompass azide-alkyne cycloadditions, Diels-Alder, thiol-ene, and oxime reactions [91]. In the case of cross-linking via Schiff base formation, polymers must possess functional groups like alcohol, amine, or hydrazide, which can react with aldehydes to form the polymer cross-linking network [92].

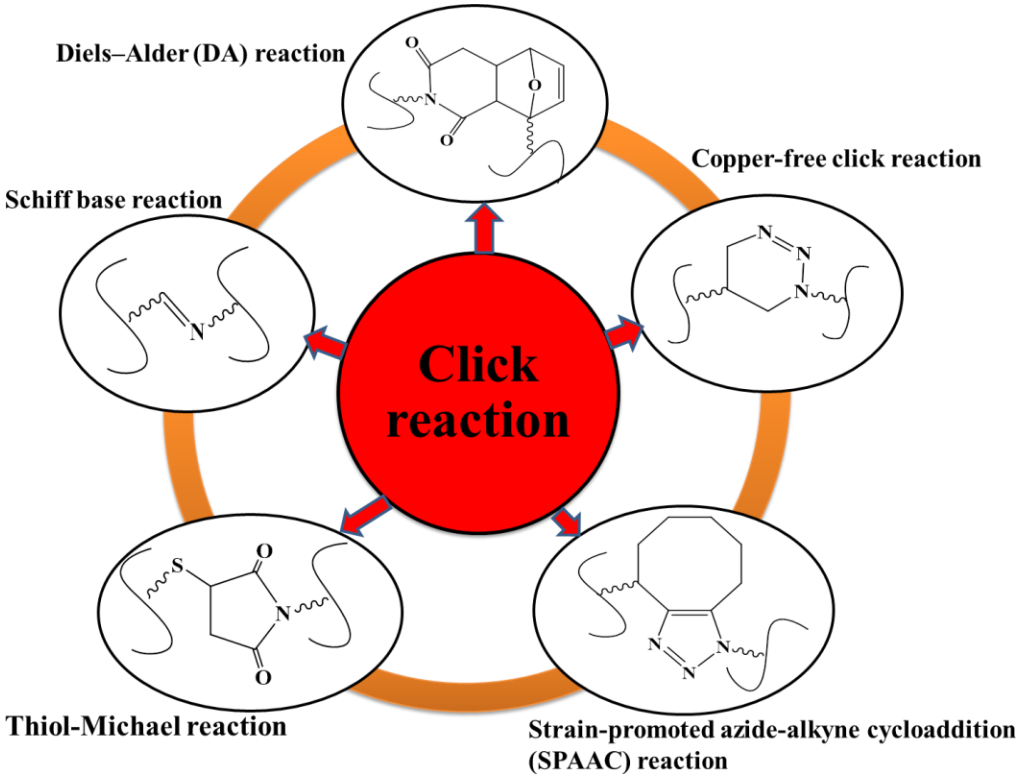

Figure 5. Click chemistry reactions employed to cross-link hydrogels.

Another mechanism involves the use of enzymes as cross-linking agents, which is considered an appealing option due to the specificity of enzymes and the mild reaction conditions required. Cross-linking via enzymes occurs in two primary ways: either through direct enzymatic catalysis of cross-link formation, as illustrated in **Figure 6**, or indirectly through enzymatic

production of a cross-linking agent such as H_2O_2. This agent is capable of oxidizing reactive structures, leading to subsequent cross-link formation [95, 96]. Jus et al. [97] examined enzymatic protein cross-linking as a greener alternative to conventional methods involving toxic chemicals. Their study investigated the utilization of tyrosinases from various sources and laccases for cross- linking gelatin and gelatin hydrolysates. Through spectroscopic analyses and oxygen consumption measurements, enzymatic oxidation of tyrosine residues was confirmed. Chromatographic techniques revealed the dimerization of a model substrate. Enzymatic cross-linking led to a significant increase in molecular weight, resulting in material precipitation. Moreover, the presence of phenolic molecules augmented the cross-linking effect. This research underscores the potential of enzymatic approaches for protein cross-linking, presenting a safer and more environmentally friendly alternative to traditional chemical methods [97]. In another investigation, Rossi et al. [96] examined the efficacy of whey protein/pectin edible films, supplemented with trans glutaminase, as water barrier coatings for fried and baked foods. They applied these hydro colloidal films to doughnuts, french fries, and taralli biscuits to evaluate their impact on moisture loss, oil absorption, and texture properties. The findings revealed notable reductions in moisture loss and oil content in coated fried foods compared to uncoated counterparts. Sensory evaluation tests indicated no discernible texture differences between coated and uncoated products. Furthermore, the edible films effectively prevented moisture absorption by taralli biscuits during storage, thereby preserving their desired texture. Overall, the study underscores the potential of whey protein/pectin edible films in enhancing the quality and shelf life of fried and baked foods [96]. Additionally, Battisti and al. [98] introduced an innovative packaging strategy involving the application of biopolymeric solutions onto raw paper sheets. These solutions comprised gelatin cross-linked with trans glutaminase enzyme, along with glycerol and citric acid. Although there was no improvement in mechanical properties, the coating exhibited effective film formation, as confirmed by various analyses. Notably, it significantly reduced water vapor permeability while maintaining the original optical properties of the paper. When employed for beef packaging, the coated papers demonstrated several advantages: decreased microbial populations after storage, enhanced stability against lipid oxidation, preserved red color, and lower pH values compared to uncoated paper. Moreover, they effectively prevented moisture loss from the beef, highlighting their promising role in food preservation and quality maintenance [98]

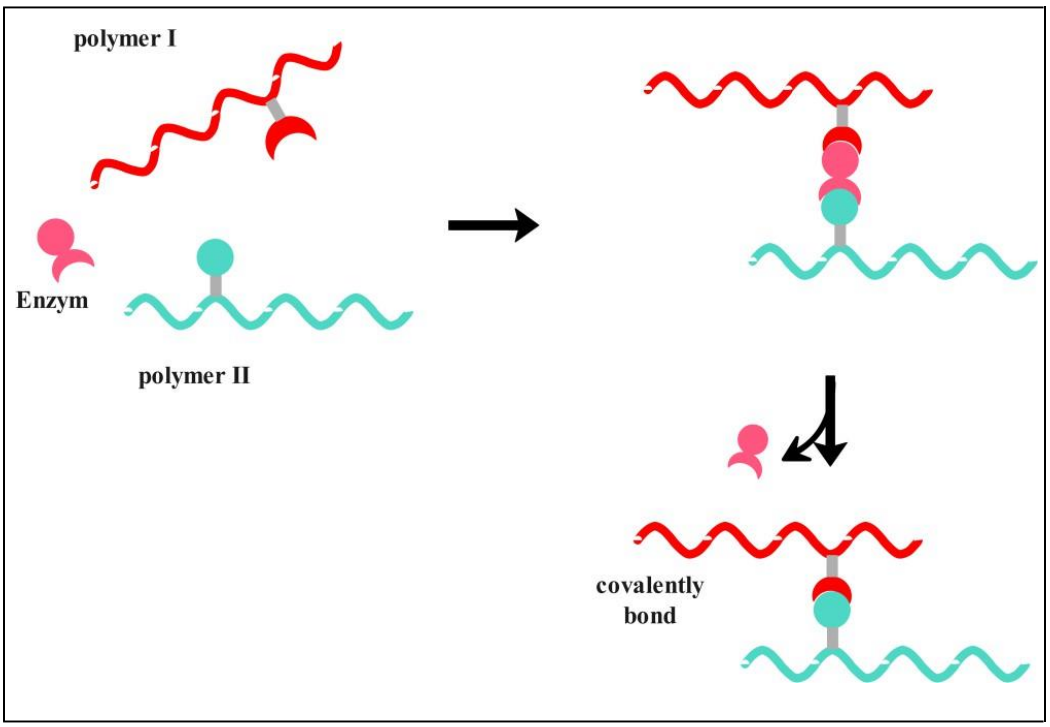

Figure 6. Schematic of enzymatic cross-linking as catalyst that assemblies two functional groups of different polymer chains. Adapted from [99].

I.4.1.2. Physical cross-linking

Physical hydrogels have recently garnered considerable interest in pharmaceutical, biomedical, and food applications, primarily due to their relatively straightforward fabrication protocol, which eliminates the need for cross-linking agents [85, 100]. These hydrogels typically feature a reversible structure characterized by continuous, dynamic, non-covalent bonds. The formation of physical hydrogels relies on intra- or intermolecular bonds that are reversible, and their association-dissociation dynamics are governed by the physical and chemical properties of the material, such as pH, temperature, ionic strength, and so forth. In contrast to chemical hydrogels, physical hydrogels feature cross-links composed of lower-energy non-covalent bonds [54, 56]. These bonds result in physical hydrogels having lower mechanical properties compared to those formed by chemical bonds [101, 102]. Various methods have been explored to synthesize physical hydrogels, including the formation of intra- and intermolecular bonds such as hydrogen bonds, hydrophobic association, and van der Waals interactions, as well as ionic cross-linking, stereo- complexation, and electrostatic interactions. Physical hydrogels derived from proteins can be created by altering the pH or subjecting the protein to temperatures exceeding its denaturation point [101].

Physical hydrogels formed by ionic cross-linking are three-dimensional polymeric networks that are cross-linked through ion interactions under mild conditions, typically at room temperature and physiological pH [86, 103, 104]. This type of cross-linking can occur through interactions between certain di- or multivalent metal ions, such as Ca^{2+}, Fe^{3+}, Cu^{2+}, Zn^{2+}, and functional groups present in the polymer, such as carboxylic groups. These interactions give rise to ionically cross-linked hydrogels [101, 104, 105], as examples the alginate hydrogels [90, 91, 105, 106].

Physically cross-linked hydrogels can be generated through the formation of hydrogen bonds, where a hydrogen atom is bonded with an atom possessing higher electronegativity, such as oxygen, nitrogen, or fluorine. In this scenario, the hydrogen atom acquires a partial positive charge, while the electronegative atom bears a partial negative charge, facilitating electrostatic interactions between them [101, 106]. Hydrogen bonds serve as physical cross-links, whether inter- or intramolecular, during hydrogel formation]. Particularly in natural polymer-based hydrogels, hydrogen bonding stands out as the primary interaction type due to the presence of numerous functional groups in their chains, including hydroxyl, amino, and carboxylic acid groups [102].

Stereo-complexation hydrogels arise from the cooperative interaction between polymer chains or molecules featuring identical chemical composition but opposite stereochemical configurations [102]. A prominent instance of such hydrogels involves polylactide copolymers. Polylactide is a biodegradable polymer sourced from renewable materials, frequently utilized in diverse biomedical and pharmaceutical contexts due to its biocompatibility and adjustable characteristics. By combining poly (l-lactide) and poly (d-lactide), both possessing differing stereoisomeric arrangements, stereo-complexation hydrogels are formed [107, 108]. One notable advantage of these hydrogels lies in their straightforward preparation, achievable by simply mixing copolymers dissolved in an aqueous solution [102].

Physical hydrogels can also be generated by exploiting electrostatic interactions between oppositely charged polyelectrolytes under appropriate conditions, eliminating the necessity for chemical cross-linkers [107, 108]. When polyanions with negative charges and polycations with positive charges are mixed to form polyelectrolyte complexes, robust and swift interaction processes occur, leading to phase separation within the solution [109]. Hydrogels offer numerous advantages, including the absence of harmful chemical cross-linkers, the rapid and

straightforward reaction under mild conditions, and the amalgamation of desired properties from two or more components [110].

Physical hydrogels formed via hydrophobic association typically result from the aggregation and association of hydrophobic groups within amphiphilic polymers, achieved through two main methods: copolymerization and crystallization (**Figure 7**).

Copolymerization of vinyl monomers with hydrophobic monomers, or the introduction of a reduced quantity of hydrophobic groups through a chemical reaction it also leads to physical hydrogels by the association of hydrophobic sequences [110]. Within an aqueous medium, these hydrophobic groups undergo association and aggregation driven by entropy, ultimately giving rise to a three-dimensional framework.

Crystallization, a method relying on the renaturation of gelatin or polysaccharides into their respective triple helical or double helical conformations during the reversible formation of sol-gel hydrogels. This process induces nucleation and growth of crystallites [110, 111]. As the helices aggregate, they form junction points influenced by temperature. At high temperatures, the helices adopt a random coil shape. As the temperature decreases, they transition to double helices and aggregate, acting as nodes that form the physical junctions (cross-linking points) of the hydrogels [111].

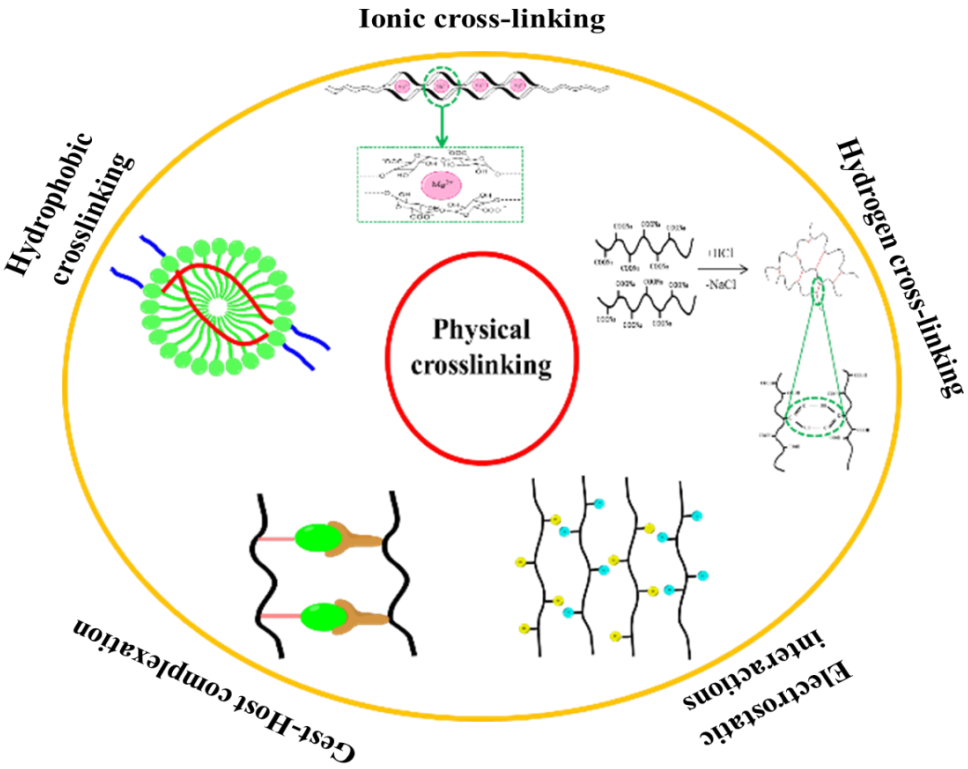

Figure 7. Different physical methods of hydrogels fabrication.

I.5. Cross-linking proteins with carbonyl derivatives of polysaccharides

I.5.1. Schiff Base Linkages

Schiff base derivatives, initially discovered in 1864 by the German chemist and Nobel laureate Hugo Schiff, represent a category of compounds formed through the reaction between amino and carbonyl groups or benzoic aldehydes, essentially belonging to the imines subclass. This reaction yields a double bond between a carbon and nitrogen atom, constituting an imine or azomethine functional group (–C=N–) [112]. Notably, Schiff base formation can occur under mild conditions, yielding water as the sole byproduct [113]. These linkages facilitate the creation of imines, hydrazones, and oximes cross-links, finding diverse applications across pharmaceuticals, biology, inorganic chemistry, and medicine. Scientists have also explored novel heterocyclic/aryl Schiff bases for developing environmentally friendly technologies, leveraging their simplicity, versatility, non-toxicity of reagents and products, and reversibility [113,115].

Hydrogels are synthesized via Schiff base cross-linking, a process involving the reaction of aldehyde/ketone groups with amines, hydrazides, and aminooxy groups present in biopolymers, leading to the formation of imines, hydrazones, and oximes cross-links, respectively. These cross-links serve as the bridges within the hydrogels [16]. Notably, hydrazones and oximes cross-links exhibit greater stability compared to imine linkages, which are condensation products of aldehyde/ketone groups with α-effect nucleophiles containing amino groups adjacent to nitrogen and oxygen atoms, respectively [16, 114, 116]. According the **Figure 8**, benzoic Schiff base hydrogels are created by linking amines, hydrazides, and aminooxy groups with benzaldehyde groups, yielding benzoic imines, benzoic hydrazides, and benzoic oximes, respectively, thereby enhancing the carbon-nitrogen double bond (–C=N–) [16, 117]. To prepare hydrogels utilizing imine, hydrazone, or oxime cross-linking, polymers need to be functionalized by incorporating aldehyde or nucleophilic groups. While primary amino groups are commonly present in many native polymers, chemical modification is essential to introduce carbonyl groups in the other reactant [113]. Two primary methods exist for functionalizing polysaccharides: oxidation of vicinal hydroxyl groups in various polysaccharides using sodium metaperiodate, or utilization of molecules containing aldehyde groups via carbodiimide chemistry [16].

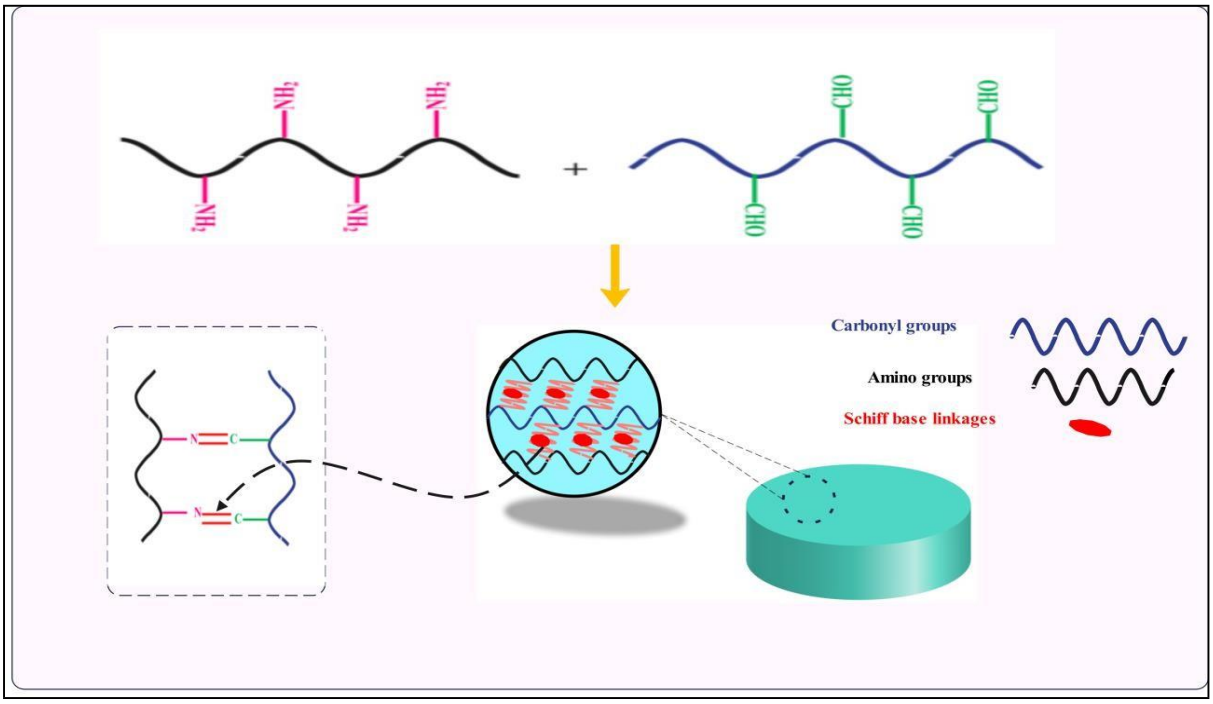

Figure 8. Representative diagram of the formation of Schiff base hydrogels[116].

I.5.2. Imine bonds based hydrogels

The imine bond constitutes a reversible dynamic covalent bond, initiated by the nucleophilic attack of amine derivatives on carbonyl groups (aldehyde/ketone) under physiological conditions [118, 119]. This reaction, termed the imine reaction, entails the elimination of water molecules upon the formation of the C=N bond either intra- or inter-molecularly through the reaction of two molecules containing amino and carbonyl groups (**Figure 9**).

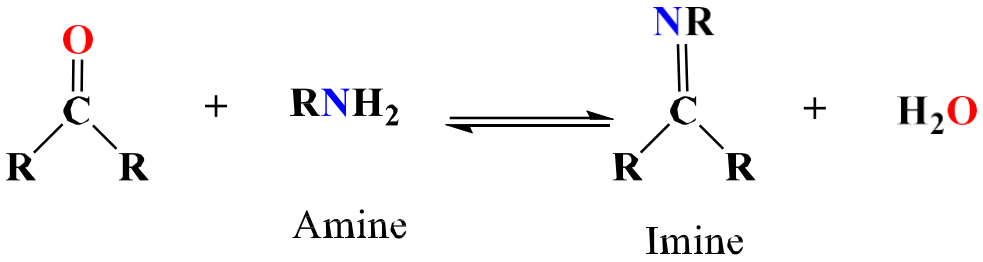

Figure 9 : Reaction between molecules containing amino and carbonyl groups.

The reaction rate can be accelerated by acid catalysis [118, 120]. The imine bond is reversible, allowing the reaction to proceed in both directions. In the forward direction, water molecules are eliminated either physically, using the Dean-Stark apparatus under azeotropic conditions, or chemically, by introducing a drying agent such as molecular sieves or $MgSO_4$ into the reaction mixture. This typically involves refluxing a mixture of compounds containing carbonyl and amine functional groups [118, 120, 121]. In the reverse direction, the addition of water to an imine can induce hydrolysis, reverting the condensation reaction to produce the initial reactants. This reversible process reaches thermodynamic equilibrium upon reheating [118, 120, 122, 123]. The imine bond finds extensive utility across various fields due to its several advantages. Firstly, it's a reversible bond, conveniently synthesized from amine and aldehyde groups. Secondly, imine compounds exhibit low toxicity levels. Furthermore, aromatic aldehydes can undergo condensation with amines to yield imines, a process offering notable advantages in organic synthesis. Aromatic imines, commonly known as Schiff bases, formed through these reactions, possess enhanced stability due to resonance stabilization within the aromatic ring, thus resisting hydrolysis under mild conditions. The region selectivity inherent to aromatic aldehydes ensures the generation of a single desired product, minimizing the formation of unwanted

byproducts. Additionally, imines exhibit sensitivity to environmental factors such as pH, concentration, and temperature, providing significant advantages in organic synthesis. This sensitivity enables precise control over reaction conditions, facilitating the fine-tuning of reactivity and selectivity. Through the adjustment of these parameters, chemists can optimize reaction rates and product yields while minimizing the formation of undesired [122].

Hydrogels for diverse applications have been extensively engineered utilizing imine bonds, primarily owing to their reversible association and dissociation behavior, which occurs without intermediates [16, 96].

Recent investigations have focused on hydrogels incorporating imine bonds. These studies often involve modifying the structural units of polysaccharides with sodium periodate to introduce aldehyde groups. The resulting oxidized polysaccharides are then utilized to create imine bond-based hydrogels, often in conjunction with cationic polysaccharides or proteins. Additionally, various biopolymers containing primary amine groups, such as gelatin and chitosan, can serve as precursors for imine cross-linking [16, 124]. For instance, Ding et al. [124], synthesized a hydrogel using two biopolymers, acrylamide-modified chitosan, and oxidized alginate, employing covalent cross-linking to establish imine bonds.They observed that the mechanical properties and self-healing capabilities of the hydrogels were impacted by both the duration of cross-linking and the pH environment. Furthermore, they anticipated that these hydrogels held promise for the advancement of self-healing materials and could be applied across a broad spectrum of biomedical fields [124].

Furthermore, Ma et al. [125] developed an injectable hydrogel by blending oxidized alginate hybrid nanoparticles with hydroxyapatite and carboxymethyl chitosan through imine formation. These hydrogels demonstrated self-healing properties, with rheological testing revealing an increase in storage modulus corresponding to higher concentrations of oxidized alginate or longer oxidation times. These findings suggest promising applications for the hydrogels in bone tissue engineering [125]. Lei et al. [126], devised a self-healing hydrogel by leveraging imine bond formation between gelatin and dialdehyde carboxymethyl cellulose. Initially, gelatin was reacted with ethylenediamine to enhance the amino group content, subsequently cross-linked with dialdehyde groups present within the carboxymethyl cellulose backbone. The outcomes revealed that these hydrogels displayed commendable self-healing ability, fatigue resistance, and self- recovery capacity, attributed to the presence of imine bonds [126]

I.5.3. Hydrazone and acyl hydrazone bonds-based hydrogels

Hydrazone or acylhydrazone bonds represent common reversible reactions, arising from the condensation of hydrazines and hydrazides, respectively, with carbonyl groups (typically ketones or aldehydes), elimination of water as shown in the **Figure 10** [128, 129].

a)

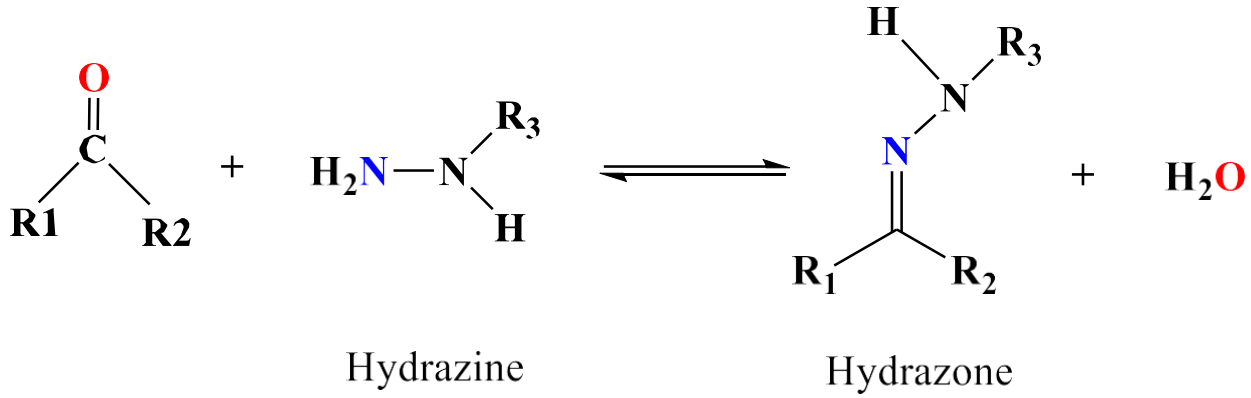

b)

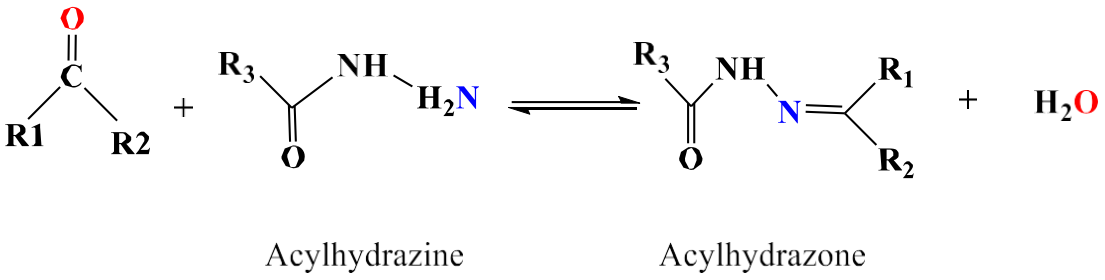

Figure 10. Schiff base : a) hydrazone linkages; b) acylhydrazone linkages.

The hydrazone bond is distinguished by its swift formation and reversibility under specific conditions, alongside its heightened stability in comparison to the imine bond. Introducing an acyl group into the hydrazide side transforms the hydrazone bond into an acyl hydrazone bond, albeit at a slower rate than the hydrazone bond [114, 116, 130]. Hydrazone or acyl hydrazone reactions mirror those of imine bonds, being reversible and capable of changing direction through hydrolysis. Under acidic conditions, the rate of formation or hydrolysis accelerates significantly, facilitating rapid bond exchange [129, 131].

Hydrazone and acyl hydrazone bonds have garnered significant attention for crafting biopolymer hydrogels across various applications, owing to their distinctive properties [121]. These hydrogels are formed through hydrazone and acyl hydrazone cross-linking, achieved by blending oxidized polysaccharides with hydrazides or acyl hydrazides. Typically, the functionalization of hydrazides involves carbodiimide chemistry, facilitating the reaction between the free carboxylic acid groups present in the biopolymer backbone and dihydrazide-containing components like adipicdihydrazide (ADA) and carbodihydrazide (CDH) [16, 124]. Researchers have investigated hydrogels utilizing hydrazone/acyl hydrazone cross-links due to their notable properties such as injectability, shear-thinning behavior, and self-healing capabilities [132, 133]. Wei and al. [132] introduced a novel biocompatible self-healing hydrogel by leveraging the dynamic interaction between carboxyethyl chitosan functionalized with adipic acid dihydrazide (ADH) and oxidized sodium alginate. They demonstrated that these hydrogels exhibited exceptional self-healing abilities without requiring external stimuli, likely attributed to the dynamic nature of imine and acyl hydrazone bonds within the hydrogel networks. Additionally, the hydrogels demonstrated favorable cytocompatibility and cell release characteristics [132]. In a separate study, Lehmann-horn et al. [133], demonstrated that oxidized hyaluronic acid (HA-ALD) could be paired with hyaluronic acid functionalized with adipic-dihydrazide (HA-ADH) to produce a self-healing and shear-thinning hydrogel suitable for bioprinting applications. Additionally, the incorporation of thiol-ene cross-linkable groups into the resulting hydrogel networks enhanced the mechanical properties of the films [133]. Yang and colleagues [134], developed a range of cellulose-based self-healing hydrogels, constructed via dynamic covalent acylhydrazone linkages. These synthesized hydrogels exhibit outstanding mechanical properties and self-healing capabilities, achieving a healing efficiency exceeding 96%. Moreover, the hydrogels demonstrate dual-responsive sol-gel transition behaviors triggered by pH and redox stimuli, suggesting potential for controlled release applications, particularly in the context of doxorubicin delivery [134].

I.5.4. Oxime bonds-based hydrogels

The oxime bond represents a reversible reaction within dynamic covalent chemistry. It forms through the condensation reaction between an aldehyde or ketone group and a

hydroxylamine functional group under mild conditions, with water being the sole byproduct (**Figure 11**) [114, 136, 137].

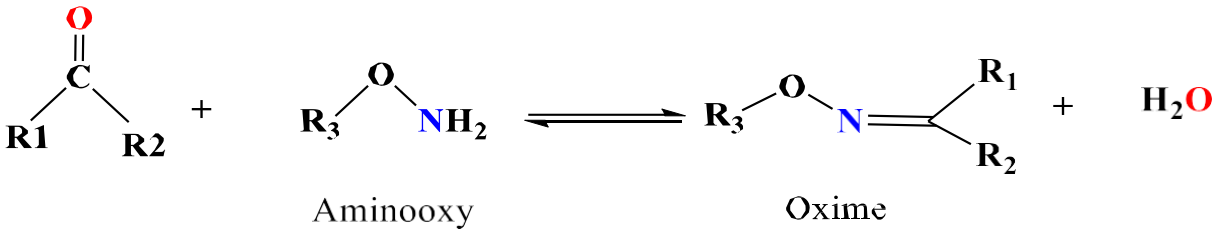

Figure 11. Schematic illustration of Schiff base oxime linkages.

As previously noted, while oxime formation displays some reversibility, this reaction provides improved hydrolytic stability compared to imine and hydrazone bonds, which poses a constraint in developing dynamic covalent bulk materials [129,130]. Furthermore, the oxime reaction offers several advantageous features, including high efficiency, chemoselectivity, formation in aqueous solvents, and non-toxicity, with water being the sole byproduct [136]. Additionally, acidic conditions catalyze oxime formation through electron transfer from adjacent oxygen [129, 138]. Due to the electron-donating resonance effect of the oxygen atom, oximes and oxime ethers exhibit lower reactivity towards nucleophilic attack compared to imines, as the sp^2 carbon atom of the oxime is less electrophilic than that of the corresponding imines [138]. Oxime bonds, with their distinctive properties, have found widespread application across various domains, including cell surface modification, hydrogel fabrication, scaffold preparation, conjugation, and biological molecule labeling [135]. In recent times, oxime cross-linking has emerged as a promising technique for bioconjugation, particularly in the creation of covalently-cross-linked hydrogels. By combining aminooxy-functionalized biopolymers with aldehyde-functionalized biopolymers, oxime-based hydrogels can be synthesized [114, 131]. Mukherjee and al. [139] introduced a self-healing hydrogel functionalized with oxime groups, capable of reversible gel-to-sol transition in acidic conditions through controlled oxime exchange. They employed conventional polymerization of *N*, *N*-dimethyl acrylamide (DMA) and diacetone acrylamide (DAA) to prepare keto-functional copolymers, which were subsequently chemically cross-linked with difunctionalalkoxyamines to form hydrogels via oxime bond formation. The researchers demonstrated that the reversible nature of oxime cross-links endowed the hydrogels with autonomous healing capabilities [139]. In another study, Lin and al. [135] synthesized

hydrogels based on poly(ethylene glycol) (PEG) utilizing oxime bonds as cross-links. They achieved this by combining dialdehyde-functionalized PEG (PEG-bCHO) with a 4-arm aminooxy cross-linker molecule. The properties of the hydrogel were found to be influenced by pH and the presence or absence of an aniline catalyst. Additionally, azide-functionalized oxime hydrogels were generated using copper (I)-catalyzed alkyne-azidecycloaddition (CuAAC) and metal-free strain-promoted alkyne-azidecycloadditions (SPAAC). This allowed for the incorporation of RGD peptides into the hydrogel post-gelation, confirming the availability of azide groups for subsequent reactions [135].

In alkene-derived oxime hydrogels, the investigation into 3D photo peptide patterning via thiol-ene chemistry has garnered attention. Payam et al. and Cole and al. [141, 142] have demonstrated a synthetic approach for hydrogel preparation utilizing a photolabile protecting group, 2-(2-nitrophenyl) propyloxycarbonyl (NPPOC), as a direct photocage for releasing aminooxy groups. Upon exposure to UV radiation, the aminooxy groups are liberated from the NPPOC photocages, subsequently interacting with aldehydes derived from poly (ethylene glycol) (PEG) end-functionalized with benzaldehyde to form oxime linkages. This enables control over the location and degree of cross-linking via photo-mediated oxime connections, facilitating systematic adjustment of mechanical properties. Moreover, the use of photo-mediated oxime linkages enables the immobilization of various biomolecules with spatiotemporal control and micron-scale resolution [141, 142].

The cross-linking of hydrogels via Schiff base linkages stands as a crucial element in the advancement of versatile and functional materials with promising applications spanning multiple domains. These hydrogels can be efficiently cross-linked through various methods, primarily utilizing imine, hydrazone, acylhydrazone, and oxime linkage formation. The flexibility offered by these cross-linking strategies enables precise control over the properties of the hydrogels, making them adaptable for a wide range of applications.

While Schiff-based hydrogels hold considerable promise for various applications, they encounter challenges related to long-term stability and biodegradability. Researchers are actively striving to tackle these issues, seeking to improve the overall performance of these hydrogels. In summary, Schiff base hydrogels and their cross-linking methods offer significant potential for the development of advanced materials. Nonetheless, ongoing research is indispensable to optimize the properties of hydrogels and surmount potential limitations.

I.6. Conclusion

In conclusion, the modification of polysaccharides through oxidation represents a versatile approach for introducing carbonyl groups, thereby facilitating their cross-linking with proteins or other polymers bearing amino groups, to fabricate hydrogels. Polysaccharides, owing to their abundance, biocompatibility, and tunable properties, serve as excellent candidates for hydrogel synthesis. The introduction of carbonyl groups using periodate oxidation or enzymatic oxidation enhances the reactivity of polysaccharides, enabling efficient cross-linking with proteins.

The formation of Schiff base linkages between the carbonyl groups in oxidized polysaccharides and proteins plays a pivotal role in hydrogel fabrication. This cross-linking mechanism offers several advantages, including simplicity, reversibility, and biocompatibility. By adjusting the oxidation conditions and protein composition, the properties of the resulting hydrogels, such as mechanical strength, swelling behavior, and degradation rate, can be tailored to suit specific applications.

Generally, polysaccharides modified by oxidation for the introduction of carbonyl groups provide a promising platform for the development of hydrogels with diverse applications in tissue engineering, drug delivery, and biomedical devices. Further research efforts aimed at optimizing the oxidation process, elucidating the cross-linking mechanisms, and exploring novel polysaccharide-protein combinations will continue to advance the field of hydrogel technology.

CHAPTER II:
Classification of Hydrogels and Their Different Biomedical Applications

Chapter II: Classification of hydrogels and their different biomedical applications

II.1. Introduction

This chapter presents the classification of hydrogels and their biomedical applications cross-linked with carbonyl derivatives of polysaccharides sequenced as follows: - Biomedical applications of film Schiff base hydrogels; - Biomedical applications of microparticles hydrogels; - Biomedical applications of nanoparticles hydrogels (nanogels).

II.2. Classification of hydrogels

Hydrogels are pivotal in material engineering, showcasing distinctive and diverse applications (**Figure 13**). Among them, Schiff-base cross-linked hydrogels have garnered considerable interest in biomedicine due to their biocompatibility, autonomous structural integrity, tissue affinity, porous architecture, adjustable characteristics, and potential for precise drug release [121]. These hydrogels form through polymeric chain cross-linking via condensation reactions involving carbonyl and amino groups, leading to Schiff bases (imine) bond formation. This resulting structure offers an ideal milieu for an array of biomedical uses, spanning from tissue engineering to drug delivery, wound mending, shape adaptation, and self-repair mechanisms. Their primary strength lies in their dynamic nature and capacity to conform to evolving conditions, rendering them exceedingly adaptable and sought-after materials across various biomedical domains.

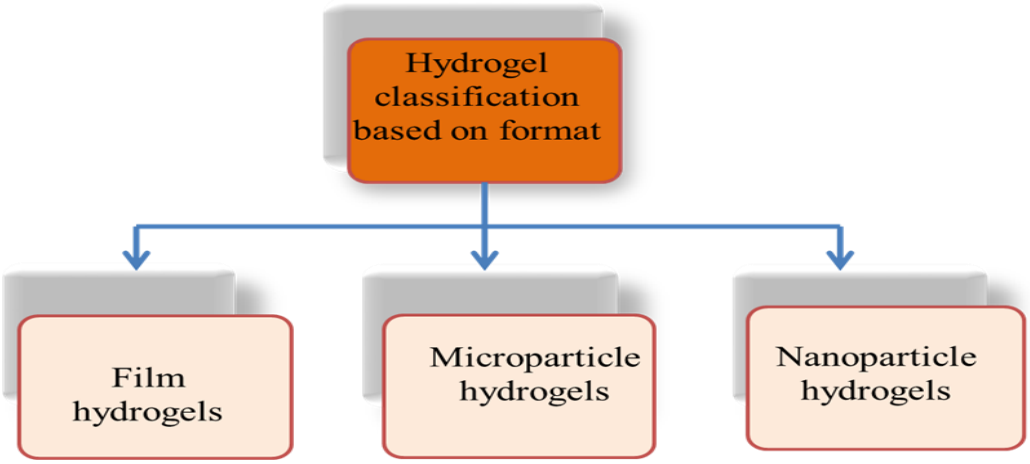

Figure 12. Hydrogels types discussed different classifications of hydrogels based on their format.

From the **Figure 12**, hydrogels synthesized through Schiff base cross-linking. Depending on the intended application, these hydrogels can be tailored into various formats, including films, membranes, rods, particles, and emulsions, utilizing different methodologies [142].

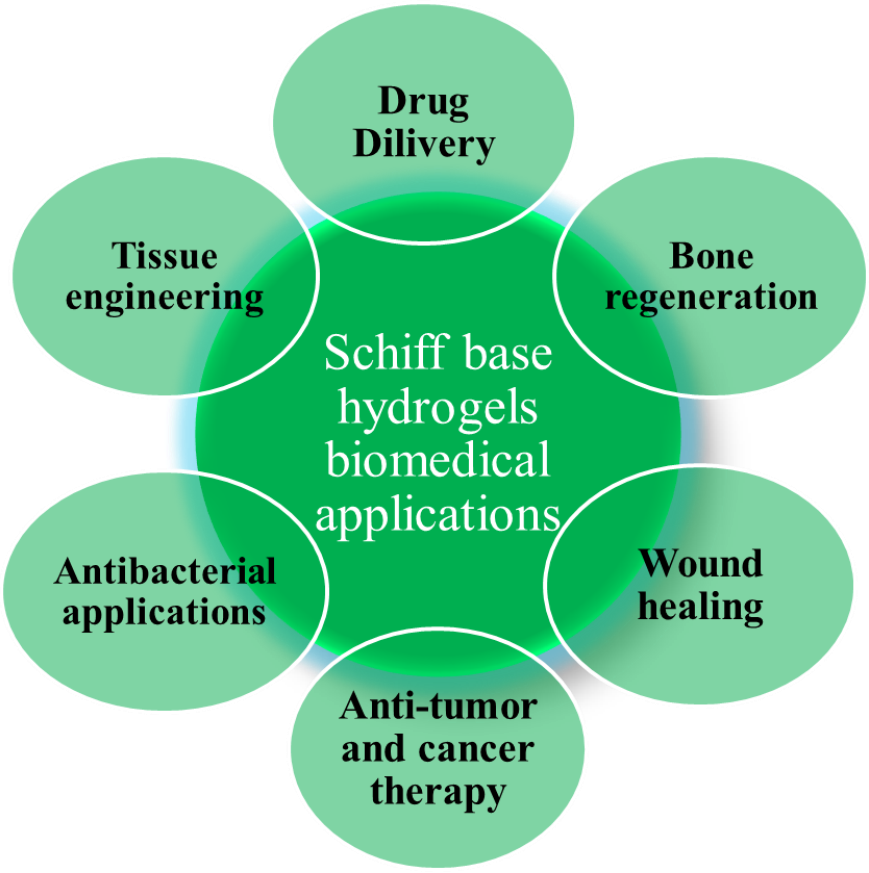

Figure.13. Different biomedical applications of cross-linked hydrogels formed by Schiff base reaction.

II.3. Hydrogels films

Hydrogels, renowned for their hydrophilic and pliable nature, retain water and mimic the extracellular matrix through their intricately cross-linked 3D structure. They boast features like significant swelling, remarkable biocompatibility, and notable adaptability in shape [143]. Recently, there's been progress in crafting hydrogel films, or membranes, with precise thickness. These films are constructed from interconnected networks of either natural polymers (such as chitosan, gelatin, carrageenan, and alginate) or synthetic polymers (including poly(vinyl alcohol), poly(acrylic acid), polyacrylamide, and poly(N-isopropyl acrylamide), among others). These films inherit both the chemical and physical traits of bulk hydrogels and exhibit rapid responsiveness and outstanding flexibility. Such characteristics render them compatible with

biological systems and sensitive to external stimuli, thus paving the way for innovative functionalities [145, 146].

In their study, Ding and al. [146], introduce a novel biofilm derived from natural polymers with Schiff base formation. This self-healable polymeric hydrogel is formed by self-crosslinking acrylamide-modified chitin (AMC) and oxidized alginate. Utilizing dynamic covalent linkages, the hydrogel achieves self-healing capabilities through Schiff base bonds between polysaccharide chains. The hydrogel's ability to self-heal is contingent upon the ratio of AMC to oxidized alginate and the surrounding pH. Notably, it exhibits complete recovery post-damage and exceptional stretchability, a unique trait in polysaccharide-based hydrogels. Furthermore, its self-healing property can be preserved through freeze-drying and reactivated upon rehydration. Moreover, the hydrogel acts as a scaffold for directing the repair of inorganic materials like hydroxyapatite. With its biocompatible and biodegradable composition, this self-healable hydrogel shows promise for a wide array of biomedical applications [146]. Additionally, Higueras et al. [147], introduce an innovative approach wherein cinnamaldehyde is tethered to chitosan films via imino-covalent bonding, providing a reversible attachment mechanism. Employing solid-phase synthesis, chitosan films are immersed in an acidified ethanolic solution containing the aldehyde, resulting in a high substitution degree nearing 70 %. The formation of the chitosan-cinnamaldehyde Schiff base is confirmed through ATR-FTIR spectroscopy. Examination of hydrolysis and cinnamaldehyde release under simulated food preservation conditions yields insights into film stability and kinetics. Evaluation of antimicrobial properties against diverse bacteria, including Listeria monocytogenes, demonstrates efficacy influenced by treatment conditions and bond hydrolysis levels. Notably, the films impede L. monocytogenes growth for an extended period under refrigeration, potentially augmenting food shelf life. Sensory analysis reveals consumer acceptance of the cinnamon aroma, opening avenues for applications in antimicrobial food packaging and beyond, especially where sustained-release systems are imperative [147]. Hydrogel films constructed from natural polymers with Schiff base formation present a versatile platform boasting diverse applications, accompanied by unique advantages and considerations. Stemming from biocompatible sources, these films hold significant promise in biomedical realms like wound care, targeted drug delivery, and tissue regeneration. Their eco-friendly derivation from renewable materials aligns with sustainability objectives. Adjustable properties, achievable through tailored compositions, enable customized

performance tailored to specific application demands. The inherent self-healing capabilities imparted by Schiff base formation bolster durability, yet challenges persist, including inherent mechanical limitations and questions surrounding biodegradability. Processing intricacies, such as gelation kinetics and film uniformity, pose hurdles that can impact scalability and reproducibility. While the potential is undeniable, a judicious evaluation of both strengths and limitations is imperative to maximize their efficacy across a spectrum of applications.

In exploring biofilms based on natural polymers with Schiff base formation, Wang and al. [148] investigated the development of a semi-interpenetrating polymeric network using chitosan and poly (vinyl alcohol) (PVA), cross-linked with glutaraldehyde. The study meticulously characterized the molecular weight and degree of deacetylation of chitosan, delving into the chemical bonds formed during the cross-linking reaction and their response to varying pH conditions. Examination of the gelation properties of the chitosan-PVA pregel solution and the resultant hydrogel's mechanical attributes yielded significant insights. FTIR spectra analysis unveiled the formation of Schiff's base (C=N) and its pH-dependent transition, underscoring chitosan's pivotal role in hydrogel formation via Schiff's base reaction with glutaraldehyde. Furthermore, the study observed an augmentation in mechanical properties with PVA incorporation but noted PVA leaching during prolonged swelling periods in acidic environments due to the hydrolysis of gel networks, particularly Schiff's base bonds. This research contributes substantially to the comprehension and optimization of chitosan-PVA hydrogels for a myriad of applications [148]. Moreover, Zhumadilova et al. [149], synthesized innovative copolymers comprising acrylic acid and Schiff base, featuring amine groups in the main chain and carboxylic groups in the side chain. These copolymers exhibited poly(ampholyte-electrolyte) behavior and formed complexes with anionic, cationic, and non-ionic polymers. The study delved into how external factors such as solvent quality, temperature, pH, and ionic strength influenced the phase and volume transitions of these complexes. This research yields valuable insights into the behavior and interactions of these copolymers and their complexes across diverse conditions, presenting potential applications across various fields [149]. These films are highly adaptable, allowing for precise tailoring to meet specific requirements like mechanical strength, swelling behavior, and responsiveness to stimuli. This versatility enables a wide range of applications spanning from biomedical needs such as drug delivery and tissue engineering to industrial and environmental uses like sensors and wastewater treatment. Moreover, their synthetic composition

ensures consistent quality and reproducibility, making them well-suited for diverse fields. However, it's important to consider potential issues such as cytotoxicity and limited biodegradability associated with certain synthetic polymers, underscoring the necessity for thorough evaluation and optimization tailored to individual applications.

Creating biomaterial structures via hydrogel film preparation has emerged as a popular and straightforward method. This approach facilitates the transformation of a diverse array of natural and synthetic polymers into cross-linked hydrogel films suitable for applications in tissue engineering, controlled drug release, and various medical contexts [151, 152].

The fabrication of hydrogel films from biopolymers via cross-linking reactions involving Schiff base linkages is garnering significant attention. This method holds promise for diverse applications, leveraging the combined benefits of biocompatibility, controlled hydrogel properties, and the unique characteristics imparted by the Schiff base reaction.

II.4. Hydrogel Particles

Schiff base hydrogel particles, whether micro or nano-sized, are spherical structures derived from either synthetic or natural polymers, and can be tailored in various sizes and shapes using techniques compatible with encapsulating biological compounds such as cells and drugs [144, 151]. These biomaterials offer unique potential, combining the advantageous properties of hydrogels—such as high water retention—with those of micro/nanoparticles, including small size and large specific surface area [152]. In recent years, hydrogel particles have gained substantial traction in the biomedical domain due to their remarkable biocompatibility, substantial loading capacity, and responsiveness to environmental factors like pH, temperature, and ionic strength [152]. According to the International Union of Pure and Applied Chemistry (IUPAC) definition, nanogels (hydrogel nanoparticles) are characterized as gel particles capable of assuming any shape with an equivalent diameter ranging from 1 nm to 100 nm. Conversely, microgels (hydrogel microparticles) are gel particles with diameters falling within the range of 100 nm to 100 μm (**Tableau 1**) [153].

Daly and al. [154], categorized hydrogel microparticles into three main groups: suspensions, granular hydrogels, and composites. In hydrogel microparticle suspensions, the particles are dispersed within a fluid (liquid), with minimal interactions between them. However, as the packing density of the particles increases, particle-particle interactions become significant, leading to the formation of granular hydrogels. Granular hydrogels predominantly exist in a

jammed or stuck state, ranging from loosely packed configurations with high porosity to ultra-close-packing states. In the latter, hydrogel microparticles deform, and interstitial spaces collapse, resulting in a loss of microporosity. Additionally, when hydrogel microparticles are integrated within a bulk hydrogel, hydrogel microparticle composites are formed [154].

Hydrogel microparticles present distinct benefits compared to larger hydrogel forms, rendering them appealing for biomedical use. Their small size enables simple administration via fine needles, catheters, or inhalation, facilitating minimally invasive delivery of cells and biologics, thereby streamlining medical procedures [155]. Moreover, the interplay among particles within granular systems induces a shear-thinning effect, allowing effortless injection followed by a transition to a solid-like state post-injection, all achieved without requiring chemical alterations [155]. Alternatively, interparticle interactions can be introduced by forming chemical bonds between polymer particles within a hydrogel through cross-linking chemistries, offering the potential to further tailor the properties of granular hydrogels[156]. Secondly, microgel systems exhibit inherent modularity, allowing for the blending of multiple hydrogel microparticle populations with diverse compositions, sizes, and contents to generate a wide array of materials. In their review, Mealy and al [157], delved into the modification of di-thiolcrosslinkers to engineer stable and cleavable microgels within granular hydrogels. These stable microgels, created using a non-degradable di-thiolcrosslinker (DTT), and cleavable microgels, integrating a peptide sequence susceptible to matrix metalloproteinase (MMP) cleavage, were laden with distinct payloads. Investigation of payload release and hydrogel degradation showcased differing responses to proteases, with cleavable hydrogels displaying swifter payload release and degradation in the presence of collagenase compared to stable hydrogels. Combining stable and cleavable microgels in a two-component granular hydrogel enabled the development of intricate materials with unique attributes, offering potential for controlled release of multiple factors and cellular infiltration within a singular hydrogel system. This study underscores the adaptability of microgel cross linkers in governing granular gel behaviors and the release dynamics of encapsulated molecules, shedding light on the design of versatile hydrogel materials for biomedical purposes. Such adaptability facilitates the customization of hydrogel formulations to address specific biomedical needs [157]. Thirdly, granular hydrogels often possess considerable porosity, stemming from the interstitial gaps between hydrogel microparticles [178]. This porosity is contingent upon the size and packing

density of the hydrogel microparticles and can be finely tuned to facilitate cellular proliferation and migration. For instance, Lee and al [158], innovatively introduced a new method by integrating a thiol-functionalized thermo-responsive polymer into oxidized hyaluronic acid microgel assemblies. This approach facilitated the development of granular hydrogels with distinct attributes, including shear-thinning and self-healing properties driven by the swift exchange rate of thiol-aldehyde dynamic covalent bonds. Moreover, the phase transition behavior of the thermo-responsive polymer acted as secondary crosslinking, bolstering stability at physiological temperatures. These granular hydrogels displayed exceptional injectability, shape retention, and mechanical robustness, positioning them as promising contenders for diverse biomedical applications. Additionally, the presence of aldehyde groups within the microgels provided covalent anchoring sites for sustained drug release, enhancing their versatility. Notably, these hydrogels could function as platforms for cell encapsulation and delivery, and they were compatible with 3D printing without necessitating supplementary post-processing steps for mechanical support. In sum, this study presents thermo-responsive granular hydrogels endowed with multifunctional capabilities, holding significant promise for biomedical research and clinical utilization [158]. Additionally, Xu and al [159]. introduced injectable lutetium-177-labeled 3D hollow porous granular hydrogels (177Lu-3D-HPGH) designed for SPECT imaging-guided intravascular brachytherapy, targeting tumors abundant in blood vessels. These hydrogels, fabricated via microfluidics and UV photo-cross-linking, exhibited outstanding attributes such as biocompatibility, chemical stability, and precise delivery capabilities. The 177Lu-3D-HPGH displayed promise in interventional brachytherapy, achieving complete tumor suppression in rabbit VX2 liver tumors. This advancement signifies a significant stride in cancer treatment modalities [159]. This characteristic holds pivotal importance in tissue engineering and regenerative medicine, where scaffolds with adequate porosity are essential for optimal cellular growth and functionality [151, 156].

Nanogels, also known as hydrogel nanoparticles, are dispersions of polymer particles formed through chemical or physical cross-linking of polymer chains, exhibiting an internal three-dimensional network structure. Typically ranging in particle size from 1 to 200 nm, nanogels represent an advanced nano-delivery carrier [160]. In comparison to microgels, nanogels boast smaller particle sizes and larger specific surface areas, rendering them advantageous for enhanced biocoupling and targeted drug delivery [143]. Hydrogel nanoparticles

have garnered attention as potential vehicles for drug delivery owing to their favorable attributes, including biocompatibility, excellent stability, tunable particle sizes, efficient drug-loading capacities, and surface customizability. This surface modification facilitates active targeting by attaching specific ligands capable of recognizing receptors on desired cells or tissues [161].

Additionally, nanogels demonstrate superior capabilities in surmounting in vivo physiological barriers, exhibiting high stability in systemic circulation, and enhancing the bioavailability of immobilized drugs. They efficiently transport bioactive substances to therapeutic doses at the target site in vivo [162]. Hydrogel nanoparticles are recognized as intelligent or smart materials due to their ability to undergo structural alterations in response to environmental changes. These environmental factors encompass variations in temperature, pH, light exposure, reduction reactions, and intracellular enzyme activity. The drug is released from intelligent nanogels within the tissue or even within the target cell. Moreover, the responsiveness to external stimuli is significantly enhanced, irrespective of the specific drug encapsulated within the nanogels [161].

Table 1. Nano/microparticles obtained through covalent cross-linking and Shiff base formation and their biomedical applications.

Crosslinking types	Materiels	Biomedical application	References
Thiol-ene coupling	Hyaluronic acid-poly(ethylene glycol)-bis(thiol)	Drug delivery	[163]
Enzymatic crosslinking	Gelatin- gelatin (using transglutaminase (mTG))	Wound healing and tissue engineering.	[164]
Enzymatic crosslinking, and Diels–Alder	furylamine (furan) and tyramine (TA) grafted Hyaluronic acid (HA) molecules(HA-furan/TA)	Cell encapsulation and delivery	[165]
Hydrazone cross-linked	Hyaluronic acid hydrazide-hyaluronic acid aldehyde Hyaluronic acid hydrazide - poly(ethylene glycol) dialdehyde	the treatment of vocal fold scarring, not just as biocompatible filler materials, repair focal defects, smooth the vocal fold margin, and potentially soften and dissolve scar tissue.	[166]

Hydrazone cross-linked	Hydrazide functionalized carboxymethyl cellulose – Aldehyde functionalized dextran (DEX-B)	cell encapsulation or drug delivery	[167]
Imine crosslinked	Hybrid bovine serum albumin-gum arabic aldehyde (BSA-GAA)	Drug delivery and other biomedical application	[168]
Imine crosslinked	Oxidized sodium alginate-chitosan	Crrier for the colon-specific delivery of anti-inflammatory drugs including 5-ASA and the enhanced therapeutic effect of ulcerative colitis.	[169]

II.5. Biomedical applications of hydrogels obtained through Schiff base chemistry

Recent years have witnessed significant strides at the intersection of polymer chemistry and biomedical sciences, yielding remarkable advancements in biomaterials. Among these breakthroughs, microparticle, nanoparticle, and film hydrogels synthesized via Schiff base reactions have emerged as highly adaptable platforms with promising applications in healthcare. These hydrogel structures exhibit precision and tunability inherent to Schiff base chemistry, rendering them well-suited for a wide array of biomedical purposes. From targeted drug delivery and tissue regeneration to diagnostic sensing and wound healing, these hydrogels possess the potential to transform medical therapies and diagnostics, paving the way for more effective and personalized interventions. This review delves into the intricate hydrogel systems achieved through Schiff base chemistry and their prospective role in shaping the future of biomedical applications.

II.5.1. Biomedical applications of film Schiff base hydrogels

Schiff-base hydrogel films have garnered considerable interest in recent years, thanks to their distinctive properties and wide-ranging applications. These films form a stable, cross-linked network through the chemical interaction between aldehydes and primary amines. The resultant hydrogel film showcases outstanding biocompatibility, adjustable mechanical attributes, and remarkable water absorption capacity. Such qualities position Schiff base hydrogel films as promising contenders for diverse applications, spanning from drug delivery and wound healing to tissue engineering.

II.5.1.1.Drug delivery

Targeted drug delivery entails the precise delivery of a medication to a particular site within the body (**Figure 14**). By employing targeted drug delivery, the medication's effectiveness is concentrated solely on a designated area, thereby reducing potential side effects and safeguarding the viability of cells in that region [170].

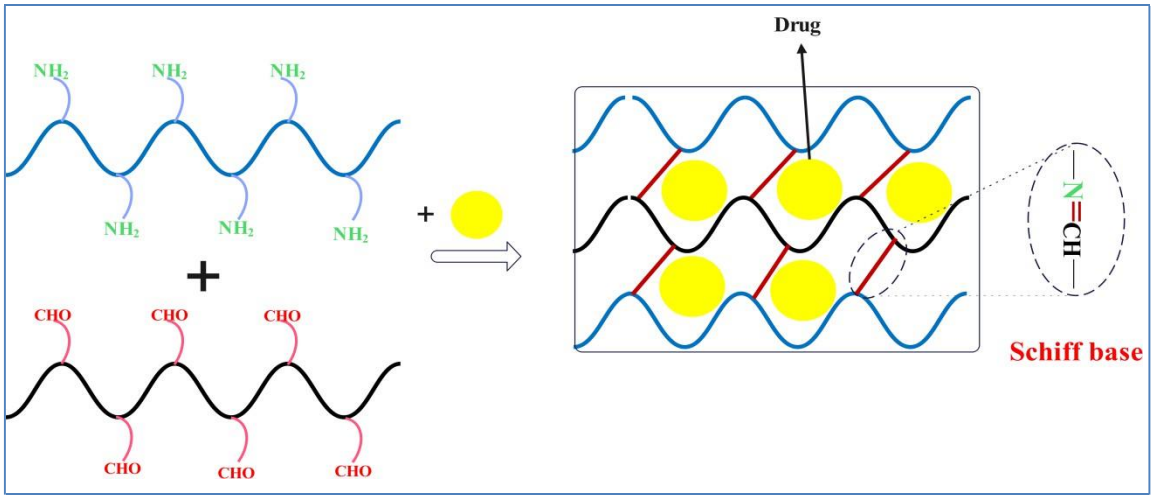

Figure 14. The immobilization of the drug in the film matrix.

Hydrogel films engineered for drug delivery epitomize a pioneering approach in pharmaceutical and biomedical sciences. Comprising water-swollen polymer networks, these films provide an exceptional platform for the controlled and targeted release of therapeutic agents. Widely embraced in biomedicine, hydrogel films boast a spectrum of attributes that have propelled their extensive utilization in drug delivery applications. Noteworthy among these attributes are superior biocompatibility, robust stability, injectable characteristics, and the ability to facilitate controlled and sustained release of therapeutics [154,22].

Schiff-based hydrogel films have surfaced as a fresh and promising avenue for sophisticated drug delivery applications. These hydrogel films present a distinctive blend of properties that render them ideal for controlled and targeted drug release. The porous structure inherent in Schiff base hydrogels plays a pivotal role in numerous applications, notably in drug delivery. These pores within Schiff base hydrogels dictate the creation of a three-dimensional matrix capable of effectively encapsulating drugs or bioactive molecules. The polymer matrix

shields the drugs from degradation, enhancing their stability and facilitating controlled release over time.

Furthermore, the porosity of the hydrogel matrix can be fine-tuned by adjusting the cross-linking density [2]. Schiff base hydrogels demonstrate remarkable responsiveness to environmental stimuli such as pH, temperature, and specific molecules. This characteristic can be harnessed to induce customized drug release profiles.

Additionally, numerous Schiff base precursors and resultant hydrogels boast biocompatibility, rendering them well-suited for biomedical applications. Dalei and al [171], provide compelling evidence for the practical implementation of in situ cross-linked chitosan-dialdehyde guar gum (CsDAGG) hydrogels in dual drug release strategies for colorectal cancer treatment. Their research involved the fabrication of various grades of CsDAGG hydrogels by adjusting the dialdehyde guar gum (DAGG) content. The investigation centered on combining curcumin with aspirin to target colon carcinoma. The hydrogels demonstrated the capacity to shield the drugs from premature absorption in the stomach and small intestine, thereby enabling a precisely controlled release within the colorectal region [171]. In a separate investigation, Hosseini and Nabid [172] concentrate on the development of pH-sensitive hydrogel films using basil seed mucilage (OBM) biopolymer as a novel approach for wound dressing and drug delivery. Through the incorporation of varying proportions of poly (vinyl alcohol) (PVA), glutaraldehyde (GA) as a cross-linker, and glycerol as a plasticizer, an optimal equilibrium of flexibility and durability was attained. The refined formulations of hydrogel films were subsequently employed to encapsulate Tetracycline hydrochloride (TH) as a model drug, revealing enhanced release profiles at pH levels 8.5 and 7.4, underscoring their potential for wound healing and drug delivery applications [172].

II.5.1.2. Tissue engineering

Tissue engineering (TE) involves the application of scientific and engineering principles to create, regenerate, enhance, or control the structure and functionality of living tissues [173]. Tissue engineering principles have gained widespread acceptance in the restoration of damaged or dysfunctional tissues and organs, aiming to restore them to their normal or improved function [174]. Given the structural similarity of hydrogels to the extracellular matrix of various tissues, they are utilized as scaffolds in regenerative medicine [175]. These scaffolds provide structural support, guide cellular organization and development, act as tissue barriers and adhesives, serve

as reservoirs for drugs, facilitate the delivery of bioactive substances that promote natural healing, and encapsulate and transport cells. Hydrogels elicit favorable tissue responses owing to their unique physical and chemical properties. Their high water content renders them highly compatible with cells, enabling specific or non-specific binding with cellular receptors. Protein and polysaccharide-based hydrogels can integrate ligands that enhance cell binding, rendering them valuable scaffolds for cell encapsulation [174]. These biomaterials can undergo chemical or physical cross-linking to yield various forms of hydrogels, serving as versatile scaffolds for a wide array of regenerative medicine applications.

Schiff base hydrogel films emerge as compelling candidates for scaffolds in tissue engineering, boasting notable attributes such as biocompatibility, customizable properties, responsiveness to stimuli, and the ability to support both cell growth and controlled drug delivery. These hydrogels hold immense potential across various regenerative medicine applications, where precise control over scaffold properties is crucial for ensuring the efficacy of tissue regeneration.In a comprehensive research endeavor, Rajalekshmi and collaborators [176]. Meticulously investigated the fibrin (FIB) integrated injectable alginate dialdehyde (ADA) - gelatin (G) hydrogel system, potentially serving as a scaffold for liver tissue regeneration. To fulfill this objective, they ingeniously formulated a hydrogel system by incorporating fibrin into ADA-G, enabling a thorough exploration of its physicochemical and rheological properties. The research encompassed a comprehensive evaluation of the hydrogel's biological characteristics, encompassing cytocompatibility, HepG2 cell viability, and the examination of crucial functional markers. These evaluations encompassed various assessments, including the indocyanine green uptake assay, Live Cell Imaging Analysis (LDL) uptake assay, glycogen storage analysis, CYP-P450 expression analysis, ammonia clearance assay, and albumin assay. The outcomes of these experiments indicate that the fibrin-incorporated ADA-G-Fib hydrogel exhibits the potential to significantly enhance cellular adhesion, proliferation, and overall functionality. These findings underscore the obtained delivery system as a highly promising candidate for applications in liver tissue regeneration [176]. In a separate investigation led by Cheng and al [177], a novel method was employed to immobilize collagen onto cellulose film without inducing conformational changes or degradation. The study explored the efficacy of periodate-oxidized regenerated cellulose films in stabilizing collagen through the Schiff base reaction, wherein NH2 groups in collagen interacted with CHO groups in the 2,3-dialdehyde cellulose (DARC) backbone[177].

The resultant composite material displayed considerable potential as a scaffold for tissue engineering applications. It exhibited notable strength in a swollen state, provided flexibility in situ, maintained a favorable equilibrium-swelling ratio, allowed for air permeability, and demonstrated remarkable biocompatibility [177]. Liu et al [178], introduced a pioneering approach involving the synthesis of methacrylate- and aldehyde-functionalized dextran, termed Dex–MA–AD. This study unveiled an innovative family of cell-encapsulating hydrogels achieved by modulating the synergy between the polymers Dex–MA–AD and gelatin. The hydrogel was fabricated via ultraviolet (UV) crosslinking, leveraging methacrylate groups on Dex–MA–AD and a Schiff base reaction between Dex–MA–AD and gelatin. These hydrogels exhibit promising potential as 3-D vascular tissue engineering scaffolds [178].

II.5.1.3. Wound healing

Hydrogel-based wound dressings play a pivotal role in various wound care strategies, addressing superficial burns, abrasions, donor sites, pressure ulcers, and chronic wounds. They create an optimal wound environment by promoting cleansing, facilitating the body's natural removal of necrotic tissue, maintaining moisture, shielding against contamination, absorbing exudate, and actively supporting the healing process [175,180]. Hydrogel treatment offers a plethora of advantages in wound care. It fosters the development of new blood vessels and the regeneration of intricate layers of skin, including hair follicles and oil-producing glands, thereby reducing scarring risk. Additionally, hydrogels serve as a protective barrier against wound desiccation, crucial for preserving moisture content, enhancing patient comfort, managing pain, and providing a soothing, cooling effect. With their high moisture content, hydrogel dressings effectively block bacteria and oxygen from entering the wound, thereby forming a protective shield against infections.

Moreover, hydrogels have demonstrated the ability to enhance fibroblast proliferation by minimizing fluid loss from the wound surface. This protective effect shields the wound from external irritants and accelerates the healing process. Hydrogel dressings also play a crucial role in maintaining an optimal microclimate for cellular activities on the wound surface, which is essential for facilitating biosynthetic reactions [175,180,181].

Schiff base hydrogel films represent a significant advancement in wound care. Comprising hydrogel materials formed through Schiff base reactions, these films offer a plethora of advantages, rendering them particularly promising for wound management [16]. Firstly, they play

a vital role in maintaining a moist wound environment, a critical factor in promoting effective wound healing. Schiff base hydrogel films facilitate tissue regeneration by preventing wound desiccation. Additionally, these hydrogel films aid in managing wound exudate, as they possess the ability to absorb excess exudate while releasing moisture into the wound bed, thereby maintaining an optimal balance and preventing maceration. Moreover, Schiff-base hydrogel films are generally well-tolerated by the skin and exhibit biocompatibility, thereby reducing the risk of irritation or allergic reactions [181]. An important advantage of these films is their non-adherent nature when in contact with the wound, which reduces the risk of trauma or damage to newly formed tissue during dressing changes [182]. Furthermore, specific Schiff base hydrogels can be engineered to respond to particular stimuli, such as changes in pH or fluctuations in temperature. This capability enables controlled drug delivery or customized wound treatment strategies[183]. Depending on their composition, Schiff base hydrogels may also exhibit inherent antimicrobial properties, enhancing their effectiveness in preventing wound infections [184,185,186]. Their ease of application and ability to conform to various wound shapes and sizes further enhance their appeal.

Guo and al [186], embarked on a novel study aimed at developing a hydrogel for wound dressing with significant potential for chronic wound healing applications. Their innovative hydrogel was synthesized through a Schiff base reaction, utilizing oxidized hyaluronic acid (OHA) and carboxymethyl chitosan (CMCS). This hydrogel was further enriched by the incorporation of active polypeptides extracted from Periplanetaamericana (PAE), commonly known as the American cockroach. The role of the peptide was likely to enhance the hydrogel's properties or functionality. Peptides sourced from natural origins like Periplanetaamericana often possess bioactive properties, such as antimicrobial, antioxidant, or wound healing effects. Hence, integrating these peptides into the hydrogel may have conferred additional therapeutic benefits, such as promoting tissue regeneration or providing antimicrobial protection. OHA/CMCS/PAE composite hydrogels hold immense promise as candidates for addressing challenges in chronic wound healing. With their robust properties and demonstrated therapeutic effects, these hydrogels offer a potential avenue for improving the management of chronic wounds, particularly in diabetic wound healing scenarios [186]. In a distinct study, Zhang and al [187], utilized a Schiff base reaction to fabricate hydrogels using oxidized sodium alginate, chitosan, and zinc oxide. These hydrogels exhibited notable swelling and porosity characteristics. Extensive in vitro

experiments were conducted to evaluate their biocompatibility with diverse cell lines, including 293T cells, blood cells, and 3T3 cells. The results were highly promising, demonstrating the favorable biocompatibility of the hydrogels. Remarkably, these hydrogels displayed exceptional antibacterial properties, effectively combatting Bacillus subtilis, Candida albicans, and Staphylococcus aureus. Concurrently, they demonstrated the ability to expedite the healing process of scalded wounds in rat models. This comprehensive investigation underscores the potential and versatility of these hydrogels in various biomedical applications [187]. In a study conducted by Oh and al [188], hydrogels were synthesized via a Schiff base reaction involving gelatin, oxidized sodium alginate, chitosan, and salicylic acid. These hydrogels showcased remarkable wound healing properties while also displaying a notable absence of toxicity [188].

II.5.2 Biomedical applications of microparticles hydrogels

In biomedical realms, microgels, characterized by their micron-scale diameters, assume a pivotal role. Their diminutive size facilitates injection and surface modification, rendering them versatile tools in the biomedical domain. With expansive specific surface areas and impressive loading capacities, microgels hold promise for localized therapeutic delivery and integration into granular scaffold structures. These hydrogel microparticles find myriad biomedical applications, including topical drug delivery, bone and soft tissue regeneration, and immunomodulation. Similarly, hydrogel microparticles synthesized through cross-linking with imine bond formation play a crucial role in biomedical contexts. These hydrogels offer tunable properties, such as responsiveness to environmental cues, biocompatibility, and controlled release of encapsulated biological molecules. Their capacity for tailored responses to physiological conditions enables precise drug targeting. Furthermore, their biocompatibility ensures harmonious interactions with living tissues, rendering them ideal for tissue engineering and regenerative medicine applications. The potential impact of Schiff base particle hydrogels on the biomedical field is substantial, promising enhanced drug delivery precision, support for tissue regeneration, and advancements in therapeutic strategies.

II.5.2.1. Schiff base micro gels for drug delivery

Hydrogel microparticles have emerged as a favored drug delivery system. Bioactive agents are either physically bound to the delivery system or encapsulated within hydrogel microparticles. Their distinctive attributes, such as high water content, adjustable porosity, ample specific surface area, capability to regulate drug release, and favorable biocompatibility and

mobility, render them exceptional carriers for a diverse array of drugs, encompassing small molecules, proteins, and nucleic acids, in comparison to conventional hydrogels [154].

The application of the Schiff-base reaction, which entails the interaction between a polysaccharide typically containing amine and aldehyde functional groups, has been instrumental in the development of diverse hydrogels and microgels relevant to biomedical contexts. Literature highlights the benefits of hydrogels synthesized via Schiff-base chemistry, such as their biocompatibility, antibacterial properties, and responsiveness to environmental factors [189]. Du and al. [189], devised drug-loaded microgels through the Schiff-base reaction involving carboxymethyl chitosan and oxidized carboxymethyl cellulose. These microgels were subsequently integrated into hydrogels, yielding a notable hydrogel-microgels composite referred to as Gel/MGs. Findings affirmed that the inclusion of microgels imparted superior stability, enhanced mechanical strength, and heightened drug release sensitivity to both acidic and alkaline conditions in vitro. Moreover, Gel/MGs wound dressings demonstrated favorable antibacterial properties, positioning them as promising candidates for wound dressing applications [189]. Su and al. [152], pioneered the development of hydrogel microparticles through the formation of Schiff bases between aldehyded dextran and ethylenediamine within water-in-oil (W/O) microemulsion system. These microgels exhibited particle sizes ranging from 800 to 1100 nm. Their groundbreaking work underscores the potential of pH-sensitive microgels as versatile and efficient drug delivery systems, holding immense promise for a wide array of biomedical applications [152]. Yan and al. [190], have recently ingeniously engineered hydrogel microparticles designed for pulmonary drug delivery. These microparticles, composed of Zn^{2+}, carboxymethyl chitosan, and hyaluronan aldehyde, were fabricated using the spray drying method. Results demonstrated that the produced hydrogel microparticles showcased a sustained drug release profile, reaching equilibrium after 24 hours in vitro. They adeptly evaded clearance by alveolar macrophages and exhibited substantially prolonged residence times in vivo, thus holding significant potential for enhancing the treatment and management of respiratory conditions [190]. In a separate investigation, Cheng and al. [191] introduced an innovative injectable hydrogel microparticle system aimed at achieving sustained release of antibiotics, specifically lysostaphin (Ls) and vancomycin (Van), at infection sites. The process involved a two-step approach: first, microfluidic encapsulation of Van within gelatin methacryloylmicrogels, followed by their incorporation into a solution of gelatin and oxidized starch prepolymer to form

a hydrogel through Schiff base reaction. The introduction of transglutaminase facilitated the creation of a dual cross-linked network scaffold for controlled drug release. This system offers sequential antibiotic release, facilitating targeted eradication of biofilm bacteria and minimizing toxicity from hydrogel degradation products, thereby presenting a promising strategy for infection treatment [191].

II.5.2.2. Schiff base microgels for cell encapsulation

Hydrogel microparticles, particularly those formed via Schiff base chemistry, have garnered significant interest as a versatile platform for cell encapsulation across diverse biomedical applications. These minute, gel-based particles are designed to encapsulate and shield individual cells or cell clusters, furnishing an optimal microenvironment for their growth, proliferation, and therapeutic functions. The hydrogel matrix of these microparticles can be precisely engineered to mimic the extracellular matrix, providing mechanical support, facilitating nutrient exchange, and enabling controlled release of bioactive molecules [154, 193]. Jang eand al. [193], devised a polysaccharide-based microgel by cross-linking oxidized dextran (ODX) with N-carboxyethyl chitosan (N-CEC) via Schiff base chemistry. They entrapped NIH-3T3 fibroblast cells (a mouse embryonic fibroblast cell line) within these microgels and evaluated cell viability. The study revealed that these microgels displayed excellent biocompatibility, indicating their potential for various biomedical uses. Moreover, the technique allows for the on-the-spot formation of microgels from two thick polymer solutions, offering versatility. This advancement could pave the way for novel biomedical research and applications [193].

II.5.2.3. Schiff base microgels for bone regeneration

Bone regeneration poses a multifaceted challenge demanding novel approaches for improved outcomes. Microparticle Schiff Base Hydrogels (MSBHs) represent a notable breakthrough in this domain. What distinguishes MSBHs is their microparticulate architecture and distinctive attributes including softness, size, injectability, porosity, and degradability. These characteristics render them well-suited for transporting drugs, bioactive agents, and cells, tailored for tissue restoration and regrowth [194]. Zhou's team [195], has developed a groundbreaking injectable system utilizing Gelatin-Methacryloyl (Gelma) hydrogel microspheres as the delivery medium. Their objective is to induce epigenetic reprogramming within micro-fluidic microsphere systems to augment bone regeneration and modulate the microenvironment during the initial fracture phase. This system is specifically engineered for targeting macrophages, employing

micro/nano microspheres Gelmaphosphatidylserine-specific liposomes (Gelma@Lip@Pla) to amplify therapeutic effects. The Gelma@Lip@Plamicrogel necessary for this purpose was synthesized through Schiff base cross-linking between residual amino groups on the low-substituted Gelma surface and aldehyde groups on the Lip@Pla surface. The researchers have validated that the Gelma@Lip@Plamicrogel holds significant promise as an extended-release platform for addressing bone defects and various immune-related conditions involving macrophages [195]. In their study, Zhang and al. [196], engineered a 3D microsphere comprising bacterial cellulose and collagen, interconnected through Malaprade and Schiff base reactions, resulting in a multi-stage structure with diverse composition. The aim was to leverage this construct in bone tissue engineering endeavors. Remarkably, this multi-level architecture exhibited outstanding biocompatibility and notably enhanced the attachment, proliferation, and osteogenic differentiation of MC3T3-E1 cells in murine models [196]. Moreover, these Schiff base-linked 'smart' hydrogels not only safeguard encapsulated drugs, peptides, and proteins against external influences but also enable controlled release by responding to fluctuations in the polymer network's swelling and shrinking, effectively functioning as an "on-off" switch for controlled drug delivery [197].

II.5.3. Biomedical applications of nanoparticles hydrogels (nanogels)

Nanogels offer a plethora of advantages, including stable size, remarkable hydrophilicity, biocompatibility, and the ability to adapt to specific environmental cues. Their minimal non-specific interaction with blood proteins lowers the likelihood of immune responses. As such, nanogels emerge as promising contenders in the realm of biomedicine. In this segment, we offer a succinct overview of recent nanogel applications spanning drug delivery, anti-tumor/cancer therapies, antibacterial interventions, nerve regeneration, and disease prevention and diagnosis.

II.5.3.1. Nanogels for drug delivery

Many nanogels demonstrate outstanding drug encapsulation efficiency and loading capacity, rendering them ideal for transporting a broad spectrum of pharmaceuticals, including both hydrophilic and hydrophobic drugs. Additionally, the structure of nanogels can be readily customized to integrate features from different materials, offering a substantial advantage for simultaneously encapsulating drugs with diverse physicochemical properties, such as small molecules, proteins, and nucleic acids [198].

Schiff base nanogels possess a distinctive capability to form and break reversible covalent bonds, enabling them to uphold a stable drug structure while facilitating controlled and responsive drug release. Researchers can tailor these nanogels to react to particular environmental cues, such as variations in pH, temperature, or enzymatic activity, thereby allowing for precise customization of drug release profiles. This adaptability proves particularly valuable across various therapeutic applications.In a pioneering investigation by Su and al. [199], a dextran-based nanogel system was devised to enhance the efficacy of Schiff base formation for drug delivery, with doxorubicin (DOX) serving as the model drug. This innovative nanogel was synthesized utilizing the inverse microemulsion technique, wherein the covalent conjugation of DOX to the nanogel was accomplished via Schiff base linkages. Notably, this nanogel exhibits a pH-dependent drug release profile attributable to its acid-sensitive Schiff base linkages, resulting in faster drug release in acidic environments compared to physiological solutions. This research underscores the fusion of nanotechnology and chemistry in the development of intelligent drug delivery systems [199]. In a noteworthy investigation, Sarika and her team [200], encapsulated curcumin, a naturally occurring therapeutic compound, within nanogels crafted from dialdehyde alginate and gelatin (AlgAld-Gel). They utilized the inverse miniemulsion technique to fabricate these nanoparticles. Their findings unequivocally underscore the efficacy of ingeniously designed nanogels in delivering curcumin specifically to breast cancer cells. This promising advancement heralds fresh opportunities for enhanced and targeted drug delivery in breast cancer treatment [200].

II.5.3.2. Nanogel for anti-tumor and cancer therapy

Schiff base nanogels are emerging as promising contenders in the realm of anti-tumor and cancer therapy, providing a versatile platform for drug delivery with a specific emphasis on targeting cancer cells. Leveraging Schiff base chemistry, these nanogels can be precisely engineered to react to the specific pH conditions prevalent in tumor microenvironments. This pH sensitivity enables controlled and selective drug release at the tumor site, thereby minimizing off-target effects and bolstering therapeutic efficacy [201]. An outstanding advantage of Schiff base nanogels lies in their capability to encapsulate a diverse array of anti-cancer drugs, spanning chemotherapeutic agents, targeted therapies, and even macromolecules like nucleic acids. This versatility facilitates tailored treatment strategies for various cancer types and stages [199, 203]. Moreover, the presence of multiple aldehyde groups on Schiff base nanogels presents opportunities for additional functionalization, such as the attachment of targeting ligands or

imaging probes. This enhances the specificity of drug delivery to cancer cells while minimizing collateral damage to healthy tissues [203].

Recent studies have showcased the potential of Schiff base nanogels to surmount drug resistance, enhance drug solubility, and elevate overall therapeutic efficacy in cancer treatment. Their biocompatibility and adjustable properties render them invaluable assets for refining anti-tumor and cancer therapies, enabling greater effectiveness and precision. As research in this domain progresses, Schiff base nanogels emerge as promising contenders for revolutionizing cancer treatment strategies.In a study led by Yu and colleagues [204], dextran-based (Dex-SS) nanogels were synthesized using a direct method that relied on the formation of disulfide intermolecular bonds and Schiff base linkages between polyaldehyde dextran and cystamine within a water-in-oil inverse microemulsion. These nanogels possess a unique attribute: they respond to both acidic and reductive environments, a crucial trait for drug delivery in cancer therapy. The innovative aspect of this research was the covalent conjugation of the anticancer drug doxorubicin (DOX) into the dextran nanogels via Schiff base linkages. This strategic drug encapsulation enabled the development of pH/GSH (glutathione) dual-responsive drug release profiles, ensuring predominant release of DOX in the acidic and reductive tumor microenvironment [204]. In their study, Bachiri and al. [168], employed gum Arabic oxidized with sodium periodate as a naturally derived, non-toxic cross-linker to fabricate hybrid bovine serum albumin-gum arabic aldehyde (BSA-GAA) nanogels via a Schiff base reaction, utilizing 5-fluorouracil (5-FU) as the model anti-cancer drug. Notably, the entire synthesis process was conducted without the use of toxic organic solvents, with fractionated coconut oil serving as the continuous phase. The outcomes of the study suggest that these biobased hybrid nanogels hold promise for various anti-cancer therapies [168]. Ziaei and colleagues [205], devised pH-responsive, in-situ forming hydrogels by employing oxidized alginate and gelatin encapsulated with doxorubicin (DOX) within chitosan/gold nanoparticles (CS/AuNPs) nanogels. The polymer chains are interconnected through Schiff-base bonds, and β-glycerophosphate (β-GP) was utilized as an ionic accelerator crosslinker. As anticipated, both the drug-loaded hydrogel and free DOX at a specific concentration induced significant cell death in MCF-7 cells, underscoring the potential of these hydrogels for localized breast cancer treatment [205].

II.5.3.3. Nanogels for antibacterial applications

The formation of bacterial biofilms presents a formidable challenge in clinical settings, frequently leading to implant failure and severe complications, including life-threatening scenarios. Effectively tackling this issue is paramount, and nanogels emerge as a promising solution.

Renowned for their stability and capacity to target specific sites, nanogel carriers facilitate the controlled release of antimicrobial agents at concentrated levels within localized areas. This notable attribute positions them as invaluable assets in combatting bacterial infections and mitigating their ensuing complications [207, 208]. Furthermore, incorporating Schiff base chemistry into nanogels amplifies their versatility for antibacterial applications. The Schiff base linkages within these nanogels can be customized to react to particular environmental stimuli, facilitating pH or other stimuli-responsive drug releases, thereby enhancing their antibacterial efficacy. This multifaceted approach holds immense promise in combating bacterial biofilms and stands to revolutionize antibacterial and anti-infection strategies in clinical settings.In a recent study by Chung and al. [208], nanogels (NGs) were engineered through precise chemical modifications. Aldehyde groups were cross- linked with primary amines using a Schiff reaction to create DNA-HCl-S-benzyl-L-cysteine (SBLC). Simultaneously, alginate acid (AA) was treated with a water-soluble derivative of carbodiimide (EDAC), resulting in AA-EDAC, which was further substituted with SBLC to yield AA-SBLC.

These modifications were incorporated into an emulsification process, yielding spherical NGs with grafted benzene rings. The authors verified that SBLC modifications notably enhanced the antimicrobial properties of the NGs.

This study presents a promising clinical solution for antibiotic-resistant biofilm strains [208]. In a separate investigation, Gao and al. [209], synthesized antimicrobial quaternized chitosan/Ag composite nanogels (QCS/Ag CNGs) via the inverse miniemulsion technique, achieving a high encapsulation efficiency of NH_2-Ag nanoparticles.

The QCS/Ag CNGs exhibit potent broad-spectrum antimicrobial properties with minimal toxicity, attributed to the synergistic action of Ag nanoparticles and QCS. These NH_2- Ag NPs are securely bound to the QCS structure through Schiff base reactions, endowing the resulting QCS/Ag CNGs with reactive groups that ensure enduring antibacterial performance on cotton fabrics. This research presents a straightforward and adaptable approach for fabricating polymer/inorganic CNGs, addressing the urgent need for antibacterial materials and fabrics [209].

II.6. Conclusion

In conclusion, the biomedical applications of hydrogels based on cross-linked proteins with carbonyl derivatives of polysaccharides offer a versatile platform with diverse forms such as films, nanoparticles, and microparticles, each holding distinct advantages in various biomedical contexts.

Film hydrogels, with their thin and flexible structure, are well-suited for wound healing, tissue engineering scaffolds, and drug delivery patches. Their ability to conform to irregular surfaces makes them particularly useful for wound dressings and ocular drug delivery systems.

Microparticle hydrogels, with their larger size and controlled release properties, are ideal for localized drug delivery, tissue engineering, and cell encapsulation. They can provide sustained release of therapeutic agents, promote tissue regeneration, and protect encapsulated cells from immune rejection.

Nanoparticle hydrogels, owing to their small size and large surface area, are excellent carriers for drug delivery, gene therapy, and imaging agents. Their ability to penetrate biological barriers and target specific tissues or cells makes them valuable tools in cancer therapy, regenerative medicine, and diagnostics.

CHAPTER III:
Hydrogels Based On Oxidized Alginate/Gelatin Cross-Linked By Schiff Base Crosslinking for Biomedical Applications

Chapter III: Hydrogels based on oxidized alginate/gelatin cross-linked by Schiff base crosslinking for biomedical applications

III.1. Introduction

This chapter first describes the chemical properties of gelatin, as well as the formation of hydrogels from oxidized alginate and gelatin cross-linked by the Schiff chemistry. He also defines the properties of this type of hydrogels such as biocompatibility, hydrophilicity, biodegradability, controlled release and cell compatibility.

III.2. Hydrogels on base alginate and gelatin

Hydrogels play a crucial role in various biomedical applications due to their unique properties, such as high water content, biocompatibility, and tunable mechanical characteristics. One promising class of hydrogels is derived from the crosslinking of oxidized alginate and gelatin through Schiff base chemistry. This innovative approach combines the advantages of alginate, a natural polysaccharide extracted from seaweed, and gelatin, a protein derived from collagen.

The crosslinking process involves the formation of Schiff base linkages, which occur through the reaction between aldehyde groups in oxidized alginate and amino groups in gelatin. This covalent bonding creates a stable network within the hydrogel, imparting it with enhanced mechanical strength and stability. The resulting hydrogel exhibits a three-dimensional structure that closely mimics the extracellular matrix found in natural tissues. These hydrogels have garnered significant attention in the biomedical field for applications such as drug delivery, tissue engineering, and wound healing. The controlled release of therapeutic agents from the hydrogel matrix is facilitated by its porous structure, offering a promising solution for targeted and sustained drug delivery. Moreover, the biocompatibility of the hydrogel makes it suitable for encapsulating cells and promoting tissue regeneration.

The Schiff base cross-linked hydrogels based on oxidized alginate and gelatin represent a versatile platform with tunable properties, making them adaptable to specific biomedical requirements. Their potential impact spans a range of applications, contributing to advancements in personalized medicine, regenerative therapies, and other areas of healthcare. As research in this field progresses, these hydrogels hold promise for addressing diverse biomedical challenges and improving patient outcomes.

III.3. Gelatin: Raw material

Gelatin production begins with the utilization of collagen-containing tissues, which can vary widely in origin. While hides, skins, and bones from mammals like pigs and cows are commonly preferred sources, gelatins are also derived from the skins of both cold and warm water fish species, with minor quantities sourced from fowl. The manufacturing process encompasses several stages, starting with the cleaning of the source tissues, followed by pre-treatment to prepare them for extraction. Gelatin extraction is then carried out, followed by processes of filtration, purification, and sterilization to refine the product. Subsequently, the gelatin is concentrated, dried, and finally milled to achieve the desired form for various applications [211, 212].

III.3.1. Process of obtaining of gelatin

The process of obtaining gelatin initiates with the thorough washing of the raw material to eliminate any impurities (**Figure 15**). For bones, a distinct procedure is followed: after washing and crushing, the degreased bone chips undergo a maceration process in acidic conditions, typically using 4±7 % hydrochloric acid, for a minimum of two days. This maceration results in the removal of mineral components such as hydroxyl apatite (Ca_5 $(PO_4)_3(OH)$) and calcium carbonate, leaving behind a sponge-like bone material known as ossein. The concentrated raw materials may then be utilized immediately or dried and stored for future use. Subsequently, depending on the source of collagen and the desired quality of the final gelatin, the raw material undergoes either acid or alkaline pre-treatment, followed by gelatin extraction [210].

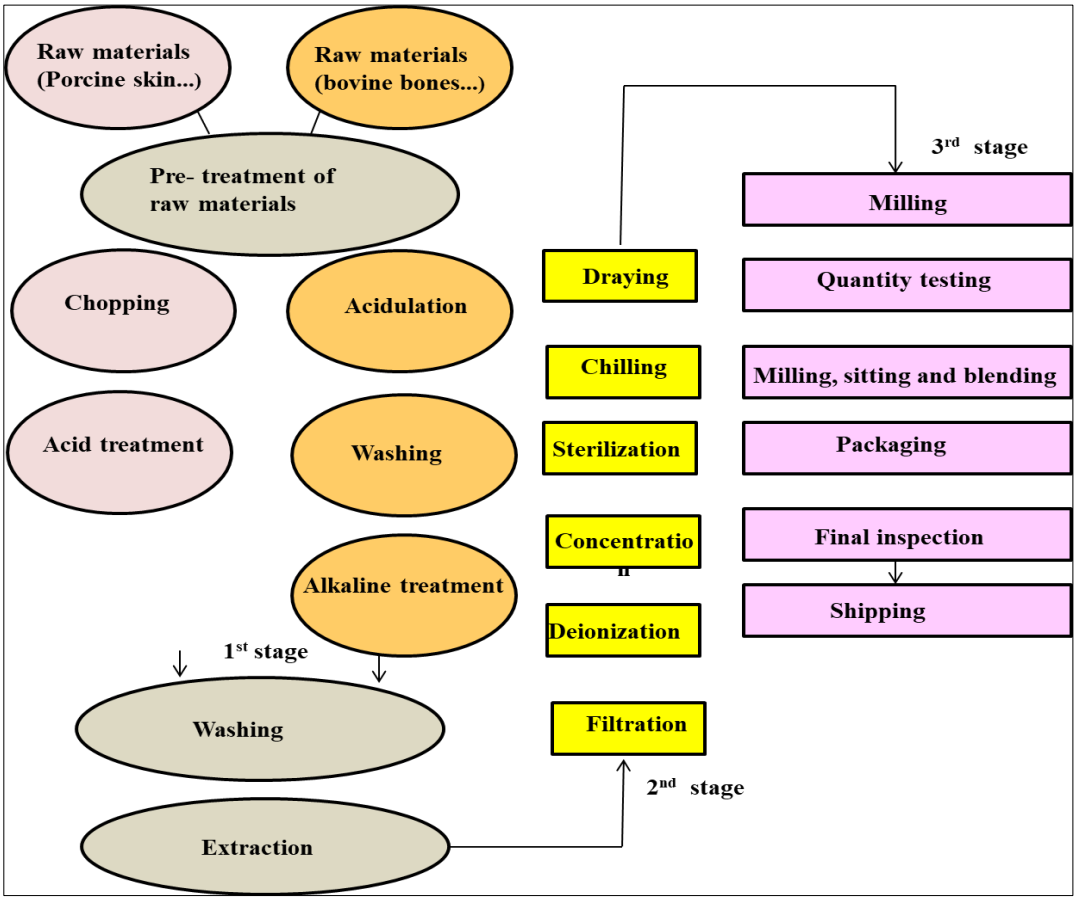

Figure 15. Industrial setup for manufacturing and production of gelatin [212].

III.3.1.1. Acid pre-treatment

The acid pre-treatment method yields type A gelatins, predominantly utilized in industrial settings. This process involves immersing the washed and hydrated rawmaterial (porcine skin, porcine bone, beef hides) in a cold dilute mineral acid solution with a pH ranging from 1.5 to 3.0 for duration of 8 to 30 hours, typically around 18 to 24 hours, adjusted according to the thickness and size of the raw material. Following treatment, the material undergoes thorough washing in running water and neutralization until the extraction pH is achieved [211, 213].

III.3.1.2. Alkaline pre-treatment

Type B gelatins are the outcome of the alkaline pre-treatment process. Various alkaline agents may be employed for this treatment, although saturated lime water ($Ca(OH)_2$) with a pH

of 12.0 stands as the most commonly used curing liquid. The washed raw material (bovine bone, beef hides and porcine bones) is placed in pits or vats alongside the liquid, with sufficient hydrated lime to maintain saturation. Throughout the process, the temperature is carefully regulated to remain below 24°C, and the mixture is periodically agitated using poles or mechanical means. The duration of this process ranges from at least 20 days to up to 6 months, typically lasting around 2 to 3 months, contingent upon the thickness and type of the raw material. Upon completion of treatment, the limed material undergoes thorough washing with water until reaching approximately neutral conditions before further treatment with dilute acid (e.g., HCl) to achieve the appropriate extraction pH [211, 213].

III.3.1.3. From extraction to final gelatin product

To extract gelatin, the pre-treated raw material is introduced into extraction kettles and immersed in hot water. Multiple extractions are performed using successive batches of hot water, typically ranging from three to five, with each extraction conducted at progressively higher temperatures within the range of 55 to 100 °C. This combined pre-treatment and extraction process results in the final gelatin product being a blend of polypeptide chains with varying compositions and molecular weights which results three primary fragments. The three primary fragments found in gelatin are: free α-chains, β-chains formed by the covalent linkage of two α-chains, and γ-chains formed by the covalent linkage of three α-chains. Additionally, the free α-chains may undergo depolymerization into sub-α-chains, which are polypeptides with lower molecular weights than a single α-chain. This non-monodisperse nature distinguishes gelatin from monodisperse proteins like globular proteins, and thus, all parameters describing the chemical and physical properties of gelatins represent average values [210].

High-quality gelatins, distinguished by their average molecular weight and gel-forming properties, are typically produced during lower temperature extractions, as they result in minimal hydrolysis of the polypeptide backbone. Subsequent extractions yield gelatin with increased depolymerization and a darker coloration. The color of gelatin is attributed to the Maillardreaction occurring between α-amino groups of amino acids in gelatin and residual carbohydrates in the raw material. At this stage, the gelatins typically have an ash content of 2 to 3%, which can be reduced through ion exchange to eliminate excess salt [210].

The aqueous gelatin solutions are concentrated by evaporation until further concentration

becomes impractical due to increased viscosity, typically reaching concentrations of 20-25% for high molecular weight gelatins and over 40% for low molecular weight varieties. Following concentration and filtration, the gelatin solutions undergo sterilization, employing both indirect methods like plate heat exchangers and direct steam sterilization. After sterilization, the solutions are cooled, leading to gel formation. For powder gelatins, gels are extruded into noodles and dried on conveyor belts using filtered, de-humidified, and microbially clean air. The drying process starts at approximately 30°C and adjusts based on gelatin dryness. The dried noodles are then crushed and milled into blends with particle sizes ranging from 0.1 to 10 mm in diameter. Commercial gelatins typically have moisture content between 8 to 12 %, requiring precise water content determination. Additionally, for use in food, pharmaceuticals, and photography, gelatins must have ash content below 2% to meet regulatory standards [210].

III.3.2. Gelatin Structure and composition

Gelatin is a high-molecular-weight polypeptide originating from the protein collagen, achieved through processes that entail the disruption of cross-linkages between polypeptide chains and the partial cleavage of polypeptide bonds [213]. The process of collagen hydrolysis into gelatin results in the formation of molecules with diverse molecular weights, but each of them is a fragment of the collagen chain from which it was cleaved [214]. Considering this characteristic, gelatin isn't a single chemical compound but rather a blend of fractions, each comprising amino acids connected by peptide bonds. These bonds form low molecular weight polypeptides, represented by the general formula where R_1, R_2, R_3, R_4 (**Figure 16**) denote various radicals. These polypeptides have molecular masses ranging from 15,000 upwards, or they may form aggregates with molecular masses falling within the range of 200,000 to 300,000, Comprising residues of 18 out of the 20 natural amino acids, with the exception of cystine and cysteine, gelatin is often referred to as a biopolymer due to the high molecular values of its constituent polypeptides. In subsequent discussions, we may also use this term to describe gelatin [214]. The gelatin structure is shown in the **Figure 17** and some idea of the average amino acid composition of gelatin is given by the generalized diagram presented in **Figure 17** given from [214, 215].

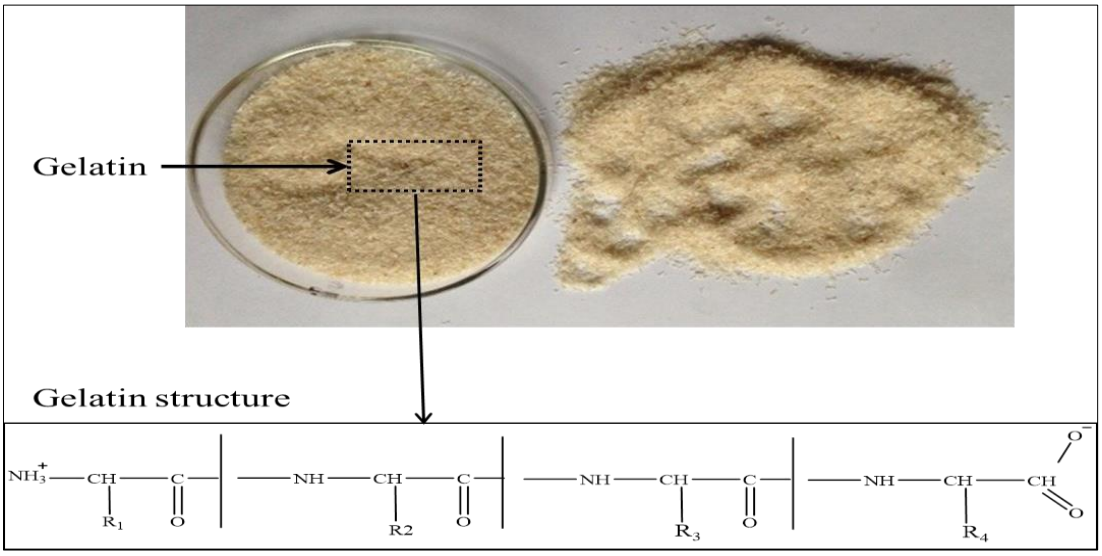

Figure 16. The structural formula of the gelatin.

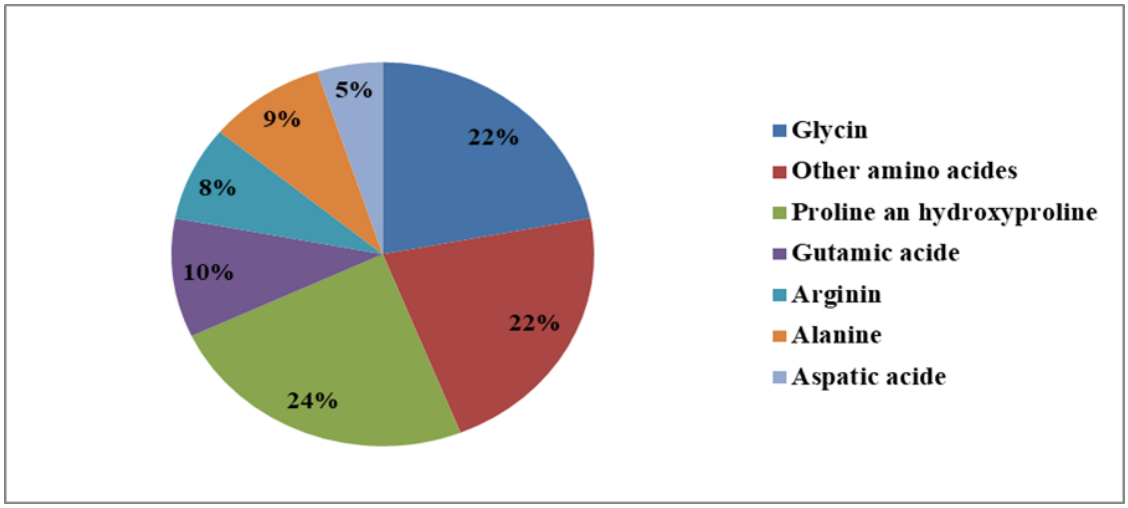

Figure 17. Amino acid composition of gelatin.

III.3.3. Gelatin properties

III.3.3.1. Viscosity

The viscosity of gelatin varies depending on several factors such as its concentration, temperature, and molecular weight distribution of its constituent polypeptides. Generally, as the concentration of gelatin increases, so does its viscosity. Similarly, higher temperatures tend to decrease the viscosity of gelatin solutions. The molecular weight distribution of the polypeptides in gelatin also influences its viscosity, with higher molecular weight fractions contributing to increased viscosity. Overall, gelatin exhibits a range of viscosities depending on its specific formulation and processing conditions [213, 217, 216 and 219].

III.3.3.2. Solubility

The solubility of gelatin is influenced by various factors including temperature, pH, and nature of solvent [218]. Gelatin exhibits excellent solubility in water, particularly at higher temperatures, where it readily forms a homogeneous solution. The solubility of gelatin decreases at lower temperatures, leading to gel formation as the solution cools. Additionally, the solubility of gelatin can be affected by pH, with optimal solubility typically occurring in slightly acidic to neutral conditions. In the presence of certain ions, such as calcium ions, gelatin may exhibit decreased solubility due to the formation of insoluble complexes [216].

III.3.3.3. Gelation

Gelatin exhibits the ability to form gels when heated and then cooled. This gelation behavior is due to the formation of a three-dimensional network of molecules, resulting in the trapping of water molecules within the gel structure. Gelatin's gelation properties find extensive use in the food industry for producing gummy candies, marshmallows, and other confectionery products [212].

III.3.3.4. Hydrophilicity

Gelatin is hydrophilic, meaning it has a high affinity for water. This property allows gelatin to form hydrogels when hydrated, making it useful in applications such as food thickening agents and wound dressings [212, 221].

III.3.3.5. Biodegradability

Gelatin is biodegradable, meaning it can be broken down by biological processes. This property makes gelatin environmentally friendly and suitable for use in applications where biodegradability is desired, such as in biomedical implants and controlled-release drug delivery systems [211].

III.3.4. Gelatin based hydrogels

Gelatin demonstrates superb biocompatibility, plasticity, and adhesiveness, rendering it a highly proficient material for the formation of films and particles [212, 213]. Furthermore, it creates a thermoreversible gel with a melting point near body temperature, a feature of particular significance in applications related to edibles and pharmaceuticals [222]. Gelatin undergoes dissolution in water through heating the solution to around 40 °C, causing collagen chains to exhibit a random coil structure above this temperature. Upon cooling, the aqueous solution undergoes a transition from sol to gel state, contingent on the concentration being sufficiently

high [215, 216]. In addition to its role in the food industry as a gelling agent in desserts, marshmallows, and gummy candies, gelatin finds application in pharmaceuticals for encapsulating drugs in softgel capsules. It is also utilized in photography, cosmetics, and various medical and laboratory settings. The diverse properties of gelatin make it a valuable and widely used biomaterial with a range of industrial and scientific applications.

Gelatin finds extensive utilization across a spectrum of industries, spanning from food production [225] to medical and pharmaceutical sectors [226]. In the realm of tissue engineering and regenerative medicine, gelatin emerges as a promising foundational substance for crafting 'intelligent' hydrogels tailored for drug administration purposes. The growing enthusiasm for gelatin in these domains arises from its array of advantageous attributes, encompassing biocompatibility, biodegradability, affordability, and ease of handling [227]. Moreover, gelatin holds the status of being deemed safe (GRAS) by the US Food and Drug Administration (FDA) for its application in food processing [227]. Moreover, it is a commonplace choice in clinical settings, where it serves as a plasma expander and acts as a stabilizing agent in various protein formulations, including vaccines [228].

Gelatin, a proteinaceous substance primarily composed of denatured and partially hydrolyzed native collagen, notably type I [229], displays limited antigenicity compared to collagen, a result of heat denaturation [230]. Crucially, gelatin preserves key bioactive sequences of collagen, such as the arginine-glycine-aspartic acid (RGD) peptide responsible for cell attachment and matrix metalloproteinase (MMP)-sensitive degradation sites, within its structure [231]. Consequently, gelatin facilitates essential cellular functions like migration, proliferation, and differentiation through integrin-mediated cell adhesion and cell-mediated enzymatic degradation [224, 225]. The main shortcoming of gelatin as a material lies in its poor mechanical properties, limiting its potential applications. These properties are intricately linked to the renaturation level of the protein. However, both mechanical and thermal stability can be significantly enhanced through crosslinking. Chemical crosslinking is particularly advantageous due to the abundance of functional side groups present in gelatin. Common crosslinking agents include glutaraldehyde, genipin, diisocyanates, carbodiimides, and polyepoxy compounds.

III.4. Alginate

Alginates are a significant class of natural polysaccharides extracted from marine brown algae, composed mainly of linear chains of 1,4-linked β-D-mannuronate (M) and 1,4-linked α-L-guluronate (G) residues and their sodium salts [233, 235]. These two different repeating

monomers could form regions with varying proportions of M residues (MM blocks), G residues (GG blocks), or alternating M and G structures (MG blocks) [236, 238]. The source and species that produce the alginate may specify the M and G residues in the alginate chain as well as the physical properties of the polymers [40]. Thanks to the excellent biocompatibility [76], biodegradability and immunogenicity, non-toxicity, and functional groups [77], the alginate has been widely used in biomedical such as drug carrier material [78], tissue engineering [18], controlled-release [236], as well as cell immobilization [237].

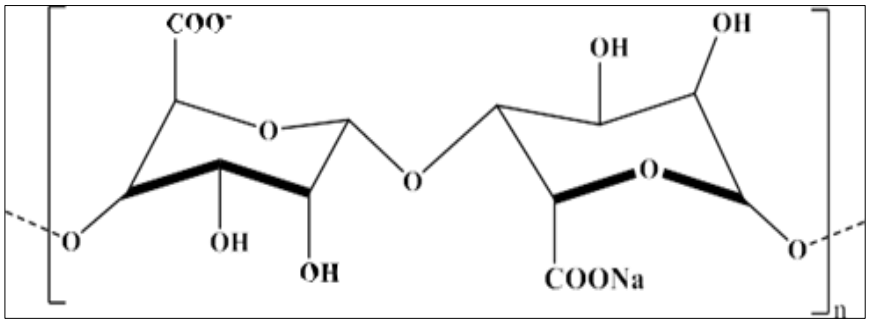

Figure 18. Schematic of chemical structure of sodium alginate molecule.

III.4.1. Periodate oxidation of sodium alginate

Periodate oxidation is an important reaction for polysaccharides modifications. Sodium alginate can be modified by the oxidation reaction using sodium periodate as oxidizing agent in an aqueous solution. The oxidized alginate molecular weight decreased [233], its reactivity and biodegradability were improved, and the application fields increased [238, 239]. The modification by oxidation of sodium alginate with sodium periodate (**Figure 19**) occurs by cleaving the dihydroxyl groups at C-2 and C-3 vicinal bonds in the uronic units forming dialdehyde groups on the alginate chains [235]. In the ring-opening reaction, aldehyde groups can be generated by selective cleavage of carbon-carbon bonds in the uronic residues resulting in a decline of the alginate molecular weight [234, 240]. The higher reactivity of the dialdehyde product occurs as a spontaneous interaction between the aldehyde groups and vicinal hydroxyl groups present on the unoxidized residues. The intramolecular and intermolecular hemiacetals that can reduce aldehyde groups' content are formed [63]. Moreover, Painter obtained that alginate possessed limited oxidation of close to 50% due to the formation of stable inter-residue hemiacetals [63]. The periodate oxidation of alginate was one of the most extensively studied oxidation. Gomez et al. oxidized the sodium alginate using sodium periodate at room

temperature for 24 hours in the dark. This oxidation resulted in a decline in the alginate stiffness by breaking the C2–C3 bond with a backbone scission as a simultaneous reaction. The molecular weight also decreased rapidly until the oxidation degree is of 10 % and then remained nearly constant. Until this oxidation degree, they observed that gel was not formed in the presence of calcium excess [44].

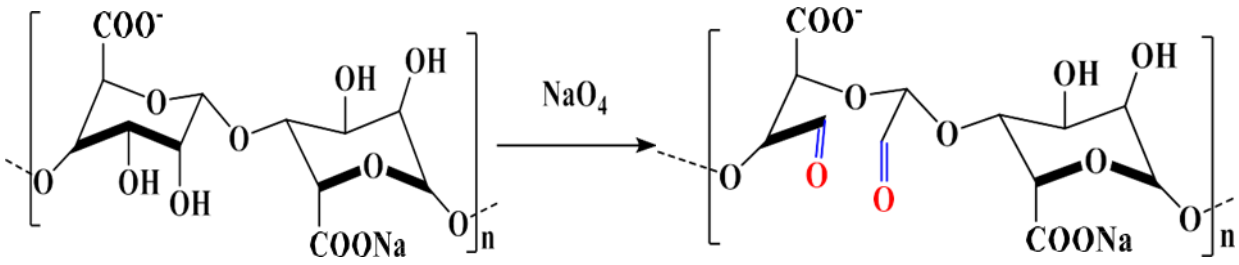

Sodium Alginate 0xidized Sodium Alginate

Figure 19. Oxidation of sodium alginate.

Ding et al. [235] synthesized oxidized sodium alginate with different sodium periodate concentrations. After that, the samples were further fractionated by graded ethanol precipitation to obtain four oxidized sodium alginate fractions with a narrower molecular weight range.

The structure and properties of OSA samples and fractions were characterized using different methods. Then the cross-linking performances of oxidized sodium alginate/fractions on collagen fiber were investigated. Generally, they observed that the molecular weight of oxidized sodium alginate plays a decisive role in improving the properties of the cross-linked collagen fiber [235].

Balakrishnan et al. [239], examined the oxidation of sodium alginate in the aqueous solution and in a 1:1 ethanol-water mixture. They compared the oxidation in these two different media to obtain a higher quantity of the oxidized product with a minimum amount of solvent in one reaction. The results show a similarity in the oxidation kinetic and facile oxidation in both mediums. Moreover, the cleavage of the dihydroxyl groups in the oxidation reaction occurs in both media, but it was extensive in the ethanol-water medium, and the product yield was higher in this medium than in water. One noteworthy advantage of oxidizing the alginate in adispersion for this study lies in its ability to yield larger quantities of the oxidized product with higher efficiency, while also consuming less solvent, making it an attractive approach for large-scale applications [239].

III.5. Hydrogels base on gelatin cross-linked with oxidized sodium alginate

Hydrogels based on gelatin cross-linked with oxidized sodium alginate represent a sophisticated biomaterial platform with a wide range of applications [215]. Gelatin, derived from collagen, offers excellent biocompatibility and contains bioactive sequences crucial for cellular functions like adhesion, proliferation, and differentiation [240]. However, gelatin's inherent poor mechanical properties limit its utility in certain applications.To address this limitation, researchers have turned to cross-linking strategies, leveraging the unique properties of oxidized sodium alginate. Sodium alginate is a natural polysaccharide derived from seaweed, known for its biocompatibility and biodegradability. When oxidized, sodium alginate gains additional functional groups, enhancing its cross-linking potential with gelatin.The cross-linking process typically involves the reaction between the aldehyde groups of oxidized sodium alginate and the amino groups of gelatin, forming stable covalent bonds (**Figure 20**). This chemical bonding results in the formation of a three-dimensional network within the hydrogel matrix, significantly improving its mechanical strength and stability.Moreover, the incorporation of oxidized sodium alginate allows for precise tuning of the hydrogel's properties, such as porosity, swelling behavior, and degradation kinetics, by adjusting the cross-linking density and degree of oxidation.

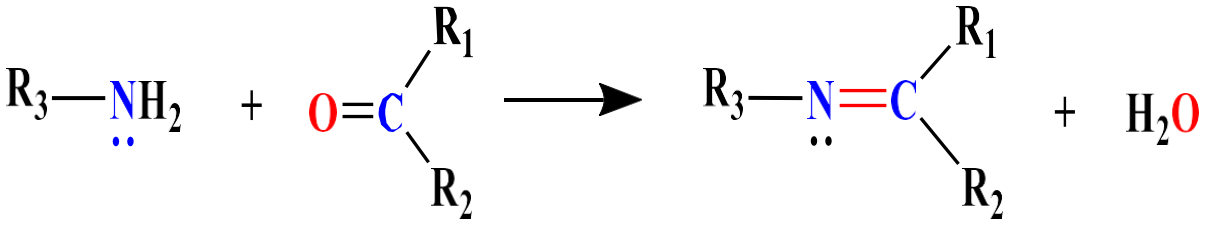

Figure 20. Reaction of an amino group with an aldehyde group.

These gelatin-based hydrogels cross-linked with oxidized sodium alginate find applications in various biomedical fields. In tissue engineering, they serve as scaffolds to support cell growth and tissue regeneration. Their controlled release properties make them ideal candidates for drug delivery systems, where therapeutics can be encapsulated within the hydrogel matrix and released in a controlled manner over time. Furthermore, the biocompatibility and tunable properties of these hydrogels make them promising candidates for other applications, including wound healing, cartilage repair, and 3D cell culture systems.

III.5.1. Gelatin/oxidized sodium alginate hydrogels properties

Both gelatin and sodium alginate hydrogels are widely studied in biomedical and

pharmaceutical fields due to their biocompatibility and tunable properties. When combined, their properties can be further modified to suit specific applications. Here are some key properties of gelatin and oxidized sodium alginate hydrogels:

III.5.1.1. Biocompatibility

Gelatin/ oxidized sodium alginate hydrogels demonstrate exceptional biocompatibility, rendering them invaluable materials in various biomedical applications. Derived from natural sources, gelatin originates from collagen found abundantly in animal tissues, while sodium alginate is extracted from seaweed. This natural origin substantially diminishes the likelihood of adverse immune reactions or toxicity, making these hydrogels inherently safer for use within the body. Furthermore, their biodegradability ensures that they can be broken down into harmless byproducts through enzymatic or hydrolytic processes, eliminating concerns associated with long-term implantation. Crucially, these hydrogels provoke minimal inflammatory responses when implanted in vivo, owing to their natural composition and the biocompatible nature of their degradation products. This characteristic not only reduces the risk of adverse reactions but also fosters an environment conducive to tissue regeneration and healing [42]. Gelatin and sodium alginate hydrogels also offer an ideal milieu for cellular interactions, supporting attachment, proliferation, and differentiation. Through careful adjustment of parameters such as crosslinking density, composition, and degradation kinetics, their biocompatibility can be further tailored to meet specific biological requirements, ensuring their suitability for a diverse array of biomedical endeavors. Thus, the biocompatibility of gelatin and oxidized sodium alginate hydrogels underscores their pivotal role in advancing fields such as tissue engineering, regenerative medicine, drug delivery, and cell therapy….etc.

III.5.1.2. Hydrophilicity

Gelatin/oxidized sodium alginate hydrogels are characterized by their hydrophilicity, a fundamental property influencing their performance in aqueous environments. These hydrogels possess hydrophilic functional groups that readily interact with water molecules through hydrogen bonding [241]. This interaction facilitates the absorption and retention of water within the hydrogel matrix, leading to swelling. The extent of swelling can be controlled by factors such as polymer concentration and crosslinking density [242]. Hydrophilicity also impacts the mechanical properties of the hydrogels, enhancing their flexibility while maintaining softness. In biomedical applications like drug delivery and tissue engineering, the hydrophilic nature of these hydrogels enables controlled release of water-soluble molecules and provides a hydrated

microenvironment conducive to cell growth and tissue regeneration. Understanding and leveraging the hydrophilic properties of gelatin and oxidized sodium alginate hydrogels are crucial for designing biomaterials tailored to specific applications in medicine and biotechnology.

III.5.1.3. Biodegradability

Gelatin/ oxidized sodium alginate hydrogels are characterized by their significant biodegradability, making them valuable in biomedical contexts. This property allows for gradual degradation through enzymatic or hydrolytic processes, eliminating the need for surgical removal post-application. The degradation rate can be controlled by adjusting factors such as polymer concentration and crosslinking density. In tissue engineering, their biodegradability supports temporary scaffolds, facilitating tissue regeneration without the risk of chronic inflammation. Additionally, in drug delivery systems, the gradual degradation of these hydrogels enables sustained release of therapeutic agents, minimizing systemic toxicity. Overall, the biodegradability of gelatin and oxidized sodium alginate hydrogels offers a versatile solution for various biomedical applications, providing controlled degradation alongside biocompatibility and therapeutic efficacy [245, 246].

III.5.1.4. Controlled Release

Gelatin/ oxidized sodium alginate hydrogels are highly effective in facilitating controlled release of bioactive substances, making them invaluable in drug delivery systems. Through careful manipulation of various factors, including polymer composition, crosslinking density, drug encapsulation methods, hydrogel structure, and environmental stimuli, these hydrogels offer precise modulation of release kinetics. Their controlled release mechanism allows for tailored drug delivery profiles, optimizing therapeutic efficacy while minimizing potential side effects. The composition of the hydrogel, its crosslinking density, and the method of drug encapsulation all contribute to determining the release kinetics. Additionally, hydrogel morphology and response to environmental stimuli further enhance their versatility in drug delivery applications [247, 248].

III.5.1.5. Cell Compatibility

Gelatin cross-linked oxidized sodium alginate based hydrogels exhibit exceptional compatibility with cells, positioning them as valuable biomaterials in various biomedical applications, particularly in tissue engineering and regenerative medicine. Derived from natural sources, gelatin from collagen and sodium alginate from seaweed, these hydrogels provide a biologically relevant environment for cell growth and function. Their hydrophilic nature

promotes cell adhesion, spreading, and proliferation, while their porous structure enhances nutrient and oxygen diffusion to encapsulated or seeded cells, mimicking the native tissue microenvironment. Furthermore, the tunable properties of these hydrogels, including crosslinking density, composition, and degradation rate, allow for customization to match specific cellular requirements. Surface modifications can also be employed to incorporate bioactive molecules or cell-adhesive peptides, further enhancing cell compatibility and promoting desired cellular responses. Overall, gelatin and oxidized sodium alginate hydrogels serve as versatile platforms for supporting cell viability, proliferation, and differentiation, paving the way for advancements in tissue engineering, drug delivery, and regenerative therapies [248, 250].

III.6. Conclusion

Hydrogels formed from oxidized alginate and gelatin cross-linked via Schiff base chemistry offer a versatile platform for various biomedical applications due to their unique properties. Oxidized alginate, derived from alginate, undergoes partial oxidation to introduce aldehyde functional groups, enabling Schiff base cross-linking with amino groups of gelatin. This cross-linking mechanism allows for control over the gel's mechanical strength, swelling behavior, and degradation rate, crucial factors for specific biomedical uses.

The resulting hydrogels exhibit excellent biocompatibility, promoting cell adhesion, proliferation, and differentiation, which are essential for tissue engineering applications. Their porous structure and high water content resemble the natural extracellular matrix, facilitating nutrient exchange and waste removal. Furthermore, the hydrogels can be tailored to mimic the biochemical and biomechanical cues of specific tissues, enhancing their ability to support tissue regeneration.

Despite these advantages, challenges remain in optimizing hydrogel properties for specific biomedical applications. Further research is needed to enhance mechanical strength, fine-tune degradation kinetics, improve long-term stability, and investigate in vivo biocompatibility and therapeutic efficacy. Additionally, the scalability and cost-effectiveness of production methods should be considered to facilitate translation from bench to bedside. Overall, hydrogels based on oxidized alginate/gelatin cross-linked by Schiff base crosslinking hold great promise for advancing biomedical technologies and addressing unmet clinical needs.

PART II: METHODS AND MATERIALS

CHAPTER IV:
Experimental Work

Chapter IV: Experimental work

IV.1. Introduction

This chapter presents the methods and materials used for the preparation and characterisation of hydrogels based on oxidised sodium alginate (OSA) and gelatin. The process involves two main steps: the preparation of OSA, followed by the formation of hydrogels films by combining OSA and gelatin. During this work/action, various analytical techniques were used, including Fourier transform infrared spectroscopy (FTIR), nuclear magnetic resonance spectroscopy (NMR) and thermogravimetric analysis (TGA), to study the chemical structure and thermal stability of OSA and sodium alginate (SA). In addition, the oxidation kinetics were monitored, the quantification of aldehyde groups and the effects of temperature were evaluated. For the hydrogels, scanning electron microscopy (SEM), FTIR and GTA were used to analyse their morphology, structure and thermal stability. Further characterisation includes measurement of amino group conversion index (CI %), assessment of swelling behaviour, encapsulation efficiency, release kinetics and antioxidant activity. This comprehensive analysis provides valuable information on the properties and potential applications of these hydrogel systems in biomedical fields.

IV.2. Methods and materials

IV.2.1. Materials

Medium molecular weight Gel type A, native sodium alginate (SA) were purchased from Sigma Aldrich; Pro solution (30%) was a gift from Apitherapy, Tween 80, p-coumaric acid (PCA), sodium meta periodate, ninhydrin, glutamic acid, dialysis membrane with pores of 14kDa were purchased from Sigma Aldrich, sodium thiosulfate, acetic acid, potassium iodide, sodium chloride, disodium phosphate, monosodium phosphate, ethanol, sodium hydroxide (NaOH), were purchase from chemical Company, Iași, Romania

IV.2.2. Methods

IV.2.2.1. Oxidized sodium alginate (OSA) Preparation

The oxidized sodium alginate (OSA) was prepared by utilizing $NaIO_4$ as an oxidizing agent and bi-distilled water as a solvent (**Figure 21**). Initially, 2 g of native sodium alginate was

dissolved in 100 mL of bi-distilled water at 80 °C. The resulting solution was then transferred into a 250 milliliter flask and allowed to cool to 30 °C. Meanwhile, 1.5 g of $NaIO_4$ was dissolved in 20 mL of bi-distilled water at room temperature and added dropwise to the sodium alginate solution at 30°C. The oxidation reaction occurred in the absence of light for duration of 24 hours.

Subsequently, the resulting solution underwent purification through dialysis against deionized ultra-pure water. Cinq changements d'eau bi-distillée sur une période de trois jours ont été réalisés au cours de la dialyse. A la fin, la solution purifiée a été lyophilisée pour obtenir l'OSA.

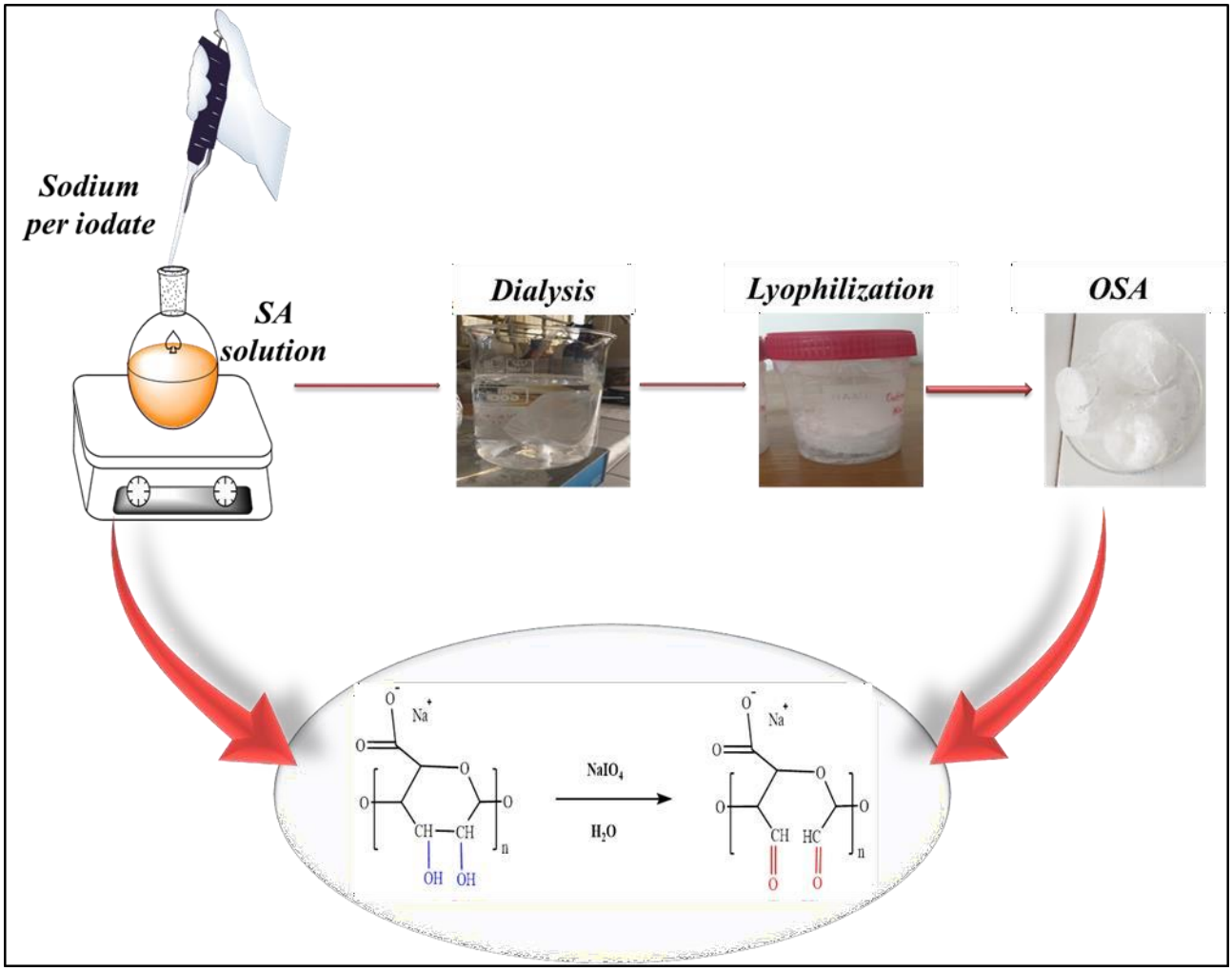

Figure 21. Protocol for the preparation of oxidized sodium alginate (OSA).

IV.2.2.2. Hydrogel Films Based on Gelatin and OSA Preparation

The hydrogels based on gelatin/oxidized sodium alginate (G/OSA) were prepared by combining OSA and gelatin at varying -CHO/-NH2 molar ratios (0.5:1; 0.75:1; 1:1; 1.5:1 mol/mol) in acetate buffer solution (ABS) at two different pH levels (pH = 5.5 and 3.7), as depicted in **Figure 22**.

Initially, a specified amount of OSA was dissolved in ABS solution at 80 °C for 30 minutes. Subsequently, 1.2 mL of a 5 % w/v Mg^{2+} aqueous solution was introduced to facilitate the interaction with carboxyl groups (COO-) within the oxidized sodium alginate chains. The mixture underwent ultrasonic treatment for 15 minutes to ensure thorough mixing.

Concurrently, 0.2 g of gelatin was dissolved in 2 mL of ABS at 40 °C. The resulting gelatin solution was then added dropwise to the OSA solution and stirred for a period of 6 hours. On the other, 3g of glycerin was incorporated to impart flexibility and prevent fragility in the resulting hydrogel

To produce hydrogels films, the polymer solution was poured into Petri dishes with a diameter of 9 cm and allowed air-dried to at room temperature. Once dried, the films were carefully removed from the Petri dishes and at room temperature for subsequent analysis. The experimental program used to obtain covalently cross-linked G/OSA based hydrogel films in ABS pH=5.5 is given by the table 2.

Table 2. Experimental program used to obtain covalently cross-linked G/OSA based hydrogel films in ABS pH = 5.5.

Samples Codes*	**Molar ratio -CHO/-NH_2**	**Number of moles of -CHO*10^{-4}**
PA1 (PB1)	0.5/1	1.69
PA2 (PB2)	0.75/1	2.535
PA3 (PB3)	1/1	3.38
PA4 (PB4)	1.5/1	5.07

*The number of moles of CHO, and the molar report CHO: NH_2 were the same for the hydrogels which prepared in ABS at pH medium of 3.7, they coded PB1, PB2, PB3, PB4. The films containing propolis and containing the same molar ratios prepared at ABS pH of 5.5 and 3.7 were coded with PAP1, PAP2, PAP3, PAP4, and PBP1, PBP2, PBP3, PBP4 respectively.

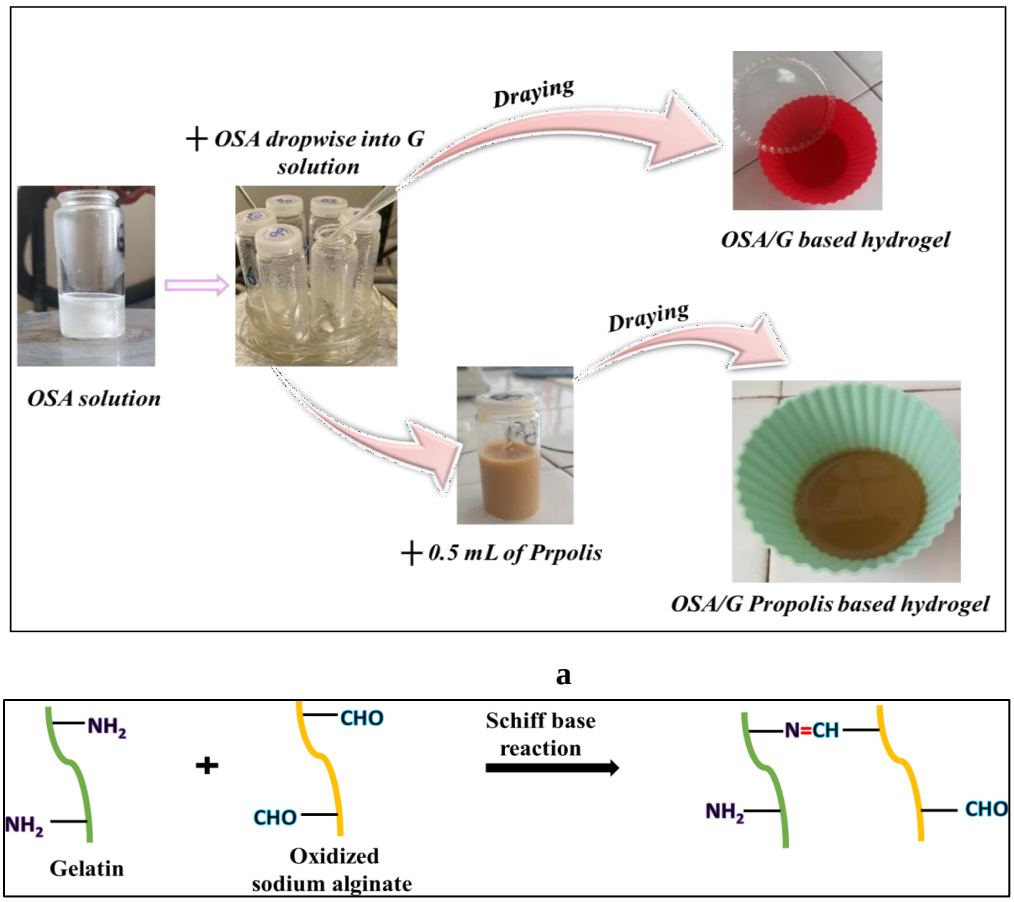

a

b

Figure 22. Schematic illustration of (a) experimental work of gelatin/ OSA based hydrogel preparation (b) Reaction of Schiff base formation between NH2 of gelatin and CHO of OSA.

IV.3. Characterizations methods

The characterization of oxidized sodium alginate (OSA) and sodium alginate (SA) involved a comprehensive array of analytical techniques. Fourier Transform Infrared (FTIR) Spectroscopy, Nuclear Magnetic Resonance (NMR) Spectroscopy, and Thermogravimetric Analysis (TGA) were employed to assess the chemical structure and thermal stability of both materials.

Additionally, quantification of aldehyde groups, investigation of oxidation kinetics, and examination of temperature effects were conducted to gain insights into the modification process.

Hydrogels with varying compositions and under different pH conditions were subjected to thorough characterization utilizing a variety of analytical methods. Scanning Electron Microscopy (SEM), FTIR spectroscopy, and TGA were employed to analyze the morphology, structure, and thermal stability of the hydrogels. Furthermore, the determination of the Amino Groups' Conversion Index (CI %), assessment of swelling behavior, evaluation of encapsulation efficiency, release kinetics, and antioxidant activity studies were performed to elucidate the properties and performance of the hydrogel formulations.

IV.3.1. Comprehensive Characterization of Oxidized Sodium Alginate (OSA), Sodium Alginate (SA), and Gelatin for Hydrogel Formulation

IV.3.1.1. Fourier-Transform Infrared Spectroscopy

The FTIR analysis aimed to elucidate the chemical structure of both sodium alginate (SA) and oxidized sodium alginate (OSA). Using a Bruker Vertex FTIR spectrophotometer (Billerica, MA, USA), spectral data were collected over a range of wavenumbers from 400 to 4000 cm^{-1}. To ensure uniformity and accuracy in measurements, SA and OSA samples were prepared as KBr pellets. This preparation method facilitates consistent spectral recordings and enables detailed analysis of functional groups and molecular vibrations within the samples.

IV.3.1.2. Nuclear magnetic resonance spectroscopy of SA and OSA

^{1}H NMR spectra were obtained using a Bruker NEO 1-400 NMR spectrometer (Billerica, MA, USA) to elucidate the molecular structure of sodium alginate (SA) before and after oxidation. The samples (SA and OSA) were dissolved in deuterium oxide (D_2O) prior to analysis, with ^{1}H NMR employed for detailed molecular characterization.

IV.3.1.3. Quantification of Aldehyde Groups in OSA

To determine the content of aldehyde groups in the resulting oxidized sodium alginate (OSA), a modified protocol based on Dellali and al. [40], was employed. The amount of aldehyde groups present in OSA was indirectly quantified through a titration method using residual sodium periodate, as described by Lange in 1961.

In this context, a 1 mL volume of the OSA solution obtained from the oxidation reaction mixture was added to a mixture containing 1 mL of 20 % KI solution and 1 mL of 37 % HCl in a beaker. The formation of iodine (I_2) was then titrated with 0.05 N $Na_2S_2O_3$ until the endpoint was reached. At the endpoint, the solution changed from blue to transparent, indicating the disappearance of iodine. This transition was visualized by the addition of 1 mL of starch solution.

Through the titration reaction, the amount of unreacted sodium periodate in the oxidation reaction was determined by subtracting the amount of $NaIO_4$ that remained unreacted from the initial amount added. To calculate the number of moles of aldehyde groups produced in the reaction, the stoichiometry of the reaction had to be taken into account. Since it takes 1 mole of $NaIO_4$ to produce 2 moles of aldehyde groups in oxidized sodium alginate, this ratio was utilized in the calculation.

IV.3.1.4. Oxidation kinetics and temperature effect studies

The kinetics of the oxidation reaction was investigated at a temperature of 30 °C. Initially, 100 mL of an aqueous solution containing 2 % w/v sodium alginate (SA) was prepared. The oxidation reaction was initiated by adding a calculated amount of sodium periodate ($NaIO_4$) with a 1:1 molar ratio of SA to $NaIO_4$, ensuring an excess of 34 % of sodium periodate, into the reaction flask. The reaction mixture was kept in a dark environment to prevent photochemical reactions. At hourly intervals over a period of 72 hours, 1 mL samples of the reaction mixture were withdrawn and titrated with sodium thiosulfate ($Na_2S_2O_3$) to monitor the progress of the oxidation reaction. The titration allowed for the determination of the amount of unreacted $NaIO_4$, indicating the extent of the oxidation reaction.The degree of oxidation (OD) was calculated using equation (1), where OD represents the extent of conversion of SA to oxidized sodium alginate (OSA) over time.

$$OD\ \% = \frac{M_R}{M_T} \qquad (\mathbf{1})$$

Where $M_{R,}$ and M_T represent the amount of $NaIO_4$ reacted and $NaIO_4$ total amount respectively.

To explore the influence of temperature on the performance of the oxidation reaction, a similar protocol to the kinetic studies was followed. However, in this experiment, the samples were prepared at different temperature settings ranging from 25 to 45 degrees Celsius (T °C) and maintained for duration of 24 hours. Following the preparation of each sample, 1 mL of the reaction mixture from each temperature setting was collected and subjected to titration with

sodium thiosulfate ($Na_2S_2O_3$). This process allowed for the determination of the extent of the oxidation reaction at each temperature condition.

IV.3.1.5. Thermogravimitric property

The thermal properties of sodium alginate (SA), oxidized sodium alginate (OSA), gelatin, and propolis were examined using a TA Instruments model TGA Q500. These experiments were carried out under a nitrogen atmosphere to prevent oxidation, with a dynamic heating rate of 10 °C min^{-1}.The temperature range for the analyses spanned from 20 to 800 °C. Alumina was utilized as the reference material throughout the experiments to ensure accurate temperature calibration and measurement.

IV.3.1.6. Gelatin Amino Groups' determination

The ninhydrin test was used to assess the concentration of amino groups in gelatin. A stock solution of 0.1% (w/v) glutamic acid in acetic acid was prepared to establish a calibration curve. This involved pouring 10 mL of the solution into a 100 mL flask and adding acetate buffer solution (pH = 5.6, 0.1 M) to mark the flask. Various volumes were withdrawn from this solution to prepare six concentrations of glutamic acid ranging from 0.04 to 0.1 mg/mL, each brought to volume with acetate buffer solution (pH = 5.6) in 5 mL volumetric flasks. For the ninhydrin test, 1 mL of each prepared glutamic acid solution with different concentrations was mixed with 2 mL of 2% ninhydrin solution in ethanol in test tubes. The mixtures were heated at 95°C for 30 minutes, resulting in a dark blue coloration. After cooling, a mixture of 8 mL ethanol and distilled water (1:1 volume ratio) was added to each tube. To calibrate the spectrophotometer, a blank solution without glutamic acid was prepared by adding 1 mL of acetate buffer (pH = 5.6) instead. Absorbances of all solutions were measured at 570 nm using a UV spectrophotometer. Finally, the initial concentrations of the solutions in mg/mL were converted to molar concentrations, indicating the number of moles of amino groups per milliliter (**Figure 23**).

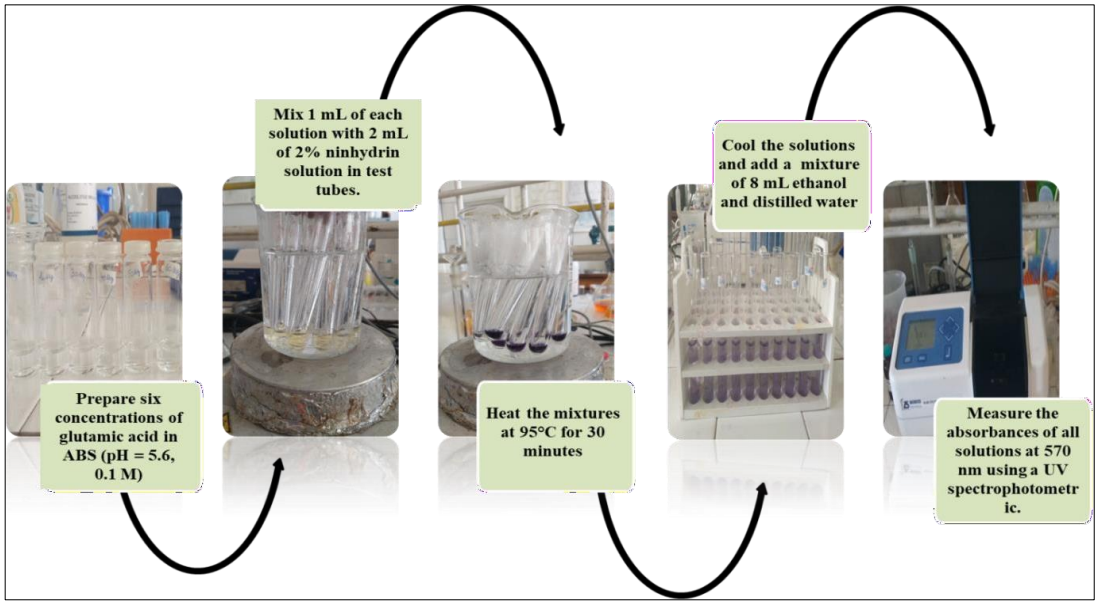

Figure 23. Experimental protocol for Gelatin Amino**.**

IV.3.2. Comprehensive Characterization of the fabricated hydrogels

IV.3.2.1. Fourier-Transform Infrared Spectroscopy

FTIR analysis was conducted to elucidate the chemical structure of gelatin/SA, gelatin/OSA, and gelatin/OSA propolis based hydrogels. Spectra were obtained using a Bruker Vertex FTIR spectrophotometer (Billerica, MA, USA). Samples were prepared as KBr pellets and analyzed over wavenumbers ranging from 400 to 4000 cm^{-1} at room temperature, with a resolution of 4 cm^{-1}.

IV.3.2.2. Thermal property

The thermal properties of SA/gelatin, OSA/gelatin, and OSA/gelatin/propolis hydrogels were investigated using a TA Instruments model TGA Q500. The experiments were performed under a nitrogen atmosphere with a dynamic heating rate of 10 °C min^{-1}. Analysis was conducted over a temperature range of 20 to 800 °C, with alumina serving as the reference material for the experiments.

IV.3.2.3. Scanning Electron Microscopy

The surface morphology of hydrogel films was examined using scanning electron microscopy (SEM) after drying and gold metallization achieved via spray deposition. Analysis

was conducted using a HITACHI SU 1510 electron microscope (Hitachi SU-1510, Hitachi Company, Chiyoda City, Tokyo, Japan).

IV.3.2.4. The Amino Groups' conversion index (CI %) Determination into Schiff Bases in Hydrogel Films

The ninhydrine test was deemed essential for assessing the concentration of unbound amino groups within the obtained films. The method described for constructing the glutamic acid calibration curve was applied in this study to standardize the experimental procedure. Fragments of the films were weighed and placed into test tubes, followed by the addition of 1 mL of 0.1 M acetate buffer with pH = 5.6 and 2 mL of 2% ninhydrine solution. After allowing the mixture to incubate at room temperature for one hour to ensure ninhydrin penetration into the films, it was then heated at 95°C for 30 minutes. Subsequently, upon cooling, an 8 mL mixture of ethanol and distilled water in a 1:1 volume ratio was introduced. The absorbance of the resulting solution was measured at 570 nm wavelength. The concentration of unbound amino groups in the hydrogel films was determined utilizing the previously established glutamic acid calibration curve. This facilitated the computation of the total number of amino groups involved in the formation of Schiff bases, utilizing the difference between the total moles of free amino groups initially added in the reaction (**Figure 24**). The conversion index was calculated using equation (2):

$$CI\ \% = \frac{N_a\ -\ N_b}{N_a} \times 100 \qquad (2)$$

Where N_a refers to the number of moles of free amino groups present before cross-linking, while N_b represents the number of moles of free amino groups present after cross-linking, The difference between N_a and N_b represents the number of amino groups that have formed covalent bonds within the hydrogel film.

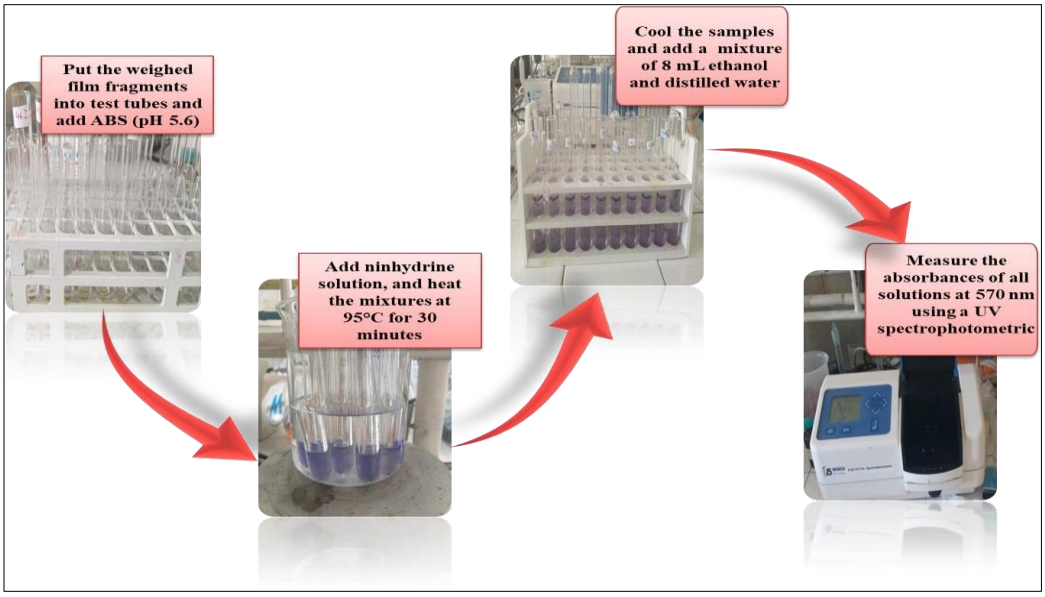

Figure 24. The amino groups' determination into Schiff bases in hydrogel films protocol.

IV.3.2.5. Swelling behavior of OSA/ gelatin based hydrogels

To evaluate the capacity of the OSA/gelatin hydrogels to absorb and retain aqueous medium without dissolution, a swelling degree experiment was conducted. This characteristic holds importance as it directly influences the diffusion rates of the active ingredient from the hydrogel matrix.

To investigate the swelling behavior of the samples, we employed a conventional gravimetric approach using buffer solutions mimicking physiological fluids: phosphate buffer at pH = 7.4 and acetate buffer resembling skin pH at pH = 5.5. The detailed procedure involved: accurately weighing dried hydrogel samples (W dry) and immersing them in 5 mL of solutions with varying pH values at 37°C. At different time intervals, the samples were removed from the solution, excess water was blotted off using filter paper, and the weight of the swollen films (W swelling films) was measured. Subsequently, the samples were returned to the solution. This process continued at regular intervals until equilibrium was achieved. The difference between the weight of the swollen films (W swelling films) and the weight of the dry films (W dry) represented the amount of solution absorbed by the hydrogels (W solution). The degree of swelling was determined by calculating the ratio of the solution retained by the films at each time interval to the weight of the completely dry film, as indicated by Equation (3).

$$Q\ \% = \frac{W_{solution}}{W_{dry}} \times 100 \qquad (3)$$

IV.3.3. Encapsulation Efficiency

To anchor the propolis within the hydrogel matrix, the propolis was initially characterized by High-Performance Liquid Chromatography (HPLC) [39], to analyze its composition. The composition of propolis is outlined below:

A solution consisting of 500 μL of propolis liquid, containing 22.75 mg of para-coumaric (PCA) acid, was incorporated into the polymer solution. The mixture was then subjected to an ultrasonic bath at 37 °C for 30 minutes. Subsequently, the solution was transferred into Petri dishes and left to dry for 48 hours.

Because of the intricate composition of propolis, determining its encapsulation and release presents practical challenges. However, researchers have indeed assessed the quantity of p-coumaric acid, which is the principal component in propolis' composition.

To ascertain the quantity of propolis that remained unimmobilized, the content of para-coumaric acid (PCA) from the hydrogels was quantified. However, before proceeding, it was necessary to establish a PCA calibration curve (**Figure 25**). The procedure was as follows: 5 mg of PCA was dissolved in 10 mL of 1 % tween solution, prepared in ABS pH = 5.5 and PBS pH = 7.4. This mixture was then transferred into a 50 mL flask and brought to a total volume of 50 mL with 1% tween solution. Seven different concentrations of PCA ranging from 0.01 to 0.05 mg/mL were prepared using varying volumes. The absorbances of these solutions were measured using a UV spectrophotometer at wavelengths of 299 nm for ABS pH = 5.5 and 287 nm for PBS pH = 7.4. The resulting calibration curve illustrates absorbance plotted against the concentration of PCA.

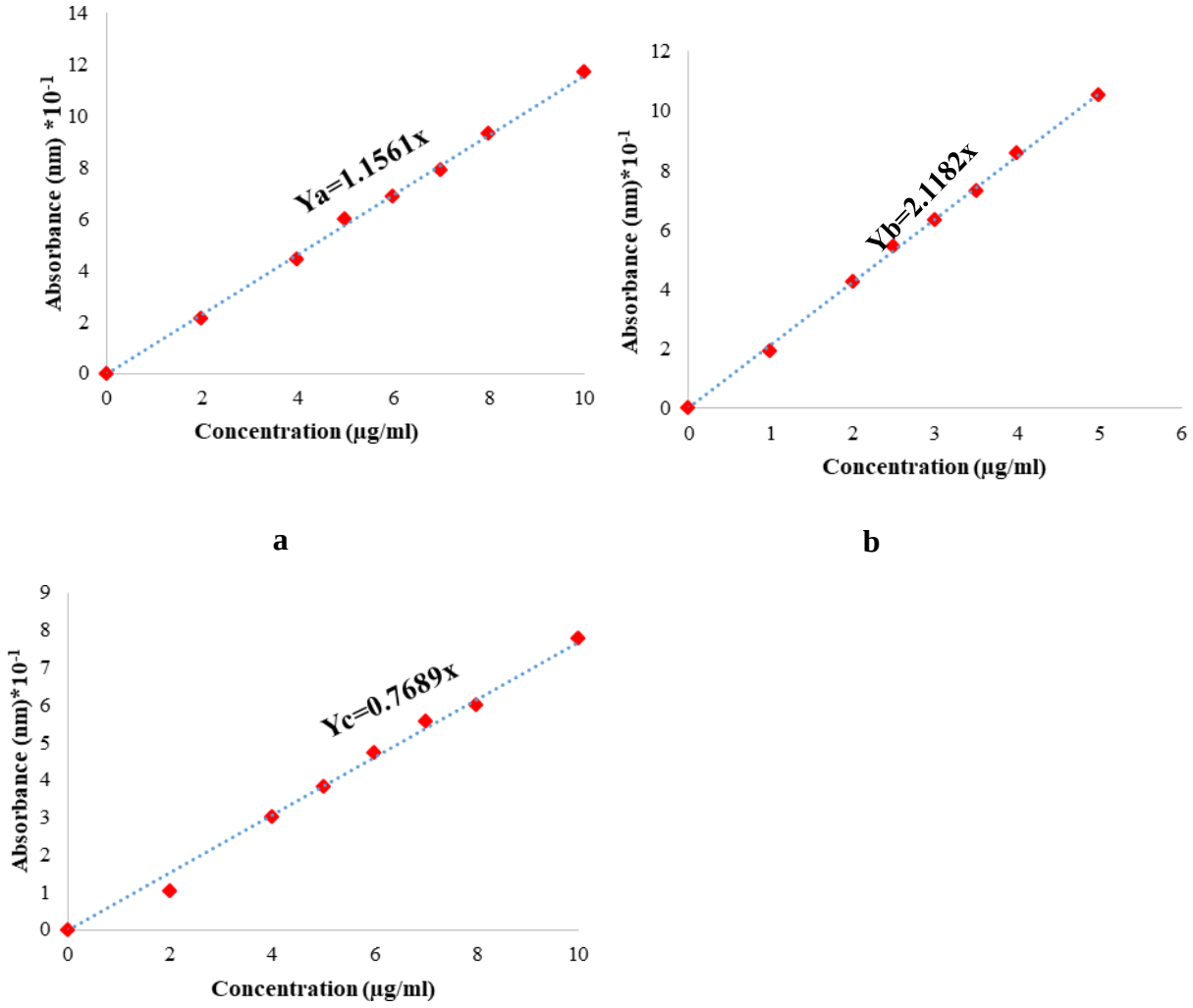

Figure 25. Calibration curve of p-coumaric acid in: (a) tween of pH 7.4 (y_a = 1.1561x); (b) tween of pH 5.5 (y_b = 2.1182x); (c) ethanol (y_c = 0.7689x).

In order to determine the propolis quantity that was not immobilized, a fragment of each film was immersed into 1mL of bi-distilled water for one hour, after that 10 mL of ethanol was added and stirred for 24 hours at 37 °C (**Figure 26**). After wile, the absorbances of the solutions in which the fragments were immersed were measured using Nano Drop UV-spectroscopy at wavelength of 311 nm.

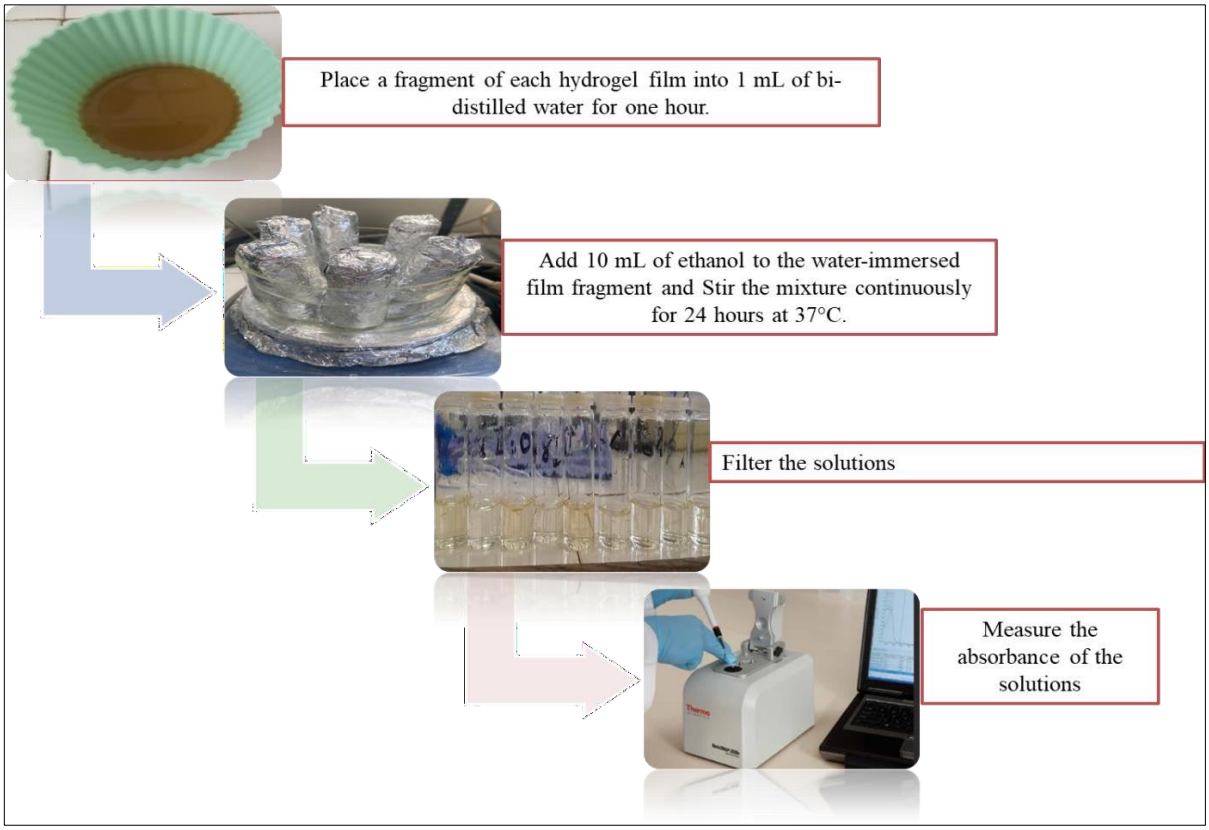

Figure 26. Encapsulation efficiency experimental work.

IV.3.4. Release efficiency

To assess the release efficiency of propolis immobilized within the hydrogel matrix, a fragment of the dried film was immersed in separate tubs containing 20 mL of buffer solutions, specifically ABS at pH=5.5 and PBS at pH=7.4. Over time, samples of 0.250 mL volume were periodically withdrawn (**Figure 27)**. To maintain a consistent volume for all samples, 3 mL of buffer solution was added after each withdrawal.

The amount of propolis released was determined spectrophotometrically, leveraging the para-coumaric acid (PCA) calibration curves previously established in the respective buffer solutions. This allowed for accurate quantification of the released propolis content**.**

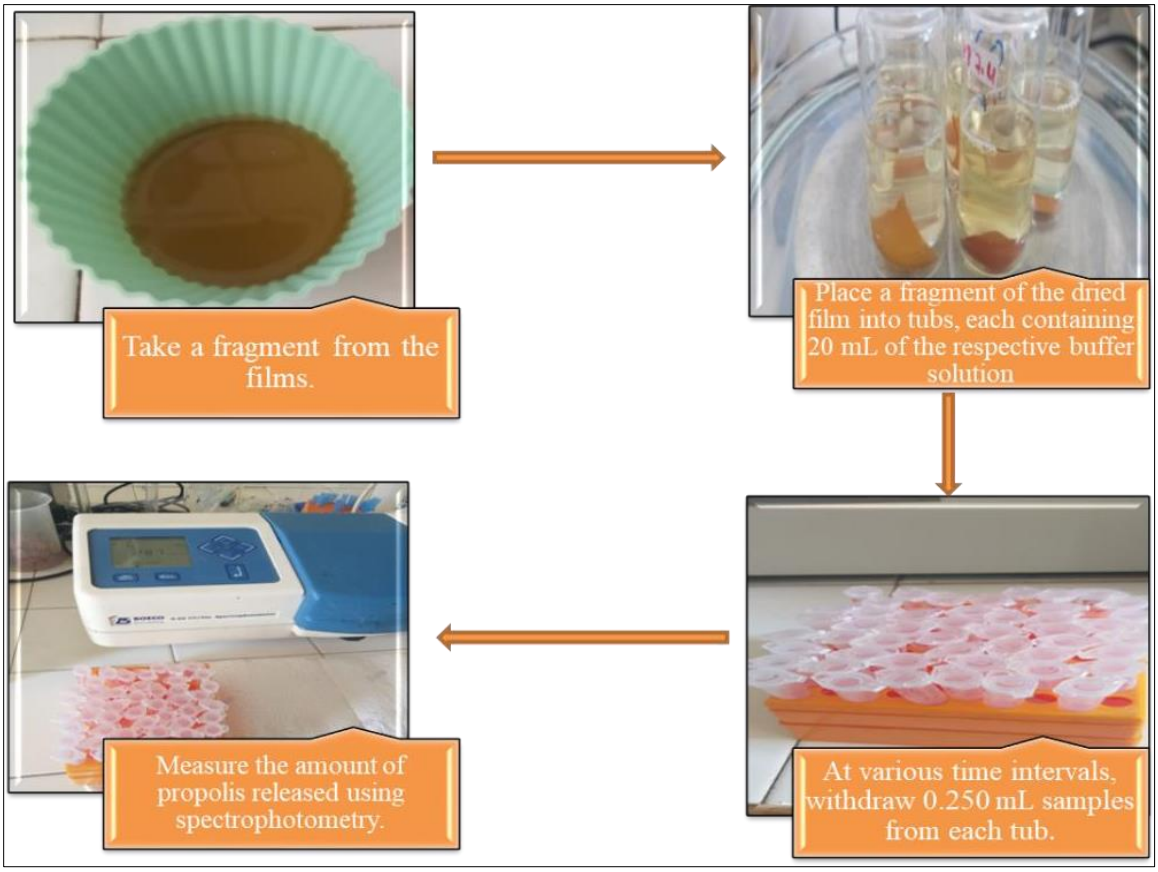

Figure 27. Release efficiency experimental protocol.

IV.3.5. Antioxidant activity

The methodology, initially outlined by Choi and al. [41], was adapted with specific adjustments for this study. Six samples of OSA/G-based hydrogels were prepared, each containing encapsulated propolis for subsequent antioxidant activity evaluation (**Figure 28 (a)**). These hydrogels were divided into two groups for further experimentation. The DPPH test of the antioxidant principle and the DPPH reaction with natural antioxidants is shown in the **Figure 28 (b)**.

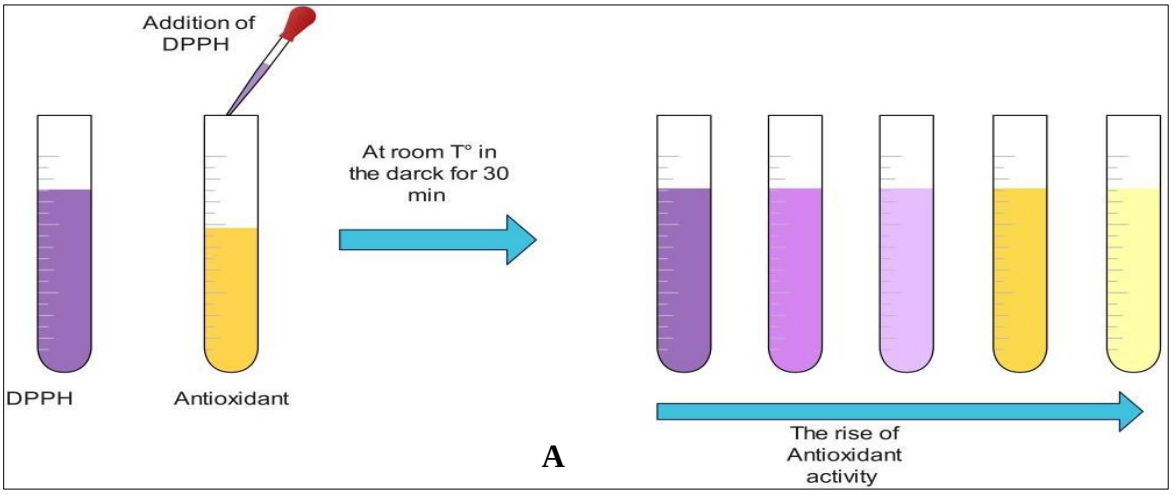

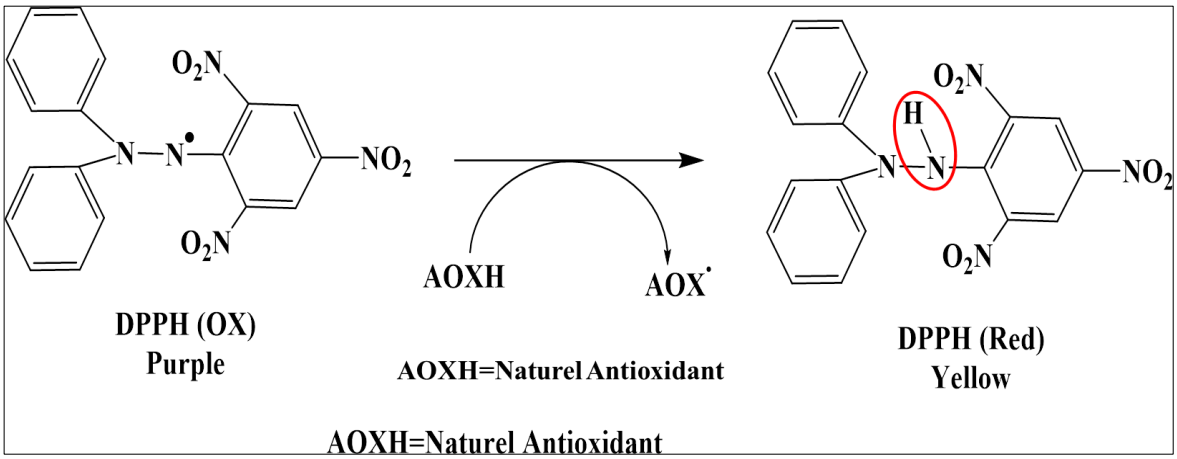

Figure 28. (**a**) DPPH antioxidant principle assay.

(**b**) DPPH reaction with natural antioxidants.

In the first group, propolis extraction was carried out by immersing half of the hydrogels directly in 20 mL of ethanol for 24 hours. Conversely, the second group of hydrogels underwent UV irradiation for 30 minutes before being subjected to the same 24-hour ethanol immersion. In parallel, a volum of 0.250 mL of free propolis was exposed to UV irradiation for 30 minutes, followed by immersion in 20 mL of ethanol. Additionally, an equivalent volume of propolis was dissolved in 20 mL of ethanol without prior UV irradiation. These procedures resulted in the creation of stock solutions for each sample (**Figure 29**).

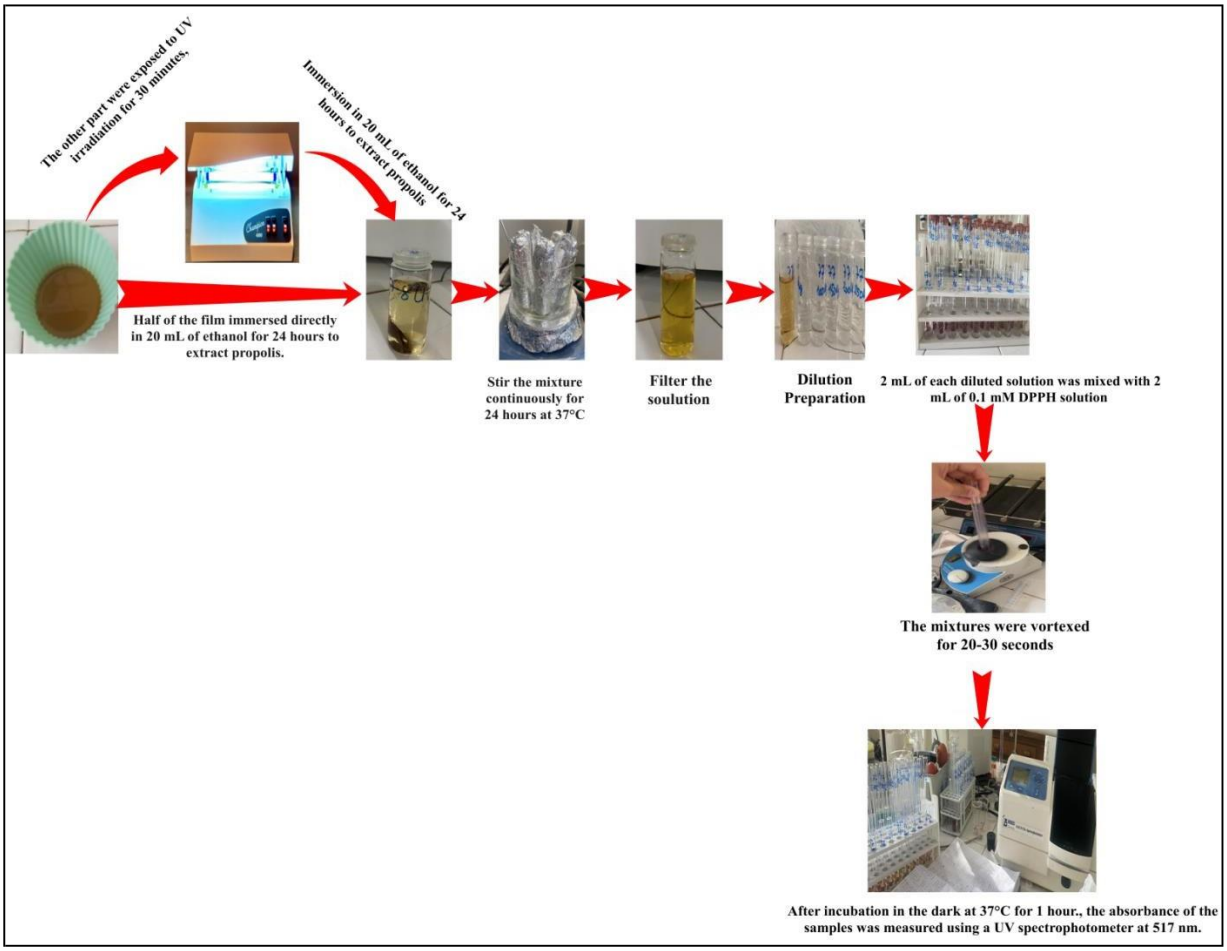

Figure 29. DPPH antioxidant assay OSA/Gelatin based film encapsulating the propolis.

To evaluate antioxidant activity, various dilutions were prepared from the stock solutions, with final propolis concentrations ranging from 5 to 25 µg/mL. In test tubes, 2 mL of each solution concentration was combined with 2 mL of a 0.1 mM DPPH solution (in ethanol). After vortexing the samples for 20–30 seconds, they were placed in the dark at a temperature of 37°C for 1 hour. Subsequently, the absorbance of the samples was measured using a UV spectrophotometer at a wavelength of 517 nm. As a reference, ascorbic acid was employed.

The resulting absorbance values were then converted into percentages representing antioxidant activity, expressed as the inhibition percentage of free radicals in DPPH (DPPH-I %). This transformation was achieved using the following relation (4):

$$I(\%) = 100 - [(A_s - A_b) \times \frac{100}{A_c}] \quad (4)$$

With: I (%): inhibition percentage.

The spectrophotometer underwent calibration using ethanol, with (As) denoting the absorbance values corresponding to diverse solution concentrations.For the blank reference (Ab), a solution containing 2 mL of ethanol and 2 mL of propolis solutions at various concentrations was employed. The absorbance of the blank was recorded for each concentration. And a control solution was prepared by combining 2 mL of ethanol with 2 mL of DPPH solution.

The IC50 value, expressed in µg/mL, was determined from the graphical representation of inhibition percentage (I %) against concentration. This value represents the concentration of the sample required to neutralize 50% of the free radicals present in the DPPH solution.

IV.4. Conclusion

The comprehensive characterization of oxidized sodium alginate (OSA), sodium alginate (SA) and gelatin for hydrogel formulation was carried out using Fourier transform infrared spectroscopy and nuclear magnetic resonance spectroscopy. Other effects were studied such as, oxidation kinetics and temperature effect studies and thermogravimetric properties as well as determination of gelatin amino groups and a comprehensive characterization of the fabricated hydrogels. The thermal properties of SA/gelatin, OSA/gelatin and OSA/gelatin/propolis hydrogels were studied using a TA Q500 TGA. Also, the surface morphology of the hydrogel films was examined by scanning electron microscopy (SEM).

The determination of the conversion index of amino groups (CI %) Shiff bases in hydrogel films as well as the swelling behavior of OSA and gelatin based hydrogels. The latter characteristic is important because it directly influences the diffusion rates of the active ingredient from the hydrogel matrix. The encapsulation efficiency was characterized by high performance liquid chromatography (HPLC) of propolis that is to be anchored in the hydrogel. The release efficiency of propolis in the hydrogel was verified by ABS at pH = 5.5 and ABS at pH = 6.5. The antioxidant activity is an important characteristic of hydrogels, the latter was evaluated by the addition of certain volumes of DPPH solution

PART III: RESULTS AND DISCUSSIONS

CHAPTER V:
Synthesis of Hydrogels Based On Oxidized Sodium Alginate Cross-Linked With Gelatin for Propolis Encapsulation

Chapter V: Synthesis of hydrogels based on oxidized sodium alginate cross-linked with gelatin for propolis encapsulation

V.1. Introduction

This chapter presents the results and discussions of the development of biocompatible gelatin-based hydrogels by cross-linking protein-free amino groups with aldehyde groups obtained by oxidation of sodium alginate. FTIR and NMR spectroscopy results confirm the presence of aldehyde groups in the oxidised alginate. The results concerning the synthesis of hydrogels with different molar ratios between oxidised alginate and gelatin, and the effects of pH and degree of cross-linking on the properties of the hydrogels were studied in this work.

V.2. FTIR Spectroscopy of SA and OSA

The FTIR analysis was carried out to detect the appearance of new chemical bonds or the modification of existing ones, which could demonstrate the oxidation of SA and the presence of aldehyde groups in the OSA. **Figure 30** shows the infrared spectra of SA and OSA after 24 hours of oxidation.

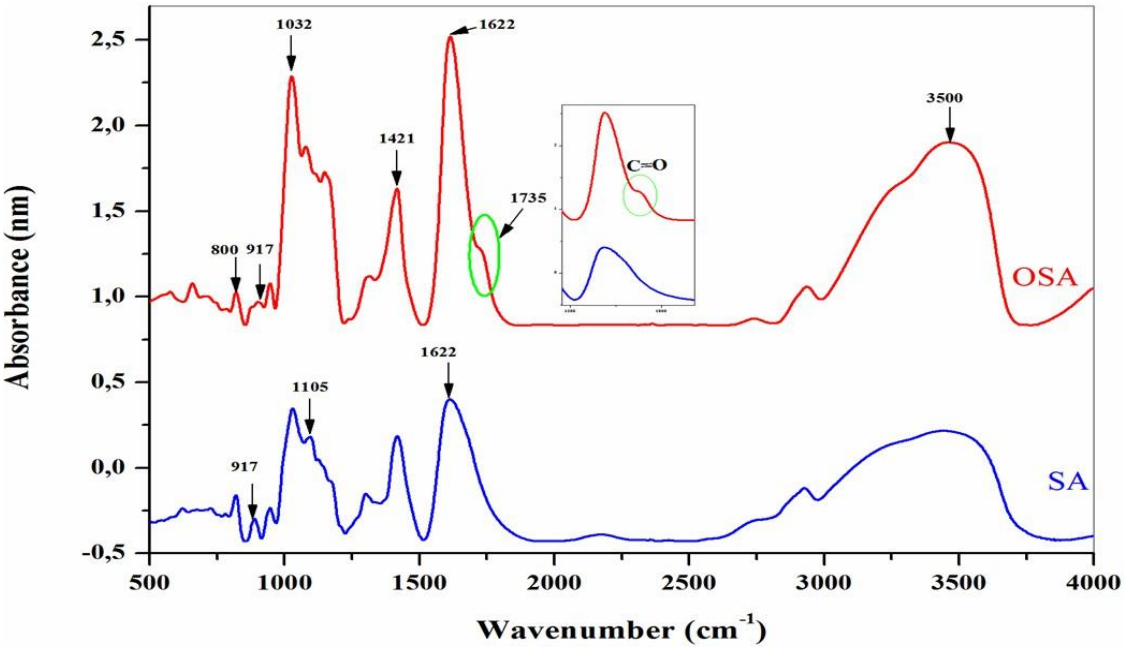

Figure 30. Fourier-transform infrared (FTIR) spectra of SA and OSA (oxidation time: 24 h)

The infrared spectra of the alginate present the typical bands of its polysaccharide structure. The broad absorption peak shown at 3465 cm^{-1} is assigned to the stretching vibration of hydroxyl groups (–OH) [38–41]. And the absorption bands at 2943, 1031 and 1105 cm^{-1} are typical peaks

of all polysaccharide derivatives. This can be attributed to the C–H stretching vibration elongation of the C–O–C groups and C–C stretching groups, respectively [248–250]. The absorption peak at 1622 and 1421 cm^{-1} is related to asymmetric and symmetric carboxylate salt groups of alginate [38–42,44,251]; the figure also shows a peak at 1312 cm^{-1} due to single bond stretching vibration C–O groups [252]. Compared to the SA infrared spectra, a new characteristic band is shown at 1735 cm^{-1} in the FTIR spectra of OSA; it is assigned to the carbonyl signal peaks of the aldehyde group -C=O, which confirmed the occurrence of the oxidation reaction [40,45,74,248,249,253–256]. This peak was too weak and, in some studies, is not detected due to the formation of intermolecular hemiacetals structures between the free aldehydes groups and neighboring hydroxyl groups on the adjacent uronic acid [40,65,248,257].

Moreover, the stretching vibration frequency of the absorption peak of -C–O bonds shifted from 1314 cm^{-1} in the SA spectrum to 1352 cm^{-1} in the spectrum of OSA [252]. These results indicated the cleavage of –C2–C3– bonds between vicinal glycols on alginate uronic acid residue by the oxidation reaction [248,251,252]. In addition, the similarity of infrared spectroscopy results of the OSA and native SA demonstrated that the periodate cleaved only the -C2–C3- bond by the oxidation reaction [60]. Absorption bands from about 800 cm^{-1} can be attributed to hemiacetals formed between the aldehyde group and vicinal hydroxyl groups in an acidic medium but could also occur in a neutral medium.

V.3. NMR Spectroscopy of SA and OSA

The oxidation of sodium alginate was confirmed by the comparison of ^{1}H NMR spectra of SA and OSA using D_2O as a solvent (**Figure 31**):

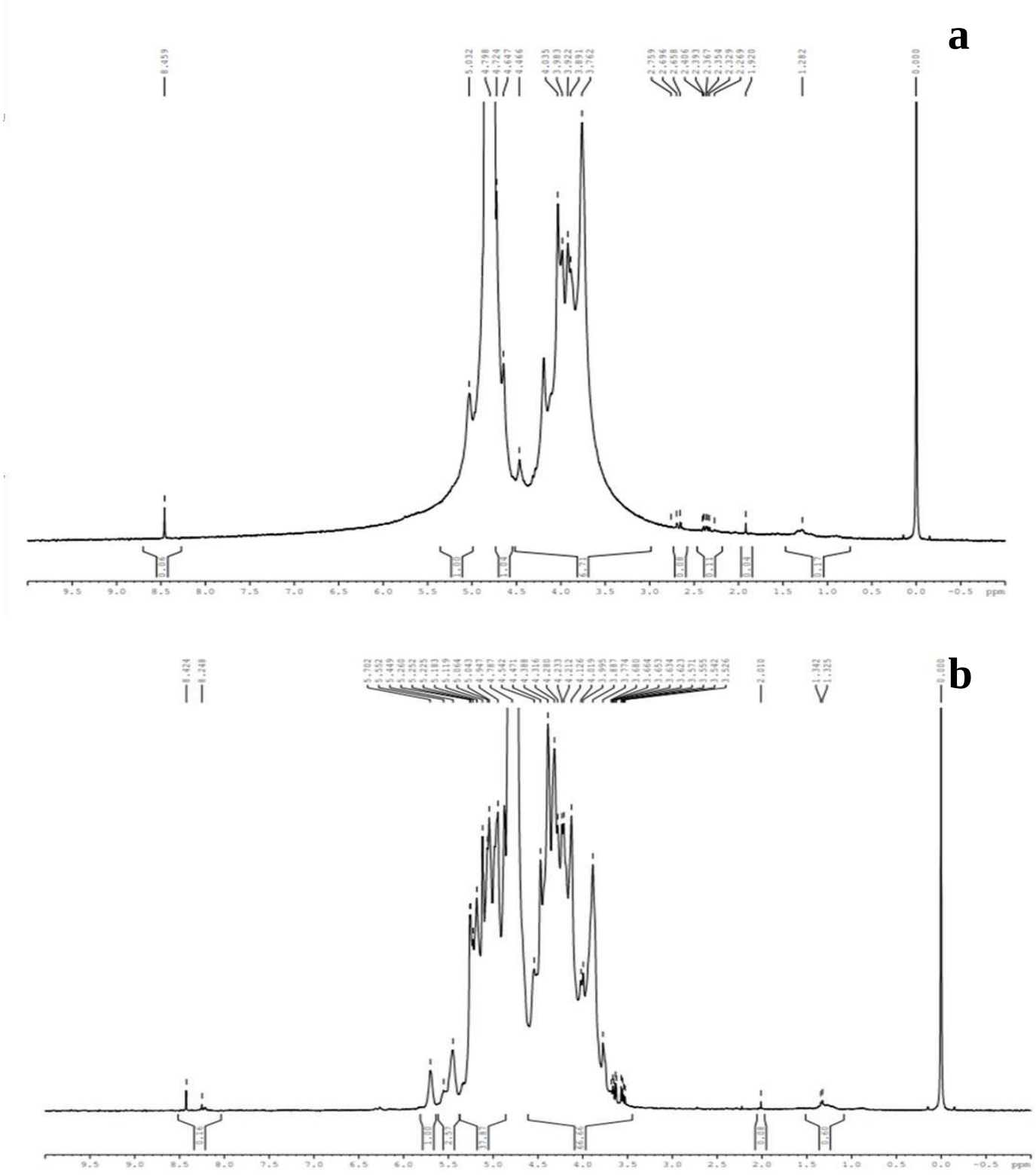

Figure 31. Proton nuclear magnetic resonance (^{1}H NMR) spectra for SA dissolved in water (a), and OSA dissolved in D_2O (b).

The ^{1}H NMR spectra of SA exhibited ranging peaks from 3.762 to 5.0 ppm corresponding to the anomeric proton of Glucuronic (G) and Mannuronic (M) units [258]. The peaks at 5.0 and 3.7 ppm were assigned to the G-1 and M-5 protons, respectively. Meanwhile, the peaks between 4.66 and 4.798 ppm corresponded to the G-5 and M-1 protons [258–260]. Compared to the OSA ^{1}H NMR spectra, a new peak at 8.24 ppm appears, which is attributed to the proton of the aldehyde groups -CHO [65, 74, 258]. Two signals at 5.449 and 5.702 ppm were assigned to the protons in hemiacetals structures [44, 252, 254, 255, 26]. These structures resulted from the adol condensation reaction between the aldehyde and contiguous hydroxyl groups in the D_2O solvent [258, 262, 263]. Moreover, the intensity of the peaks at 3.7 and 5.0 ppm that correspond to the signals of protons of M-5 and G-1 were decreased, and the signal of the G-5 proton was modified. The above results confirmed the oxidation of sodium alginate using $NaIO^4$ and the change of surroundings caused by the cleavage of the vicinal -C2-C3- bonds [264]. In some cases, the peak of aldehyde groups did not appear due to the equilibrium of the aldehydes in water with their hydrated forms, and they react with the unreacted hydroxyl groups of the SA chain [260].

V.4. Oxidation reaction kinetic of SA

The kinetics of the SA oxidation in the presence of $NaIO_4$ was studied by determining the consumption of sodium periodate during the reaction. **Figure 32** shows the obtained results.

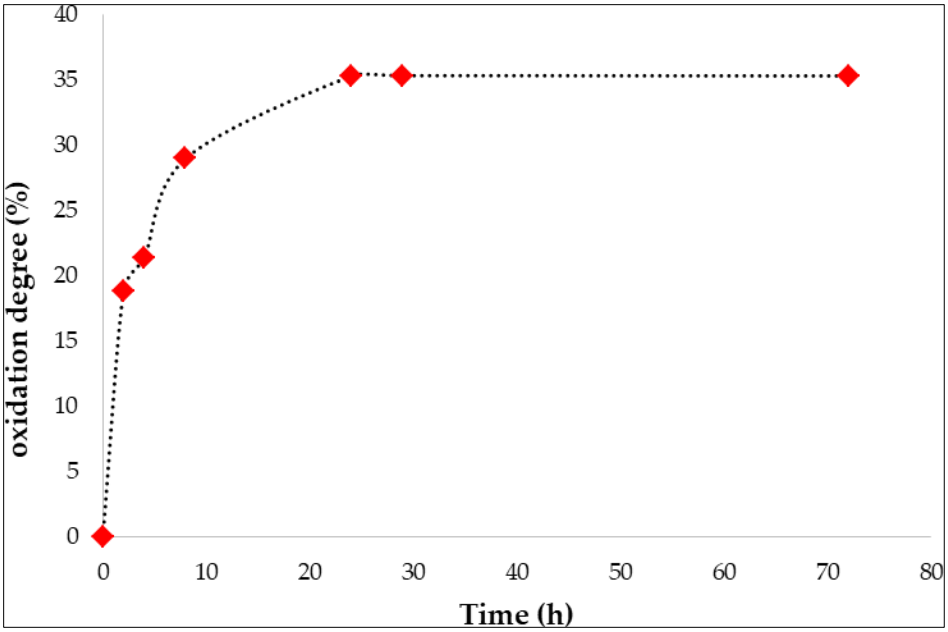

Figure 32. Variation in time of the oxidation degree of SA.

In an aqueous solution, SA was oxidized in the dark using sodium periodate as an oxidizing agent at room temperature for 24 hours. Different reaction times were used to determine the maximum oxidation degree value and optimize the oxidation reaction parameters (**Figure 32**). The sodium periodate cleaved the vicinal dihydroxyl groups in the SA chains at C2-C3. The aldehyde groups were generated, and the degradation of the polymer occurred [44, 251].

The result shows that the oxidation degree gradually increases with time until 24 h, reaching the value of 35.26 %. After 24 h, the oxidation degree value was maintained almost constant until 72 h, meaning that not all the vicinal hydroxyl groups were oxidized, and the SA was only partially oxidized. Similar results were found in the literature, in which the oxidation degree increases over time up to 24 hours [74].

The maximum degree of oxidation varies between (35% and 50%) due to the formation of stable inter-residue hemiacetals between an aldehyde group and a hydroxyl group in the monomeric units resulting in the protection of the hydroxyl group from further oxidation [38, 63, 239, 265].

V.5. Temperature influence on the oxidation degree

The effect of temperature on the degree of oxidation of SA was studied by keeping the duration of the reaction constant (t = 24 h). **Figure 33** shows the results obtained.

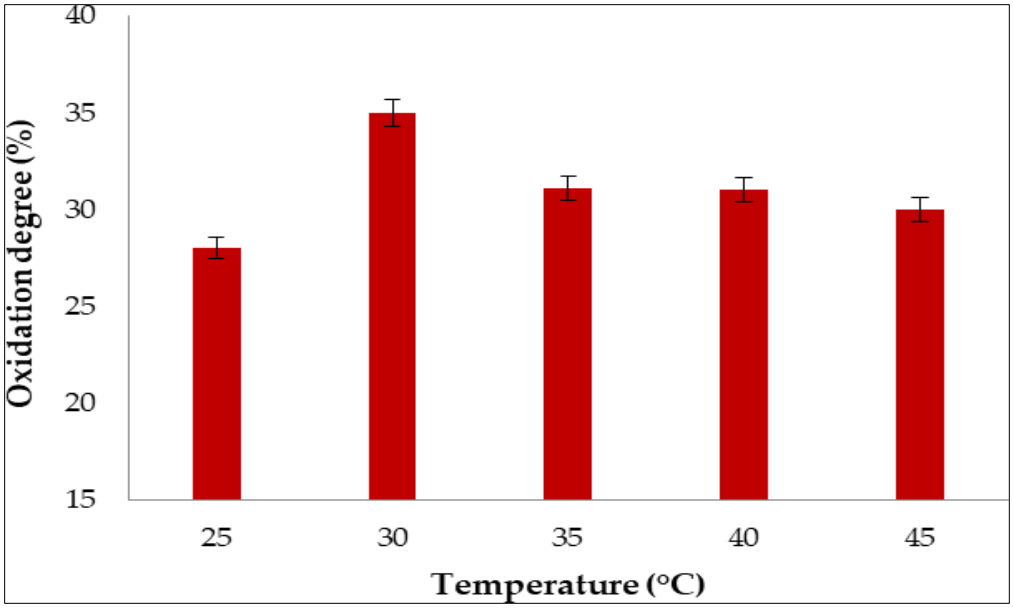

Figure 33. Variation of SA oxidation degree as a function of temperature (t = 24 h).

In order to study the effect of temperature on the oxidation reaction, different oxidation degrees were determined at various reaction temperatures varying from 25 °C to 45 °C (**Figure 33**). The results show that the oxidation degree was higher when the temperature increased to 30 °C, reaching an oxidation degree of 35%. Increasing the temperature up to 45 °C leads to a decrease in oxidation degree to 30%. This diminish in the oxidation degree is in agreement with the decomposition of periodate, which affects the aldehyde groups yield more or less if the oxidation reaction occurs at temperatures over 45°C as already reported by Chemin et al. and Li et al [266, 267]. At higher temperatures, the periodate ion (IO^{4-}) can undergo a series of reactions that result in the formation of iodate (IO^{3-}) and oxygen (O^{2}) gas. This process can lead to incomplete or inefficient oxidation and reduces the effectiveness of periodate as an oxidant in the reaction, which can induce lower yields or undesirable byproducts.

V.6. FTIR spectroscopy of the hydrogels

Figure 34 illustrates the FTIR spectra of Gel, Pro, P'2, PA3, and PAP3 hydrogels at a pH of 5.5 (with and without Pro) to establish the new absorption bands.

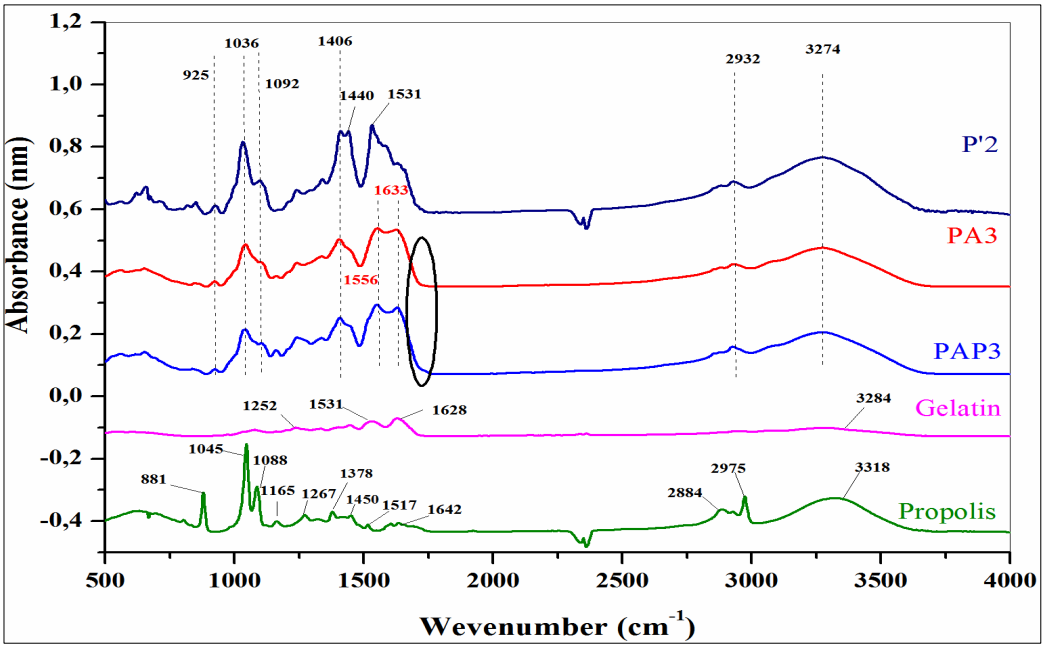

Figure 34. FTIR analysis of hydrogels (P'2 SA/G 1:1, PA3 OSA/G 1:1, PAP3 OSA/G/Pro hydrogels), Gel and Pro.

The FTIR spectrum presented in **Figure 34** reveals distinctive absorption bands corresponding to the protein structure of the Gel. Notably, the peaks at 1628, 1531, 1250, cm^{-1} are assigned to the -N–H stretching vibration peaks for amide I, amide II, amide III [268,269]. On the other hand, the bands around 1036 and 1092 cm^{-1}, which refer to the -C-O and -CO-C vibration of groups in mannuronic and guluronic units, respectively, and 925 cm^{-1} assigned to -C-O vibration of groups in a-configuration of the guluronic units, these bounds are attributed to the saccharide structure of SA [270]. The bands at 1421 cm^{-1} are attributed to -COO- (in the SA and OSA, Figure 30) shifted to a lower wavenumber in the hydrogels samples to 1406 cm-1, confirming the ionic cross-linking of SA with Mg^{2+} [271]. Moreover, the absorption band at 3274 cm^{-1} could be attributed to the stretching vibration of the -O-H group (from the SA or OSA) bonded to the -N-H group (from the Gel). The peak of this band in the SA and OSA was at the wavenumber of 3500 cm-1 and 3284 cm^{-1} in the Gel spectrum, respectively. The maximum intensity of this bond exhibited a reduction in polymers compared to the spectra of the individual polymer, proving the interaction of this group in the cross-linking reaction [271, 272].

FTIR spectrum of the PA3 and PAP hydrogels verified the interactions between the carbonyl group from the OSA and the amino groups from the Gel to produce the Schiff base cross-linking. The presence of -N=C- bonds confirms the realization of the cross-linking reaction.

In Figure 8, the PA3 and PAP3 spectra present two intense bonds at 1556 and 1633 cm^{-1} due to the -N=C- stretching, which suggests the formation of the Schiff base bonds [273–276]. The band's broadening at 1633 cm^{-1} attributed to 'Schiff's base is likely a result of overlap with the band at 1628 cm^{-1} corresponding to amide I of uncrosslinked Gel [275]. Furthermore, the absorption peak corresponding to the aldehyde group in OSA at 1735 cm^{-1} vanished, and a distinct peak emerged at 1633 cm^{-1}, indicative of a -C=N- double bond leading to the formation of a hydrogel network [277].

The FTIR spectrum of Pro showed the presence of phenolic compounds or their esters (-O-H at 3318 cm^{-1}, -C-O- at 2884 cm^{-1}, and -C-H aromatic at 2975 cm^{-1}) [278]. The peaks observed in the range of 1642 cm^{-1} are attributed to the -C=O and -C=C- stretching vibrations of flavonoids, as well as the -N-H asymmetric stretching of amino acids. Furthermore, a strong agreement is noted between the signals in the analyzed sample and the literature [279] for phenols and flavonoids. This correspondence serves as a robust indicator of the presence of both types of compounds in the extract. The characteristic signals for these compounds include stretching and bending vibrations at 1450 cm^{-1}, vibrations and bending at 1378 cm^{-1}, and vibrations and bending at 1088 cm^{-1}. The peak at 1267 cm^{-1} is attributed to the hydrocarbons' asymmetrical -O-H and -C-CO bending. The peaks at 1043 cm^{-1} and 880 cm^{-1} are also associated with primary and secondary alcohols. Specifically, ethanol exhibits a symmetrical stretching at 881-880 cm^{-1}, aligning with the fact that the extracts are dissolved in ethanol [279]. Moreover, the minor peak at 1517 cm^{-1} might be attributed to the flavonoids or aromatic ring, and the bound at 1165 cm^{-1} corresponds to the lipid or the tertiary alcohol groups [280].

V.7. Thermogravimetric analysis (TGA)

Thermogravimetric analysis of pure materials (SA, Gelatin, propolis) and OSA, as well as P'2, PA3, and PAP3 hydrogels, are presented in **Figure 35**, and the main data are summarized in **Table 3**.

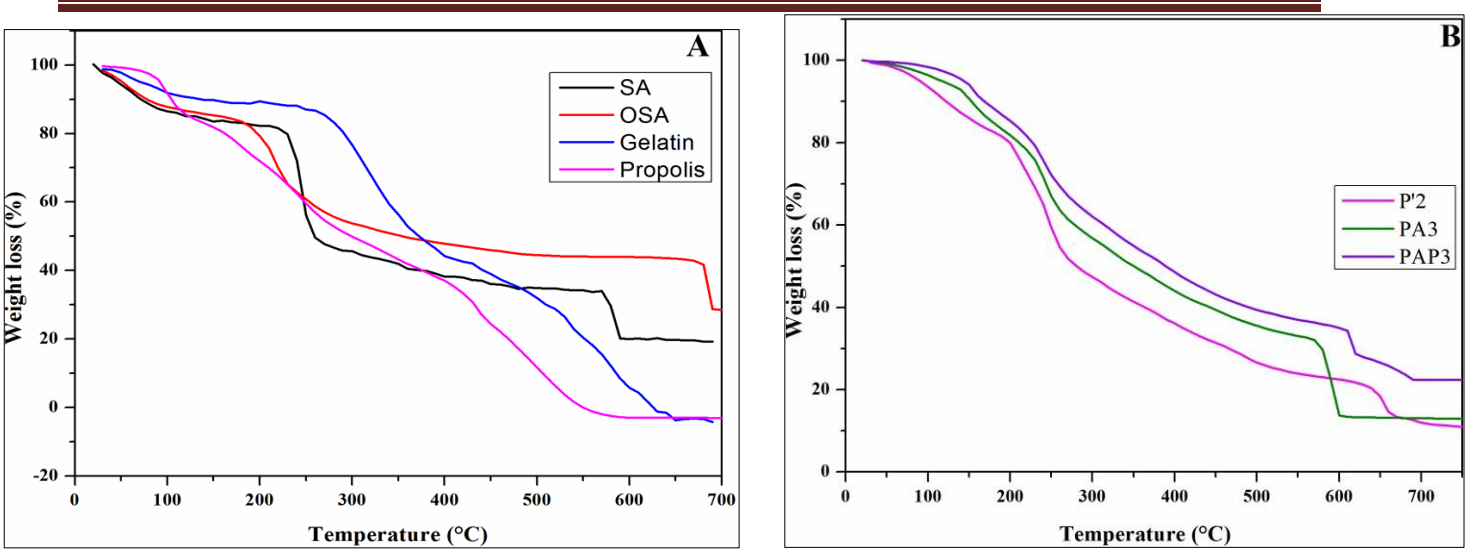

Figure 35. Thermogravimetric analysis curves of A) SA, OSA, Gel, and Pro; B) hydrogels.

TGA is a robust method for evaluating the thermal stability of composite hydrogels. It provides a foundation for indirectly investigating the interactions among the components of these hydrogels. This is achieved by comparing key parameters, such as the final mass loss, the rate of weight loss at the final stage, and the Tmax, which refers to the temperature at which the maximum rate of weight loss occurs during the thermal decomposition across different samples. **Figure 35A** shows that the thermogravimetric curve of Gel displays three stages of thermal degradation. The first stage of weight loss is perceived across the temperature ranges of 38-115 °C, accompanied by a weight loss of 7.86%, possibly due to the release of free-binding water and volatile components loss. In the second stage, 45.68% weight loss in the temperature range of 230-420°C related to the decomposition of molecules with low molecular weights in the Gel [281].

Table 3. Thermal characteristics of SA, OSA, Gel, P'2, PA3 and PAP3.

Samples	Temperature range (°C)	Weight loss (%)	Final residual fraction (%)	T_{max} (°C)
SA	40-100 200-290 558-601	13.45 37.15 13.8	19.18	240

OSA	40-100 170-300 658-700	9.33 30.54 14.77	28.71	219
Gelatin	38-115 230-420 470-660	7.86 45.68 36.32	0	310
Propolis	40-130 140-300 390-600	15.38 33.08 38.26	0	440
P'2	53.18-164 180-295 611-680	14.01 35.24 10.15	10.55	250
PA3	130-190 200-285 557-610	11.08 20.35 19.1	13	240
PAP3	131-180 200-280 600-690	8.21 19.99 7.13	22.39	237

Between temperatures of 470 to 660 °C, the third phase of weight reduction became evident with a weight loss of 36.32%, referring to the complete thermal decomposition of Gel chains [276]. On the other side, from the TGA curve of Pro, it can be appreciated that the Pro thermal stability sample was assessed by three main degeneration stages where the significant decrease

observed in the temperature of 440 °C indicated a substantial reduction in the weight of the samples. The first degradation stage occurred in the temperature range between 40 and 130 °C, with mass losses of approximately 15.38%. This indicates the breaking of hydrogen bonds, subsequently releasing water molecules and other volatile compounds with low molecular weight [282, 284].

Besides SA and OSA, the TGA curve also illustrates three phases. From **Table 3**, the first phase saw 13.45% and 9.33% weight loss for SA and OSA at a temperature below 100°C due to the evaporation of free and bound water in the samples [245]. At 170-300°C, significant weight was reduced by about 37.15% and 30.54% for SA and OSA, respectively, which might be attributed to the dehydration of hydroxyl groups along the alginate backbone and the thermal decomposition of mannuronic acid (M) and guluronic acid (G) residues, which known as hexuronic acid segments [279]. In the temperature range between 560°C-700°C, due to the more carbonization decomposition and decarboxylation of the residues [285] compared to the Gel and SA, OSA exhibits a higher residual fraction (28.71%) as well as a lower degradation rate. Moreover, the temperatures at which the maximum rate of weight loss occurred during the thermal decomposition were 240°C and 219°C for SA and OSA, and all these results confirmed the higher thermal stability. We determined from the results that oxidized functional groups, such as carbonyl groups, may contribute to increased thermal stability by introducing stronger chemical bonds and modifying the overall molecular structure. These modifications can make the polysaccharide more resistant to thermal decomposition. During the second stage, 33.08% weight loss was observed at a temperature range of 140-300°C, which might have contributed to the degradation of phenolics, carbohydrates, and amino acids [282, 283, 286]. At higher temperatures, the elimination of other organic compounds occurs. This process is minorly related to the combined decomposition of amino acidsand fiber, continuing until the final residues are obtained [282, 283]. On the other hand, it can be seen from **Figure 35b** that the hydrogels TGA curve of all hydrogels showed three stages, the first one at approximately temperature range of 53.18-164

°C, 130-190° C, 130-181°C with weight loss of 14.01%, 11.08%, 8.21% for P’2, PA3, PAP3 respectively. These temperature ranges correspond to the removal of adsorbed and bound water and the loss of volatile compounds. The second stage was in the temperature range of 180-295°C, 200-285 °C, and 200-280 °C with weight loss of 35.24%, 20.35%, and 19.99% for P’2, PA3, and PAP3, respectively, which might describe the degradation of peptide bonds within

protein chains and the hydroxylic gropes within the hydrogels. The third stage for P'2 hydrogel occurred in the rage of 611-680°C with a weight loss of 10.15% due to the decomposition of the Gel residual chain. However, for PA3 and PAP3 samples, the decomposition occurred between 557 and 610°C 600 and 690°C for PA3 and PAP3, respectively, with weight loss of 19.1% and 13%, which contributed to the decomposition of thermally stable structures such as imine bound. Table 2 shows that the P'2 hydrogel presents a lower weight loss rate with a lower final fraction residual of 10.55% compared to the PA3 (13%) or PAP3 (22.39%) Schiff base-based hydrogels. Moreover, the Tmax reduces with the introduction of the aldehyde groups into the hydrogel matrix, which means that the P'2 exhibits a higher Tmax (250 °C) compared to PA3 (240 °C) and PAP3 (237 °C) hydrogels. Therefore, the Schiff base hydrogels PA3 and PAP3 demonstrated more excellent stability against thermal degradation than the SA/Gel-based hydrogels 'P'2. This suggests that the cross-linking of Gel/OSA with an imine bond significantly improved the thermal stability [285]. Moreover, the addition of Pro within the OSA/ Gel matrix hydrogel makes the hydrogel more thermally stable, as it was confirmed on the sample PAP3.

V.8. Scanning electron microscopy (SEM) analysis

SEM analysis was conducted to visualize the film's surface and cross-section morphology. To demonstrate how the incorporation of OSA in the film matrix and the addition of Pro affect the morphology of the hydrogel films, we selected P'2, PA3, and PAP3 samples for this aim. The molar ratios of -CH=O/-NH_2 used to obtain the films were 1:1 for both samples, adding 0.5 ml of Pro to the PAP3 sample.

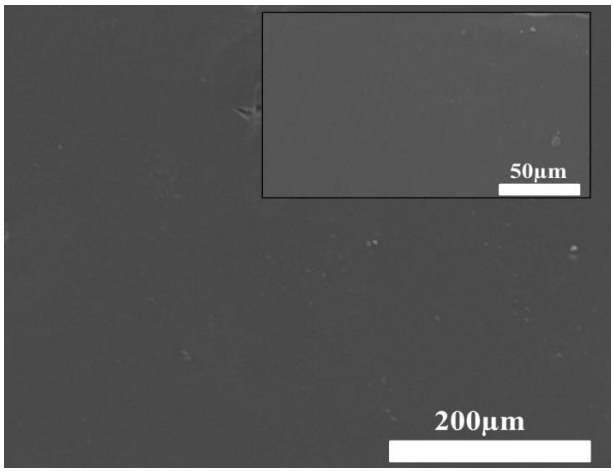

a

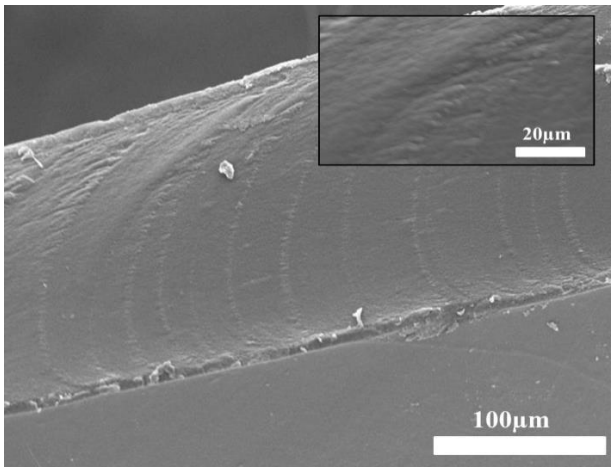

b

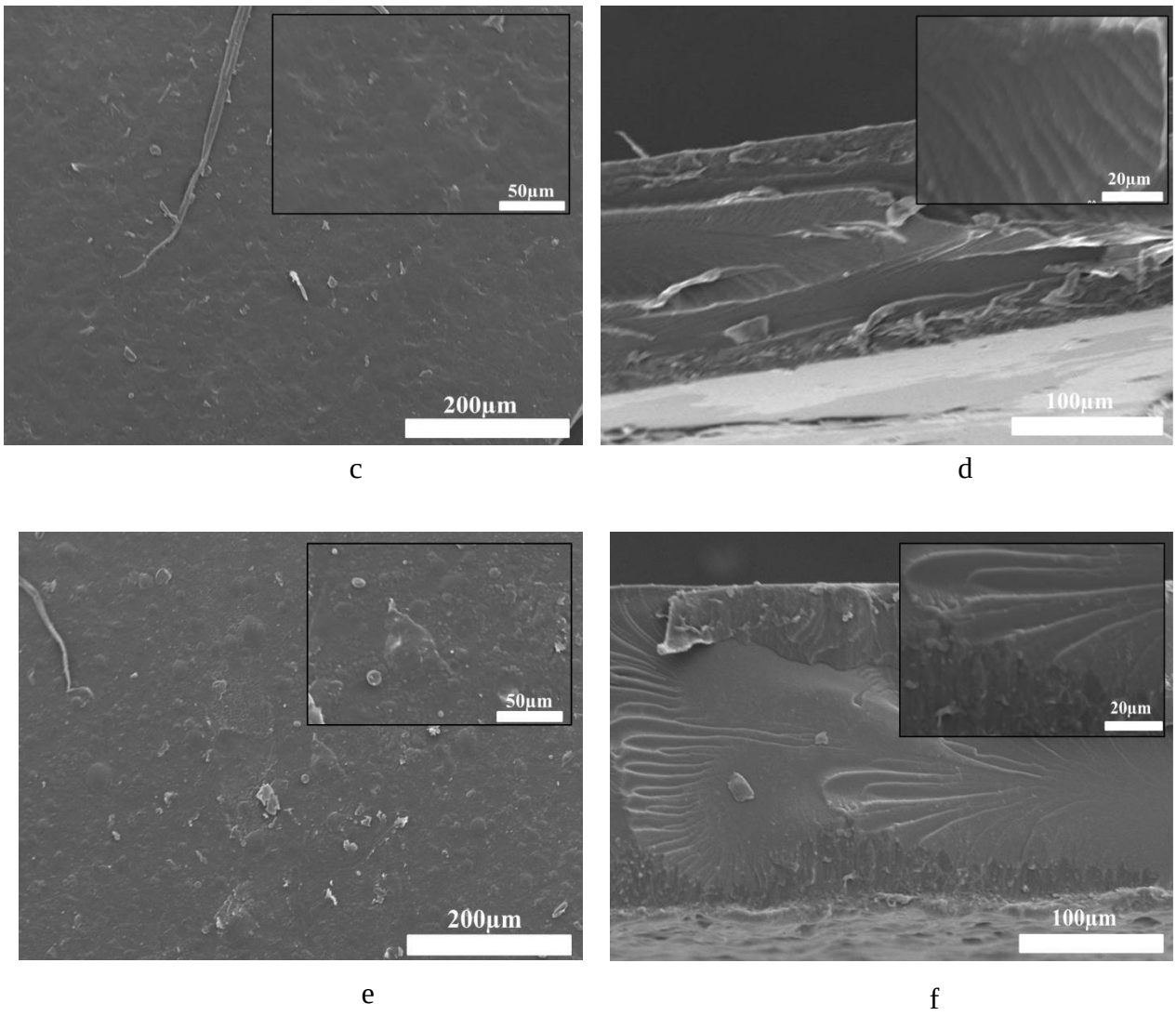

Figure 36. Scanning electron microscopy photographs of the samples
a) PSA2 surface b) PSA2 cross-section
c) POA3 surface d) POA3 cross-section
e) POAP3 cross-section f) POAP3 cross-section.

Figure 36 displays SEM surface images as well as the cross-section for SA/ Gel, OSA/ Gel, and OSA/ Gel/ Pro hydrogels to evidence the effect of cross-linking by Schiff base links, as well as the introduction of the Pro in the hydrogel matrix. It can be seen that the roughness of the hydrogel surface increased with the addition of the OSA and the Pro in the hydrogel matrix. The SA/Gel P'2 hydrogel showed a compact, smooth, continuous, flat surface morphology. However, the OSA/Gel base hydrogel surface exhibits a rough, dense, and slightly porous morphology. Incorporating Pro into the hydrogel matrix increases the roughnessof the hydrogels.

The cross-section morphology of the native P'2 was compact and lacked any distinctive

pores structure. On the other hand, the OSA/ Gel and OSA/Gel/Pro composite hydrogels indicated less compact morphology. As illustrated in **Figure 36 (f)**, the incorporation of Pro into the OSA/Gel matrix is evident in a more densely packed structure [276].

V.9. Amino groups conversion index determination

The number of moles of free amino groups from Gel was determined using the ninhydrine test. This information was essential in order to prepare the hydrogel films. We used different molar ratios between the free amino groups from Gel and aldehyde groups from OSA.

Based on the glutamic acid calibration curve and the ninhydrin test, the free amino groups presented in the native Gel (found at 1.69×10^{-3} mol/g) and in the obtained hydrogels were determined. Hence, by the difference between the number of initial free amino groups in Gel and those determined in the films, the conversion index of amino groups obtained in Schiff's bases in hydrogel films was established based on Equation (2) from methods. **Table 4** shows the values of the conversion index for the hydrogels in correlation with Pro's encapsulation efficiency.

Table 4. Conversion index of the samples with Pro.

Samples* codes	**Molar ratio -CHO: NH_2**	**Conversion index (%)**
PAP1	0.5:1	63.60
PAP2	0.75:1	72.40
PAP3	1:1	78.24
PAP4	1.5:1	81.78
PBP1	0.5 :1	60.79
PBP2	0.75 :1	71.93
PBP3	1 :1	76.47
PBP4	1.5 :1	79.36

The average percentage of free amino groups after cross-linking reaction at different pH (3.7 and 5.5) and different molar ratios CHO/NH_2 was determined by using the ninhydrine test. The results are shown in **Figure.37**:

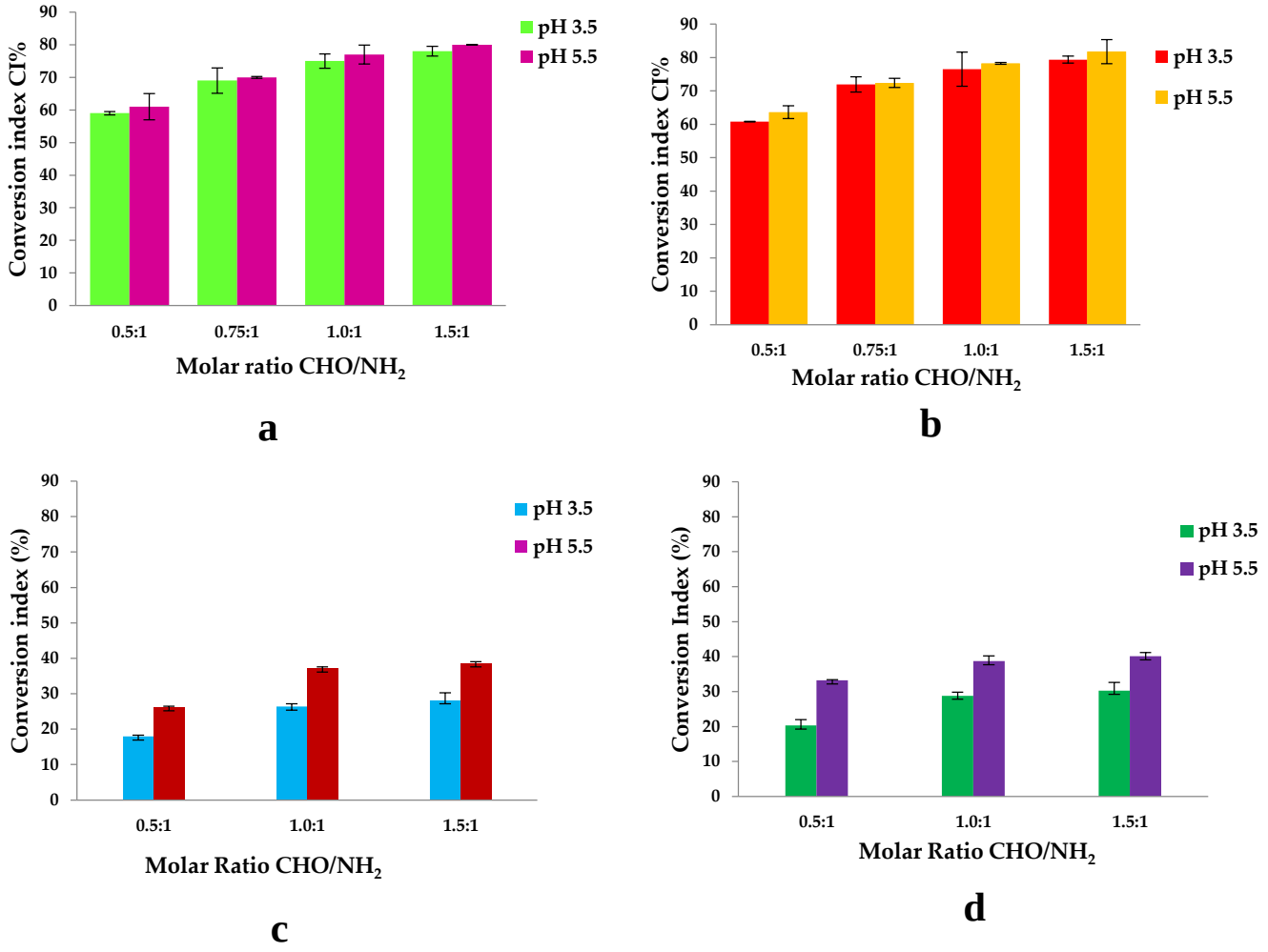

Figure 37. The variation of the amino group's conversion index values in function of the molar CHO/NH_2 ratios and pH (t reaction =6 hr, T reaction =37 °C)

(a) samples with OSA without propolis obtain at pH 3.5 and5.5

(b) samples with OSA with propolis obtain at pH 3.5 and5.5

(c) samples with SA without propolis obtain at pH 3.5 and5.5

(d) samples with SA with propolis obtain at pH 3.5 and5.5.

Table 5. The CI (%) for the hydrogels obtained by chemical cross-linking and the physical interaction between Gel and OSA, respectively, by the interaction of the amine groups of Gel with the carboxylic groups of SA.

Samples	pH of the medium	Molar ratio CHO/NH_2	CI Chemical crosslinking+ physical interaction (%)	CI Physical interaction (%)	CI Chemical crosslinking+ physical Interaction − CI Physical interaction = CI Chemical crosslinking (Schiff base crosslinking) (%)
PB1	3.7	0.5:1	59.31±0.50	17.96±0.38	41.35
PB2	3.7	1:1	75.04±2.10	26.36±0.82	48.67
PB3	3.7	1.5:1	78.53±1.50	28.14±2.15	50.39
PA1	5.5	0.5:1	61.19±3.90	32.15±0.71	34.79
PA2	5.5	1:1	77.98±2.90	37.15±0.40	40.82
PA3	5.5	1.5:1	80.67±0.04	38.57±0.44	42.09
PBP1	3.7	0.5:1	60.70±0.13	20.27±1.70	40.52
PBP2	3.7	1:1	76.47±5.10	28.80±0.97	47.66
PBP3	3.7	1.5:1	79.36±1.03	30.21±2.41	49.15
PAP1	5.5	0.5:1	63.60±1.91	33.21±0.20	30.41
PAP2	5.5	1:1	78.24±0.28	38.69±1.49	39.54
PAP3	5.5	1.5:1	81.78±3.60	40.07±1.04	41.71

The hydrogels were prepared using different molar ratios between the amino groups from Gel and the aldehyde groups from OSA. The number of moles of amino groups from Gel was maintained constant for all the samples namely 3.38×10^{-3} moles, and the number of moles of carbonyl groups from OSA was varied by variation of OSA amount. The pH of the medium in which the biopolymers were dissolved before obtaining the hydrogel was 3.5 and 5.5. The magnesium ions were added to the OSA solution before adding the Gel to avoid the ionic complexation between the Gel and OSA. **Figure 37** shows that the CI values increase when the -CHO/-NH_2 molar ratio increases from 0.5:1 to 1.5:1. The pH medium's value does not significantly influence the CI values obtained. It increases from 59% to 78% for pH=3.5 and from 61% to 80% for pH=5.5; the difference between the values obtained at pHs = 3.5 and 5.5 are small and statistically insignificant. This means that the degree of cross-linking is higher as the amount of OSA increases, because the reaction of aldehyde groups facilitates hydrogel formation [261,279]. The IC values of hydrogels with immobilized active ingredient increased from 60% to 79% at pH=3.5 and from 63% to 83% at pH=5.5; these values are close to those obtained in the absence of propolis. The difference observed between samples with propolis and those without is minimal and has no statistical significance. This suggests that, although there is a slight variation, propolis components do not interact significantly with gelatin amino groups. Although minor interactions, such as hydrogen bonds, may occur, these are likely to be disrupted at the reaction temperature of 100°C, where the ninhydrin reaction takes place. This means that

the presence of propolis has no significant effect on the interaction with gelatin under these conditions.

Because Pro contains various compounds, they may interact with amino acids and protein groups from Gel to form several bonds such as covalent binding, hydrogen bonding, and electrostatic interactions, which can slightly increase the CI values.

On the other hand, the aldehyde groups within OSA might form hemiacetals with the hydroxyl groups. Thus, not all the resulting aldehyde groups are available to react with the amino groups from the Gel to form Schiff bases (or imine bonds), and this could describe the incomplete reactivity of amino groups even in the case of excess aldehyde groups theoretically presented in the OSA. Moreover, it must be noted that some intermolecular interactions exist, such as hydrogen bonds, which could block the free amino groups [287].

Another parameter affecting the cross-linking reaction is the pH of an acidic medium. Figure 5 shows that the conversion index at pH =3.7 is slightly lower than at pH 5.5. In both acidic media, protonated amine groups in the gel facilitate the crosslinking reaction with aldehyde groups [288]. The isoelectric point of Gel type A is found at a pH value between 7 and 8.5. At this pH, the charge of the protein is neutral, and its functional groups do not react. The literature mentions rapid gelation before the isoelectric point until pH=7, where the amino groups are protonated [289]. A negative charge could be generated on the Gel backbone above the isoelectric point because the proteins have an amphoteric character [290]; in this pH range, the substituting –COOH groups on the main chain of the protein are found in dissociated form, respectively as carboxylate ions. The pKa of the carboxyl groups is at pH 3.5. At this pH, electrostatic interactions between the carboxyl groups of the OSA and the protonated amine groups of the gel did not occur. The CI values are slightly higher at pH=5.5 because, at this pH value, the free amino groups within Gel may react not only with the aldehyde groups but also with the carboxylic groups that did not participate in the ionic cross-linking with Mg^{2+} and form also polyelectrolyte complexes. Since steric hindrances can occur between macromolecules, it is not possible to obtain a 100% conversion index of amino groups to Schiff bases, even if a -CHO/-NH_2 molar ratio of 1.5:1 (so, excess of –CHO groups) was used.

To elucidate the specific Schiff base cross-linking within the film and explore the potential formation of electrostatic interactions between amino groups from gelatin and -COOH groups from OSA at two different pH levels, twelve films (six without Pro and six with Pro) were studied. The free amino groups were quantified by dosing them with ninhydrin after drying the

hydrogel films. The results are illustrated in Table 5 and **Figures 37c** and 37d. It is important to note that the films were prepared with sodium alginate to facilitate this test.

It should be noted that the CI (%) values are annotated as follows:

CI chemical crosslinking+ physical interaction (%) represents the overall involvement of amino groups in both chemical bonds and physical interactions.

CI physical interactions (%) indicates the percentage of amino groups exclusively involved in physical interactions.

CI chemical crosslinking+ physical interaction–CI Physical interaction = CI chemical cross-linking (Schiff base) (%), which exclusively involved the Schiff base interaction between the amino and the CHO groups.

A first finding is that, indeed, it was found that in non-chemically cross-linked samples, some of the amino groups from Gel did not participate in the reaction with ninhydrin, obviously because $–NH_2$ groups were involved in stable interactions with carboxylic groups of SA. It is assumed that the same effect occurs when cross-linked samples are obtained, i.e., some of the amino groups of Gel react with the OSA carbonyl groups, and others interact with the carboxylic group of OSA. These interactions could explain the high CI values corresponding to these samples, which do not correctly express the CI of amino groups into Schiff bases.

Thus, for the samples prepared at a pH of 3.5, the P1 sample, CI Schiff base (%) difference was 41.35%. According to the molar ratio of the functional groups involved in the P1 sample, the maximum theoretical value of the cross-linking reaction is 50% (0.5 moles of -CH=O for 1 mol of $-NH_2$). In the case of the P2 sample, CI Schiff base (%) was significant at 48.67% and the molar ratio was 1:1. For the P3 sample the difference was 50.39%, corresponding to given that the molar ratio between these two types of functional groups was 1.5:1. For the samples which prepared at pH = 5.5, P'1 the Schiff base (%) difference was 34.79%, while the maximum theoretical value of the corresponding CI being 50% (the molar ratio was0.5 moles of -CH=O for 1 mol of $-NH_2$). Likewise, in the case of the P'2 sample, there was a notable difference of 40.82%, considering the molar ratio between these two types of functional groups was set at 1:1. In the case of sample P'3, characterized by a molar ratio of 0.5 moles of -CHO groups for 1 mol of $-NH_2$ groups, the observed difference was 42.09%.

The observed difference in physical cross-linking between amino groups from Gel and carboxylic groups from SA in samples prepared at pH 3.5 versus those at pH 5.5 is likely influenced by several factors.

The difference observed in the physical cross-linking between Gel amino groups and SA carboxyl groups in samples prepared at pH 3.5 compared with those prepared at pH 5.5 is probably influenced by several factors. At pH values of 3.5 or 5.5, the NH_2 groups of gelatin are protonated, as these pH values are below the isoelectric point of gelatin. At pH values above 3.5 (pka for COOH groups), carboxyl groups can be deprotonated, forming carboxylate ions that can be found in oxidized alginate in a large number as the pH value of the cross-linking reaction medium increases. These carboxylate groups can react with amino groups instantly, leading to the formation of polyelectrolyte complexes and preventing the formation of Schiff bases, which occurs after a few hours. Generally, the carboxylate groups of anionic polysaccharides are fully deprotonated under basic pH conditions, increasing their reactivity in such complex-forming processes.

The results confirme that the Schiff base cross-linking crosslinking for the samples abtained at pH 5.5 were slightly lower compared to those at pH 3.5, which confirmed that the although pH has an influence on cross-linking, the variation in pH does not significantly affect the Schiff base formation between gelatin and OSA groups.

V.10. The molar ratio -CHO/-NH_2 influences on the swelling degree.

The swelling degree (Q %) was determined to evaluate the capacity of the OSA/G hydrogels to absorb and retain the aqueous solution at different pH mediums. The Q% is an essential property of hydrogels with biomedical applications because the diffusion of the encapsulated bioactive principle from the polymer matrix depends on it. The swelling degree of the hydrogels with/without propolis, with different -CHO/-NH_2 molar ratio values, was measured until equilibrium in two different pH mediums (pH= 5.5 and pH=7.4) at 37^0C. The results are shown in **Figure 38** and **Figure 39** .

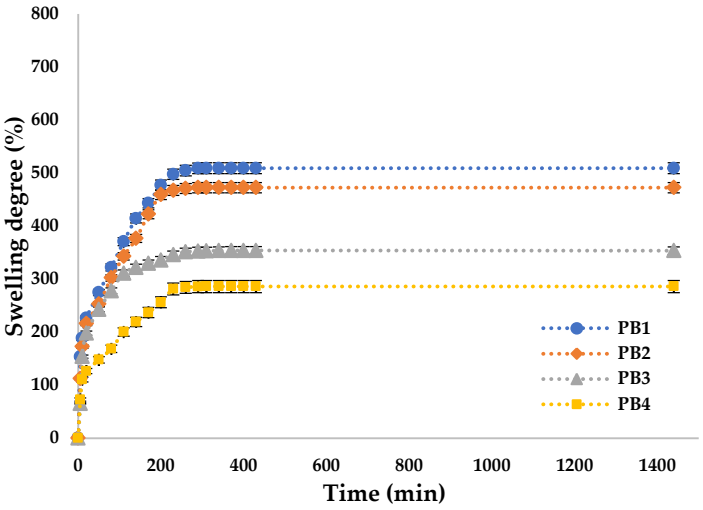
Swelling degree (%)
Time (min)
PB1
PB2
PB3
PB4

(a)

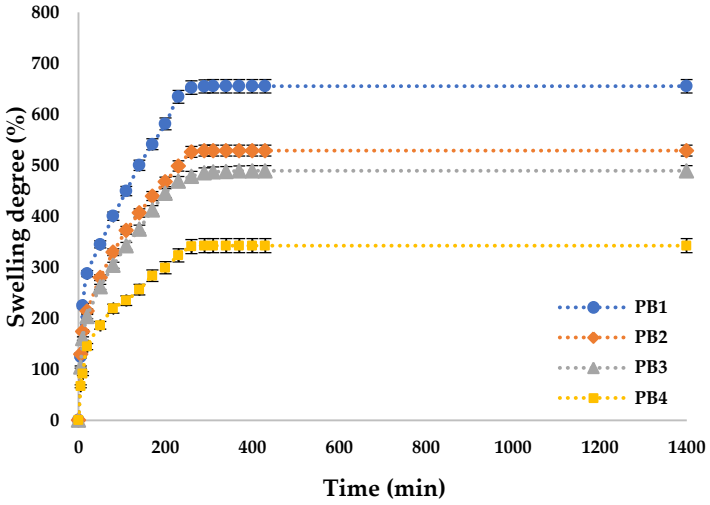
Swelling degree (%)
Time (min)
PB1
PB2
PB3
PB4

(b)

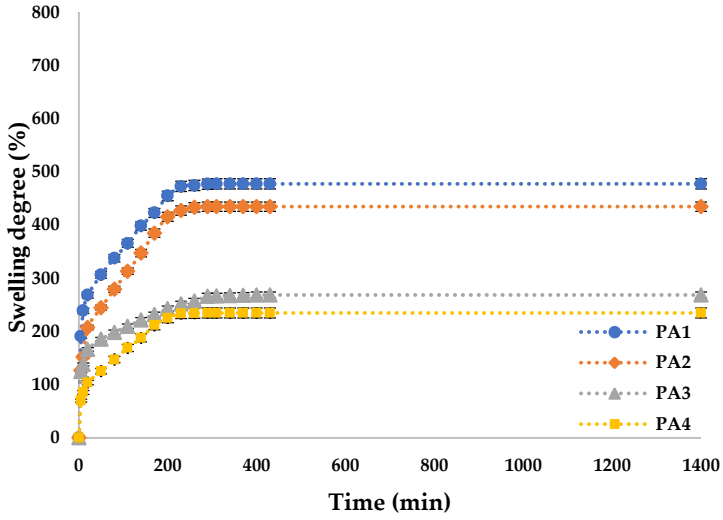
Swelling degree (%)
Time (min)
PA1
PA2
PA3
PA4

(c)

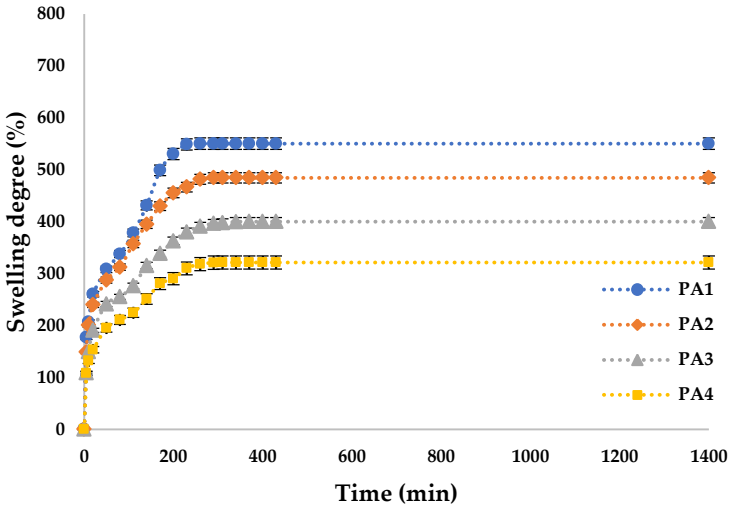
Swelling degree (%)
Time (min)
PA1
PA2
PA3
PA4

(d)

Figure 38. The swelling degree kinetics at different -CHO/-NH_2 molar ratios of
(a) hydrogels prepared at pH= 3.5 immersed in acetate buffer solution (ABS) at pH= 5.5
(b) hydrogels prepared at pH= 3.5 immersed in phosphate buffer solution (PBS) at pH= 7.4
(c) hydrogels prepared at pH= 5.5 immersed in acetate buffer solution at pH= 5.5
(d) hydrogels prepared at pH= 5.5 immersed in phosphate buffer solution pH = 7.4.

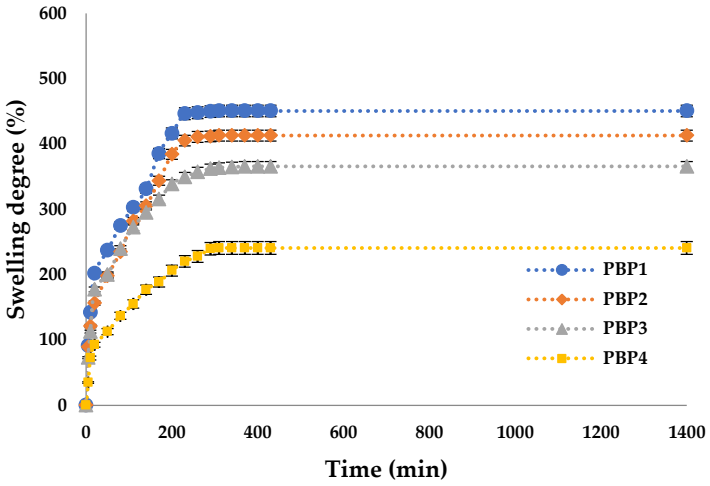

(a)

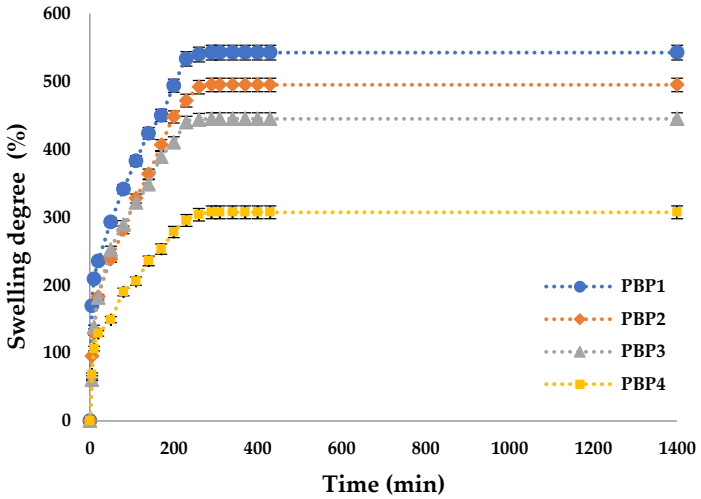

(b)

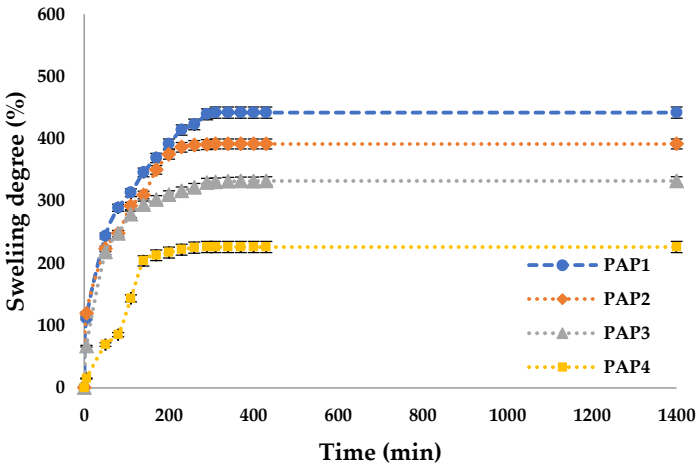

(c)

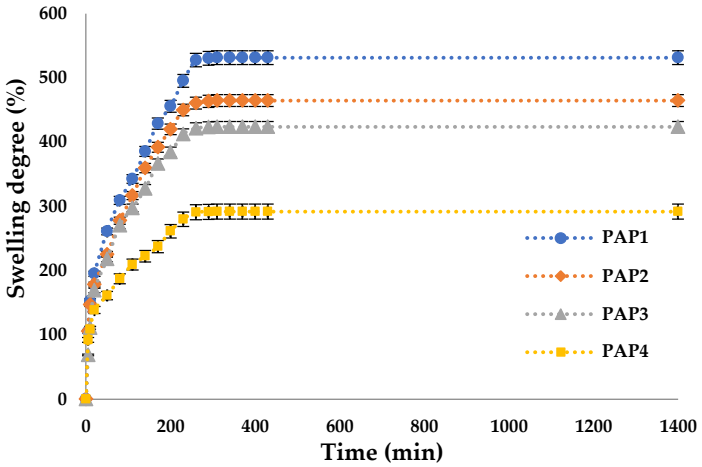

(d)

Figure 39. The swelling degree kinetics at different -CHO/-NH_2 molar ratios of
(a) hydrogels prepared at pH= 3.5 with Pro immersed in acetate buffer solution (ABS) at pH= 5.5
(b) hydrogels prepared at pH= 3.5 with Pro immersed in phosphate buffer solution (PBS) at pH= 7.4
(c) hydrogels prepared at pH= 5.5 with Pro immersed in acetate buffer solution at pH= 5.5

(d) hydrogels prepared at pH= 5.5 with Pro immersed in phosphate buffer solution pH= 7.4.

Figure 38 shows that Q% values were higher at pH=7.4 than at pH=5.5 because the hydrogels contain OSA in their structure. Therefore, the basic pH induces the formation of carboxylate anions from the acid groups that did not participate in the cross-linking with Mg^{2+} ions or in interactions with amino groups, which leads to the electrostatic repulsions between the polysaccharide chains and has an effect on the relaxation of the network, facilitating the diffusion of higher amounts of water.

The isoelectric point of Gel type A is found at around pH=7.4. At this pH, the interactions of the functional groups within the protein are weak, and the hydrogen bonds do not form. At pH = 5.5, several hydrogen bonds could be formed in the hydrogel films, leading to lower adsorption of the swelling medium. These intermolecular attraction forces predominantly have, as a consequence polymer-polymer interactions and not medium-polymer interactions resulting in a smaller amount of medium absorbed by these hydrogel [291].

The variation in the degree of swelling of the material is inversely proportional to the degree of crosslinking, meaning that as the degree of crosslinking increases, the degree of swelling decreases. This relationship is influenced by the molar ratio of amino groups to carbonyl groups used in the crosslinking process. Whereas, carboxyl groups in oxidized sodium alginate significantly influence the swelling behavior of the hydrogels prepared. They introduce additional hydrophilic sites, increasing the hydrogel's capacity to absorb water. These results were confirmed in the work of Baron et al. [292] and Tincu (Iurciuc) et al. [293], they demonstrated similar findings. These results align well with the conversion index, confirming the expected behavior of the material under varying cross-linking conditions.

Figure 39 shows that the addition of Pro leads to a slightly decreased swelling degree compared to the ones that don’t contain the active principle. The active principle is located within the pores of the polymer matrix, reducing the aqueous solution's absorption. Additionally, propolis is poorly soluble in water and can make the film hydrophobic, leading to lower aqueous solution absorption and, consequently, a lower degree of swelling.

V. 11. Encapsulation Efficiency

As previously mentioned, propolis's encapsulation and release have been indirectly assessed through the encapsulation and release of the p-coumaric acid it contains.

Figure 40 presents the results obtained for the encapsulation efficiency of Pro for the OSA/Gel-based hydrogels prepared in two different pH mediums.

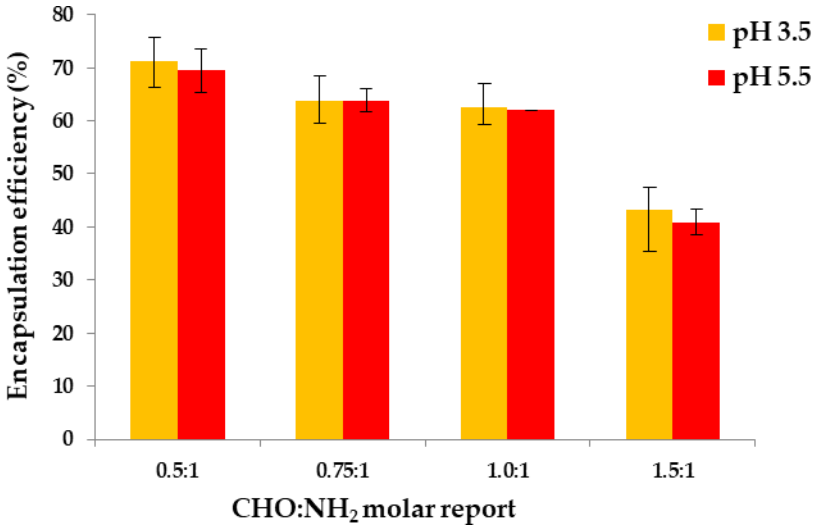

Figure 40. Pro encapsulation efficiency in OSA/Gel-based hydrogels obtained at different pH mediums, at different -CHO/-NH_2 molar ratios.

Due to the biocompatibility of the biopolymers used in the OSA/Gel-based hydrogels preparation, this study further aims to confirm their feasibility for the encapsulation and release of active compounds. The selection of Pro as a drug model involved assessing its encapsulation efficiency within OSA/G-based hydrogels, which was determined by evaluating the presence of p-coumaric acid as a crucial component of Pro [The volume of Pro solution (with 30% concentration) was 500 µl which contains 22.75 mg of p-coumaric acid)].

The results are presented in Figure 13. It was found that the encapsulation efficiency of p-coumaric acid decreased with the increase of the OSA quantity within the hydrogel matrix, which means that the encapsulation efficiency decreased when the cross-linking degree was higher. With the increase of the molar ratio in favor of the -CHO groups, thus of the cross-linking degree, the polymer network meshes become smaller and cannot immobilize a large amount of Pro. However, a higher Pro amount could be immobilized at a lower cross-linking degree.

V. 12. Release kinetics of Pro from hydrogel films

The release kinetic studies were performed in vitro in two different pH mediums (pH = 7.4-PBS 0.1 M and pH = 5.5-ABS. 0.1 M using tween 80 of 1% w/w concentration) at 37ºC for 3 hours until equilibrium. Para-coumaric acid was only dosed to study the release efficiency of Pro from the hydrogels; the results obtained are presented in **Figure 41**.

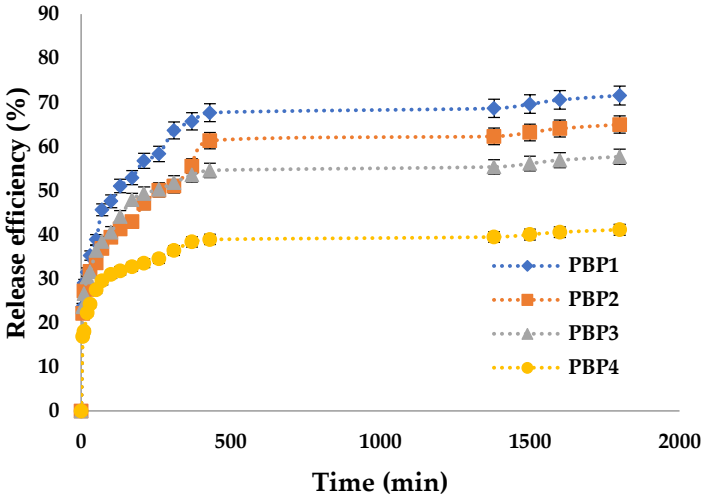

(a)

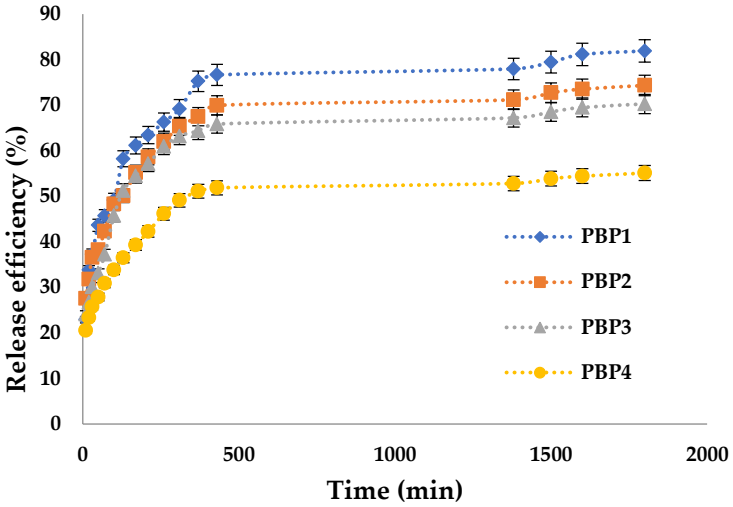

(b)

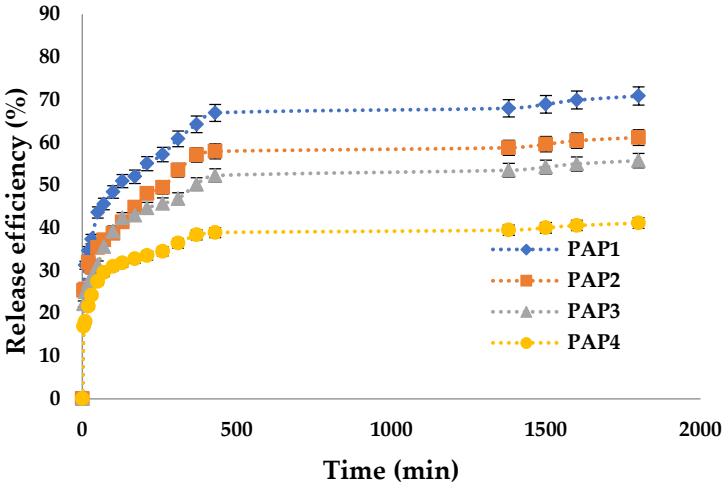

(c)

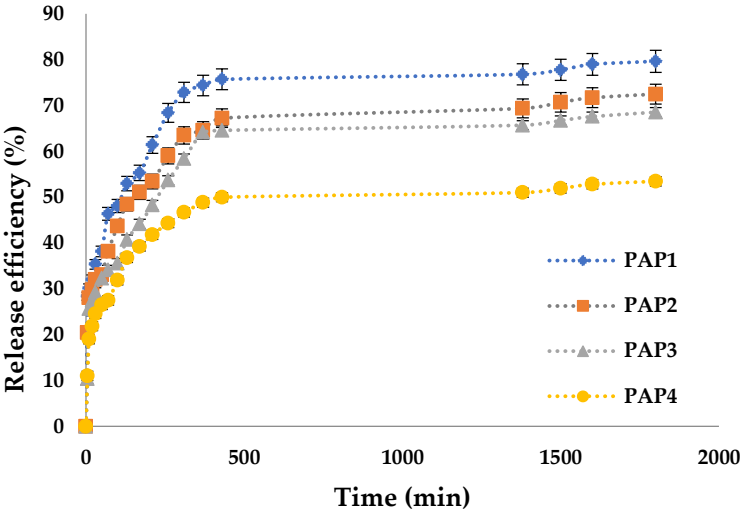

(d)

Figure 41. The p-coumaric acid release kinetics in time at different -CHO/-NH_2 molar ratio of (a) hydrogels prepared at pH= 3.5 immersed in acetate buffer solution pH= 5.5 (b) hydrogels prepared at pH= 3.5 immersed in phosphate-buffer solution pH= 7.4 (c) hydrogels prepared at pH= 5.5 immersed in acetate buffer solution pH= 5.5 (d) hydrogels prepared at pH= 5.5 immersed in phosphate buffer solution pH= 7.4

A controlled release is achieved when the active compound can diffuse out of the film's network gradually in a limited time with appropriate dosage. Hence, drug waste is avoided and a suitable treatment effect is reached.

The release of the bioactive principle was rapid in the first phase of the study due to the

higher concentration gradient of the drug present at the start of the test, which could act as a driving force for the drug release from the OSA/Gel hydrogels network. The release rate decreases over time until the equilibrium; this decrease might be caused by the thickness of the film that acts as a diffusion barrier [29,288,289]. These results are due to the hydrogel's dense matrix, where strong physical interactions between drug and hydrogel thus limiting drug release from the hydrogel. The work of Kapare et al [61] showed similar results for the encapsulation of propolis on a polyvinyl alcohol (PVA)-based hydrogel, according to a research paper by Kapare et al [294], they demonstrated similar results, obtaining by encapsulation of propolis on polyvinyl alcohol (PVA) hydrogel based hydrogel.

It was reported that the drug release depends on the interaction between the polymer network and the drug, the hydrogel swelling behavior in an aqueous solution, and the solubility of the drug [35,36]. The OSA/Gel-based hydrogels could be used in biomedical applications for controlled and sustained release of the bioactive principle. It was found that the release efficiency was higher in the PBS 0.1 M at pH=7.4, compared with the release efficiency values obtained in ABS. 0.1 M. pH=5.5. The maximum p-coumaric acid release efficiency was 82% in PBS at pH=7.4 after 1800 minutes; when it was used the hydrogel synthesized at pH=3.7 with immobilized Pro (molar ratio -CHO/-NH_2 was 0.5/1). Also, the p-coumaric acid release efficiency values increased when the cross-linking density (or molar ratio) of the OSA/Gel-based hydrogel was lower. The Pro (p-coumaric acid) release kinetics from OSA/Gel-based hydrogels are consistent with the degree of hydrogel swelling. The results show that the hydrogels with a smaller –CHO/-NH_2 molar ratio had a higher swelling degree and released a higher p-coumaric acid amount in both pH mediums. These results confirmed that the release efficiency increased with the decrease of the cross-linking degree due to the influence of the polymer network mesh size, which was higher in hydrogels with a lower cross-linking degree. An identic effect was observed in many studies. Sarmah et al. Yan et al. and Gull et al. suggest that increased cross-linking density in the hydrogel structure impedes drug release. The tight cross-linking network limits the movement of drug molecules, slowing the rate of release or reducing the efficiency of drug release. Thus, a high degree of cross-linking limits drug diffusion from the hydrogel matrix [295–297].

V. 13. Antioxidant activity

DPPH possesses an unpaired electron capable of accepting either electrons or hydrogen ions, leading to a color reaction. This characteristic makes it a straightforward and ideal model

for assessing free radical scavenging activity. In the scope of this investigation, we assessed the DPPH free radical scavenging activity of OSA/G Pro-encapsulated hydrogels; OSA/G Pro-encapsulated UV-irradiated hydrogels, free Pro, UV-irradiated free Pro, and utilized ascorbic acid as a standard. The assessment involved determining the inhibition percentage of free radicals from DPPH, and based on these findings, the antioxidant activity was expressed through IC50. The examination of antioxidant activity focused on the immobilized Pro within hydrogel films, allowing for an exploration of the impact of constituent polymers and the molar ratio between polymers on this crucial feature of the active principle. Additionally, the study considered the influence of UV irradiation on the hydrogels and Pro as an active principle. In essence, a lower IC50 value signifies higher antioxidant activity. As mentioned earlier, the IC50 value was calculated from the graphical representation depicting the inhibition percentage versus concentration, expressed in µg/mL. The findings from these analyses are presented in **Figure 42**.

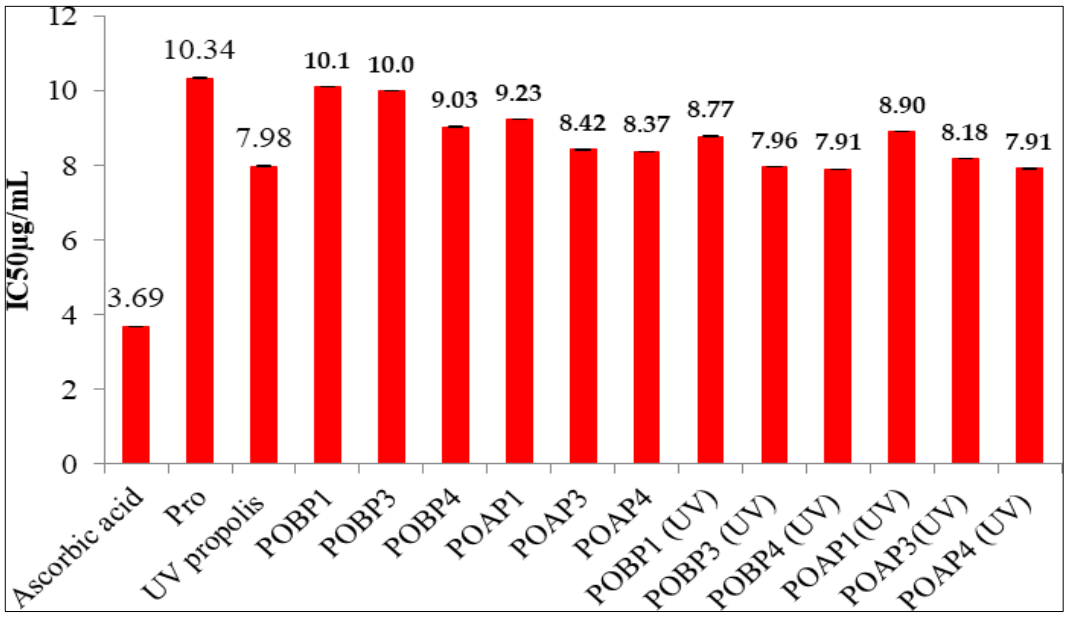

Figure 42. The obtained IC50 values for the analyzed samples (I made the standard deviation but it doesn't apeare because thr deference is too smal).

UV irradiation can significantly affect the antioxidant activity of propolis. Studies show that exposure to UV light can alter propolis's free radical scavenging capacity, either enhancing or reducing its effectiveness, depending on the preparation and form of the propolis. For instance, a study found that UV irradiation decreased the antioxidant activity of propolis drops, whereas propolis spray showed an increase in antioxidant activity after UV exposure. This difference may be due to the formulation and how each reacts with UV-induced oxidative stress [298,299].

Furthermore, another study demonstrated that propolis methanolic extracts exhibited strong

antioxidant activity and provided protection against UV-induced oxidative damage in skin cells, suggesting a potential photoprotective role [299].

These findings suggest that while UV irradiation can sometimes diminish the antioxidant potential of propolis, specific formulations may benefit from UV exposure in terms of increased activity, which can be explored for applications like skin protection against UV damage.

The investigation revealed that the IC50 values for both free Pro and OSA/G Pro-encapsulated hydrogels decrease with an increased amount in the films. This trend was observed for both UV-irradiated and non-irradiated samples and under both pH mediums. Notably, at a pH medium of 5.5, the IC50 value is lower than at a pH of 3.5, suggesting that the antioxidant activity of Pro-loaded hydrogel films intensifies with a higher degree of cross-linking in the hydrogel film. Another noteworthy observation is that the IC50 value decreases upon exposing the samples to UV irradiation. UV irradiation of Pro results in a lower IC50 value than free Pro, indicating enhanced antioxidant activity. This effect is also observed in UV-irradiated, encapsulated propolis, suggesting that UV exposure boosts the antioxidant activity of both free and encapsulated forms. This increase in activity is likely due to the degradation of polyphenols under UV light, which produces lower molecular weight products. Some studies have shown that UV irradiation can increase the antioxidant activity of propolis, particularly in certain formulations like propolis sprays. This enhancement is likely due to the alteration of phenolic compounds, such as flavonoids and phenolic acids, which become more reactive after UV exposure. UV light might also activate latent antioxidants in propolis, making them more effective at scavenging free radicals. Additionally, synergistic effects between modified and existing antioxidants in propolis could further boost its antioxidant potential. However, the impact of UV irradiation is not uniform across all propolis forms, as drops, for example, have been observed to experience a decrease in activity after UV exposure [298,299].

Acompelling correlation emerged from the results, revealing that the antioxidant content increases concomitantly with the rise in Schiff base cross-linking. Antioxidants inherent in Pro play a crucial role in neutralizing harmful free radicals, exerting their protective effects.

The observed increase in antioxidant activity in both Pro and Pro encapsulated in hydrogel films following UV irradiation can be attributed to a complex interplay of factors. Propolis contains several antioxidant compounds, including phenolics and prenylates such as flavonoids, *p-coumaric* acid, ferulic acid, caffeic acid and drupanine [55,300], it has inherent properties that contribute to its ability to neutralize free radicals and counter oxidative stress, as highlighted by

Andritoiu et al [55]. UV irradiation acts as a catalyst in this phenomenon, inducing changes in the chemical composition and properties of the natural substances within Pro. This process has the potential to either form new compounds or modify existing ones. UV light has been recognized for its capacity to activate phytochemicals by breaking chemical bonds or initiating specific reactions. Such activation can result in the scavenging of free radicals, thereby bolstering the protective capabilities of Pro against oxidative stress and consequently enhancing its overall antioxidant properties [301]. Moreover, UV irradiation has been shown to generate reactive oxygen species (ROS) within Pro. While ROS are commonly associated with oxidative damage, at lower levels, they can paradoxically stimulate the production of endogenous antioxidants within organisms. In the context of Pro exposed to UV light, this phenomenon may trigger the synthesis of its own antioxidants as a defense mechanism [302]. Ebrahimi et al. [303] have demonstrated that exposure of chlorophylls to UV-A light can lead to the generation of singlet oxygen (a reactive oxygen species). Singlet oxygen can oxidize neighboring molecules, and the oxidative stress caused by oxygen triggers a series of biochemical events within the extract, ultimately leading to the synthesis and accumulation of secondary metabolites, including phenolic compounds. Consequently, this intrinsic response contributes to an overall augmentation of antioxidant activity. This dual action of UV light—activating existing phytochemicals and stimulating the synthesis of endogenous antioxidants creates a synergistic effect that reinforces the antioxidant potential of Pro. This phenomenon is confined to Pro alone and extends to hydrogel films encapsulating propolis, highlighting the adaptability and responsiveness of this composite system to UV irradiation. These findings underscore the intricate relationship between UV exposure, the chemical dynamics of Pro and the resulting enhancement of its antioxidant properties, offering valuable insights into potential applications in biomedical and therapeutic contexts.

Indeed, the closer the antioxidant activity of the propolis extracted from the films is to that of unirradiated free propolis, the more effectively the polymer matrix protects the encapsulated propolis. This demonstrates the protective role of the hydrogel film, which helps to preserve the integrity and functionality of the propolis when exposed to UV light. In medical applications, this protective mechanism is crucial for maintaining the therapeutic efficacy of propolis in various formulations.

V14. Conclusion

This study successfully developed biocompatible hydrogels based on gelatin by cross-

linking protein-free amino groups with aldehyde groups obtained through sodium alginate oxidation. The hydrogels were synthesized with different molar ratios between the oxidized alginate and gelatin, and the effects of pH and cross-linking degree were investigated. The presence of aldehyde groups in the oxidized alginate was confirmed through FTIR and NMR spectroscopy.

The results showed that increasing the molar ratio NH_2/CHO led to higher conversion index values of amino groups of gelatin and improved hydrogel stability. However, it also resulted in decreased swelling degree values in different pH mediums. The encapsulation efficiency of propolis increases when the concentrations of oxidized alginate in the hydrogel decrease, while the release efficiency of immobilized propolis decreases with an increase in the cross-linking degree, being in concordance with the swelling degree. By Pro immobilization, its antioxidant activity is not affected. The values of IC 50 of encapsulated Pro are very close to or lower than that of free Pro. The results show that the antioxidant activity increases if the samples are UV irradiated or have more oxidized alginate within the polymeric matrix. These findings also show that the hydrogel films could be UV irradiated for sterilization and used as wound dressing to treat different skin diseases. These findings provide valuable insights into the design and optimization of hydrogels for propolis immobilization and controlled release applications. The developed hydrogels have the potential for use in various biomedical and pharmaceutical fields, such as drug delivery systems or wound healing applications.

GENERAL CONCLUSION

General Conclusion

This study successfully developed biocompatible hydrogels based on gelatin by cross-linking amino groups (-NH_2), devoid of free proteins with aldehyde groups (-CHO) generated through the oxidation of sodium alginate with sodium periodate $NaIO_4$.

1. The results showed, on the one hand, that the degree of oxidation increased progressively with time up to 24 h, reaching a value of 35.26%; it remained practically constant up to 72 h. On the other hand, the optimum temperature at which the degree of oxidation reached the maximum value (35%) was 30°C, but increasing the temperature to 45°C resulted in a decrease in the degree of oxidation to 30%.
2. The presence of aldehyde groups in oxidized sodium alginate (OSA) was confirmed using FTIR spectroscopy, new stretching bonds at 1735 cm^{-1}; and NMR spectroscopy, a new stretching links appears at 8.24 ppm, which is attributed to the proton of the aldehyde groups -CHO.
3. The results confirmed that oxidized functional groups, such as carbonyl groups, can contribute to increased thermal stability of OSA.
4. The Schiff hydrogels OSA/Gel were synthesized with different molar ratios of –NH2 groups of gelatin to –CHO groups from oxidized alginate, at different pH values (3.5 and 5.5). FTIR analysis showed the appearance of new bonds at 1556 cm-1 and 1633 cm^{-1} for the OSA/gel hydrogels, confirming the presence of -N=C- bonds. TGA analysis of the composite hydrogels showed that the imine bond significantly improved the thermal stability. SEM results of the film surface and cross section showed that the roughness of the hydrogel surface increased with the addition of OSA and Pro to the hydrogel matrix. On the other hand, OSA/Gel and OSA/Gel/Pro composite hydrogels showed less compact morphology.
5. Increasing the -NH_2/-CHO molar ratio significantly increased the rate of conversion of the gelatin amino groups, leading to improved hydrogel stability but reduced swelling in different pHs mediums (5.5 and 7.4). Propolis encapsulation efficiency was higher at lower concentrations of oxidised alginate in the hydrogel, while higher degrees of cross-linking led to a reduction in propolis release efficiency, in agreement with the degree of swelling.
6. Importantly, the antioxidant activity of immobilized propolis remained intact, with IC50 values for encapsulated propolis being comparable or lower than those of free propolis. Additionally, UV irradiation or increased oxidized alginate within the matrix enhanced

antioxidant activity. These findings suggest that the hydrogels can be sterilized via UV irradiation and serve as wound dressings for treating skin conditions.

The successful development of these hydrogels represents a significant advancement in biomaterials research, providing a platform for further exploration and application in health care and environmental sustainability.

Future research could focus on optimizing the formulation and exploring additional biopolymer combinations to enhance the functionality and applicability of these innovative materials in various biomedical fields.

PERSPECTIVES

Perspectives

Hydrogels based on OSA/Gel/Pro represent a promising area in biomaterials research with significant biomedical potential. These hybrid hydrogels leverage the complementary features of proteins and polysac-charides, offering biocompatibility, biodegradability, and tailored properties.

These hydrogels are particularly promising for tissue engineering, drug delivery, and regenerative medicine, serving as scaffolds, delivery systems, and implantable devices. Their biodegradability reduces long-term adverse effects, and their ability to encapsulate bioactive molecules enhances therapeutic outcomes.

However, several challenges and opportunities lie ahead. Optimization of synthesis methods, including cross-linking efficiency and gelation kinetics, is essential to achieve reproducible and scalable production of hydrogels with consistent properties. Compre-hensive characterization and evaluation of their biocompatibility, mechanical properties, and degradation behavior are crucial to ensure their safety and efficacy in clinical trials. Furthermore, exploring novel formulations, such as hybrid hydrogels with enhanced stimuli responsiveness or multifunctional capabilities, holds promise for addressing unmet needs in regenerative medicine and drug delivery.

References

1. Ho, T.C.; Chang, C.C.; Chan, H.P.; Chung, T.W.; Shu, C.W.; Chuang, K.P.; Duh, T.H.; Yang, M.H.; Tyan, Y.C. Hydrogels: Properties and Applications in Biomedicine. *Molecules* **2022**, *27*, 1–29, doi:10.3390/molecules27092902.

2. Chai, Q.; Jiao, Y.; Yu, X. Hydrogels for Biomedical Applications: Their Characteristics and the Mechanisms behind Them. *Gels* **2017**, *3*, doi:10.3390/gels3010006.

3. Mahinroosta, M.; Jomeh Farsangi, Z.; Allahverdi, A.; Shakoori, Z. Hydrogels as Intelligent Materials: A Brief Review of Synthesis, Properties and Applications. *Mater. Today Chem.* **2018**, *8*, 42–55, doi:10.1016/j.mtchem.2018.02.004.

4. Kaith, B.S.; Singh, A.; Sharma, A.K.; Sud, D. Hydrogels: Synthesis, Classification, Properties and Potential Applications—A Brief Review. *J. Polym. Environ.* **2021**, *29*, 3827–3841, doi:10.1007/s10924-021-02184-5.

5. Shivani Chaudhary, Vijay Prakash Jain, G.J. The Composition of Polysaccharides: Monosaccharides and Binding, Group Decorating, Polysaccharides Chains. In *Innovation in Nano-Polysaccharides for Eco-sustainability*; 2022; pp. 83–118.

6. Ren, Y.; Bai, Y.; Zhang, Z.; Cai, W.; Del Rio Flores, A. The Preparation and Structure Analysis Methods of Natural Polysaccharides of Plants and Fungi: A Review of Recent Development. *Molecules* **2019**, *24*, doi:10.3390/molecules24173122.

7. Zong, A.; Cao, H.; Wang, F. Anticancer Polysaccharides from Natural Resources: A Review of Recent Research. *Carbohydr. Polym.* **2012**, *90*, 1395–1410, doi:10.1016/j.carbpol.2012.07.026.

8. Yu, Z.J.; Li, Q.; He, X.; Wang, X.; Wen, Y.; Zeng, L.; Yu, W.; Hu, P.; Chen, H. A Multifunctional Hydrogel Based on Nature Polysaccharide Fabricated by Schiff Base Reaction. *Eur. Polym. J.* **2023**, *197*, 112330, doi:10.1016/j.eurpolymj.2023.112330.

9. Alavarse, A.C.; Frachini, E.C.G.; da Silva, R.L.C.G.; Lima, V.H.; Shavandi, A.; Petri, D.F.S. Crosslinkers for Polysaccharides and Proteins: Synthesis Conditions, Mechanisms, and Crosslinking Efficiency, a Review. *Int. J. Biol. Macromol.* **2022**, *202*, 558–596, doi:10.1016/j.ijbiomac.2022.01.029.

10. Mo, C.; Xiang, L.; Chen, Y. Advances in Injectable and Self-Healing Polysaccharide Hydrogel Based on the Schiff Base Reaction. *Macromol. Rapid Commun.* **2021**, *42*, 1–18, doi:10.1002/marc.202100025.

11. Yang, C.; Gao, L.; Liu, X.; Yang, T.; Yin, G.; Chen, J.; Guo, H.; Yu, B.; Cong, H. Injectable Schiff Base Polysaccharide Hydrogels for Intraocular Drug Loading and Release. *J. Biomed. Mater. Res. - Part A* **2019**, *107*, 1909–1916, doi:10.1002/jbm.a.36677.

12. Zhou, L.; Chen, M.; Guan, Y.; Zhang, Y. Multiple Responsive Hydrogel Films Based on Dynamic Schiff Base Linkages. *Polym. Chem.* **2014**, *5*, 7081–7089, doi:10.1039/c4py00868e.

13. Xing, L.; Sun, J.; Tan, H.; Yuan, G.; Li, J.; Jia, Y.; Xiong, D.; Chen, G.; Lai, J.; Ling, Z.; et al. Covalently Polysaccharide-Based Alginate/Chitosan Hydrogel Embedded Alginate Microspheres for BSA Encapsulation and Soft Tissue Engineering. *Int. J. Biol. Macromol.* **2019**, *127*, 340–348, doi:10.1016/j.ijbiomac.2019.01.065.

14. Weng, L.; Rostamzadeh, P.; Nooryshokry, N.; Le, H.C.; Golzarian, J. In Vitro and in Vivo Evaluation of Biodegradable Embolic Microspheres with Tunable Anticancer Drug Release. *Acta Biomater.* **2013**, *9*, 6823–6833, doi:10.1016/j.actbio.2013.02.017.

15. Li, Y.; Liu, C.; Tan, Y.; Xu, K.; Lu, C.; Wang, P. In Situ Hydrogel Constructed by Starch- Based Nanoparticles via a Schiff Base Reaction. *Carbohydr. Polym.* **2014**, *110*, 87–94, doi:10.1016/j.carbpol.2014.03.058.

16. Xu, J.; Liu, Y.; Hsu, S. Hydrogels Based on Schi Ff Base Linkages For. *Molecules* **2019**, *24*, 1–21.

17. Su, M.; Ruan, L.; Dong, X.; Tian, S.; Lang, W.; Wu, M.; Chen, Y.; Lv, Q.; Lei, L. Current State of Knowledge on Intelligent-Response Biological and Other Macromolecular Hydrogels in Biomedical Engineering: A Review. *Int. J. Biol. Macromol.* **2023**, *227*, 472– 492, doi:10.1016/j.ijbiomac.2022.12.148.

18. Drury, J.L.; Mooney, D.J. Hydrogels for Tissue Engineering: Scaffold Design Variables and Applications. *Biomaterials* **2003**, *24*, 4337–4351, doi:10.1016/S0142-9612(03)00340-5.

19. Tomasik, P. Chemical Modifications of Polysaccharides. *Chem. Funct. Prop. Food Saccharides* **2003**, *2013*, 123–130, doi:10.1155/2013/417672.

20. Schwartz, S.J.; Cooperstone, J.L.; Cichon, M.J.; Joachim, H. V; Monica, G. *Colorants Fennema's Food Chemistry Ed Damodaran S, Parkin L. K.*; 2017; ISBN 9780333227794.

21. Davari, N.; Bakhtiary, N.; Khajehmohammadi, M.; Sarkari, S.; Tolabi, H.; Ghorbani, F.; Ghalandari, B. *Protein-Based Hydrogels: Promising Materials for Tissue Engineering*; 2022; Vol. 14; ISBN 8613003133.

22. Abdalla, T.H.; Nasr, A.S.; Bassioni, G.; Harding, D.R.; Kandile, N.G. Fabrication of Sustainable Hydrogels-Based Chitosan Schiff Base and Their Potential Applications. *Arab. J. Chem.* **2022**, *15*, 103511, doi:10.1016/j.arabjc.2021.103511.

23. Review, T. Bio-Based Composite Hydrogels for Biomedical Applications.

24. Yin, B.; Gosecka, M.; Bodaghi, M.; Crespy, D.; Youssef, G.; Dodda, J.M.; Wong, S.H.D.; Imran, A. Bin; Gosecki, M.; Jobdeedamrong, A.; et al. Engineering Multifunctional Dynamic Hydrogel for Biomedical and Tissue Regenerative Applications. *Chem. Eng. J.* **2024**, *487*, 150403, doi:10.1016/j.cej.2024.150403.

25. Kristiansen, K.A.; Ballance, S.; Potthast, A.; Christensen, B.E. An Evaluation of Tritium and Fluorescence Labelling Combined with Multi-Detector SEC for the Detection of Carbonyl Groups in Polysaccharides. *Carbohydr. Polym.* **2009**, *76*, 196–205, doi:10.1016/j.carbpol.2008.10.006.

26. Aristizabal Bedoya, D.; Figueroa, F.N.; Macchione, M.A.; Strumia, M.C. *Advanced Biopolymeric Systems for Drug Delivery*; 2020; ISBN 978-3-030-46922-1.

27. Matricardi, P.; Di Meo, C.; Coviello, T.; Hennink, W.E.; Alhaique, F. Interpenetrating Polymer Networks Polysaccharide Hydrogels for Drug Delivery and Tissue Engineering. *Adv. Drug Deliv. Rev.* **2013**, *65*, 1172–1187, doi:10.1016/j.addr.2013.04.002.

28. Jaipan, P.; Nguyen, A.; Narayan, R.J. Gelatin-Based Hydrogels for Biomedical Applications. *MRS Commun.* **2017**, *7*, 416–426, doi:10.1557/mrc.2017.92.

29. Buhus, G.; Peptu, C.; Popa, M.; Desbrières, J. Controlled Release of Water Soluble Antibiotics by Carboxymethylcellulose- And Gelatin-Based Hydrogels Crosslinked with Epichlorohydrin. *Cellul. Chem. Technol.* **2009**, *43*, 141–151.

30. Skopinska-Wisniewska, J.; Tuszynska, M.; Olewnik-Kruszkowska, E. Comparative Study of Gelatin Hydrogels Modified by Various Cross-Linking Agents. *Materials (Basel).* **2021**, *14*, 1–17, doi:10.3390/ma14020396.

31. Buhus, G.; Popa, M.; Desbrieres, J. Hydrogels Based on Carboxymethylcellulose and Gelatin for Inclusion and Release of Chloramphenicol. *J. Bioact. Compat. Polym.* **2009**, *24*, 525–545, doi:10.1177/0883911509349687.

32. Rao, Z.; Dong, Y.; Liu, J.; Zheng, X.; Pei, Y.; Tang, K. Genipin-Crosslinked Gelatin- Based Composite Hydrogels Reinforced with Amino-Functionalized Microfibrillated Cellulose. *Int. J. Biol. Macromol.* **2022**, *222*, 3155–3167, doi:10.1016/j.ijbiomac.2022.10.088.

33. Schacht, E.; Bogdanov, B.; Van Den Bulcke, A.; De Rooze, N. Hydrogels Prepared by Crosslinking of Gelatin with Dextran Dialdehyde. *React. Funct. Polym.* **1997**, *33*, 109– 116, doi:10.1016/s1381-5148(97)00047-3.

34. Khorshidi, S.; Karkhaneh, A. A Self-Crosslinking Tri-Component Hydrogel Based on Functionalized Polysaccharides and Gelatin for Tissue Engineering Applications. *Mater. Lett.* **2016**, *164*, 468–471, doi:10.1016/j.matlet.2015.11.041.

35. Brownlee, I.A.; Seal, C.J.; Wilcox, M.; Dettmar, P.W.; Pearson, J.P. Applications of Alginates in Food. **2009**, 211–228, doi:10.1007/978-3-540-92679-5_9.

36. Sanchez-Ballester, N.M.; Bataille, B.; Soulairol, I. Sodium Alginate and Alginic Acid as Pharmaceutical Excipients for Tablet Formulation: Structure-Function Relationship. *Carbohydr. Polym.* **2021**, *270*, 118399, doi:10.1016/j.carbpol.2021.118399.

37. Li, J.; He, J.; Huang, Y. Role of Alginate in Antibacterial Finishing of Textiles. *Int. J. Biol. Macromol.* **2017**, *94*, 466–473, doi:10.1016/j.ijbiomac.2016.10.054.

38. Ding, W.; Zhou, J.; Zeng, Y.; Wang, Y. nan; Shi, B. Preparation of Oxidized Sodium Alginate with Different Molecular Weights and Its Application for Crosslinking Collagen Fiber. *Carbohydr. Polym.* **2017**, *157*, 1650–1656, doi:10.1016/j.carbpol.2016.11.045.

39. Kristiansen, K.A.; Potthast, A.; Christensen, B.E. Periodate Oxidation of Polysaccharides

for Modification of Chemical and Physical Properties. *Carbohydr. Res.* **2010**, *345*, 1264– 1271, doi:10.1016/j.carres.2010.02.011.

40. Emami, Z.; Ehsani, M.; Zandi, M.; Foudazi, R. Controlling Alginate Oxidation Conditions for Making Alginate-Gelatin Hydrogels. *Carbohydr. Polym.* **2018**, *198*, 509–517, doi:10.1016/j.carbpol.2018.06.080.

41. Kong, X.; Chen, L.; Li, B.; Quan, C.; Wu, J. Applications of Oxidized Alginate in Regenerative Medicine. *J. Mater. Chem. B* **2021**, *9*, 2785–2801, doi:10.1039/d0tb02691c.

42. Reakasame, S.; Boccaccini, A.R. Oxidized Alginate-Based Hydrogels for Tissue Engineering Applications: A Review. *Biomacromolecules* **2018**, *19*, 3–21, doi:10.1021/acs.biomac.7b01331.

43. Chi, J.; Li, A.; Zou, M.; Wang, S.; Liu, C.; Hu, R.; Jiang, Z.; Liu, W.; Sun, R.; Han, B. Novel Dopamine-Modified Oxidized Sodium Alginate Hydrogels Promote Angiogenesis and Accelerate Healing of Chronic Diabetic Wounds. *Int. J. Biol. Macromol.* **2022**, *203*, 492–504, doi:10.1016/j.ijbiomac.2022.01.153.

44. Gomez, C.G.; Rinaudo, M.; Villar, M.A. Oxidation of Sodium Alginate and Characterization of the Oxidized Derivatives. *Carbohydr. Polym.* **2007**, *67*, 296–304, doi:10.1016/j.carbpol.2006.05.025.

45. Hu, Y.; Chen, T.; Dong, X.; Mei, Z. Preparation and Characterization of Composite Hydrogel Beads Based on Sodium Alginate. *Polym. Bull.* **2015**, *72*, 2857–2869, doi:10.1007/s00289-015-1440-2.

46. Pettignano, A.; Häring, M.; Bernardi, L.; Tanchoux, N.; Quignard, F.; Díaz Díaz, D. Self- Healing Alginate-Gelatin Biohydrogels Based on Dynamic Covalent Chemistry: Elucidation of Key Parameters. *Mater. Chem. Front.* **2017**, *1*, 73–79, doi:10.1039/c6qm00066e.

47. Rottensteiner, U.; Sarker, B.; Heusinger, D.; Dafinova, D.; Rath, S.N.; Beier, J.P.; Kneser, U.; Horch, R.E.; Detsch, R.; Boccaccini, A.R.; et al. In Vitro and in Vivo Biocompatibility of Alginate Dialdehyde/Gelatin Hydrogels with and without Nanoscaled Bioactive Glass for Bone Tissue Engineering Applications. *Materials (Basel).* **2014**, *7*, 1957–1974, doi:10.3390/ma7031957.

48. D'Auria, F.D.; Tecca, M.; Scazzocchio, F.; Renzini, V.; Strippoli, V. Effect of Propolis on Virulence Factors of Candida Albicans. *J. Chemother.* **2003**, *15*, 454–460, doi:10.1179/joc.2003.15.5.454.

49. Sevinç-Özakar, R.; Seyret, E.; Özakar, E.; Adıgüzel, M.C. Nanoemulsion-Based Hydrogels and Organogels Containing Propolis and Dexpanthenol: Preparation, Characterization, and Comparative Evaluation of Stability, Antimicrobial, and Cytotoxic Properties. *Gels* **2022**, *8*, doi:10.3390/gels8090578.

50. Al-Hatamleh, M.A.I.; Alshaer, W.; Hatmal, M.M.; Lambuk, L.; Ahmed, N.; Mustafa, M.Z.; Low, S.C.; Jaafar, J.; Ferji, K.; Six, J.L.; et al. Applications of Alginate-Based Nanomaterials in Enhancing the Therapeutic Effects of Bee Products. *Front. Mol. Biosci.*

2022, *9*, 1–33, doi:10.3389/fmolb.2022.865833.

51. Ordóñez, R.M.; Zampini, I.C.; Moreno, M.I.N.; Isla, M.I. Potential Application of Northern Argentine Propolis to Control Some Phytopathogenic Bacteria. *Microbiol. Res.* **2011**, *166*, 578–584, doi:10.1016/j.micres.2010.11.006.

52. Sforcin, J.M.; Bankova, V. Propolis: Is There a Potential for the Development of New Drugs? *J. Ethnopharmacol.* **2011**, *133*, 253–260, doi:10.1016/j.jep.2010.10.032.

53. Burdock, G.A. Review of the Biological Properties and Toxicity of Bee Propolis (Propolis). *Food Chem. Toxicol.* **1998**, *36*, 347–363, doi:10.1016/S0278-6915(97)00145-2.

54. Gonçalves, I.S.; Lima, L.R.; Berretta, A.A.; Amorim, N.A.; Pratavieira, S.; Corrêa, T.Q.; Nogueira, F.A.R.; Barud, H.S. Antimicrobial Formulation of a Bacterial Nanocellulose/Propolis-Containing Photosensitizer for Biomedical Applications. *Polymers (Basel).* **2023**, *15*, doi:10.3390/polym15040987.

55. Andritoiu, C.V.; Lungu, C.; Danu, M.; Ivanescu, B.; Andriescu, C.E.; Vlase, L.; Havarneanu, C.; Iurciuc, C.E.; Popa, M. Evaluation of the Healing Effect of Ointments Based on Bee Products on Cutaneous Lesions in Wistar Rats. *Pharmaceuticals* **2021**, *14*, doi:10.3390/ph14111146.

56. Cunha, A.G.; Gandini, A. Turning Polysaccharides into Hydrophobic Materials: A Critical Review. Part 1. Cellulose. *Cellulose* **2010**, *17*, 875–889, doi:10.1007/s10570-010-9434-6.

57. Ding, W.; Wang, Y. nan; Zhou, J.; Shi, B. Effect of Structure Features of Polysaccharides on Properties of Dialdehyde Polysaccharide Tanning Agent. *Carbohydr. Polym.* **2018**, *201*, 549–556, doi:10.1016/j.carbpol.2018.08.111.

58. Malaprade, L. Oxidation of Some Polyalcohols by Periodic Acid-Applications. *Comptes Rendus* **1928**, *186*, 382–384.

59. Malaprade, L. Action of Polyalcohols on Periodic Acid. Analytical Application. *Bull. Soc. Chim. Fr.* **1928**, *43*, 683–696.

60. P. (F.) Fleury and J. Lange, C.. No Title. *Acad. Sci* **1932**, *195*, 1395.

61. Jaušovec, D.; Vogrinčič, R.; Kokol, V. Introduction of Aldehyde vs. Carboxylic Groups to Cellulose Nanofibers Using Laccase/TEMPO Mediated Oxidation. *Carbohydr. Polym.* **2015**, *116*, 74–85, doi:10.1016/j.carbpol.2014.03.014.

62. Abdul Ghafar , Pavel Gurikov , Raman Subrahmanyam , Kirsti Parikka , Maija Tenkanen , Irina Smirnova, K.S.M. Mesoporous Guar Galactomannan Based Biocomposite Aerogels through Enzymatic Crosslinking. *Compos. Part A Appl. Sci. Manuf.* **2017**, *94*, 93–103, doi:https://doi.org/10.1016/j.compositesa.2016.12.013.

63. Painter Oxidation during Periodate Ox of Alginate 1979.

64. Parikka, K.; Master, E.; Tenkanen, M. Oxidation with Galactose Oxidase: Multifunctional Enzymatic Catalysis. *J. Mol. Catal. B Enzym.* **2015**, *120*, 47–59,

doi:10.1016/j.molcatb.2015.06.006.

65. Kholiya, F.; Chaudhary, J.P.; Vadodariya, N.; Meena, R. Synthesis of Bio-Based Aldehyde from Seaweed Polysaccharide and Its Interaction with Bovine Serum Albumin. *Carbohydr. Polym.* **2016**, *150*, 278–285, doi:10.1016/j.carbpol.2016.05.022.

66. Ding, W.; Wu, Y. Sustainable Dialdehyde Polysaccharides as Versatile Building Blocks for Fabricating Functional Materials: An Overview. *Carbohydr. Polym.* **2020**, *248*, 116801, doi:10.1016/j.carbpol.2020.116801.

67. Parikka, K.; Leppänen, A.S.; Pitkänen, L.; Reunanen, M.; Willför, S.; Tenkanen, M. Oxidation of Polysaccharides by Galactose Oxidase. *J. Agric. Food Chem.* **2010**, *58*, 262– 271, doi:10.1021/jf902930t.

68. Filip Mollerup, Matti Haara, Kirsti Parikka, Chunlin Xu, Maija Tenkanen, E.M. Enzymatic Oxidation of Plant Polysaccharides Adsorbed to Cellulose Surfaces. *N. Biotechnol.* **2014**, *31*, S7–S8, doi:10.1016/j.nbt.2014.05.1631.

69. Patel, I.; Ludwig, R.; Haltrich, D.; Rosenau, T.; Potthast, A. Studies of the Chemoenzymatic Modification of Cellulosic Pulps by the Laccase-TEMPO System. *Holzforschung* **2011**, *65*, 475–481, doi:10.1515/HF.2011.035.

70. Aracri, E.; Vidal, T. Enhancing the Effectiveness of a Laccase – TEMPO Treatment Has a Biorefining Effect on Sisal Cellulose Fibres. **2012**, 867–877, doi:10.1007/s10570-012- 9686-4.

71. Xu, S.; Song, Z.; Qian, X. Introducing Carboxyl and Aldehyde Groups to Softwood- Derived Cellulosic Fibers by Laccase / TEMPO-Catalyzed Oxidation. **2013**, 2371–2378, doi:10.1007/s10570-013-9985-4.

72. Wongsagon, R.; Shobsngob, S.; Varavinit, S. Preparation and Physicochemical Properties of Dialdehyde Tapioca Starch. *Starch/Staerke* **2005**, *57*, 166–172, doi:10.1002/star.200400299.

73. Çaykara, T.; Demirci, S.; Eroğlu, M.S.; Güven, O. Poly(Ethylene Oxide) and Its Blends with Sodium Alginate. *Polymer (Guildf).* **2005**, *46*, 10750–10757, doi:10.1016/j.polymer.2005.09.041.

74. Muhammad, M.; Willems, C.; Rodríguez-fernández, J.; Gallego- Ferrer, G.; Groth, T. Synthesis and Characterization of Oxidized Polysaccharides for in Situ Forming Hydrogels. *Biomolecules* **2020**, *10*, 1–18, doi:10.3390/biom10081185.

75. Criegee, R. An Oxidative Fission of Glycols (II. Communication. On Oxidations with Lead (IV)-Salts)). *Ber. Dtsch. Chem. Ges. B* **1931**, *64*, 260–266.

76. Venkatesan, J.; Bhatnagar, I.; Manivasagan, P.; Kang, K.H.; Kim, S.K. Alginate Composites for Bone Tissue Engineering: A Review. *Int. J. Biol. Macromol.* **2015**, *72*, 269–281, doi:10.1016/j.ijbiomac.2014.07.008.

77. Venkatesan, J.; Nithya, R.; Sudha, P.N.; Kim, S.K. *Role of Alginate in Bone Tissue*

Engineering; 1st ed.; Elsevier Inc., 2014; Vol. 73; ISBN 9780128002681.

78. Lai, H.L.; Abu'Khalil, A.; Craig, D.Q.M. The Preparation and Characterisation of Drug- Loaded Alginate and Chitosan Sponges. *Int. J. Pharm.* **2003**, *251*, 175–181, doi:10.1016/S0378-5173(02)00590-2.

79. Bobbitt, J.M. Periodate Oxidation of Carbohydrates. *Adv. Carbohydr. Chem.* **1956**, *11*, 1–41, doi:10.1016/S0096-5332(08)60115-0.

80. © 1945 Nature Publishing Group. **1945**.

81. Taniguchi, N.; Objectives, L. Amino Acids and Proteins N Taniguchi C0002 C0002 2.

82. Whitford, D. *P Roteins*; 2013; ISBN 0471498939.

83. Sun, P.D.; Foster, C.E.; Boyington, J.C. Overview of Protein Structural and Functional Folds. *Curr. Protoc. Protein Sci.* **2004**, *Chapter 17*, 1–189, doi:10.1002/0471140864.ps1701s35.

84. Syariah, K.B.; Ilmu, G. *No* 主観的健康感を中心とした在宅高齢者における健康関連指標に関する共分散構造分析*Title*; ISBN 9780815341055.

85. Bharskar, G. A Review on Hydrogel. **2020**, doi:10.20959/wjpps20207-16602.

86. Maitra, J.; Shukla, V.K. Cross-Linking in Hydrogels - A Review. *Am. J. Polym. Sci.* **2014**, *4*, 25–31, doi:10.5923/j.ajps.20140402.01.

87. Su, J. Thiol-Mediated Chemoselective Strategies for in Situ Formation of Hydrogels. *Gels* **2018**, *4*, doi:10.3390/gels4030072.

88. Trengove, A.; Duchi, S.; Onofrillo, C.; O'Connell, C.D.; Di Bella, C.; O'Connor, A.J. Microbial Transglutaminase Improves Ex Vivo Adhesion of Gelatin Methacryloyl Hydrogels to Human Cartilage. *Front. Med. Technol.* **2021**, *3*, 1–14, doi:10.3389/fmedt.2021.773673.

89. Li, Z.; Lin, Z. Recent Advances in Polysaccharide-based Hydrogels for Synthesis and Applications. *Aggregate* **2021**, *2*, 1–26, doi:10.1002/agt2.21.

90. Hennink, W.E.; van Nostrum, C.F. Novel Crosslinking Methods to Design Hydrogels. *Adv. Drug Deliv. Rev.* **2012**, *64*, 223–236, doi:10.1016/j.addr.2012.09.009.

91. Madduma-Bandarage, U.S.K.; Madihally, S. V. Synthetic Hydrogels: Synthesis, Novel Trends, and Applications. *J. Appl. Polym. Sci.* **2021**, *138*, 1–23, doi:10.1002/app.50376.

92. Peppas, N.A.; Khare, A.R. Preparation, Structure and Diffusional Behavior of Hydrogels in Controlled Release. *Adv. Drug Deliv. Rev.* **1993**, *11*, 1–35, doi:10.1016/0169- 409X(93)90025-Y.

93. Weerasinghe, M.A.S.N.; Dodo, O.J.; Rajawasam, C.W.H.; Raji, I.O.; Wanasinghe, S. V.; Konkolewicz, D.; De Alwis Watuthanthrige, N. Educational Series: Turning Monomers into Crosslinked Polymer Networks. *Polym. Chem.* **2023**, *14*, 4503–4514,

doi:10.1039/d3py00912b.

94. Ullah, F.; Othman, M.B.H.; Javed, F.; Ahmad, Z.; Akil, H.M. Classification, Processing and Application of Hydrogels: A Review. *Mater. Sci. Eng. C* **2015**, *57*, 414–433, doi:10.1016/j.msec.2015.07.053.

95. Azeredo, H.M.C.; Waldron, K.W. Crosslinking in Polysaccharide and Protein Films and Coatings for Food Contact - A Review. *Trends Food Sci. Technol.* **2016**, *52*, 109–122, doi:10.1016/j.tifs.2016.04.008.

96. Rossi Marquez, G.; Di Pierro, P.; Esposito, M.; Mariniello, L.; Porta, R. Application of Transglutaminase-Crosslinked Whey Protein/Pectin Films as Water Barrier Coatings in Fried and Baked Foods. *Food Bioprocess Technol.* **2014**, *7*, 447–455, doi:10.1007/s11947- 012-1045-9.

97. Jus, S.; Stachel, I.; Fairhead, M.; Meyer, M.; Thöny-Meyer, L.; Guebitz, G.M. Enzymatic Cross-Linking of Gelatine with Laccase and Tyrosinase. *Biocatal. Biotransformation* **2012**, *30*, 86–95, doi:10.3109/10242422.2012.646036.

98. Battisti, R.; Fronza, N.; Vargas Júnior, Á.; Silveira, S.M. da; Damas, M.S.P.; Quadri, M.G.N. Gelatin-Coated Paper with Antimicrobial and Antioxidant Effect for Beef Packaging. *Food Packag. Shelf Life* **2017**, *11*, 115–124, doi:10.1016/j.fpsl.2017.01.009.

99. Calva-Estrada, S.J.; Jiménez-Fernández, M.; Lugo-Cervantes, E. Protein-Based Films: Advances in the Development of Biomaterials Applicable to Food Packaging. *Food Eng. Rev.* **2019**, 78–92, doi:10.1007/s12393-019-09189-w.

100. Pruett, S.B.; Fan, R.; Zheng, Q.; Schwab, C. Patterns of Immunotoxicity Associated with Chronic as Compared with Acute Exposure to Chemical or Physical Stressors and Their Relevance with Regard to the Role of Stress and with Regard to Immunotoxicity Testing. *Toxicol. Sci.* **2009**, *109*, 265–275, doi:10.1093/toxsci/kfp073.

101. Lee, K.Z.; Jeon, J.; Jiang, B.; Subramani, S.V.; Li, J.; Zhang, F. Protein-Based Hydrogels and Their Biomedical Applications. *Molecules* **2023**, *28*, 1–16, doi:10.3390/molecules28134988.

102. Abdallah, M. Development of Hydrogels and Study the Effect of Their Mechanical Properties on Podocyte Behaviors. **2020**, 23–27.

103. Lee, K.Y.; Mooney, D.J. Alginate: Properties and Biomedical Applications. *Prog. Polym. Sci.* **2012**, *37*, 106–126, doi:10.1016/j.progpolymsci.2011.06.003.

104. Taylor, D.L.; in het Panhuis, M. Self-Healing Hydrogels. *Adv. Mater.* **2016**, *28*, 9060– 9093, doi:10.1002/adma.201601613.

105. Shi, F.K.; Zhong, M.; Zhang, L.Q.; Liu, X.Y.; Xie, X.M. Robust and Self-Healable Nanocomposite Physical Hydrogel Facilitated by the Synergy of Ternary Crosslinking Points in a Single Network. *J. Mater. Chem. B* **2016**, *4*, 6221–6227, doi:10.1039/c6tb01606e.

106. Feng, Z.; Zuo, H.; Gao, W.; Ning, N.; Tian, M.; Zhang, L. A Robust, Self-Healable, and Shape Memory Supramolecular Hydrogel by Multiple Hydrogen Bonding Interactions. *Macromol. Rapid Commun.* **2018**, *39*, 1–7, doi:10.1002/marc.201800138.

107. Kulkarni, A.D.; Vanjari, Y.H.; Sancheti, K.H.; Patel, H.M.; Belgamwar, V.S.; Surana, S.J.; Pardeshi, C. V. Polyelectrolyte Complexes: Mechanisms, Critical Experimental Aspects, and Applications. *Artif. Cells, Nanomedicine Biotechnol.* **2016**, *44*, 1615–1625, doi:10.3109/21691401.2015.1129624.

108. Rembaum, A. Polyelectrolyte Complexes. *J. Macromol. Sci. Part A - Chem.* **1969**, *3*, 87– 99, doi:10.1080/10601326908053794.

109. Tang, S.; Zhao, L.; Yuan, J.; Chen, Y.; Leng, Y. *Physical Hydrogels Based on Natural Polymers*; Elsevier Inc., 2019; ISBN 9780128164211.

110. K. R. Kamath and K. Park Biodegradable Hydrogels in Drug Delivery. *Adv. Drug Deliv. Rev.* **1993**, *11*, 59–84, doi:10.1016/0169-409X(93)90027-2.

111. Jeong, B.; Kim, S.W.; Bae, Y.H. Thermosensitive Sol-Gel Reversible Hydrogels. *Adv. Drug Deliv. Rev.* **2002**, *54*, 37–51, doi:10.1016/S0169-409X(01)00242-3.

112. Kajal, A.; Bala, S.; Kamboj, S.; Sharma, N.; Saini, V. Schiff Bases: A Versatile Pharmacophore. *J. Catal.* **2013**, *2013*, 1–14, doi:10.1155/2013/893512.

113. Zhang, Z.; He, C.; Chen, X. Hydrogels Based on PH-Responsive Reversible Carbon- Nitrogen Double-Bond Linkages for Biomedical Applications. *Mater. Chem. Front.* **2018**, *2*, 1765–1778, doi:10.1039/c8qm00317c.

114. Coden, I.; Mohammad, N.; Uddin, E.; Uddin, S.; Babar, I.H.; Hossain, S.; Bitu, N.A.; Khan, N.; Asraf, A.; Hossen, F. International Journal of Chemistry and Exploring Schiff Base Chemistry- An Overview. **2021**, *9*, 18–31.

115. Kalia, J.; Raines, R.T. Hydrolytic Stability of Hydrazones and Oximes. *Angew. Chemie - Int. Ed.* **2008**, *47*, 7523–7526, doi:10.1002/anie.200802651.

116. Qu, X.; Yang, Z. Benzoic-Imine-Based Physiological-PH-Responsive Materials for Biomedical Applications. *Chem. - An Asian J.* **2016**, *11*, 2633–2641, doi:10.1002/asia.201600452.

117. Meyer, C.D.; Joiner, C.S.; Stoddart, J.F. Template-Directed Synthesis Employing Reversible Imine Bond Formation. *Chem. Soc. Rev.* **2007**, *36*, 1705–1723, doi:10.1039/b513441m.

118. Zhang, Y.; Pham, C.Y.; Yu, R.; Petit, E.; Li, S.; Barboiu, M. Dynamic Hydrogels Based on Double Imine Connections and Application for Delivery of Fluorouracil. *Front. Chem.* **2020**, *8*, doi:10.3389/fchem.2020.00739.

119. Belowich, M.E.; Stoddart, J.F. Dynamic Imine Chemistry. *Chem. Soc. Rev.* **2012**, *41*, 2003–2024, doi:10.1039/c2cs15305j.

120. Mandewale, M.C.; Thorat, B.; Patil, U.; Yamgar, R. Review: Synthesis and Applications of Schiff Bases. *Int. J. Chem. Pharm. Sci.* **2015**, *3*, 1919–1928.

121. Yu, R. Nouveaux Hydrogels à Liaison Imine Double Préparés à Partir d ' O- Carboxyméthyl Chitosane et de Jeffamine Par Chimie Covalente Dynamique Pour Applications Biomédicales To Cite This Version : HAL Id : Tel-03346833. **2021**.

122. Eric Lutz; Lutz, E. Dynamic Covalent Surfactants for the Controlled Release of Bioactive Volatiles. **2014**, 1–254.

123. Muir, V.G.; Burdick, J.A. Chemically Modified Biopolymers for the Formation of Biomedical Hydrogels. *Chem. Rev.* **2021**, *121*, 10908–10949, doi:10.1021/acs.chemrev.0c00923.

124. Ding, F.; Shi, X.; Wu, S.; Liu, X.; Deng, H.; Du, Y.; Li, H. Flexible Polysaccharide Hydrogel with PH-Regulated Recovery of Self-Healing and Mechanical Properties. *Macromol. Mater. Eng.* **2017**, *302*, 1–9, doi:10.1002/mame.201700221.

125. Ma, L.; Su, W.; Ran, Y.; Ma, X.; Yi, Z.; Chen, G.; Chen, X.; Deng, Z.; Tong, Q.; Wang, X.; et al. Synthesis and Characterization of Injectable Self-Healing Hydrogels Based on Oxidized Alginate-Hybrid-Hydroxyapatite Nanoparticles and Carboxymethyl Chitosan. *Int. J. Biol. Macromol.* **2020**, *165*, 1164–1174, doi:10.1016/j.ijbiomac.2020.10.004.

126. Lei, J.; Li, X.; Wang, S.; Yuan, L.; Ge, L.; Li, D.; Mu, C. Facile Fabrication of Biocompatible Gelatin-Based Self-Healing Hydrogels. *ACS Appl. Polym. Mater.* **2019**, *1*, 1350–1358, doi:10.1021/acsapm.9b00143.

127. Lehn, J.M. Dynamers: Dynamic Molecular and Supramolecular Polymers. *Prog. Polym. Sci.* **2005**, *30*, 814–831, doi:10.1016/j.progpolymsci.2005.06.002.

128. Patenaude, M.; Smeets, N.M.B.; Hoare, T. Designing Injectable, Covalently Cross-Linked Hydrogels for Biomedical Applications. *Macromol. Rapid Commun.* **2014**, *35*, 598–617, doi:10.1002/marc.201300818.

129. Apostolides, D.E.; Patrickios, C.S. Dynamic Covalent Polymer Hydrogels and Organogels Crosslinked through Acylhydrazone Bonds: Synthesis, Characterization and Applications. *Polym. Int.* **2018**, *67*, 627–649, doi:10.1002/pi.5554.

130. Fan, L.; Ge, X.; Qian, Y.; Wei, M.; Zhang, Z.; Yuan, W.E.; Ouyang, Y. Advances in Synthesis and Applications of Self-Healing Hydrogels. *Front. Bioeng. Biotechnol.* **2020**, *8*, 1–14, doi:10.3389/fbioe.2020.00654.

131. Wang, H.; Zhu, D.; Paul, A.; Cai, L.; Enejder, A.; Yang, F.; Heilshorn, S.C. Covalently Adaptable Elastin-Like Protein–Hyaluronic Acid (ELP–HA) Hybrid Hydrogels with Secondary Thermoresponsive Crosslinking for Injectable Stem Cell Delivery. *Adv. Funct. Mater.* **2017**, *27*, 1–11, doi:10.1002/adfm.201605609.

132. Wei, Z.; Yang, J.H.; Liu, Z.Q.; Xu, F.; Zhou, J.X.; Zrínyi, M.; Osada, Y.; Chen, Y.M. Novel Biocompatible Polysaccharide-Based Self-Healing Hydrogel. *Adv. Funct. Mater.* **2015**, *25*, 1352–1359, doi:10.1002/adfm.201401502.

133. Lehmann-horn, K.; Sagan, S.A.; Bernard, C.C.A.; Sobel, A.; Zamvil, S.S.; Wanna, A.G.B.; Noble, J.H.; Carlson, M.L.; Gifford, H.; Dietrich, M.S.; et al. 3D Extrusion Bioprinting of Single- and Double-Network Hydrogels Containing Dynamic Covalent Crosslinks. *Laryngoscope* **2014**, 2–31.

134. Yang, X.; Liu, G.; Peng, L.; Guo, J.; Tao, L.; Yuan, J.; Chang, C.; Wei, Y.; Zhang, L. Highly Efficient Self-Healable and Dual Responsive Cellulose-Based Hydrogels for Controlled Release and 3D Cell Culture. *Adv. Funct. Mater.* **2017**, *27*, 1–10, doi:10.1002/adfm.201703174.

135. Lin, F.; Yu, J.; Tang, W.; Zheng, J.; Defante, A.; Guo, K.; Wesdemiotis, C.; Becker, M.L. Peptide-Functionalized Oxime Hydrogels with Tunable Mechanical Properties and Gelation Behavior. *Biomacromolecules* **2013**, *14*, 3749–3758, doi:10.1021/bm401133r.

136. Collins, J.; Nadgorny, M.; Xiao, Z.; Connal, L.A. Doubly Dynamic Self-Healing Materials Based on Oxime Click Chemistry and Boronic Acids. *Macromol. Rapid Commun.* **2017**, *38*, 1–7, doi:10.1002/marc.201600760.

137. Grover, G.N.; Braden, R.L.; Christman, K.L. Oxime Cross-Linked Injectable Hydrogels for Catheter Delivery. *Adv. Mater.* **2013**, *25*, 2937–2942, doi:10.1002/adma.201205234.

138. Lu, B., Yu, J., Zhang, X., & Chen, G. Recent Advances on Catalytic Asymmetric Hydrogenation of Oximes and Oxime Ethers. *Tetrahedron Lett.* **2024**, *136*, doi:https://doi.org/10.1016/j.tetlet.2024.154914.

139. Mukherjee, S.; Hill, M.R.; Sumerlin, B.S. Self-Healing Hydrogels Containing Reversible Oxime Crosslinks. *Soft Matter* **2015**, *11*, 6152–6161, doi:10.1039/c5sm00865d.

140. Farahani, P.E.; Adelmund, S.M.; Shadish, J.A.; DeForest, C.A. Photomediated Oxime Ligation as a Bioorthogonal Tool for Spatiotemporally-Controlled Hydrogel Formation and Modification. *J. Mater. Chem. B* **2017**, *5*, 4435–4442, doi:10.1039/c6tb03400d.

141. Deforest, C.A.; Tirrell, D.A. A Photoreversible Protein-Patterning Approach for Guiding Stem Cell Fate in Three-Dimensional Gels. *Nat. Mater.* **2015**, *14*, 523–531, doi:10.1038/nmat4219.

142. Ahmed, E.M. Hydrogel : Preparation , Characterization , and Applications : A Review. *J. Adv. Res.* **2015**, *6*, 105–121, doi:10.1016/j.jare.2013.07.006.

143. Yang, S.; Wang, F.; Han, H. Biomedical Technology Fabricated Technology of Biomedical Micro-Nano Hydrogel. **2023**, *2*, 31–48, doi:10.1016/j.bmt.2022.11.012.

144. Dong, M.; Jiao, D.; Zheng, Q.; Wu, Z.L. Recent Progress in Fabrications and Applications of Functional Hydrogel Films. *J. Polym. Sci.* **2023**, *61*, 1026–1039, doi:10.1002/pol.20220451.

145. Yazdi, M.K.; Vatanpour, V.; Taghizadeh, A.; Taghizadeh, M.; Ganjali, M.R.; Munir, M.T.; Habibzadeh, S.; Saeb, M.R.; Ghaedi, M. Hydrogel Membranes: A Review. *Mater. Sci. Eng. C* **2020**, *114*, doi:10.1016/j.msec.2020.111023.

146. Ding, F.; Wu, S.; Wang, S.; Xiong, Y.; Li, Y.; Li, B.; Deng, H.; Du, Y.; Xiao, L.; Shi, X. A Dynamic and Self-Crosslinked Polysaccharide Hydrogel with Autonomous Self-Healing Ability. *Soft Matter* **2015**, *11*, 3971–3976, doi:10.1039/c5sm00587f.

147. Higueras, L.; López-Carballo, G.; Gavara, R.; Hernández-Muñoz, P. Reversible Covalent Immobilization of Cinnamaldehyde on Chitosan Films via Schiff Base Formation and Their Application in Active Food Packaging. *Food Bioprocess Technol.* **2015**, *8*, 526–538, doi:10.1007/s11947-014-1421-8.

148. Wang, T.; Turhan, M.; Gunasekaran, S. Selected Properties of PH-Sensitive, Biodegradable Chitosan-Poly(Vinyl Alcohol) Hydrogel. *Polym. Int.* **2004**, *53*, 911–918, doi:10.1002/pi.1461.

149. Zhumadilova, G.; Yashkarova, M.; Bimendina, L.; Kudaibergenov, S. Interpolymer Complexes of Novel Linear and Crosslinked Acrylic Acid-Schiff Base Copolymers. *Polym. Int.* **2003**, *52*, 876–882, doi:10.1002/pi.994.

150. Marinucci, L.; Lilli, C.; Guerra, M.; Belcastro, S.; Becchetti, E.; Stabellini, G.; Calvi, E.M.; Locci, P. Biocompatibility of Collagen Membranes Crosslinked with Glutaraldehyde or Diphenylphosphoryl Azide: An in Vitro Study. *J. Biomed. Mater. Res. - Part A* **2003**, *67*, 504–509, doi:10.1002/jbm.a.10082.

151. Reddy, N.; Reddy, R.; Jiang, Q. Crosslinking Biopolymers for Biomedical Applications. *Trends Biotechnol.* **2015**, *33*, 362–369, doi:10.1016/j.tibtech.2015.03.008.

152. Su, H.; Jia, Q.; Shan, S. Synthesis and Characterization of Schiff Base Contained Dextran Microgels in Water-in-Oil Inverse Microemulsion. *Carbohydr. Polym.* **2016**, *152*, 156– 162, doi:10.1016/j.carbpol.2016.06.091.

153. Kubicek, C.P. *Synthetic Biopolymers*; 2015; ISBN 9783319227085.

154. Daly, A.C.; Riley, L.; Segura, T.; Burdick, J.A. Hydrogel Microparticles for Biomedical Applications. *Nat. Rev. Mater.* **2020**, *5*, 20–43, doi:10.1038/s41578-019-0148-6.

155. Highley, C.B.; Song, K.H.; Daly, A.C.; Burdick, J.A. Jammed Microgel Inks for 3D Printing Applications. *Adv. Sci.* **2019**, *6*, doi:10.1002/advs.201801076.

156. Griffin, D.R.; Weaver, W.M.; Scumpia, P.; Di Carlo, D.; Segura, T. Scaffolds Assembled From Annealed Building Blocks. *Nat. Mater.* **2015**, *14*, 737–744, doi:10.1038/nmat4294.Accelerated.

157. Mealy, J.E.; Chung, J.J.; Jeong, H.H.; Issadore, D.; Lee, D.; Atluri, P.; Burdick, J.A. Injectable Granular Hydrogels with Multifunctional Properties for Biomedical Applications. *Adv. Mater.* **2018**, *30*, doi:10.1002/adma.201705912.

158. Lee, H.P.; Cai, K.X.; Wang, T.C.; Davis, R.; Deo, K.; Singh, K.A.; Lele, T.P.; Gaharwar, A.K. Dynamically Crosslinked Thermoresponsive Granular Hydrogels. *J. Biomed. Mater. Res. - Part A* **2023**, *111*, 1577–1587, doi:10.1002/jbm.a.37556.

159. Xu, X.; Chen, H.; He, P.; Zhao, Z.; Gao, X.; Liu, C.; Cheng, H.; Jiang, L.; Wang, P.;

Zhang, Y.; et al. 3D Hollow Porous Radio-Granular Hydrogels for SPECT Imaging- Guided Cancer Intravascular Brachytherapy. *Adv. Funct. Mater.* **2023**, *33*, doi:10.1002/adfm.202215110.

160. Zhang, Z.; Hao, G.; Liu, C.; Fu, J.; Hu, D.; Rong, J.; Yang, X. Recent Progress in the Preparation, Chemical Interactions and Applications of Biocompatible Polysaccharide- Protein Nanogel Carriers. *Food Res. Int.* **2021**, *147*, 110564, doi:10.1016/j.foodres.2021.110564.

161. Hajebi, S.; Rabiee, N.; Bagherzadeh, M.; Ahmadi, S.; Rabiee, M.; Roghani-Mamaqani, H.; Tahriri, M.; Tayebi, L.; Hamblin, M.R. Stimulus-Responsive Polymeric Nanogels as Smart Drug Delivery Systems. *Acta Biomater.* **2019**, *92*, 1–18, doi:10.1016/j.actbio.2019.05.018.

162. Chen, L. chun; Kong, Y. ping; Zheng, Y.; Zhang, S. yu; Zhang, L. yu; Wang, J. ying Preparation of Coix Seed Oil Bioactive Delivery Systems Based on Homologous Polysaccharides and Proteins. *Int. J. Biol. Macromol.* **2020**, *151*, 376–383, doi:10.1016/j.ijbiomac.2020.02.171.

163. Hachet, E.; Sereni, N.; Pignot-paintrand, I.; Ravaine, V.; Szarpak-jankowska, A.; Auzély- velty, R. Journal of Colloid and Interface Science Thiol-Ene Clickable Hyaluronans : From Macro-to Nanogels. **2014**, *419*, 52–55.

164. Hou, S.; Lake, R.; Park, S.; Edwards, S.; Jones, C.; Jeong, K.J. Injectable Macroporous Hydrogel Formed by Enzymatic Cross-Linking of Gelatin Microgels. *ACS Appl. Bio Mater.* **2018**, *1*, 1430–1439, doi:10.1021/acsabm.8b00380.

165. Ma, T.; Gao, X.; Dong, H.; He, H.; Cao, X. High-Throughput Generation of Hyaluronic Acid Microgels via Microfluidics-Assisted Enzymatic Crosslinking and/or Diels–Alder Click Chemistry for Cell Encapsulation and Delivery. *Appl. Mater. Today* **2017**, *9*, 49–59, doi:10.1016/j.apmt.2017.01.007.

166. Jia, X.; Yeo, Y.; Clifton, R.J.; Jiao, T.; Kohane, D.S.; Kobler, J.B.; Zeitels, S.M.; Langer, R. Hyaluronic Acid-Based Microgels and Microgel Networks for.Pdf. **2006**, 3336–3344.

167. Kesselman, L.R.B.; Shinwary, S.; Selvaganapathy, P.R.; Hoare, T. Synthesis of Monodisperse, Covalently Cross-Linked, Degradable ―Smart‖ Microgels Using Microfluidics. *Small* **2012**, *8*, 1092–1098, doi:10.1002/smll.201102113.

168. Bashiri, G.; Shojaosadati, S.A.; Abdollahi, M. Synthesis and Characterization of Schiff Base Containing Bovine Serum Albumin-Gum Arabic Aldehyde Hybrid Nanogels via Inverse Miniemulsion for Delivery of Anticancer Drug. *Int. J. Biol. Macromol.* **2021**, *170*, 222–231, doi:10.1016/j.ijbiomac.2020.12.150.

169. Chen, C.; Liu, M.; Lü, S.; Gao, C.; Chen, J. In Vitro Degradation and Drug-Release Properties of Water-Soluble Chitosan Cross-Linked Oxidized Sodium Alginate Core-Shell Microgels. *J. Biomater. Sci. Polym. Ed.* **2012**, *23*, 2007–2024, doi:10.1163/092050611X601720.

170. Usta, A.; Asmatulu, R. Hydrogels in Various Biomedical Applications. **1845**, 248–257.

171. Dalei, G.; Das, S.; Ranjan Jena, S.; Jena, D.; Nayak, J.; Samanta, L. In Situ Crosslinked Dialdehyde Guar Gum-Chitosan Schiff-Base Hydrogels for Dual Drug Release in Colorectal Cancer Therapy. *Chem. Eng. Sci.* **2023**, *269*, 118482, doi:10.1016/j.ces.2023.118482.

172. Hosseini, M.S.; Nabid, M.R. Synthesis of Chemically Cross-Linked Hydrogel Films Based on Basil Seed (Ocimum Basilicum L.) Mucilage for Wound Dressing Drug Delivery Applications. *Int. J. Biol. Macromol.* **2020**, *163*, 336–347, doi:10.1016/j.ijbiomac.2020.06.252.

173. Hunziker, E.; Spector, M.; Libera, J.; Gertzman, A.; Woo, S.L.Y.; Ratcliffe, A.; Lysaght, M.; Coury, A.; Kaplan, D.; Vunjak-Novakovic, G. Translation from Research to Applications. *Tissue Eng.* **2006**, *12*, 3341–3364, doi:10.1089/ten.2006.12.3341.

174. Subramanian, K.G.; Vijayakumar, V. Hydrogels: Classification, Synthesis, Characterization, and Applications. *Encycl. Biomed. Polym. Polym. Biomater.* **2015**, 3879– 3892, doi:10.1081/e-ebpp-120049894.

175. Tan, H.; Marra, K.G. Injectable, Biodegradable Hydrogels for Tissue Engineering Applications. *Materials (Basel).* **2010**, *3*, 1746–1767, doi:10.3390/ma3031746.

176. Rajalekshmi, R.; Kaladevi Shaji, A.; Joseph, R.; Bhatt, A. Scaffold for Liver Tissue Engineering: Exploring the Potential of Fibrin Incorporated Alginate Dialdehyde–Gelatin Hydrogel. *Int. J. Biol. Macromol.* **2021**, *166*, 999–1008, doi:10.1016/j.ijbiomac.2020.10.256.

177. Cheng, Y.; Lu, J.; Liu, S.; Zhao, P.; Lu, G.; Chen, J. The Preparation, Characterization and Evaluation of Regenerated Cellulose/Collagen Composite Hydrogel Films. *Carbohydr. Polym.* **2014**, *107*, 57–64, doi:10.1016/j.carbpol.2014.02.034.

178. Liu, Y.; Chan-Park, M.B. Hydrogel Based on Interpenetrating Polymer Networks of Dextran and Gelatin for Vascular Tissue Engineering. *Biomaterials* **2009**, *30*, 196–207, doi:10.1016/j.biomaterials.2008.09.041.

179. Bale, S.; Banks, V.; Haglestein, S.; Harding, K.G. A Comparison of Two Amorphous Hydrogels in the Debridement of Pressure Sores. *J. Wound Care* **1998**, *7*, 65–68, doi:10.12968/jowc.1998.7.2.65.

180. Jones, A.; Vaughan, D. Hydrogel Dressings in the Management of a Variety of Wound Types: A Review. *J. Orthop. Nurs.* **2005**, *9*, doi:10.1016/S1361-3111(05)80001-9.

181. Wang, W.; Xiang, L.; Gong, L.; Hu, W.; Huang, W.; Chen, Y.; Asha, A.B.; Srinivas, S.; Chen, L.; Narain, R.; et al. Injectable, Self-Healing Hydrogel with Tunable Optical, Mechanical, and Antimicrobial Properties. *Chem. Mater.* **2019**, *31*, 2366–2376, doi:10.1021/acs.chemmater.8b04803.

182. Zhao, X.; Wu, H.; Guo, B.; Dong, R.; Qiu, Y.; Ma, P.X. Antibacterial Anti-Oxidant Electroactive Injectable Hydrogel as Self-Healing Wound Dressing with Hemostasis and Adhesiveness for Cutaneous Wound Healing. *Biomaterials* **2017**, *122*, 34–47, doi:10.1016/j.biomaterials.2017.01.011.

183. Xin, Y.; Yuan, J. Schiff's Base as a Stimuli-Responsive Linker in Polymer Chemistry. *Polym. Chem.* **2012**, *3*, 3045–3055, doi:10.1039/c2py20290e.

184. Antony, R.; Arun, T.; Manickam, S.T.D. A Review on Applications of Chitosan-Based Schiff Bases. *Int. J. Biol. Macromol.* **2019**, *129*, 615–633, doi:10.1016/j.ijbiomac.2019.02.047.

185. Mohammadhashemi, Z.; Zohuriaan-Mehr, M.J.; Jahanmardi, R. Antibacterial Activity Induction into Superabsorbent Hydrogel via Schiff-Base-Metal Coordination Modification. *Polym. Bull.* **2023**, *80*, 8045–8065, doi:10.1007/s00289-022-04434-5.

186. Guo, F.; Liu, Y.; Chen, S.; Lin, Y.; Yue, Y. A Schiff Base Hydrogel Dressing Loading Extracts from Periplaneta Americana for Diabetic Wound Healing. *Int. J. Biol. Macromol.* **2023**, *230*, 123256, doi:10.1016/j.ijbiomac.2023.123256.

187. Zhang, M.; Qiao, X.; Han, W.; Jiang, T.; Liu, F.; Zhao, X. Alginate-Chitosan Oligosaccharide-ZnO Composite Hydrogel for Accelerating Wound Healing. *Carbohydr. Polym.* **2021**, *266*, 118100, doi:10.1016/j.carbpol.2021.118100.

188. Oh, G.W.; Kim, S.C.; Kim, T.H.; Jung, W.K. Characterization of an Oxidized Alginate- Gelatin Hydrogel Incorporating a COS-Salicylic Acid Conjugate for Wound Healing. *Carbohydr. Polym.* **2021**, *252*, 117145, doi:10.1016/j.carbpol.2020.117145.

189. Du, S.; Chen, X.; Chen, X.; Li, S.; Yuan, G.; Zhou, T.; Li, J.; Jia, Y.; Xiong, D.; Tan, H. Covalent Chitosan-Cellulose Hydrogels via Schiff-Base Reaction Containing Macromolecular Microgels for PH-Sensitive Drug Delivery and Wound Dressing. *Macromol. Chem. Phys.* **2019**, *220*, doi:10.1002/macp.201900399.

190. Yan, Y.; Wu, Q.; Miao, S.; Ren, P.; Wu, Y.; Shen, Y. A Hydrogel Microparticle with Sustained Release Properties for Pulmonary Drug Delivery. *React. Funct. Polym.* **2023**, *183*, 105489, doi:10.1016/j.reactfunctpolym.2022.105489.

191. Cheng, H.; Liu, H.; Shi, Z.; Xu, Y.; Lian, Q.; Zhong, Q.; Liu, Q.; Chen, Y.; Pan, X.; Chen, R.; et al. Long-Term Antibacterial and Biofilm Dispersion Activity of an Injectable in Situ Crosslinked Co-Delivery Hydrogel/Microgel for Treatment of Implant Infection. *Chem. Eng. J.* **2022**, *433*, 134451, doi:10.1016/j.cej.2021.134451.

192. Hunt, N.C.; Grover, L.M. Cell Encapsulation Using Biopolymer Gels for Regenerative Medicine. *Biotechnol. Lett.* **2010**, *32*, 733–742, doi:10.1007/s10529-010-0221-0.

193. Jang, Y.; Cha, C.; Jung, J.; Oh, J. Interfacial Compression-Dependent Merging of Two Miscible Microdroplets in an Asymmetric Cross-Junction for In Situ Microgel Formation. *Macromol. Res.* **2018**, *26*, 1143–1149, doi:10.1007/s13233-019-7013-8.

194. Wang, K.; Wang, Z.; Hu, H.; Gao, C. Supramolecular Microgels/Microgel Scaffolds for Tissue Repair and Regeneration. *Supramol. Mater.* **2022**, *1*, 100006, doi:10.1016/j.supmat.2021.100006.

195. Zhou, X.; Xi, K.; Bian, J.; Li, Z.; Wu, L.; Tang, J.; Xiong, C.; Yu, Z.; Zhang, J.; Gu, Y.; et al. Injectable Engineered Micro/Nano-Complexes Trigger the Reprogramming of Bone

Immune Epigenetics. *Chem. Eng. J.* **2023**, *462*, 142158, doi:10.1016/j.cej.2023.142158.

196. Zhang, W.; Wang, X. chuan; Li, X. yue; Zhang, L. le; Jiang, F. A 3D Porous Microsphere with Multistage Structure and Component Based on Bacterial Cellulose and Collagen for Bone Tissue Engineering. *Carbohydr. Polym.* **2020**, *236*, 116043, doi:10.1016/j.carbpol.2020.116043.

197. Shekhar, S.; Chaudhary, V.; Sharma, B.; Kumar, A.; Bhagi, A.K.; Singh, K.P. Sustainable Polysaccharide Hydrogels Based on Dynamic Schiff Base Linkages as Versatile Building Blocks for Fabricating Advanced Functional Materials. *J. Polym. Environ.* **2023**, *31*, 1257–1278, doi:10.1007/s10924-022-02685-x.

198. Duan, Q.-Y.; Zhu, Y.-X.; Jia, H.-R.; Wang, S.-H.; Wu, F.-G. Nanogels: Synthesis, Properties, and Recent Biomedical Applications. *Prog. Mater. Sci.* **2023**, *139*, 101167, doi:10.1016/j.pmatsci.2023.101167.

199. Su, H.; Zhang, W.; Wu, Y.; Han, X.; Liu, G.; Jia, Q.; Shan, S. Schiff Base-Containing Dextran Nanogel as PH-Sensitive Drug Delivery System of Doxorubicin: Synthesis and Characterization. *J. Biomater. Appl.* **2018**, *33*, 170–181, doi:10.1177/0885328218783969.

200. Sarika, P.R.; James, N.R.; Anil kumar, P.R.; Raj, D.K. Preparation, Characterization and Biological Evaluation of Curcumin Loaded Alginate Aldehyde–Gelatin Nanogels. *Mater. Sci. Eng. C* **2016**, *68*, 251–257, doi:10.1016/j.msec.2016.05.046.

201. Li, Z.; Huang, J.; Wu, J. PH-Sensitive Nanogels for Drug Delivery in Cancer Therapy. *Biomater. Sci.* **2021**, *9*, 574–589, doi:10.1039/d0bm01729a.

202. Damiri, F.; Rojekar, S.; Bachra, Y.; Varma, R.S.; Andra, S.; Balu, S.; Pardeshi, C.V.; Patel, P.J.; Patel, H.M.; Paiva-Santos, A.C.; et al. Polysaccharide-Based Nanogels for Biomedical Applications: A Comprehensive Review. *J. Drug Deliv. Sci. Technol.* **2023**, *84*, doi:10.1016/j.jddst.2023.104447.

203. Narayanan, K.B.; Bhaskar, R.; Han, S.S. Recent Advances in the Biomedical Applications of Functionalized Nanogels. *Pharmaceutics* **2022**, *14*, doi:10.3390/pharmaceutics14122832.

204. Yu, K.; Yang, X.; He, L.; Zheng, R.; Min, J.; Su, H.; Shan, S.; Jia, Q. Facile Preparation of PH/Reduction Dual-Stimuli Responsive Dextran Nanogel as Environment-Sensitive Carrier of Doxorubicin. *Polymer (Guildf).* **2020**, *200*, 122585, doi:10.1016/j.polymer.2020.122585.

205. Alioghli Ziaei, A.; Erfan-Niya, H.; Fathi, M.; Amiryaghoubi, N. In Situ Forming Alginate/Gelatin Hybrid Hydrogels Containing Doxorubicin Loaded Chitosan/AuNPs Nanogels for the Local Therapy of Breast Cancer. *Int. J. Biol. Macromol.* **2023**, *246*, 125640, doi:10.1016/j.ijbiomac.2023.125640.

206. Ahmed, E.M. Hydrogel: Preparation, Characterization, and Applications: A Review. *J. Adv. Res.* **2015**, *6*, 105–121, doi:10.1016/j.jare.2013.07.006.

207. Keskin, D.; Zu, G.; Forson, A.M.; Tromp, L.; Sjollema, J.; van Rijn, P. Nanogels: A Novel

Approach in Antimicrobial Delivery Systems and Antimicrobial Coatings. *Bioact. Mater.* **2021**, *6*, 3634–3657, doi:10.1016/j.bioactmat.2021.03.004.

208. Chung, F.Y.; Huang, C.R.; Chen, C.S.; Chen, Y.F. Natural Nanogels Crosslinked with S- Benzyl-L-Cysteine Exhibit Potent Antibacterial Activity. *Biomater. Adv.* **2023**, *153*, 213551, doi:10.1016/j.bioadv.2023.213551.

209. Gao, F.; Mi, Y.; Wu, X.; Yao, J.; Qi, Q.; Chen, W.; Cao, Z. Preparation of Quaternized Chitosan/Ag Composite Nanogels in Inverse Miniemulsions for Durable and Antimicrobial Cotton Fabrics. *Carbohydr. Polym.* **2022**, *278*, doi:10.1016/j.carbpol.2021.118935.

210. Haug, I.J.; Draget, K.I. Gelatin. *Handb. Hydrocoll. Second Ed.* **2009**, 142–163, doi:10.1533/9781845695873.142.

211. Rather, J.A.; Akhter, N.; Ashraf, Q.S.; Mir, S.A.; Makroo, H.A.; Majid, D.; Barba, F.J.; Khaneghah, A.M.; Dar, B.N. A Comprehensive Review on Gelatin: Understanding Impact of the Sources, Extraction Methods, and Modifications on Potential Packaging Applications. *Food Packag. Shelf Life* **2022**, *34*, 100945, doi:10.1016/j.fpsl.2022.100945.

212. Alipal, J.; Mohd Pu'ad, N.A.S.; Lee, T.C.; Nayan, N.H.M.; Sahari, N.; Basri, H.; Idris, M.I.; Abdullah, H.Z. A Review of Gelatin: Properties, Sources, Process, Applications, and Commercialisation. *Mater. Today Proc.* **2019**, *42*, 240–250, doi:10.1016/j.matpr.2020.12.922.

213. Liu, D.; Nikoo, M.; Boran, G.; Zhou, P.; Regenstein, J.M. Collagen and Gelatin. *Annu. Rev. Food Sci. Technol.* **2015**, *6*, 527–557, doi:10.1146/annurev-food-031414-111800.

214. Mikhailov, O. V. Gelatin as It Is: History and Modernity. *Int. J. Mol. Sci.* **2023**, *24*, doi:10.3390/ijms24043583.

215. Wang, Q.Q.; Liu, Y.; Zhang, C.J.; Zhang, C.; Zhu, P. Alginate/Gelatin Blended Hydrogel Fibers Cross-Linked by Ca 2+ and Oxidized Starch: Preparation and Properties. *Mater. Sci. Eng. C* **2019**, *99*, 1469–1476, doi:10.1016/j.msec.2019.02.091.

216. Erukhimovich, I.; de la Cruz, M.O. Phase Equilibria and Charge Fractionation in Polydisperse Polyelectrolyte Solutions. **2004**, 1804–1812, doi:10.1002/polb.

217. Qiao, C.; Chen, G.; Li, Y.; Li, T. Viscosity Properties of Gelatin in Solutions of Monovalent and Divalent Salts. *Korea Aust. Rheol. J.* **2013**, *25*, 227–231, doi:10.1007/s13367-013-0023-8.

218. Jahangir, M.U.; Wong, S.Y.; Afrin, H.; Nurunnabi, M.; Li, X.; Arafat, M.T. Understanding the Solubility and Electrospinnability of Gelatin Using Teas Approach in Single/Binary Organic Solvent Systems. *Bull. Mater. Sci.* **2023**, *46*, doi:10.1007/s12034-022-02834-x.

219. Ahmady, A.; Abu Samah, N.H. A Review: Gelatine as a Bioadhesive Material for Medical and Pharmaceutical Applications. *Int. J. Pharm.* **2021**, *608*, 121037, doi:10.1016/j.ijpharm.2021.121037.

220. Yang, X.J.; Zheng, P.J.; Cui, Z.D.; Zhao, N.Q.; Wang, Y.F.; Yao, K. De Swelling Behaviour and Elastic Properties of Gelatin Gels. *Polym. Int.* **1997**, *44*, 448–452, doi:10.1002/(SICI)1097-0126(199712)44:4<448::AID-PI845>3.0.CO;2-M.

221. Boanini, E.; Rubini, K.; Panzavolta, S.; Bigi, A. Chemico-Physical Characterization of Gelatin Films Modified with Oxidized Alginate. *Acta Biomater.* **2010**, *6*, 383–388, doi:10.1016/j.actbio.2009.06.015.

222. Achet, D.; He, X.W. Determination of the Renaturation Level in Gelatin Films. *Polymer (Guildf).* **1995**, *36*, 787–791, doi:10.1016/0032-3861(95)93109-Y.

223. Pezron, I.; Djabourov, M.; Leblond, J. Conformation of Gelatin Chains in Aqueous Solutions: 1. A Light and Small-Angle Neutron Scattering Study. *Polymer (Guildf).* **1991**, *32*, 3201–3210, doi:10.1016/0032-3861(91)90143-7.

224. Ross-Murphy, S.B. Structure and Rheology of Gelatin Gels: Recent Progress. *Polymer (Guildf).* **1992**, *33*, 2622–2627, doi:10.1016/0032-3861(92)91146-S.

225. Gomez-Guillen, M.C.; Gimenez, B.; Lopez-Caballero, M.E.; Montero, M.P. Functional and Bioactive Properties of Collagen and Gelatin from Alternative Sources: A Review. *Food Hydrocoll.* **2011**, *25*, 1813–1827, doi:10.1016/j.foodhyd.2011.02.007.

226. Djagny, K.B.; Wang, Z.; Xu, S. Gelatin: A Valuable Protein for Food and Pharmaceutical Industries: Review. *Crit. Rev. Food Sci. Nutr.* **2001**, *41*, 481–492, doi:10.1080/20014091091904.

227. Klotz, B.J.; Gawlitta, D.; Rosenberg, A.J.W.P.; Malda, J.; Melchels, F.P.W. Gelatin- Methacryloyl Hydrogels: Towards Biofabrication-Based Tissue Repair. *Trends Biotechnol.* **2016**, *34*, 394–407, doi:10.1016/j.tibtech.2016.01.002.

228. Elzoghby, A.O. Gelatin-Based Nanoparticles as Drug and Gene Delivery Systems: Reviewing Three Decades of Research. *J. Control. Release* **2013**, *172*, 1075–1091, doi:10.1016/j.jconrel.2013.09.019.

229. Young, S.; Wong, M.; Tabata, Y.; Mikos, A.G. Gelatin as a Delivery Vehicle for the Controlled Release of Bioactive Molecules. *J. Control. Release* **2005**, *109*, 256–274, doi:10.1016/j.jconrel.2005.09.023.

230. Ljubljana, D. Biomaterials and Their Biocompatibility : Review and Perspectives. **2011**, 1–36.

231. Van Den Steen, P.E.; Dubois, B.; Nelissen, I.; Rudd, P.M.; Dwek, R.A.; Opdenakker, G. *Biochemistry and Molecular Biology of Gelatinase B or Matrix Metalloproteinase-9 (MMP-9)*; 2002; Vol. 37; ISBN 1040923029077.

232. Nichol, J.W.; Koshy, S.T.; Bae, H.; Hwang, C.M.; Yamanlar, S.; Khademhosseini, A. Cell-Laden Microengineered Gelatin Methacrylate Hydrogels. *Biomaterials* **2010**, *31*, 5536–5544, doi:10.1016/j.biomaterials.2010.03.064.

233. Heino, J.; Huhtala, M.; Käpylä, J.; Johnson, M.S. Evolution of Collagen-Based Adhesion

Systems. *Int. J. Biochem. Cell Biol.* **2009**, *41*, 341–348, doi:10.1016/j.biocel.2008.08.021.

234. Yang, J.S.; Xie, Y.J.; He, W. Research Progress on Chemical Modification of Alginate: A Review. *Carbohydr. Polym.* **2011**, *84*, 33–39, doi:10.1016/j.carbpol.2010.11.048.

235. Pawar, S.N.; Edgar, K.J. Alginate Derivatization: A Review of Chemistry, Properties and Applications. *Biomaterials* **2012**, *33*, 3279–3305, doi:10.1016/j.biomaterials.2012.01.007.

236. Ramesh Babu, V.; Sairam, M.; Hosamani, K.M.; Aminabhavi, T.M. Preparation of Sodium Alginate-Methylcellulose Blend Microspheres for Controlled Release of Nifedipine. *Carbohydr. Polym.* **2007**, *69*, 241–250, doi:10.1016/j.carbpol.2006.09.027.

237. Orive, G.; Ponce, S.; Hernández, R.M.; Gascón, A.R.; Igartua, M.; Pedraz, J.L. Biocompatibility of Microcapsules for Cell Immobilization Elaborated with Different Type of Alginates. *Biomaterials* **2002**, *23*, 3825–3831, doi:10.1016/S0142-9612(02)00118-7.

238. AB, Lansdown, P.M. An Evaluation of the Local Reaction and Biodegradation of Calcium Sodium Alginate (Kaltostat) Following Subcutaneous Implantation in the Rat. *R. Coll. Surg. Edinburgh* **1994**, *39*, 284–288.

239. Balakrishnan, B.; Lesieur, S.; Labarre, D.; Jayakrishnan, A. Periodate Oxidation of Sodium Alginate in Water and in Ethanol-Water Mixture: A Comparative Study. *Carbohydr. Res.* **2005**, *340*, 1425–1429, doi:10.1016/j.carres.2005.02.028.

240. Bello, A.B.; Kim, D.; Kim, D.; Park, H.; Lee, S.H. Engineering and Functionalization of Gelatin Biomaterials: From Cell Culture to Medical Applications. *Tissue Eng. - Part B Rev.* **2020**, *26*, 164–180, doi:10.1089/ten.teb.2019.0256.

241. Michalak, I. 3D Cultures and Bioprinting. **2021**, 1–24.

242. Bashir, S.; Hina, M.; Iqbal, J.; Rajpar, A.H.; Mujtaba, M.A.; Alghamdi, N.A.; Wageh, S.; Ramesh, K.; Ramesh, S. Fundamental Concepts of Hydrogels: Synthesis, Properties, and Their Applications. *Polymers (Basel).* **2020**, *12*, 1–60, doi:10.3390/polym12112702.

243. Zabidi, N.A.; Nazri, F.; Syafinaz, I.; Amin, M.; Salahuddin, M.; Basri, M.; Basha, R.K.; Othman, S.H. Jo Ur Na l P. *Int. J. Biol. Macromol.* **2022**, *2*, 33–47, doi:10.1016/j.ijbiomac.2024.135177.

244. Yu, G.; Niu, C.; Liu, J.; Wu, J.; Jin, Z.; Wang, Y.; Zhao, K. Preparation and Properties of Self-Cross-Linking Hydrogels Based on Chitosan Derivatives and Oxidized Sodium Alginate. *ACS Omega* **2023**, *8*, 19752–19766, doi:10.1021/acsomega.3c01401.

245. Merati, F.; Mehryab, F.; Mortazavi, S.A.; Haeri, A. An Experimental Design Approach for Development of Crocin-Loaded Microparticles Embedded in Gelatin/Oxidized Alginate- Based Hydrogel. *J. Pharm. Innov.* **2023**, 1812–1826, doi:10.1007/s12247-023-09755-0.

246. Liu, C.; Qin, W.; Wang, Y.; Ma, J.; Liu, J.; Wu, S.; Zhao, H. 3D Printed Gelatin/Sodium Alginate Hydrogel Scaffolds Doped with Nano-Attapulgite for Bone Tissue Repair. *Int. J. Nanomedicine* **2021**, *16*, 8417–8432, doi:10.2147/IJN.S339500.

247. Hoang Thi, T.T.; Lee, Y.; Le Thi, P.; Park, K.D. Oxidized Alginate Supplemented Gelatin Hydrogels for the In Situ Formation of Wound Dressing with High Antibacterial Activity. *Macromol. Res.* **2019**, *27*, 811–820, doi:10.1007/s13233-019-7115-3.

248. Wang, H.; Chen, X.; Wen, Y.; Li, D.; Sun, X.; Liu, Z.; Yan, H.; Lin, Q. A Study on the Correlation between the Oxidation Degree of Oxidized Sodium Alginate on Its Degradability and Gelation. *Polymers (Basel).* **2022**, *14*, doi:10.3390/polym14091679.

249. Sun, X.; Ma, C.; Gong, W.; Ma, Y.; Ding, Y.; Liu, L. Biological Properties of Sulfanilamide-Loaded Alginate Hydrogel Fibers Based on Ionic and Chemical Crosslinking for Wound Dressings. *Int. J. Biol. Macromol.* **2020**, *157*, 522–529, doi:10.1016/j.ijbiomac.2020.04.210.

250. Babić Radić, M.M.; Filipović, V. V.; Vukomanović, M.; Runić, J.N.; Tomić, S.L. Degradable 2-Hydroxyethyl Methacrylate/Gelatin/Alginate Hydrogels Infused by Nanocolloidal Graphene Oxide as Promising Drug Delivery and Scaffolding Biomaterials. *Gels* **2022**, *8*, doi:10.3390/gels8010022.

251. Chi, J.; Ai Li; Mingyu Zou; Shuo Wang; Chenqi Liu; Hu, R.; Jiang, Z.; Liu, W.; Sun, R.; Baoqin Han Novel Dopamine-Modified Oxidized Sodium Alginate Hydrogels Promote Angiogenesis and Accelerate Healing of Chronic Diabetic Wounds. *Int. J. Biol. Macromol.* **2022**, *203*, 492–504.

252. Resmi, R.; Parvathy, J.; John, A.; Joseph, R. Injectable Self-Crosslinking Hydrogels for Meniscal Repair: A Study with Oxidized Alginate and Gelatin. *Carbohydr. Polym.* **2020**, *234*, 115902, doi:10.1016/j.carbpol.2020.115902.

253. Abou-Zeid, R.E.; Awwad, N.S.; Nabil, S.; Salama, A.; Youssef, M.A. Oxidized Alginate/Gelatin Decorated Silver Nanoparticles as New Nanocomposite for Dye Adsorption. *Int. J. Biol. Macromol.* **2019**, *141*, 1280–1286, doi:10.1016/j.ijbiomac.2019.09.076.

254. He, Y.; Tian, Y.; Zhang, W.; Wang, X.; Yang, X.; Li, B.; Ge, L.; Bai, D.; Li, D. Fabrication of Oxidized Sodium Alginate-Collagen Heterogeneous Bilayer Barrier Membrane with Osteogenesis-Promoting Ability. *Int. J. Biol. Macromol.* **2022**, *202*, 55– 67, doi:10.1016/j.ijbiomac.2021.12.155.

255. Ghanbari, M.; Salavati-Niasari, M.; Mohandes, F. Thermosensitive Alginate-Gelatin- Nitrogen-Doped Carbon Dots Scaffolds as Potential Injectable Hydrogels for Cartilage Tissue Engineering Applications. *RSC Adv.* **2021**, *11*, 18423–18431, doi:10.1039/d1ra01496j.

256. Fan, L.-H.; Pan, X.-R.; Zhou, Y.; Chen, L.-Y.; Xie, W.-G.; Long, Z.-H.; Zheng, H. Preparation and Characterization of Crosslinked Carboxymethyl Chitosan–Oxidized Sodium Alginate Hydrogels. *J. Appl. Polym. Sci.* **2011**, *122*, 2331–2337, doi:10.1002/app.34041.

257. Córdova, B.M.; Jacinto, C.R.; Alarcón, H.; Mejía, I.M.; López, R.C.; de Oliveira Silva, D.; Cavalheiro, E.; Venâncio, T.; Dávalos, J.Z.; Valderrama, A.C. Chemical Modification of

Sodium Alginate with Thiosemicarbazide for the Removal of Pb(II) and Cd(II) from Aqueous Solutions. *Int. J. Biol. Macromol.* **2018**, *120*, 2259–2270, doi:10.1016/j.ijbiomac.2018.08.095.

258. Liang, L.; Liu, T.; Ouyang, Q.; Li, S.; Li, C. Solid Phase Synthesis of Oxidized Sodium Alginate-Tobramycin Conjugate and Its Application for Infected Wound Healing. *Carbohydr. Polym.* **2022**, *295*, 119843, doi:10.1016/j.carbpol.2022.119843.

259. Tian, M.; Chen, X.; Gu, Z.; Li, H.; Ma, L.; Qi, X.; Tan, H.; You, C. Synthesis and Evaluation of Oxidation-Responsive Alginate-Deferoxamine Conjugates with Increased Stability and Low Toxicity. *Carbohydr. Polym.* **2016**, *144*, 522–530, doi:10.1016/j.carbpol.2016.03.014.

260. Ossipov, D.A.; Piskounova, S.; Varghese, O.P.; Hilborn, J. Functionalization of Hyaluronic Acid with Chemoselective Groups via a Disulfide-Based Protection Strategy for in Situ Formation of Mechanically Stable Hydrogels. *Biomacromolecules* **2010**, *11*, 2247–2254, doi:10.1021/bm1007986.

261. Amer, H.; Nypelö, T.; Sulaeva, I.; Bacher, M.; Henniges, U.; Potthast, A.; Rosenau, T. Synthesis and Characterization of Periodate-Oxidized Polysaccharides: Dialdehyde Xylan (DAX). *Biomacromolecules* **2016**, *17*, 2972–2980, doi:10.1021/acs.biomac.6b00777.

262. Dahlmann, J.; Krause, A.; Möller, L.; Kensah, G.; Möwes, M.; Diekmann, A.; Martin, U.; Kirschning, A.; Gruh, I.; Dräger, G. Fully Defined in Situ Cross-Linkable Alginate and Hyaluronic Acid Hydrogels for Myocardial Tissue Engineering. *Biomaterials* **2013**, *34*, 940–951, doi:10.1016/j.biomaterials.2012.10.008.

263. Bai, Z.; Dan, W.; Yu, G.; Wang, Y.; Chen, Y.; Huang, Y.; Yang, C.; Dan, N. Tough and Tissue-Adhesive Polyacrylamide/Collagen Hydrogel with Dopamine-Grafted Oxidized Sodium Alginate as Crosslinker for Cutaneous Wound Healing. *RSC Adv.* **2018**, *8*, 42123– 42132, doi:10.1039/c8ra07697a.

264. Tian, M.; Chen, X.; Li, H.; Ma, L.; Gu, Z.; Qi, X.; Li, X.; Tan, H.; You, C. Long-Term and Oxidative-Responsive Alginate-Deferoxamine Conjugates with a Low Toxicity for Iron Overload. *RSC Adv.* **2016**, *6*, 32471–32479, doi:10.1039/c6ra02674e.

265. Gao, C.; Liu, M.; Chen, J.; Zhang, X. Preparation and Controlled Degradation of Oxidized Sodium Alginate Hydrogel. *Polym. Degrad. Stab.* **2009**, *94*, 1405–1410, doi:10.1016/j.polymdegradstab.2009.05.011.

266. Chemin, M.; Rakotovelo, A.; Ham-Pichavant, F.; Chollet, G.; Da Silva Perez, D.; Petit- Conil, M.; Cramail, H.; Grelier, S. Periodate Oxidation of 4-O-Methylglucuronoxylans: Influence of the Reaction Conditions. *Carbohydr. Polym.* **2016**, *142*, 45–50, doi:10.1016/j.carbpol.2016.01.025.

267. Li, H.; Wu, B.; Mu, C.; Lin, W. Concomitant Degradation in Periodate Oxidation of Carboxymethyl Cellulose. *Carbohydr. Polym.* **2011**, *84*, 881–886, doi:10.1016/j.carbpol.2010.12.026.

268. Rizky, S.; Budhijanto; Wintoko, J. Modification of Bioadhesive Based on Crosslinked

Alginate and Gelatin. *Mater. Today Proc.* **2023**, doi:10.1016/j.matpr.2023.03.775.

269. Ji, Y.; Yang, X.; Ji, Z.; Zhu, L.; Ma, N.; Chen, D.; Jia, X.; Tang, J.; Cao, Y. DFT-Calculated IR Spectrum Amide I, II, and III Band Contributions of N-Methylacetamide Fine Components. *ACS Omega* **2020**, *5*, 8572–8578, doi:10.1021/acsomega.9b04421.

270. Derkach, S.R.; Voron'ko, N.G.; Sokolan, N.I.; Kolotova, D.S.; Kuchina, Y.A. Interactions between Gelatin and Sodium Alginate: UV and FTIR Studies. *J. Dispers. Sci. Technol.* **2020**, *41*, 690–698, doi:10.1080/01932691.2019.1611437.

271. Zhang, X.; Miao, F.; Niu, L.; Wei, Y.; Hu, Y.; Lian, X.; Zhao, L.; Chen, W.; Huang, D. Berberine Carried Gelatin/Sodium Alginate Hydrogels with Antibacterial and EDTA- Induced Detachment Performances. *Int. J. Biol. Macromol.* **2021**, *181*, 1039–1046, doi:10.1016/j.ijbiomac.2021.04.114.

272. Afjoul, H.; Shamloo, A.; Kamali, A. Freeze-Gelled Alginate/Gelatin Scaffolds for Wound Healing Applications: An in Vitro, in Vivo Study. *Mater. Sci. Eng. C* **2020**, *113*, 110957, doi:10.1016/j.msec.2020.110957.

273. Issa, R.M.; Khedr, A.M.; Rizk, H. H NMR, IR and UV/VIS Spectroscopic Studies of Some Schiff Bases Derived from 2-Aminobenzothiazole and 2-Amino-3-Hydroxypyridine. *J. Chinese Chem. Soc.* **2008**, *55*, 875–884, doi:10.1002/jccs.200800131.

274. Sharma, S.; Jain, P.; Tiwari, S. Dynamic Imine Bond Based Chitosan Smart Hydrogel with Magnified Mechanical Strength for Controlled Drug Delivery. *Int. J. Biol. Macromol.* **2020**, *160*, 489–495, doi:10.1016/j.ijbiomac.2020.05.221.

275. Sarker, B.; Papageorgiou, D.G.; Silva, R.; Zehnder, T.; Gul-E-Noor, F.; Bertmer, M.; Kaschta, J.; Chrissafis, K.; Detsch, R.; Boccaccini, A.R. Fabrication of Alginate-Gelatin Crosslinked Hydrogel Microcapsules and Evaluation of the Microstructure and Physico- Chemical Properties. *J. Mater. Chem. B* **2014**, *2*, 1470–1482, doi:10.1039/c3tb21509a.

276. Amiryaghoubi, N.; Fathi, M.; Safary, A.; Javadzadeh, Y.; Omidi, Y. In Situ Forming Alginate/Gelatin Hydrogel Scaffold through Schiff Base Reaction Embedded with Curcumin-Loaded Chitosan Microspheres for Bone Tissue Regeneration. *Int. J. Biol. Macromol.* **2024**, *256*, 128335, doi:10.1016/j.ijbiomac.2023.128335.

277. Baniasadi, H.; Mashayekhan, S.; Fadaoddini, S.; Haghirsharifzamini, Y. Design, Fabrication and Characterization of Oxidized Alginate-Gelatin Hydrogels for Muscle Tissue Engineering Applications. *J. Biomater. Appl.* **2016**, *31*, 152–161, doi:10.1177/0885328216634057.

278. Wijaya, H.; Yuliana, N.D.; Wijaya, C.H.; Nasrullah, N. Classification of Trigona Spp Bee Propolis from Four Regions in Indonesia Using FTIR Based Metabolomic Approach Classification of Trigona Spp Bee Propolis from Four Regions in Indonesia Using FTIR Metabolomics Approach. *13th ASEAN Food Conf.* **2013**, 1–8.

279. Mohd, K.; Ibrahim, N.; Zakaria, A.J.; Ismail, Z.; Ahmad, Y.; Mohd, K.S. Application of GCMS and FTIR Fingerprinting in Discriminating Two Species of Malaysian Stingless Bees Propolis. *Artic. Int. J. Eng. Technol.* **2018**, *7*, 106–112.

280. Wu, Y.W.; Sun, S.Q.; Zhao, J.; Li, Y.; Zhou, Q. Rapid Discrimination of Extracts of Chinese Propolis and Poplar Buds by FT-IR and 2D IR Correlation Spectroscopy. *J. Mol. Struct.* **2008**, *883–884*, 48–54, doi:10.1016/j.molstruc.2007.12.009.

281. Hassan, M.A.; El-aziz, S.A.; Nabil-adam, A.; Tamer, T.M. Formulation of Novel Bioactive Gelatin Inspired by Cinnamaldehyde for Combating Multi-Drug Resistant Bacteria: Characterization, Molecular Docking, Pharmacokinetic Analyses, and in Vitro Assessments. *Int. J. Pharm.* **2024**, 123827, doi:10.1016/j.ijpharm.2024.123827.

282. Pant, K.; Thakur, M.; Chopra, H.K.; Dar, B.N.; Nanda, V. Assessment of Fatty Acids, Amino Acids, Minerals, and Thermal Properties of Bee Propolis from Northern India Using a Multivariate Approach. *J. Food Compos. Anal.* **2022**, *111*, 104624, doi:10.1016/j.jfca.2022.104624.

283. Ligarda-Samanez, C.A.; Choque-Quispe, D.; Moscoso-Moscoso, E.; Huamán-Carrión, M.L.; Ramos-Pacheco, B.S.; De la Cruz, G.; Arévalo-Quijano, J.C.; Muñoz-Saenz, J.C.; Muñoz-Melgarejo, M.; Quispe-Quezada, U.R.; et al. Microencapsulation of Propolis and Honey Using Mixtures of Maltodextrin/Tara Gum and Modified Native Potato Starch/Tara Gum. *Foods* **2023**, *12*, doi:10.3390/foods12091873.

284. Pant, K.; Thakur, M.; Chopra, H.K.; Nanda, V. Encapsulated Bee Propolis Powder: Drying Process Optimization and Physicochemical Characterization. *Lwt* **2022**, *155*, 112956, doi:10.1016/j.lwt.2021.112956.

285. Li, Z.; Guo, J.; Guan, F.; Yin, J.; Yang, Q.; Zhang, S.; Tian, J.; Zhang, Y.; Ding, M.; Wang, W. Oxidized Sodium Alginate Cross-Linked Calcium Alginate/Antarctic Krill Protein Composite Fiber for Improving Strength and Water Resistance. *Colloids Surfaces A Physicochem. Eng. Asp.* **2023**, *656*, 130317, doi:10.1016/j.colsurfa.2022.130317.

286. Chouhan, K.B.S.; Mukherjee, S.; Mandal, V. Reconfiguring Extraction of Phenolics & Flavonoids through a Solvent-Free Gravity Assisted Model for the Complete Recovery of Target Analytes from Moringa Leaves: A Complete Overhauling Attempt in the Field of Botanical Extraction. *Sustain. Chem. Pharm.* **2022**, *29*, 100805, doi:10.1016/j.scp.2022.100805.

287. Dellali, M.; Iurciuc, C.E.; Savin, C.L.; Spahis, N.; Djennad, M.; Popa, M. Hydrogel Films Based on Chitosan and Oxidized Carboxymethylcellulose Optimized for the Controlled Release of Curcumin with Applications in Treating Dermatological Conditions. *Molecules* **2021**, *26*, doi:10.3390/molecules26082185.

288. Schacht, E.; Nobels, M.; Vansteenkiste, S.; Demeester, J.; Franssen, J.; Lemahieu, A. Some Aspects of the Crosslinking of Gelatin by Dextran Dialdehydes. *Polym. Gels Networks* **1993**, *1*, 213–224, doi:10.1016/0966-7822(93)90001-X.

289. Van Vlierberghe, S.; Dubruel, P.; Schacht, E. Biopolymer-Based Hydrogels as Scaffolds for Tissue Engineering Applications: A Review. *Biomacromolecules* **2011**, *12*, 1387– 1408, doi:10.1021/bm200083n.

290. Iurciuc-Tincu, C.E.; Atanase, L.I.; Ochiuz, L.; Jérôme, C.; Sol, V.; Martin, P.; Popa, M.

Curcumin-Loaded Polysaccharides-Based Complex Particles Obtained by Polyelectrolyte Complexation and Ionic Gelation. I-Particles Obtaining and Characterization. *Int. J. Biol. Macromol.* **2020**, *147*, 629–642, doi:10.1016/j.ijbiomac.2019.12.247.

291. Joy, J.; Gupta, A.; Jahnavi, S.; Verma, R.S.; Ray, A.R.; Gupta, B. Understanding the in Situ Crosslinked Gelatin Hydrogel. *Polym. Int.* **2016**, *65*, 181–191, doi:10.1002/pi.5042.

292. Baron, R.I.; Culica, M.E.; Biliuta, G.; Bercea, M.; Gherman, S.; Zavastin, D.; Ochiuz, L.; Avadanei, M.; Coseri, S. Physical Hydrogels of Oxidized Polysaccharides and Poly(Vinyl Alcohol) Forwound Dressing Applications. *Materials (Basel).* **2019**, *12*, doi:10.3390/ma12091569.

293. Tincu, C.E.; Daraba, O.M.; Jérôme, C.; Popa, M.; Ochiuz, L. Albumin-Based Hydrogel Films Covalently Cross-Linked with Oxidized Gellan with Encapsulated Curcumin for Biomedical Applications. *Polymers (Basel).* **2024**, *16*, 1–37, doi:10.3390/polym16121631.

294. Kapare, H.S.; Giram, P.S.; Raut, S.S.; Gaikwad, H.K.; Paiva-Santos, A.C. Formulation Development and Evaluation of Indian Propolis Hydrogel for Wound Healing. *Gels* **2023**, *9*, 1–19, doi:10.3390/gels9050375.

295. Sarmah, D.; Rather, M.A.; Sarkar, A.; Mandal, M.; Sankaranarayanan, K.; Karak, N. Self- Cross-Linked Starch/Chitosan Hydrogel as a Biocompatible Vehicle for Controlled Release of Drug. *Int. J. Biol. Macromol.* **2023**, *237*, 124206, doi:10.1016/j.ijbiomac.2023.124206.

296. Yan, S.; Wu, S.; Zhang, J.; Zhang, S.; Huang, Y.; Zhu, H.; Li, Y.; Qi, B. Controlled Release of Curcumin from Gelatin Hydrogels by the Molecular-Weight Modulation of an Oxidized Dextran Cross-Linker. *Food Chem.* **2023**, *418*, 135966, doi:10.1016/j.foodchem.2023.135966.

297. Gull, N.; Khan, S.M.; Butt, O.M.; Islam, A.; Shah, A.; Jabeen, S.; Khan, S.U.; Khan, A.; Khan, R.U.; Butt, M.T.Z. Inflammation Targeted Chitosan-Based Hydrogel for Controlled Release of Diclofenac Sodium. *Int. J. Biol. Macromol.* **2020**, *162*, 175–187, doi:10.1016/j.ijbiomac.2020.06.133.

298. Olczyk, P.; Komosinska-Vassev, K.; Ramos, P.; Mencner, L.; Olczyk, K.; Pilawa, B. Free Radical Scavenging Activity of Drops and Spray Containing Propolis - An EPR Examination. *Molecules* **2017**, *22*, doi:10.3390/molecules22010128.

299. Karapetsas, A.; Voulgaridou, G.P.; Konialis, M.; Tsochantaridis, I.; Kynigopoulos, S.; Lambropoulou, M.; Stavropoulou, M.I.; Stathopoulou, K.; Aligiannis, N.; Bozidis, P.; et al. Propolis Extracts Inhibit UV-Induced Photodamage in Human Experimental in Vitro Skin Models. *Antioxidants* **2019**, *8*, doi:10.3390/antiox8050125.

300. Arruda, C.; Ribeiro, V.P.; Mejía, J.A.A.; Almeida, M.O.; Goulart, M.O.; Candido, A.C.B.B.; dos Santos, R.A.; Magalhães, L.G.; Martins, C.H.G.; Bastos, J.K. Green Propolis: Cytotoxic and Leishmanicidal Activities of Artepillin C, p-Coumaric Acid, and Their Degradation Products. *Rev. Bras. Farmacogn.* **2020**, *30*, 169–176, doi:10.1007/s43450-020-00043-3.

301. GOTI, Giulio, MANAL, Kavyasree, SIVAGURU, Jayaraman, et al The Impact of UV Light on Synthetic Photochemistry and Photocatalysis. *Nat. Chem.* **2024**, *16*, 684–692.

302. Wei, M.; He, X.; Liu, N.; Deng, H. Role of Reactive Oxygen Species in Ultraviolet- Induced Photodamage of the Skin. *Cell Div.* **2024**, *19*, 1–9, doi:10.1186/s13008-024- 00107-z.

303. Ebrahimi, P.; Hoxha, L.; Mihaylova, D.; Nicoletto, M.; Lante, A. UV-A Treatment of Phenolic Extracts Impacts Colour, Bioactive Compounds, and Antioxidant Activity. *J. Sci. Food Agric.* **2024**, doi:10.1002/jsfa.13780.

APPENDIX

Appendix

Stability test for the tested hydrogels by Lowry method: Immersion medium pH=7.4

samples obtained in pH 7.4	Time (h)	PH	MT(g)	MF(g)	Initial amount of protein in samples (mg)	A1	A2	A3	C1 (mg)	C2(mg)	C3(mg)	Average C	STDEV	Proteins diffused 1 %	Proteins diffused 2 %	Proteins diffused3 %	Average	STDEV
GSA I(7.4)	4	7.4	0.6253	0.0519	16.600032	0.019	0.019	0.022	5.9375	5.9375	6.875	6.25	0.4419417	37.552293	37.552293	43.481603	39.52873	2.7951033
	6					0.029	0.026	0.028	9.0625	8.125	8.75	8.645833333	0.389756	57.316658	51.387349	55.340222	54.68141	2.4650494
GSA II (7.4)	4	7.4	0.6806	0.058	18.551095	0.025	0.023	0.023	7.8125	7.1875	7.1875	7.395833333	0.2946278	50.951793	46.87565	46.87565	48.234364	1.9215124
	6					0.047	0.044	0.045	14.6875	13.75	14.0625	14.16666667	0.389756	95.789371	89.675156	91.713228	92.392585	2.541922
GOSAI (7.4)	4	7.4	0.8491	0.0813	19.149688	0.016	0.016	0.015	5	5	4.6875	4.895833333	0.1473139	21.651099	21.651099	20.297905	21.200034	0.6379016
	6					0.027	0.027	0.03	8.4375	8.4375	9.375	8.75	0.4419417	36.536229	36.536229	40.59581	37.889423	1.9137049
GOSAII (7.4)	4	7.4	0.8133	0.0763	17.97197	0.016	0.016	0.016	5	5	5	5	0	16.418744	16.418744	16.418744	16.418744	0
	6					0.017	0.017	0.018	5.3125	5.3125	-	5.3125	0	17.444915	17.444915	-	17.444915	0

Appendix

Stability test for a tested hydrogels by Lowry method: Immersion medium pH=5.5

samples obtained in pH 7.4	Time (h)	PH	MT(g)	MF(g)	Initial amount of protein in samples (mg)	A1	A2	A3	C1 (mg)	C2(mg)	C3(mg)	Average C	STDEV	Proteins diffused 1 %	Proteins diffused 2 %	Proteins diffused3 %	Average	STDEV
GOSAI (7.4)	4	5.5	0.8491	0.0747	17.5951	0.002	0.003	0.003	0.625	0.9375	0.9375	0.833333333	0.147314	3.952873	5.929309	5.929309	5.270497	0.931701
	6					0.007	0.007	0.07	2.1875	2.1875	21.875	8.75	9.280777	13.83506	13.83506	138.3506	55.34022	58.69717
GOSAII (7.4)	4	5.5	0.8133	0.081	19.91885	0.006	0.006	0.006	1.875	1.875	1.875	1.875	0	12.22843	12.22843	12.22843	12.22843	0
	6					0.008	0.009	0.01	2.5	2.8125	3.125	2.8125	0.255155	16.30457	18.34265	20.38072	18.34265	1.664079
GOSA-I (5.5)	4	7.4	0.6944	0.0686	19.75806	0.008	0.005	0.005	2.5	1.5625	1.5625	1.875	0.441942	10.82555	6.765968	6.765968	8.119162	1.913705
	6					0.01	0.011	0.012	3.125	3.4375	3.75	3.4375	0.255155	13.53194	14.88513	16.23832	14.88513	1.104878
GOSA-II (5.5)	4	7.4	0.7196	0.0539	14.98054	0.005	0.005	0.006	1.5625	1.5625	1.875	1.666666667	0.147314	5.130857	5.130857	6.157029	5.472915	0.483742
	6					0.008	0.007	0.006	2.5	2.1875	1.875	2.1875	0.255155	8.209372	7.1832	6.157029	7.1832	0.837866
GOSA-I (5.5)	4	5.5	0.6944	0.0639	18.40438	0.003	0.005	0.004	0.9375	1.5625	1.25	1.25	0.255155	3.078514	5.130857	4.104686	4.104686	0.837866
	6					0.008	0.007	0.008	2.5	2.1875	2.5	2.395833333	0.147314	8.209372	7.1832	8.209372	7.867315	0.483742
GOSA-II (5.5)	4	5.5	0.7196	0.0764	21.23402	0.001	0.001	0.001	0.3125	0.3125	0.3125	0.3125	0	1.026171	1.026171	1.026171	1.026171	0
	6					0.006	0.008	0.005	1.875	2.5	1.5625	1.979166667	0.389756	6.157029	8.209372	5.130857	6.499086	1.279861

Appendix

Stability for examined hydrogels by Lowry method: Immersion medium pH=5.5

samples obtained 6 MAY 2022	Time (h)	PH	MT(g)	MF(g)	Initial amount of protein in samples (mg)	A1	A2	A3	C1 (mg)	C2(mg)	C3(mg)	Average C	STDEV	Proteins diffused 1 %	Proteins diffused 2 %	Proteins diffused3 %	Average	STDEV
GOS AI (5.5)-24	4	5.5	0.681	0.045	13.21586	0.001	0.001	0.002	0.3125	0.3125	0.625	0.416666667	0.147314	1.976436	1.976436	3.952873	2.635249	0.931701
	6					0.004	0.004	0.004	1.25	1.25	1.25	1.25	0	7.905746	7.905746	7.905746	7.905746	0
GOS AII (5.5)-24	4	5.5	0.7089	0.045	12.69573	0.004	0.005	0.004	1.25	1.5625	1.25	1.354166667	0.147314	8.152287	10.19036	8.152287	8.831644	0.960756
	6					0.01	0.01	0.01	3.125	3.125	3.125	3.125	0	20.38072	20.38072	20.38072	20.38072	0
GOS A-I (5.5)-24	4	7.4	0.681	0.052	15.27166	0.005	0.006	0.007	1.5625	1.875	2.1875	1.875	0.255155	6.765968	8.119162	9.472356	8.119162	1.104878
	6					0.005	0.006	0.006	1.5625	1.875	1.875	1.770833333	0.147314	6.765968	8.119162	8.119162	7.668098	0.637902
GOS A-II (5.5)-24	4	7.4	0.7089	0.0376	10.60798	0.01	0.011	0.012	3.125	3.4375	3.75	3.4375	0.255155	10.26171	11.28789	12.31406	11.28789	0.837866
	6					0.011	0.012	0.015	3.4375	3.75	4.6875	3.958333333	0.531148	11.28789	12.31406	15.39257	12.99817	1.744156
GSAI	4	5.	0.64	0.05	16.081	0.0	0.0	0.0	4.68	5	5.312	5	0.2551	15.392	16.418	17.444	16.418	0.8378

Appendix

(5.5)-24		5	67	2	65	15	16	17	75		5		55	57	74	92	74	66
	6					0.0019	0.0015	0.0016	5.9375	4.6875	5	5.208333333	0.531148	19.49726	15.39257	16.41874	17.10286	1.744156
GSAII (5.5)-24	4	5.5	0.7193	0.049	13.62436	0.01	0.011	0.011	3.125	3.4375	3.4375	3.333333333	0.147314	10.26171	11.28789	11.28789	10.94583	0.483742
	6					0.011	0.013	0.015	3.4375	4.0625	4.6875	4.0625	0.51031	11.28789	13.34023	15.39257	13.34023	1.675731
GSA-I (5.5)-24	4	7.4	0.6467	0.039	12.06123	0.016	0.016	0.016	5	5	5	5	0	16.41874	16.41874	16.41874	16.41874	0
	6					0.016	0.017	0.018	5	5.3125	5.625	5.3125	0.255155	16.41874	17.44492	18.47109	17.44492	0.837866
GSA-II (5.5)-24	4	7.4	0.7193	0.0415	11.539	0.02	0.022	0.022	6.25	6.875	6.875	6.666666667	0.294628	20.52343	22.57577	22.57577	21.89166	0.967484
	6					0.046	0.041	0.041	14.375	12.8125	12.8125	13.33333333	0.73657	47.20389	42.07303	42.07303	43.78332	2.418709

Appendix

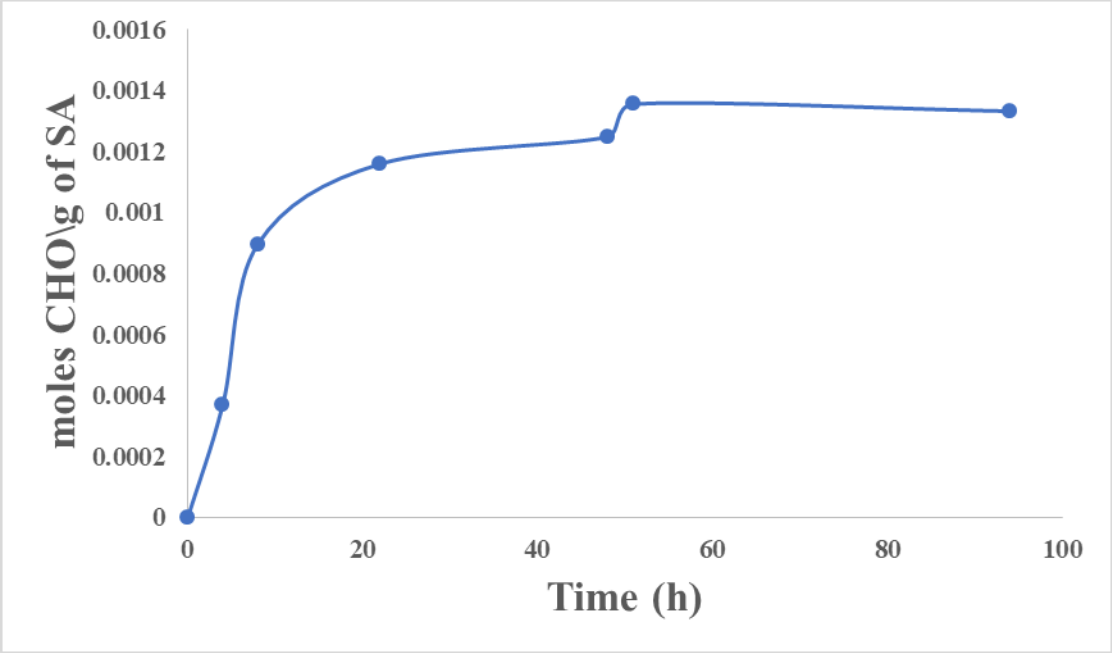

Figure for the carbonyl groups generated over the time

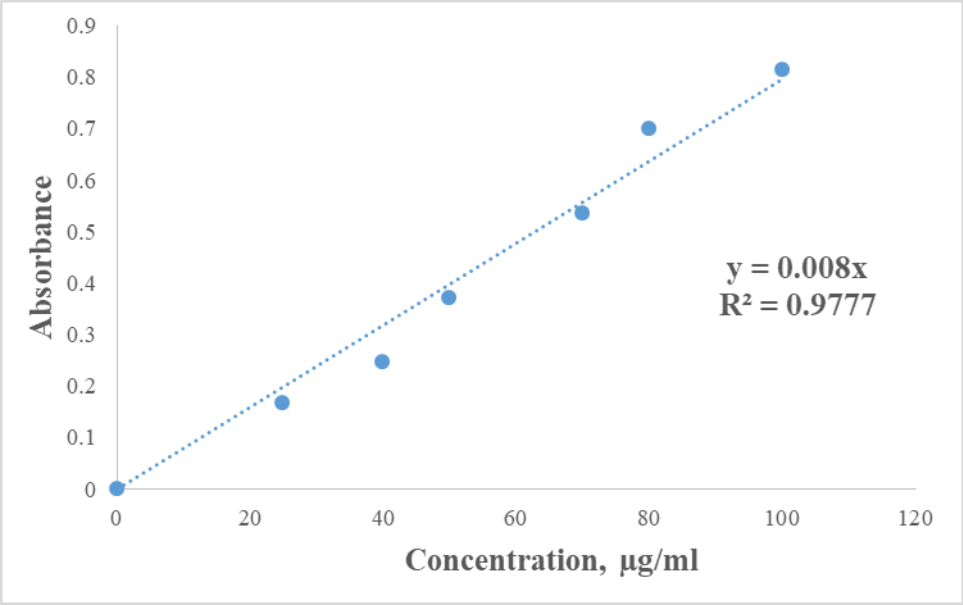

Glutamic acid calibration curve for ninhydrine test

Appendix

Table of the Antioxidant activity expressed by IC50 for the analyzed samples ((UV) means that the sample which exposed to UV irradiation).

Sample	**IC50 µg/mL**
Ascorbic acid	3.69±0.0076
Free Pro	10.33±0.0085
Free Pro (UV)	7.97±0.0074
PBP1	10.10±0.0052
PBP3	10.00±0.0076
PBP4	9.03±0.0079
PAP1	9.23±0.0098
PAP3	8.42±0.0049
PAP4	8.37±0.005
PBP1(UV)	8.77±0.0093
PBP3(UV)	7.96±0.0018
PBP4 (UV)	7.91±0.0009
PAP1 (UV)	8.90±0.0062
PAP3 (UV)	8.18±0.0032
PAP4 (UV)	7.91±0.0064